UNIVERSIDADE DE BRASÍLIA
PROGRAMA DE PÓS-GRADUAÇÃO EM PATOLOGIA MOLECULAR

Avaliação da função, estrutura e mecanismos de ação de análogos de mastoparano-L gerados por estratégia *in silico*

Karen Garcia Nogueira Oshiro

Brasília – DF
Junho de 2023

UNIVERSIDADE DE BRASÍLIA
PROGRAMA DE PÓS-GRADUAÇÃO EM PATOLOGIA MOLECULAR

Avaliação da função, estrutura e mecanismos de ação de análogos de mastoparano-L gerados por estratégia *in sílico*

Autor: Karen Garcia Nogueira Oshiro
Orientador: Prof. Dr. Octávio Luiz Franco
Coorientador: Prof. Dr. Marlon Henrique e Silva Cardoso

"Tese apresentada, como parte das exigências para obtenção do título de Doutor em Patologia Molecular, no Programa de Pós-Graduação em Patologia Molecular da Universidade de Brasília - Área de concentração: Bioquímica"

Brasília – DF
Junho de 2023

"*Science, my lad, is made up of mistakes, but they are mistakes which it is useful to make, because they lead little by little to the truth.*"

Jules Verne, A Journey to the Center of the Earth

AGRADECIMENTOS

Gratidão ao Universo, pela vida, saúde e à resiliência. Gratidão ao companheirismo, porque nenhum trabalho se faz sozinho.

Agradeço meus pais Almir Oshiro e Eni G. Nogueira e aos meus irmãos Kleiton e Murilo pelo apoio, suporte e compreensão nas ausências durante a realização deste trabalho. Aos meus avós Yushin e Kiyo Oshiro, sei que estariam orgulhosos com esse momento, agradeço a trajetória de vida e por serem exemplo, vocês ainda são presentes. As minhas doidas de quatro patas, Anastácia e Tequila, que sempre ofereciam carinho e tornavam a volta para a casa mais leve.

Agradeço a minha prima e amiga, Rosa Elena e família, Jaqueline e minhas companhias de domingo, por todo apoio, incentivo e por sempre ser presente na minha vida, nos momentos de felicidade e nos períodos difíceis. Aos meus padrinhos, Takahiro e Celina Morikawa, pelo apoio, incentivo nos estudos e compreensão com o universo acadêmico. Padrinho, gostaria que tivesse visto esse diploma chegar. A minha amiga de longa data, Natália Y. pelo companheirismo. Aos familiares e amigos que sempre me incentivaram, obrigada pelos momentos de descontração e apoio.

Esther, minha dupla de sempre, pelo companheirismo nos dias bons e ruins, por toda ajuda dentro e fora do laboratório, você faz parte desse título. Aos amigos que a academia trouxe, Betty, Marlon, e o filhote Dan, por fazerem parte dessa jornada, cheia de boas histórias, por me deixarem fazer parte da família brasiliense de vocês.

Bruno M., obrigada por todo amor, carinho, apoio e imensa compreensão nos momentos difíceis, obrigada por seu otimismo, por não me deixar sozinha nos momentos de desespero, por confiar no meu trabalho e incentivar a caminhada.

Aos meus apoiadores psicológicos Dr. Pedro e Gustavo, obrigada por todo suporte e pelos aprendizados compartilhados, vocês foram muito importantes nessa jornada. Além disso, este trabalho foi desenvolvido ao longo da pandemia do Covid-19, dessa forma, agradeço a todos os profissionais da ciência e saúde por sua dedicação.

Ao meu orientador, Octávio L. Franco, pela oportunidade e investimento na minha carreira acadêmica, ao meu orientador e amigo Marlon H. Cardoso pelos ensinamentos, pela jornada acadêmica, pelo suporte, por não me deixar desistir quando o caminho estava turbulento, obrigada por ser exemplo e inspiração.

Ao meu time do laboratório e amizades que a academia trouxe: Alexandre Duarte, Bruna Monges, Esther Vilas Boas, Ingrid Batista, Joelma Rosetto, Julia Pereira, Luccas Pires, Patrícia Souza, Raquel Quigua, Samilla Rezende, Simone Sanches, pelas horas eternas de companhia durante os experimentos, pela troca de ideias e experiências. Vocês foram a força essencial para esses experimentos serem realizados e a companhia ideal para as coisas fluírem de forma mais leve. “Não diga que a canção está perdida, tente outra vez!”.

Aos membros da minha banca de qualificação, pelas sugestões e correções. Aos participantes da banca de defesa, por aceitarem o convite e dedicação à leitura e correção desta tese.

Aos professores do Programa de Pós-Graduação em Patologia Molecular da UnB que de alguma forma ajudaram em minha formação. Ao Programa de Pós-Graduação em Biotecnologia da UCDB e ao Laboratório *S-Inova Biotech* pela estrutura e suporte no desenvolvimento dos experimentos, a todos os técnicos que auxiliaram a realização deste trabalho.

A todos os colaboradores das instituições: Centro de Análises Proteômicas e Bioquímicas, UCB; Laboratório de RMN, UFG; *Institute for Molecular Bioscience*, *UQ*; Laboratório de Purificação de Proteínas e suas Funções Biológicas, UFMS.

A CAPES, por financiar minha bolsa de estudos e as instituições de fomento CNPq e FUNDECT.

Todos que contribuíram e fizeram parte desse projeto, muito obrigada!

SUMÁRIO

LISTA DE ILUSTRAÇÕES

ABREVIATURAS E SÍMBOLOS

α – do grego *alpha*

ADN – Ácido desoxirribonucleico (do inglês *DNA, deoxyribonucleic acid*)

ARN – Ácido ribonucleico (do inglês *RNA, ribonucleic acid*)

APBS, *Adaptive Poisson-Boltzmann Solver*

β – do grego *betha*

CBM – concentração bactericida mínima (do inglês *MBC, minimal bactericidal concentration*)

CIM – concentração inibitória mínima (do inglês *MIC, minimal inhibitory concentration*)

DC – Dicroísmo circular (do inglês *CD, circular dichroism*)

DSS – 4,4-dimethyl-4-silapentane-1-sulfonic acid

ESKAPE – ***E****nterococcus faecium*, ***S****taphylococcus aureus*, ***K****lebsiella pneumoniae*, ***A****cinetobacter baumannii*, ***P****seudomonas aeruginosa* e ***E****nterobacter spp.*

FQ – Fluoroquinolona

MALDI-ToF – *matrix-assisted laser desorption/ionization - time of flight*

μ – do grego *micro* (fator 10^{-6})

MDSA – *molecular dynamics simulated annealing protocol*;

OMS – Organização Mundial da Saúde

PAMs – Peptídeos antimicrobianos (do inglês *AMP, antimicrobial peptide*)

PDH – peptídeos de defesa do hospedeiro (do inglês *HDPs, host defense peptides*)

PDB – *Protein Data Bank*;

POPC – 1-palmitoyl-2-oleoyl-sn-glycero-3-phosphocholine;

POPG – 1-palmitoyl-2-oleoylphosphatidylglycerol;

RIF – Rifamicina

RG – *Radius of gyration*

RMN – Ressonância Magnética Nuclear (do inglês *NMR, nuclear magnetic resonance*)

RMSD – root *mean square deviation*

RMSF – *root mean square fluctuation*

ROS - Espécies reativas de oxigênio (do inglês *ROS, reactive oxygen species*)

RPS – Ressonância Plasmônica de Superfície (do inglês SPR, *surface plasmon resonance*)

SASA – *solvent accessible area*

SCS – *Secondary chemical shifts*

TFE – 2,2,2-trifluoroethanol

RESUMO

Escherichia coli consiste em uma bactéria altamente versátil capaz de adquirir fatores de virulência específicos, resultando em patótipos que podem causar uma gama de doenças infecciosas, como infecções no trato urinário, gastroenterite, sepse entre outras. Consequentemente, há uma necessidade de identificar novos fármacos antimicrobianos considerando o desenvolvimento de resistência bacteriana a um amplo espectro de antibióticos. Os mastoparanos são em sua maioria peptídeos catiônicos com propriedades farmacológicas multifuncionais. Mastoparans-R1 e R4 foram projetados computacionalmente com base no mastoparano-L nativo de vespas e têm potencial terapêutico aprimorado para o controle de infecções bacterianas. Aqui avaliamos se esses peptídeos mantêm sua atividade contra cepas de *E. coli* em uma faixa de concentração fisiológica de sal. Descobrimos que os mastoparanos-R1 e R4 preservaram sua atividade nas condições testadas, incluindo atividades antibacterianas em concentrações salinas fisiológicas. A estrutura secundária geral dos peptídeos foi investigada usando espectroscopia de dicroísmo circular em uma variedade de solventes. Não foram observadas alterações significativas na estrutura secundária (arranjo aleatório em soluções aquosas e α-hélice em ambientes hidrofóbicos e aniônicos). As estruturas tridimensionais de mastoparano-R1 e R4 foram elucidadas por espectroscopia de ressonância magnética nuclear, revelando segmentos α-helicoidais anfipáticos para Leu3-Ile13 (mastoparano-R1) e Leu3-Ile14 (mastoparano-R4). Possíveis mecanismos de associação de membrana para mastoparano-R1 e R4 foram investigados por ressonância plasmônica de superfície e estudos de extravasamento de carboxifluorosceína com bicamadas lipídicas e vesículas sintéticas de POPC e POPC/POPG (4:1). Mastoparano-L teve a maior afinidade para ambos os sistemas de membrana, enquanto os dois análogos tiveram associação mais fraca, porém com maior seletividade em lisar membranas aniônicas. Esses achados também corroboram com simulações de dinâmica molecular, onde os peptídeos mastoparano-R1 e R4 têm maiores interações com membranas miméticas bacterianas em comparação com modelo de membranas de mamíferos. Apesar de apresentarem algumas diferenças em seus perfis funcional e estrutural, o análogo de mastoparano-R1 se destacou pela sua melhor atividade contra o isolado clínico, maior potencial bacteriostático, bactericida (2 - 2 μM), seletividade para lise de vesícula aniônica em concentração ~3x menor do que vesícula zwiteriônica. Este estudo reforça o potencial do mastoparano-R1 como candidato a fármaco, bem como modelo para estudo e desenvolvimento de peptídeos antimicrobianos mais seletivos.

Palavras-chave: mastoparanos, peptídeo antimicrobiano, biologia estrutural.

ABSTRACT

Escherichia coli consists of a highly versatile bacterium capable of acquiring specific virulence factors, resulting in pathotypes that can cause a range of infectious diseases, such as urinary tract infections, gastroenteritis, and sepsis, among others. Consequently, there is a need to identify new antimicrobial drugs considering the development of bacterial resistance to a broad antibiotics spectrum. Mastoparans are cationic peptides with multifunctional pharmacological properties. Mastoparans-R1 and R4 were computationally designed based on native mastoparan-L from wasps and have improved therapeutic potential for bacterial infection control. Here we evaluated whether these peptides maintain their activity against Escherichia coli strains under a range of salt concentrations. We found that mastoparans-R1 and R4 preserved their activity under the conditions tested, including having antibacterial activities at physiological salt concentrations. The overall peptide structures were investigated by using circular dichroism spectroscopy in a range of solvents. Nonsignificant modifications in the secondary structure were observed (random coil in aqueous solutions and α-helix in hydrophobic and anionic environments). The three-dimensional structures of mastoparan-R1 and R4 were elucidated through nuclear magnetic resonance spectroscopy, revealing amphipathic α-helical segments for Leu3-Ile13 (mastoparan-R1) and Leu3-Ile14 (mastoparan-R4). Possible membrane-association mechanisms for mastoparan-R1 and R4 were investigated through surface plasmon resonance and leakage studies of carboxyfluorescein with lipid bilayers and synthetic vesicles of POPC and POPC/POPG (4:1). Mastoparan-L had the highest affinity for both membrane systems, whereas the two analogs had the weaker association, but improved selectivity for lysing anionic membranes. This finding was also supported by molecular dynamics simulations, in which mastoparan-R1 and R4 were found to have greater interactions with bacteria-like membranes compared to model mammalian membranes. Despite having a few differences in their functional and structural profiles, the mastoparan-R1 analog stood out for the better activity against the clinical isolate, greater bacteriostatic, bactericidal potential (2 - 2 μM), selectivity for anionic vesicle lysis at ~3x lower concentration than zwitterionic vesicle. This study reinforces the potential of mastoparan-R1 as a drug candidate, as well as a model for the study and development of more selective antimicrobial peptides.

Keywords: *mastoparan; antimicrobial peptide; structural biology.*

1. INTRODUÇÃO

1.1 Infecções bacterianas multirresistentes

As infecções bacterianas e persistentes estão entre as maiores ameaças para a saúde humana, impactando diretamente para altos níveis de morbidade e mortalidade (Fisher et al., 2017). Segundo dados da Organização Mundial da Saúde OMS, (WHO, 2001) pacientes com infecções causadas por bactérias resistentes possuem um maior risco de desfechos clínicos inefetivos e falecimento. Somado a isso, estima-se que 13 milhões de mortes possam ser atribuídas a eventos de infecções bacterianas até o ano de 2050 (WHO, 2017). Alguns fatores podem ser levados em conta para o favorecimento, surgimento e o ressurgimento de doenças infecciosas, como por exemplo, a adaptação e a mudança microbiana, susceptibilidade humana à infecção, mudanças nos ecossistemas, desigualdade social, globalização e o uso indiscriminado de antibióticos (Morens et al., 2004; Karmali, 2018). Além desses fatores, diante da pandemia causada pela COVID-19, foi registrado um aumento de relatos de bactérias patogênicas relacionadas ao uso excessivo de antibióticos, enfatizando a necessidade de pesquisas nessa área (Akram et al., 2023).

O uso indiscriminado de antibióticos pode causar impacto na pressão seletiva de cepas bacterianas patogênicas. Dentro deste contexto, a OMS descreveu uma lista prioritária de bactérias resistentes a antibióticos afim de se priorizar o desenvolvimento de novos e eficazes tratamentos (WHO, 2017). O grupo *ESKAPE* de bactérias patogênicas, que inclui *Enterococcus faecium*, *Staphylococcus aureus*, *Klebsiella pneumoniae*, *Acinetobacter baumannii*, *Pseudomonas aeruginosa* e *Enterobacter* spp., são conhecidos por sua capacidade de serem resistentes a tratamentos com antibióticos e estão associados a incidência de infecções multirresistentes em ambientes hospitalares (Oliveira et al., 2020). Além disso, patógenos do grupo *ESKAPE* tendem a ser associados ao maior risco de mortalidade, resultando em aumento dos custos de saúde (Founou et al., 2017).

Nesta lista, organismos pertencentes a família das *Enterobacteriaceaes* foram considerados patógenos de nível crítico, pois possuem um alto nível de morbidade e mortalidade (WHO, 2017). A família das *Enterobacteriaceaes* constitui uma das mais abundantes, incluindo uma ampla variedade de bactérias Gram-negativas, as quais fazem parte da microbiota nativa dos seres humanos e animais. Entretanto, esta família também apresenta uma gama de bactérias patogênicas, incluindo espécies dos gêneros *Salmonella*, *Proteus*, *Shigella* e *Escherichia* (Huang et al., 2006). Dentre estas, *Escherichia coli* caracteriza-se por um bacilo Gram-negativo, anaeróbio facultativo que pode ser imóvel ou

móvel, com flagelos peritríquios, podendo colonizar o intestino de vertebrados e invertebrados e faz parte da microbiota normal de humanos desde as primeiras horas de nascimento (Kaper et al., 2004). Além disso, considera-se *E. coli* uma bactéria altamente versátil e, evolutivamente, várias estirpes adquiriram fatores de virulência específicos, gerando patotipos capazes de se adaptar a novos nichos e de causar um amplo espectro de doenças (Kaper et al., 2004). Estes patotipos podem causar desde infecções extra intestinais, no trato urinário, meningite e sepse (Nataro and Kaper, 1998; Okeke and Nataro, 2001; Huang et al., 2006). Embora não esteja diretamente reconhecida dentro do grupo *ESKAPE*, patotipos de *E. coli* multirresistentes costumam ser identificadas como uma das principais causas de infecções agravantes, tanto na comunidade quanto nos serviços de saúde, considerando assim, esse patógeno como uma preocupação crítica de saúde pública (Oliveira et al., 2020).

Bactérias podem ser altamente eficientes na síntese e compartilhamento de genes levando ao desenvolvimento e propagação de mecanismos de resistência aos antibióticos (Peleg and Hooper, 2010). Dessa forma, a resistência bacteriana pode ocorrer naturalmente, mas também pode ser adquirida através da transferência de genes de resistência entre as próprias bactérias ou de outras fontes (Oliveira et al., 2020). Mecanismos de resistência resultaram no desenvolvimento simultâneo de bactérias resistentes a várias classes de antibióticos, sendo assim, essas cepas ficaram conhecidas também como “superbactérias” (Alanis, 2005). Estes microrganismos podem ser intrinsecamente resistentes a determinados antibióticos, podendo também adquirir resistência através de mutações em seus genes cromossômicos e por transferência horizontal de genes (Blair et al., 2015).

A resistência intrínseca de uma bactéria a um antibiótico específico pode ser explicada pela sua capacidade de resistir à ação deste fármaco como resultado de características estruturais ou funcionais inerentes, como por exemplo, a ausência de um alvo susceptível de um antibiótico específico (Blair et al., 2015). Estudos levaram à identificação de diversos genes responsáveis pela resistência intrínseca a diferentes classes de antibióticos, incluindo β-lactâmicos, fluoroquinolonas (FQ) e aminoglicosídeos (Nikaido, 2009; Blair et al., 2015). Estudos com bactérias Gram-negativas têm mostrado mecanismos que visam a forma como os medicamentos são transportados, incluindo a atividade seletiva de porinas, bloqueio de penetração de drogas e bombas de efluxo (Nikaido, 2009; Llarrull et al., 2010).

Mecanismos como o de permeabilização de membrana acontecem onde possa haver a redução da permeabilidade da membrana externa e limitar a entrada de antibiótico na célula

bacteriana (Figura 1). Isto pode ser possível pela regulação negativa da porinas ou pela substituição de porinas por canais mais seletivos (Fernández and Hancock, 2012). A regulação de efluxo acontece onde as bombas de efluxo bacterianas transportam ativamente diversos antibióticos para fora da célula e podem ser os principais contribuintes para a resistência intrínseca de bactérias (Fernández and Hancock, 2012). Podemos citar também as alterações em alvos dos antibióticos por mutação, onde as alterações na estrutura alvo impedem a ligação eficiente do antibiótico (Figura 1), porém ainda permitindo o alvo de realizar a sua função (Wright, 2011).

A resistência adquirida pode ocorrer por meio de mutações pontuais ou através da aquisição de outro material genético (Hollenbeck and Rice, 2012). O tipo mais frequente de resistência adquirida pode ser transmitido horizontalmente através da conjugação de plasmídeos (Figura 1) (Alanis, 2005) ou através do movimento de transposons (Hollenbeck and Rice, 2012). Um exemplo de resistência mutacional consiste no desenvolvimento de resistência a rifamicina (RIF). A RIF bloqueia a transcrição bacteriana por inibição da polimerase de ácido ribonucleico (RNA) dependente do ácido desoxirribonucleico (DNA) (Munita and Arias, 2016). Essas mutações resultam na diminuição da afinidade do fármaco por seu alvo, o qual geralmente poupa a atividade catalítica da polimerase, permitindo a transcrição (Floss and Yu, 2005). Hooper e colaboradores (2002) mostraram outro exemplo bem caracterizado de resistência mutacional envolvendo fluoroquinolonas. O mecanismo de resistência FQ ocorre através do desenvolvimento de mutações cromossômicas nos genes que codificam as subunidades de enzimas ligadas ao DNA, as quais alteram a replicação do DNA (DNA-girase e topoisomerase). O nível de resistência adquirido por alterações em desenvolvimento em uma das enzimas dependerá da potência com a qual o agente antimicrobiano inibe ou inativa o alvo (Hooper, 2002). Além disso, foi relatada a existência de regiões multirresistentes compostas por elementos móveis, como integrons e transposons, os quais uma vez combinados, podem contribuir ativamente para a resistência bacteriana (Osborn and Böltner, 2002; Wellington et al., 2013).

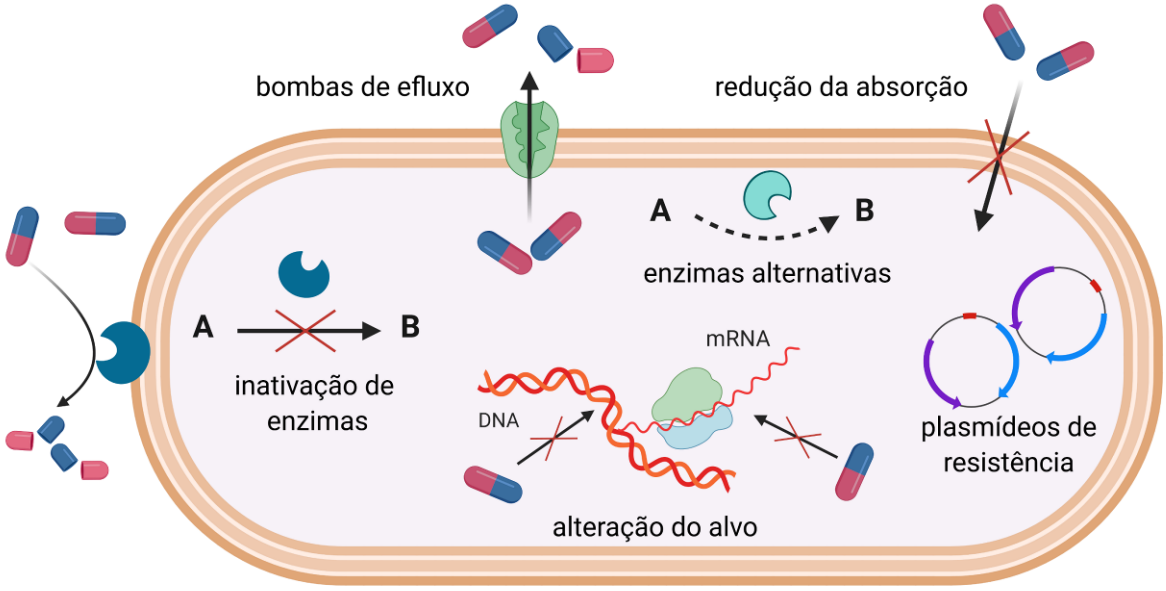

Figura 1. Mecanismos de ação antimicrobiana associados ao desenvolvimento de resistência em bactérias. Dentre os diversos mecanismos pelos quais as bactérias podem se tornar resistentes aos antibióticos ilustramos a produção de enzimas alternativas ou inativação anzimática (ex: β-lactamases, aminoglicosídeo fosfotransferase ou modificases), bombas de efluxo que podem causar a expulsão de antibióticos, modificação da permeabilidade da membrana celular, alteração da via metabólica e a alteração do alvo, bem como a transferência horizontal de genes com o compartilhamento de plasmídeos. Figura criada com o auxílio da ferramenta *BioRender*.

Além destes mecanismos citados, uma das formas das bactérias tornarem-se resistentes tanto física quanto quimicamente pode ser através da formação de biofilmes (O'Toole et al., 2000). A susceptibilidade a antibióticos pode ser apresentada por células imersas em biofilme podendo ser considerada multifatorial e pode variar dependendo da espécie e composição genética do(s) organismo(s), do tipo de agente antimicrobiano, do estágio de desenvolvimento do biofilme além das condições ambientais (Hall and Mah, 2017). Estudos indicam que os mecanismos de resistência podem estar ligados à virulência das cepas e mecanismos de adaptação para sobreviver sob condições de estresse (Martínez and Baquero, 2002). Em casos de exposição constante, por exemplo, a agentes antimicrobianos, limitação de nutrientes e alteração de temperatura, cepas bacterianas podem vir a se desenvolver e formar comunidades multicelulares aderentes a superfícies bióticas e/ou abióticas, denominadas biofilmes (Costerton et al., 1999; de la Fuente-Núñez et al., 2013).

Biofilmes podem ser definidos como um consórcio estruturado uni ou polimicrobiano, possuindo uma matriz extracelular de polissacarídeo(s), proteínas e DNA (de la Fuente-Núñez et al., 2013). O desenvolvimento de biofilmes inicia-se a partir de células bacterianas planctônicas (livre-nadantes) que se aderem às superfícies formando colônias que, com o tempo, passam a secretar uma matriz extracelular e, assim, criam uma barreira física (Kostakioti et al., 2013) (Figura 2). Outro mecanismo utilizado pelas bactérias para desencadear a formação de biofilmes, bem como mediar sua maturação, denomina-se *quorum sensing*, sendo este definido como a regulação da expressão gênica em resposta às flutuações da densidade populacional celular (Miller and Bassler, 2001). Uma vez desenvolvido o biofilme, células maduras dentro dessa população podem se dispersar, sendo uma fase essencial para o fechamento do ciclo dos biofilmes, permitindo que as células se espalhem e colonizem novas superfícies (Figura 2) (O'Toole et al., 2000; Miller and Bassler, 2001; de la Fuente-Núñez et al., 2013).

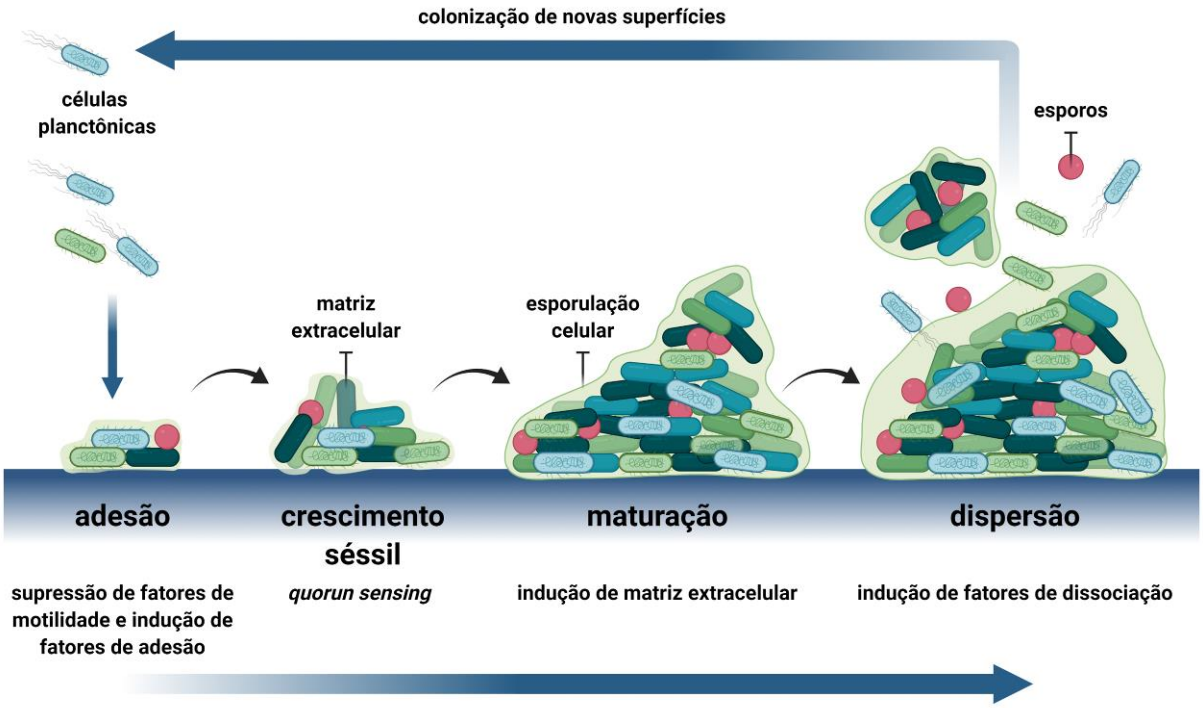

Figura 2. Representação esquemática do desenvolvimento de biofilmes bacterianos destacando os estágios de adesão, crescimento séssil, maturação e dispersão. Figura criada com o auxílio da ferramenta *BioRender*.

Alguns autores afirmam que as infecções hospitalares podem ser, em sua maioria, causadas por biofilmes bacterianos (Costerton et al., 1999; Weiss and McMichael, 2004;

Römling and Balsalobre, 2012), representando 65 % a 80 % das infecções bacterianas em humanos (de la Fuente-Núñez et al., 2013). A formação de biofilmes caracteriza-se, portanto, como um processo de desenvolvimento orientado ambientalmente que aumenta a resistência ao estresse exógeno, permitindo a sobrevivência de microrganismos em condições desfavoráveis (de la Fuente-Núñez et al., 2013). Devido à seleção de microrganismos resistentes a antibióticos, aliado a decrescente taxa de descoberta/desenvolvimento destes, pesquisadores vem buscando o desenvolvimento de novos compostos bioativos eficazes no combate a estes microrganismos (Gallo et al., 2002; de la Fuente-Núñez et al., 2013; Cardoso et al., 2016). Dentro deste cenário, peptídeos antimicrobianos (PAMs) têm sido considerados como uma alternativa aos tratamentos antibacterianos convencionais (Marr et al., 2006; Lai and Gallo, 2009; Kumar et al., 2018).

1.3 Peptídeos de Defesa do Hospedeiro (PDH)

Peptídeos de defesa do hospedeiro (PDH), constituem um grupo diversificado de moléculas que podem ser produzidos como parte do sistema de defesa (sistema imune inato) do hospedeiro e desempenham um papel importante durante um processo de infecção (Zasloff et al., 1988; Hancock and Diamond, 2000). Os PDH podem ser produzidos por uma variedade de células do corpo, incluindo células epiteliais, neutrófilos e macrófagos, e são encontradas em uma variedade de tecidos, incluindo pele, membranas mucosas e trato gastrointestinal, dessa forma, agem como uma primeira linha de defesa contra patógenos invasores, interrompendo a integridade de suas membranas celulares (Hancock and Diamond, 2000; Yeung et al., 2011)

Além de suas propriedades antimicrobianas, também podem desempenhar várias outras funções no corpo. Eles podem modular a resposta imune recrutando e ativando células imunes, e demonstraram ter propriedades anti-inflamatórias e cicatrizantes (Hancock and Sahl, 2006). Os PDH podem estar associados no papel na regulação da microbiota, a comunidade de microrganismos que vivem no corpo, matando ou inibindo seletivamente o crescimento de bactérias nocivas enquanto promovem o crescimento de bactérias benéficas (Teng et al., 2023). Essas moléculas receberam atenção nos últimos anos devido ao seu potencial como uma nova classe de antibióticos. Com o surgimento de bactérias resistentes a antibióticos, há uma necessidade urgente de novos agentes antimicrobianos, e os PDH oferecem um caminho promissor para o desenvolvimento de medicamentos. No entanto, também existem desafios no uso de PDH como fármacos, incluindo sua suscetibilidade à

degradação por proteases e seu potencial toxicidade em altas concentrações (Yeung et al., 2011; Haney et al., 2019).

De forma geral, essas moléculas podem ser um componente importante do sistema imunológico inato e desempenham um papel vital na defesa do hospedeiro contra patógenos. Mais pesquisas sobre a estrutura e função dos PDH podem levar ao desenvolvimento de novas terapias para uma variedade de doenças infecciosas, dessa forma, dentro do grupo dos PDH surge como alternativa a classe dos peptídeos antimicrobianos (PAMs) (Teng et al., 2023). Esta classe de moléculas bioativas pode ser produzida por diversos tecidos e tipos celulares em uma variedade de espécies, incluindo plantas, animais invertebrados, vertebrados, fungos e bactérias (Brogden, 2005). Essas moléculas são responsáveis por possuir reconhecimento molecular, assim como por diversas atividades biológicas, incluindo sua atuação como neurotransmissores, hormônios, toxinas e antibióticos (Izadpanah and Gallo, 2005; Magana et al., 2020).

1.2 Peptídeos antimicrobianos (PAMs)

PAMs consistem em moléculas relativamente pequenas (<10 kDa), catiônicas e anfipáticas (organização de uma face hidrofóbica e outra hidrofílica) (Brogden, 2005), sendo em sua maioria constituídas de 6 a 50 resíduos de aminoácidos e possuindo carga líquida positiva (Scott et al., 1999; Hancock and Patrzykat, 2002; Bradshaw, 2003). A presença de resíduos como arginina, lisina e histidina influenciam diretamente no caráter catiônico dos PAMs (Hancock and Scott, 2000). Alguns estudos mostram que a carga líquida destes peptídeos está relacionada às suas atividades antimicrobiana, hemolítica e citotóxica (Lorin et al., 2005). Além disso, os perfis estruturais e propriedades físico-químicas desempenham papéis importantes na determinação da atividade antibacteriana, toxicidade e biodisponibilidade (Magana et al., 2020).

Baseados em suas características físico-químicas, peptídeos catiônicos podem possuir diversas conformações estruturais (Dennison et al., 2005). Pesquisadores vêm relatando que os PAMs podem ser agrupados com base em quatro classes principais: α-hélice (Figura 3a), folha-β (Figura 3b), peptídeos lineares ou em *coil* (Figura 3c), incluindo a mistura de α-hélice e folha-β (Figura 3d) (Giuliani et al., 2007). Entretanto, existe uma gama de estruturas que estes peptídeos podem adotar, como por exemplo, estruturas em *loop* e peptídeos estendidos, estruturas em grampos (*β-hairpin*) (Blanco et al., 1994; Hancock and Lehrer, 1998), peptídeos cíclicos (Joo, 2012), além de peptídeos com composições de

aminoácidos únicos (Epand and Vogel, 1999), bem como peptídeos L- e D-enantiômeros, diasteroisomeros e retro-inversos (Petsko, 1992; Cardoso et al., 2018). Estruturas helicoidais dependem de fatores como a disposição dos resíduos de aminoácidos ao longo da sequência, a cadeia lateral destes resíduos, sua carga (positiva ou negativa), isomeria dos resíduos (L- ou D-aminoácidos) e o ambiente em que estão inseridos (Papo and Shai, 2003). Já as estruturas em folha-β podem se organizar nos sentidos paralelo e antiparalelo. Para isto geralmente os peptídeos se formam a partir de cadeias polipeptídicas determinadas, geralmente, pela presença de resíduos de cisteína responsáveis pela formação de ligações dissulfeto, conferindo maior estabilidade estrutural ao peptídeo (Broekaert et al., 1997; Braff and Gallo, 2006).

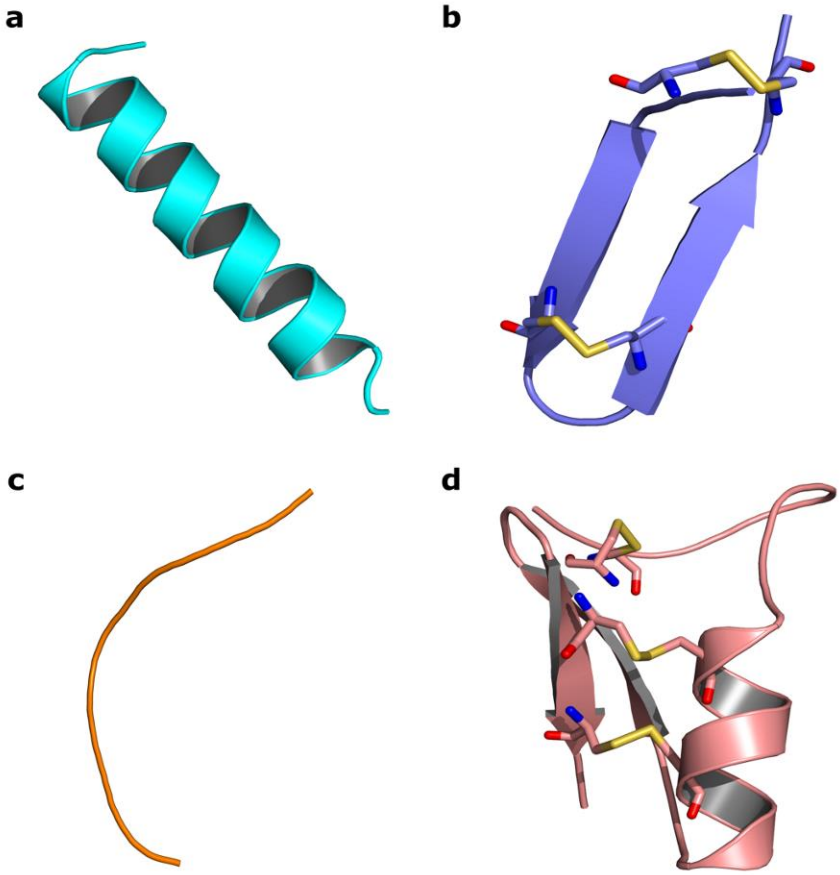

Figura 3. Estruturas tridimensionais de peptídeos antimicrobianos. Em **(a)** conformação de α-hélice, magainina-2 (PDB 2MAG); **(b)** conformação em folha-β, tachyplesina-I (PDB 1WO1); **(c)** estrutura estendida ou *coil*, indolicidina (PDB 1G89); **(d)** mistura de α-hélice e folha-β, defensina-A de inseto (PDB 1ICA). Ligações dissulfeto destacadas em *sticks* amarelo, átomos de nitrogênio em azul e átomos de oxigênio em vermelho.

As propriedades físico-químicas dos peptídeos antimicrobianos estão relacionadas com seus efeitos antibacterianos, tais como constituintes de aminoácidos, comprimento dos peptídeos, presença de resíduos com carga positiva, composição lipídica, característica de hidrofobicidade, carga líquida da molécula e a helicidade da estrutura espacial estrutura (Carratalá et al., 2020; Koehbach & Craik, 2019). Os constituintes ou o arranjo da cadeia lateral afetaram fortemente a potente atividade antimicrobiana e a especificidade para o alvo microbiano de PAMs (Li et al., 2014). Com base em seu conteúdo e proporção de aminoácidos, essas moléculas podem ser ainda categorizadas como peptídeos ricos em determinados resíduos de aminoácidos, como por exemplo, alanina (Cardoso et al., 2016), prolina (Otvos, 2002), e arginina (Chan, 2006). Estudos também revelam que alterações nas porções N- e C-terminais também podem conferir maiores estabilidades estruturais para esses peptídeos (Alvares et al., 2018; Zhu et al., 2021).

PAMs adotam diferentes conformações, tornando-os atraentes como moléculas multifuncionais que interagem com diferentes partes do microrganismo alvo. Essa capacidade de adaptação a diferentes ambientes (flexibilidade estrutural) pode ajudar os PAMs a superar os diversos mecanismos de defesa que os microrganismos utilizam para evadir os agentes antimicrobianos (Koehbach and Craik, 2019; Park et al., 2022). A flexibilidade dessas moléculas pode ser considerada um fator importante para sua atividade antimicrobiana e pode ajudar a explicar seu amplo espectro de ação e capacidade de superar os mecanismos de defesa dos microrganismos (Benfield and Henriques, 2020). No entanto, vale ressaltar que essa característica também pode desencadear efeitos indesejados, incluindo altas taxas de citotoxicidade, hemólise, baixa biodisponibilidade, degradação proteolítica, instabilidade plasmática, bem como sensibilidade ao sal, uma vez que interagem eletrostaticamente com as membranas microbianas (Gan et al., 2021). Portanto, o desenho de PAMs precisa considerar outros parâmetros além da flexibilidade, incluindo distribuição de carga, momento hidrofóbico e hidrofobicidade (Cardoso et al., 2020).

As propriedades biofísicas dos peptídeos também podem estar intimamente relacionadas com sua atividade antimicrobiana. Com alvo de paredes celulares bacterianas carregadas negativamente, a alta carga líquida positiva e a anfipaticidade podem explicar a alta afinidade por membranas (Gan et al., 2021). Para a maioria dos PAMs, a alta afinidade por membranas microbianas contribui para a natureza anfipática geral, o que demonstrou que a interação da membrana não era exclusiva dos peptídeos α-helicoidais (Y.-H. Huang et al., 2009; jarva, 2018). Outros fatores como o pH, temperatura e a concentração de sal também

afetam fortemente a eficácia dos PAMs em erradicar bactérias (Hale and Hancock, 2007; Benfield and Henriques, 2020). Em ambiente de pH ligeiramente ácido, a atividade antimicrobiana pode promover a protonação de certos aminoácidos é promovido, como histidina, ácido aspártico ou ácido glutâmico (Salas-Ambrosio, 2020). A carga líquida de PAMs catiônicos pode favorecer sua ligação com superfícies bacterianas carregadas negativamente, entretanto, em ambiente com maiores concentrações de sal podem interferir no equilíbrio dos gradientes iônicos e dificultando o vazamento do conteúdo celular (Mohanram and Bhattacharjya, 2016; Park et al., 2022). De forma geral, além das características físico-químicas, o ambiente em que estão inseridos podem alterar os diversos mecanismos de ação associados.

1.3 Mecanismos de ação

O equilíbrio anfifílico mostra-se importante para os PAMs, influenciando tanto a atividade antibacteriana quanto sua seletividade. A conformação anfifílica pode ser benéfica para a segregação da cadeia lateral catiônica hidrofílica e hidrofóbica (Chen et al., 2007). Estudos indicam que a interação de PAMs com membranas tende a se dividir em duas classes de mecanismos: (i) disrupção de membranas e (ii) alvos intracelulares (Powers and Hancock, 2003; Lee and Lee, 2015). Ainda que não exista um consenso universal relacionado aos mecanismos de ação dessas moléculas, os modelos de permeabilização de membrana têm sido propostos no meio acadêmico e aceitos com base em diversas investigações (Nguyen et al., 2011). Interações peptídeo-membrana tornam-se de fundamental importância na compreensão dos mecanismos de ação destas moléculas, uma vez que os PAMs possuem como característica sua capacidade de interagir com membranas bacterianas (Hancock and Rozek, 2002). Este mecanismo molecular e a via de permeabilização de membranas podem variar de acordo com o peptídeo. Além disso, alterações na sequência de aminoácidos, composição lipídica da membrana e concentração de peptídeo também podem interferir no mecanismo de ação (Shai, 2002).

Durante a permeabilização de membranas pode-se observar a liberação de íons e metabólitos intracelulares, interrupção de processos respiratórios, despolarização da membrana e, por fim, a morte celular (Pelegrini et al., 2011). Estas interações podem ser realizadas de diversas formas, onde na maioria das vezes apresentam-se descritas como formação de poros, sendo divididos em poro toroidal, modelo barril e modelo carpete (ou tapete) e modelo detergente (Figura 3a) (Nguyen et al., 2011). A formação de poros

geralmente pode ser coordenada pelos grupos lipídicos com a parte polar e os feixes da hélice que se orientam de forma vertical no interior da membrana. O modelo toroidal, por exemplo, constitui poros toroidais nas bicamadas lipídicas, agregando-se às camadas de forma intercalada. Já no modelo barril as hélices peptídicas formam um feixe na membrana com um lúmen central, muito semelhante a um barril composto de peptídeos helicoidais. O mecanismo de formação em carpete refere-se à desorganização da membrana por ação colaborativa dos peptídeos, onde os PAMs se ligam a superfície de forma paralela ao grupamento fosfato, causando uma disrupção mais severa da bicamada lipídica. Semelhante a este modelo, o modelo detergente pode acarretar interações desfavoráveis à superfície da membrana, produzindo um efeito que eventualmente desintegra a membrana, formando micelas e colapsando a bicamada (Yang et al., 2001; Reddy et al., 2004; Brogden, 2005).

Sabe-se que regiões hidrofílicas (podendo ser carregadas positivamente) facilitam a interação dos peptídeos com as superfícies microbianas carregadas negativamente e grupos da bicamada de fosfolipídios que levam a penetração da membrana celular (Shai, 2002). Sendo assim podemos mencionar ainda que, além dos mecanismos de ação envolvendo membranas celulares, PAMs podem exibir ação intracelular (Figura 2b) (Cardoso et al., 2019), incluindo a inibição da replicação e transcrição de DNA (Figura 2c), inibição de síntese de RNA (Figura 2d) e inibição da função ribossomal da síntese de proteínas (Figura 2e) (Mayor and Pagano, 2007). Os PAMs podem ainda inativar proteínas chaperonas, necessárias para o dobramento adequado de proteínas essenciais para o microrganismo alvo (Figura 2f) (Hale and Hancock, 2007). Além disso, peptídeos também podem causar a inibição da respiração celular e indução da formação de espécies de oxigênio reativas (ROS) (Figura 2g), podendo causar dano à integridade da membrana da célula mitocondrial, causando efluxo de ATP e NADH (Figura 2g) (Hale and Hancock, 2007; Lee and Lee, 2015).

PAMs também podem causar modificações no sítio de enzimas, como por exemplo, enzimas de inativação de aminoglicosídeos, impedindo a ação enzimática e ocasionando a perturbação de alvos intracelulares (Kumar et al., 2018), bem como podendo modular diferentes cascatas do sistema imunológico (imunomoduladores) (Brogden, 2005; Jenssen et al., 2006). Diante desta promiscuidade funcional e diversidade estrutural (Franco, 2011), podemos observar a razão pela qual PAMs têm se tornado tão atraentes como futuras moléculas terapêuticas.

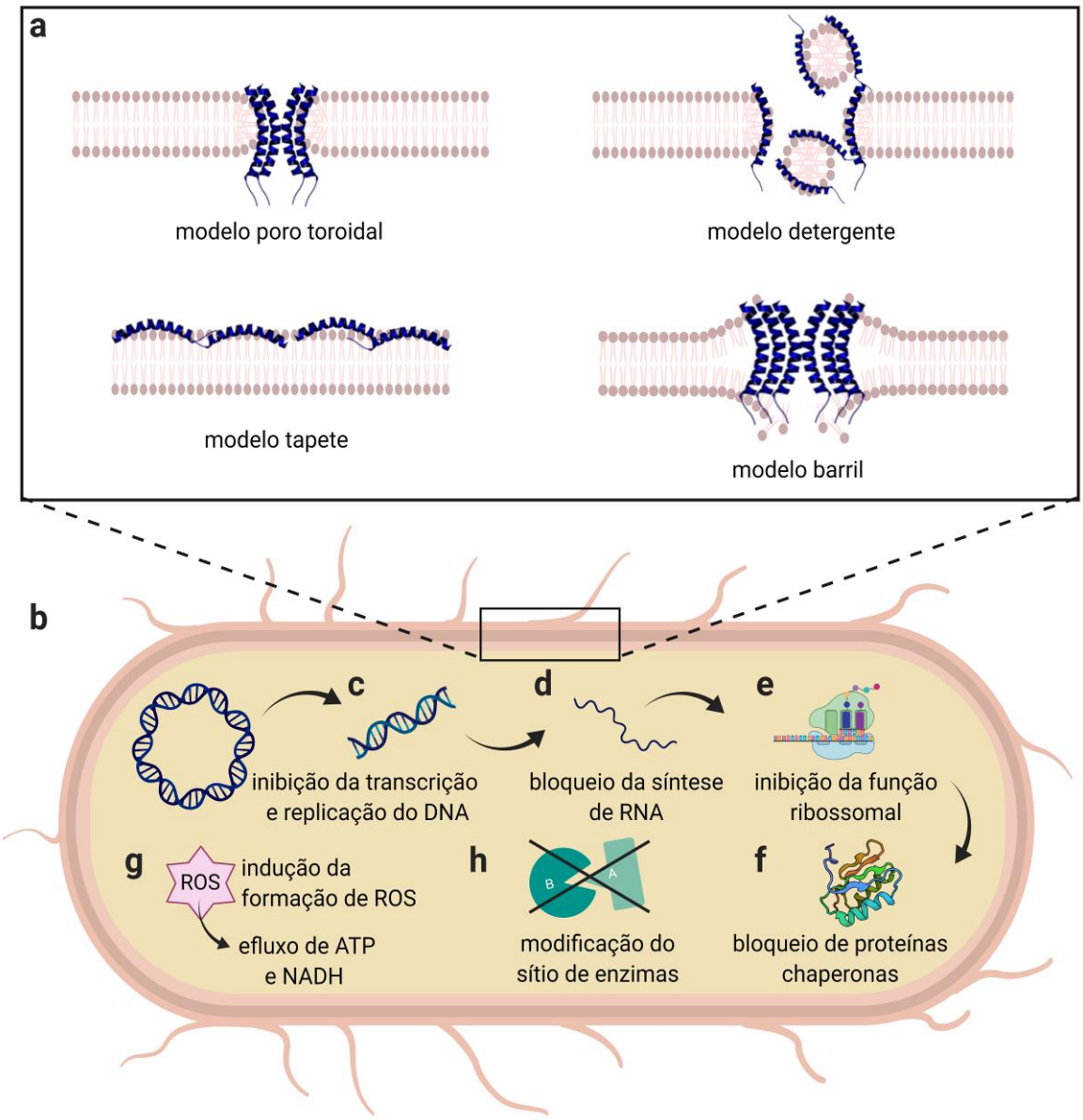

Figura 2. Mecanismos de ação de PAMs. (**a)** Mecanismos de ação em membranas, destacando a formação de poro toroidal, modelo carpete, modelo detergente e modelo barril. (**b)** Mecanismos de ação intracelular propostos para os PAMs em células bacterianas, podendo atuar: **(c)** na inibição da transcrição e replicação do DNA, **(d)** no bloqueio da síntese de RNA, **(e)** na inibição das funções ribossomais e síntese proteica, **(f)** no bloqueio de proteínas chaperonas necessárias para dobramento adequado de proteínas e **(g)** inibição da respiração celular e indução da formação de ROS e dano à integridade da membrana da célula mitocondrial e efluxo de ATP e NADH e **(h)** na modificação do sítio de enzimas. Figura criada com o auxílio da ferramenta *BioRender*.

1.4 Seleção e optimização de PAMs

Diversas estratégias de desenho para desenvolver PAMs podem ser empregadas visando a optimização, seletividade e mecanismo de ação. A otimização de PAMs pode ser uma etapa crítica em seu desenho (Blondelle and Lohner, 2010). Isso envolve modificar a sequência e, consequentemente, estrutura do peptídeo para aumentar sua atividade antimicrobiana, minimizando sua toxicidade frente as células hospedeiras (Porto et al., 2018b). Diferentes técnicas de otimização, como substituições de aminoácidos, podem ser usadas para aumentar a atividade de peptídeos que demonstram algum tipo de bioatividade já relatada (Souza et al., 2015). Projetar peptídeos com especificidade para patógenos-alvo também podem ser alcançados por meio do uso de diferentes estratégias, como a seleção de peptídeos com base em sua atividade contra cepas bacterianas específicas ou o uso de métodos combinatórios para criar bibliotecas de peptídeos com diversas sequências (Holland and Goldberg, 1989; Blondelle and Lohner, 2010; Dong et al., 2014).

Diversos algoritmos vêm sendo utilizados para predizer a estrutura e função de peptídeos (Morgenstern et al., 2006). Para isso, ferramentas computacionais vêm sendo desenvolvidas seguindo duas principais estratégias, a de métodos empíricos e a de aprendizado de máquina (*machine learning*) (Porto et al., 2012). Algoritmos baseados em métodos empíricos podem ser qualitativos, e funcionam baseados na probabilidade de uma sequência de entrada (*input*) comparada com sequências de PAMs conhecidos em bases de dados para prever uma possível função (Wang et al., 2008). Os algoritmos de aprendizado de máquina podem ser baseados em inteligência artificial, buscando reconhecimento de padrões (Kotsiantis et al., 2007). Outro foco em especial tem sido dado ao modelo quantitativo de relação estrutura-ativa (QSAR) que utiliza descritores físico-químicos para prever a atividade biológica de peptídeos a partir da sequência primária de aminoácidos (Mitchell, 2014; Neves et al., 2018). De forma geral, estes algoritmos são fundamentados em um conjunto de informações conhecidas que podem prever a informação de saída com base na informação de entrada (Davies and Shamu, 2014). Dentre as diversas estratégias que podem ser aplicadas diversas técnicas ou abordagens computacionais.

Uma das técnicas computacionais que pode ser aplicada consiste em abordagens estocásticas, as quais visam a otimização de peptídeos através de processos aleatórios para realizar alterações. Outra abordagem se dá através de algoritmos evolutivos que geram sucessivas gerações de mutações e deleções na sequência buscando aprimorar as características que lhe conferem a atividade (Hiss et al., 2010; Kliger, 2010). Os algoritmos

evolutivos são chamados assim, pois sua otimização geralmente tende a ser inspirada na natureza, como uma estratégia de evolução propriamente dita (Holland and Goldberg, 1989). Geralmente, estes métodos compartilham o conceito de variação e seleção *in silico*, onde, de forma geral, através de um conjunto de informações (genes ou sequências, por exemplo), busca pontualmente por um "indivíduo" mais apto. Dessa forma, através da variação podem produzir descendentes (homólogos) com caráteres melhorados ou que favoreçam uma ação específica (Hiss et al., 2010).

PAMs podem ser considerados moléculas promissoras para aplicações de cunho terapêutico, visto que possuem especificidade, atividade biológica e toxicidade. Contudo, na maioria dos casos, diversos parâmetros devem ser levados em consideração para sua otimização e, embora não seja abrangente, uma variedade de métodos para a geração de novos candidatos a PAMs podem ser descritas, com ênfase em tecnologias computacionais (Blondelle and Lohner, 2010; Monte et al., 2012). Bibliotecas peptídicas possuem uma alta diversidade e tornaram-se instrumentos para a investigação e compreensão de sistemas biológicos em nível proteico. Estratégias de transcriptômica e proteômica, por exemplo, permitem que cada vez mais bancos de dados sejam preenchidos com diversas moléculas de potencial biológico (Monte et al., 2012). Neste contexto, algoritmos podem ser utilizados em bancos de dados visando à busca de novas moléculas bioativas (Holland and Goldberg, 1989; Porto et al., 2018a).

O desenvolvimento de PAMs como substâncias terapêuticas requer o cumprimento de certas características (Fjell et al., 2012). Em suma, os métodos de redesenho têm sido utilizados para melhor compreensão estrutural e funcional de sequências através das propriedades físico-químicas envolvidas nestes processos de otimização. Associados aos métodos citados acima outras metodologias têm sido aplicadas como ferramentas de predição da atividade antimicrobiana a partir das sequências dos peptídeos gerados, como por exemplo, o *Collection of Antimicrobial Peptides (CAMP*$_{R3}$) (Waghu et al., 2015). Este banco de dados permite que seus usuários prevejam o potencial que uma sequência possui para ser um PAM, através de quatro algoritmos, sendo eles máquina de vetores de suporte (SVM), conhecida como um robusto algoritmo utilizado como ferramenta de inteligência artificial (Schneider and Wrede, 1998); *random forest* (RF) composto por um grupo gerado aleatoriamente de árvores (Scornet et al., 2015); análise discriminante (AD) que descreve uma distribuição de probabilidade ao longo de um número potencialmente infinito de sequências (Eddy, 1998;

Chiang et al., 2004); e rede neural artificial (ANN) que pode emular a aprendizagem humana, raciocínio e tomada de decisão (Davies and Shamu, 2014).

Embora a capacidade antimicrobiana seja uma característica importante no desenvolvimento de terapêuticas baseadas em peptídeos, a ausência de toxicidade significativa é uma característica tão importante quanto uma boa atividade antimicrobiana (Irazazabal et al., 2016; dos Santos Cabrera et al., 2019). Nesse sentido, a identificação das propriedades físico-químicas que impulsionam as atividades biológicas dos PAMs é uma ferramenta importante no planejamento racional para a otimização desses peptídeos (Torres et al., 2019). Assim, a modulação de parâmetros físico-químicos, como carga, anfipaticidade, hidrofobicidade, momento hidrofóbico e propensão helicoidal, que em uma correlação complexa influenciam os processos que direcionam a interação peptídeo-membrana, tem permitido, em alguns casos, a melhoria de peptídeos mais seletivos (Dong et al., 2014; Porto et al., 2018b; Park et al., 2022).

1.5 Mastoparanos

Diante da diversidade de PAMs considerados uma alternativa aos tratamentos antibacterianos convencionais os venenos de artrópodes representam uma fonte em potencial para a prospecção de moléculas biologicamente ativas (Marr et al., 2006; Lai and Gallo, 2009). O veneno de vespas contém inúmeras substâncias bioativas com potenciais aplicações fisiológicas, farmacológicas e terapêuticas (Monteiro et al., 2009). O veneno das vespas pode variar em sua composição entre espécies, sendo que a maioria dos componentes do veneno da vespa são geralmente categorizados como proteínas de alto peso molecular, moléculas bioativas e peptídeos de baixo peso molecular (Monteiro et al., 2009; Dongol et al., 2014; dos Santos Cabrera et al., 2019). Esses peptídeos incluem mastoparanos, que podem ser diferenciados, de acordo com suas subfamílias, Vespinae e Polistinae (Dongol et al., 2014). Entre os peptídeos curtos derivados de veneno descritos até o momento, mastoparanos encontram-se bem caracterizados (Hirai et al., 1979; Moreno and Giralt, 2015).

Podemos citar os mastoparanos como exemplo de peptídeos multifuncionais. Em sua maioria, os mastoparanos caracterizam-se como peptídeos catiônicos, anfipáticos, geralmente organizados em α-hélice (ambiente dependente), sendo constituídos de 10 a 14 resíduos de aminoácidos (Nakajima et al., 1986; de Santana et al., 2022). Os mastoparanos possuem diversos mecanismos de ação, os quais podem estar diretamente relacionados ao tipo celular com o qual interagem. Quando ligados a mastócitos, estes peptídeos causam degranulação,

secreção de histamina e, consequentemente, vasodilatação (Konno et al., 2000; Ho et al., 2001). Em células do sistema imunológico colaboram na cascata de sinais, recrutando mais células para o local de inflamação, como por exemplo, indução do processo de quimiotaxia de neutrófilos e células T auxiliares (Argiolas and Pisano, 1984; Hancock and Diamond, 2000). Os mastoparanos podem ainda causar a ativação de fosfolipases A2, as quais aumentam lesões teciduais e edemas (Argiolas and Pisano, 1984). Em células sanguíneas há relatos de que mastoparanos possuem atividade hemolítica e citotóxica (Hirai et al., 1979; Tosteson et al., 1985; Higashijima et al., 1988; Konno et al., 2001). Outra atividade importante dessa classe de PAMs parece estar ligada a transdução de sinal via proteína G (Higashijima et al., 1988; Jones and Howl, 2006).

Ademais, membros dessa classe de peptídeos podem ser eficazes no combate a fungos, cepas bacterianas, incluindo atividades bacteriostáticas e bactericidas e ação antibiofilme (Konno et al., 2006; de Souza et al., 2011; Lin et al., 2011; Vila-Farres et al., 2012; de Azevedo et al., 2015; das Neves et al., 2019). Ainda que exista uma variedade de mastoparanos isolados de diversas espécies de vespas, podemos contar também com os mastoparanos modificados, tornando esta família de peptídeos atrativos para buscas de novas funções. Com base nisso, um número crescente de investigações tem se dedicado a melhorar não só a seletividade celular de mastoparanos como também suas atividades biológicas (Silva et al., 2017; Alvares et al., 2018). Além disso, ao otimizar o potencial antimicrobiano e imunomodulador de peptídeos semelhantes ao mastoparano, efeitos hemolíticos e citotóxicos podem ser reduzidos em células de mamíferos, tornando esses peptídeos atraentes para fins clínicos (de Lacorte Singulani et al., 2019; Oshiro et al., 2019).

Um modelo linguístico foi usado como base para o desenvolvimento de uma nova ferramenta de bioinformática, denominada algoritmo *Joker*, que executa a inserção de padrões na sequência modelo para gerar PAMs otimizados (Porto et al., 2018a). Dessa forma, Oshiro e colaboradores. (2019) utilizaram dois peptídeos bioinspirados em mastoparano-L (Hirai et al., 1979), denominados mastoparano-R1 e mastoparano-R4, obtidos através do algoritmo *Joker* (Figura 5), com o objetivo de potencializar e estender suas atividades antimicrobianas, bem como reduzir seus efeitos tóxicos para as células de mamíferos quando comparados ao peptídeo progenitor. Anteriormente, os peptídeos R1 e R4 foram capazes de inibir as cepas de *E. coli* (ATCC 25922, BL21, KPC+), cepas de *Staphylococcus aureus* (ATCC12600, MRSA) e *Pseudomonas aeruginosa* (PAO1 e PA14). Além disso, estes peptídeos foram capazes de erradicar os biofilmes pré-formados de *P. aeruginosa* (PAO1). Em adição, os peptídeos de

estudo foram ainda avaliados em relação a seu potencial hemolítico perante eritrócitos humanos, onde foi observado que, a 100 μM, mastoparano-L induziu mais de 45% de hemólise, enquanto R1 e R4 causaram menos de 10% (Oshiro et al., 2019). Com esses resultados em mente, no presente estudo, mastoparano-R1 e R4 foram avaliados em concentrações salinas fisiológicas, buscando entender como propriedades físico-químicas e estruturas poderiam afetar sua afinidade por membranas bacterianas e atividade antibacteriana.

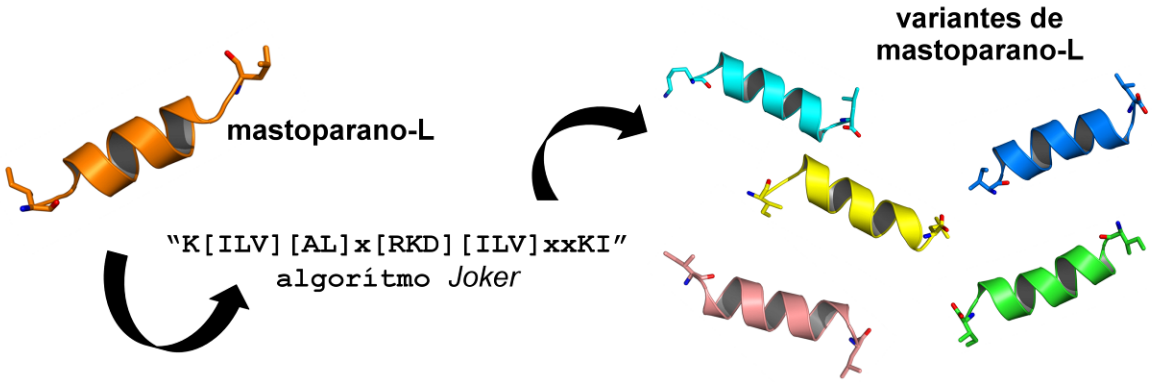

Peptídeos	Sequências	carga líquida
mastoparano-L	I N L K A L A A L A K K I L	+3
mastoparano-R1	K I L K R L A A K I K K I L	+6
mastoparano-R2	I K L L A R I A L K I K I L	+4
mastoparano-R3	I N K I A L R I L A K I I L	+3
[I^5R^8]*	I N L K I L A R L A K K I L	+4
mastoparano-R4	I N L K K L A A R I K K K I	+6

Figura 4. Variantes de mastoparano-L obtidos por desenho auxiliado por computador. Quatro variantes de mastoparano foram geradas usando o algoritmo *Joker* de acordo com o padrão α-helicoidal "K [ILV] [AL] x [RKD] [ILV] xxKI" e usando a sequência mastoparano-L como modelo. Os resíduos destacados em vermelho correspondem aos resíduos modificados nas variantes R1 a R4 em comparação com mastoparano-L. *A sequência projetada (INLKILARLAKKIL) apresentou correspondência completa com um mastoparano previamente descrito ([I^5R^8]) (Irazazabal et al., 2016), portanto, não foi utilizado. Figura adaptada de (Oshiro et al., 2019).

2. JUSTIFICATIVA

Ao longo dos anos o uso indiscriminado de antibióticos tem facilitado com que microrganismos desenvolvam respostas de resistência a antibióticos tornando-os, assim, patógenos considerados multirresistentes. As bactérias podem ser eficientes na síntese e no compartilhamento de genes envolvidos no desenvolvimento de mecanismos de resistência a antibióticos, levando a resultados negativos na clínica. Essa ineficiência pode estar relacionada à resistência intrínseca de uma bactéria a um antibiótico específico, o que pode ser explicado por sua capacidade de resistir à ação desse fármaco como resultado de características estruturais ou funcionais inerentes. Portanto, a disseminação dos fatores de resistência aos antibióticos, juntamente com o uso indevido desses medicamentos, tornou o desenho de medicamentos um amplo campo de pesquisa. Neste âmbito, os PAMs surgem como uma alternativa em resposta a esses patógenos, uma vez que são conhecidos por fazer parte do sistema imune inato de diversos organismos, atuando como primeira linha de defesa do hospedeiro. PAMs derivados de toxina de vespas são denominados, em sua maioria, mastoparanos. Mastoparanos são peptídeos de vespa de ocorrência natural que possuem potencial farmacêutico devido às suas propriedades multifuncionais, além disso estes peptídeos possuem diversos mecanismos de ação, porém passíveis de causar danos celulares, incluindo toxicidade contra células de mamíferos e hemólise de eritrócitos humanos. Dois peptídeos derivados do mastoparano-L, denominados mastoparano-R1 e mastoparano-R4, foram projetados por um algoritmo computacional denominado *Joker*, com o objetivo de potencializar a atividade antimicrobiana, bem como reduzir os efeitos tóxicos em células de mamífero. Mastoparano-R1 e R4 tiveram atividade antimicrobiana contra várias cepas, com os resultados notáveis obtidos contra cepas de *E. coli* (ATCC 25922, BL21) e *K. pneumoniae* carbapenemase gene positivo (KPC+). Os peptídeos foram avaliados quanto ao potencial hemolítico contra eritrócitos humanos e, a 100 μM, o mastoparano-L induziu mais de 45% de hemólise, enquanto R1 e R4 causaram menos de 10% de hemólise. Dada a importância desses achados, o presente estudo visou investigar o impacto das atividades antimicrobianas de R1 e R4 ao longo do tempo e em concentrações fisiológicas de sal. Além disso, buscamos obter informações sobre a relação entre suas propriedades físico-químicas, características estruturais e sua afinidade por membranas zwiteriônica e aniônica influenciando, assim, na sua seletividade celular.

3. OBJETIVO

3.1 Objetivo geral

Avaliar a atividade antibacteriana dos peptídeos mastoparano-R1 e R4 em concentrações salinas fisiológicas, buscando entender como as propriedades físico-químicas e estruturais podem afetar sua afinidade por membranas bacterianas.

3.1 Objetivos específicos

a. Sintetizar e purificar os peptídeos mastoparano-L, mastoparano-R1 e mastoparano-R4;
b. Avaliar o crescimento das cepas em meio caldo com 0 mM NaCl e 150 mM NaCl e estabelecer a padronização de unidades formadoras de colônias ($UFC.mL^{-1}$) para cada cepa em suas respectivas condições;
c. Determinar a cinética da concentração inibitória mínima (CIM) dos peptídeos mastoparano-L, R1 e R4 perante cepa susceptível e resistente de *E. coli* ao longo do tempo e determinar a concentração bactericida mínima (CBM) dos peptídeos frente essas cepas;
d. Realizar a caracterização da estrutura secundária dos peptídeos em diferentes ambientes miméticos através de Dicroísmo Circular (DC);
e. Realizar a caracterização da estrutura tridimensional dos peptídeos R1 e R4 em SDS através de Ressonância Magnética Nuclear (RMN);
f. Avaliar o potencial dos peptídeos se ligarem e romperem vesículas unilamelares simulando diferentes constituições de membranas, bem como observar a interação peptídeo-membrana avaliando o grau de associação, dissociação e afinidade dos peptídeos por membranas miméticas;
g. Avaliar o comportamento das estruturas de R1 e R4 nas mesmas constituições de membrana através de dinâmica molecular.

4. ARTIGO DE PESQUISA

Artigo 1, submetido na revista *FEBS Journal*:

Decifrando a estrutura e o mecanismo de ação dos peptídeos mastoparanos projetados por computador.

Resumo: Os mastoparanos são peptídeos catiônicos com propriedades farmacológicas multifuncionais. Mastoparanos-R1 e R4 foram projetados computacionalmente com base no mastoparan-L nativo de vespas e têm potencial terapêutico aprimorado para o controle de infecções bacterianas. Aqui avaliamos se esses peptídeos mantêm sua atividade contra cepas de *E. coli* em uma concentração fisiológica de sal. Descobrimos que os mastoparanos-R1 e R4 preservaram sua atividade nas condições testadas, incluindo atividades antibacterianas em concentrações salinas fisiológicas. A estrutura geral dos peptídeos foi investigada usando espectroscopia de dicroísmo circular em uma variedade de solventes. Não foram observadas alterações significativas na estrutura secundária (enrolamento aleatório em soluções aquosas e α-hélice em ambientes hidrofóbicos e aniônicos). As estruturas tridimensionais de mastoparano-R1 e R4 foram elucidadas por espectroscopia de ressonância magnética nuclear, revelando segmentos α-helicoidais anfipáticos para Leu3-Ile13 (mastoparano-R1) e Leu3-Ile14 (mastoparano-R4). Possíveis mecanismos de associação de membrana para mastoparano-R1 e R4 foram investigados por ressonância plasmônica de superfície e estudos de vazamento com bicamadas lipídicas sintéticas POPC e POPC/POPG (4:1). Mastoparano-L teve a maior afinidade para ambos os sistemas de membrana, enquanto os dois análogos tiveram associação mais fraca, mas melhoraram a seletividade para lisar membranas aniônicas. Essa descoberta também foi apoiada por simulações de dinâmica molecular, nas quais se descobriu que mastoparano-R1 e R4 têm maiores interações com membranas semelhantes a bactérias em comparação com modelo de membranas de mamíferos. Apesar de apresentarem algumas diferenças em seus perfis funcional e estrutural, o análogo de mastoparano-R1 se destacou com melhor atividade, maior potencial bacteriostático e seletividade para lise de membranas aniônicas. Este estudo reforça o potencial do mastoparano-R1 como candidato a medicamento.

The FEBS Journal

FEBS PRESS
science publishing by scientists

Deciphering the structure and mechanism-of-action of computer-designed mastoparan peptides

Journal:	*The FEBS Journal*
Manuscript ID	Draft
Manuscript Type:	Original Article
Date Submitted by the Author:	n/a
Complete List of Authors:	Oshiro, Karen; Universidade de Brasilia, Programa de Pós-Graduação em Patologia Molecular Freitas, Carlos Daniel; UFG, Laboratório de RMN, Instituto de Química Rezende, Samilla ; UCDB, S-Inova Biotech, Programa de Pós-Graduação em Biotecnologia Orozco, Raquel Marcela; UCDB, quigua0710@gmail.com Chan, Lai ; The University of Queensland Institute for Molecular Bioscience, Australian Research Council Centre of Excellence for Innovations in Peptide and Protein Science Lawrence, Nicole; The University of Queensland Institute for Molecular Bioscience, Australian Research Council Centre of Excellence for Innovations in Peptide and Protein Science Liao, Luciano; UFG, Laboratório de RMN, Instituto de Química Macedo, Maria Lígia; UFMS, Laboratório de Purificação de Proteínas e suas Funções Biológicas Craik, David; The University of Queensland, IMB Institute for Molecular Bioscience ; Cardoso, Marlon; Universidade de Brasília, Programa de Pós-Graduação em Patologia Molecular, Faculdade de Medicina; Universidade Católica Dom Bosco, S-inova, Programa de Pós-Graduação em Biotecnologia Franco, Octavio; Universidade Catolica de Brasilia, Biotecnologia e Ciencias Genomicas
Key Words:	

Deciphering the structure and mechanism-of-action of computer-designed mastoparan peptides

Karen G. N. Oshiro[a,b,c], Carlos D. P. Freitas[d], Samilla B. Rezende[b,c], Raquel M. Q. Orozco[b,c], Lai Y. Chan[e], Nicole Lawrence[e], Luciano M. Lião[d], Maria L. R. Macedo[f], David J. Craik[e], Marlon H. Cardoso[a,b,c,f *] and Octávio L. Franco[a,b,c*]

[a] Programa de Pós-Graduação em Patologia Molecular, Faculdade de Medicina, Universidade de Brasília, Brasília/DF, 70910900, Brazil;

[b] S-inova Biotech, Programa de Pós-Graduação em Biotecnologia, Universidade Católica Dom Bosco, Campo Grande/MS, 79117900, Brazil;

[c] Centro de Análises Proteômicas e Bioquímicas, Pós-Graduação em Ciências Genômicas e Biotecnologia, Universidade Católica de Brasília, Brasília/DF, 70790160, Brazil;

[d] Laboratório de RMN, Instituto de Química, Universidade Federal de Goiás, Goiânia/GO, 74690900, Brazil;

[e] Institute for Molecular Bioscience, Australian Research Council Centre of Excellence for Innovations in Peptide and Protein Science, The University of Queensland, Brisbane, QLD, 4072, Australia;

[f] Laboratório de Purificação de Proteínas e suas Funções Biológicas, Universidade Federal de Mato Grosso do Sul, Campo Grande/MS, 79070900, Brazil.

[*]**Corresponding author(s):** Prof. Marlon H. Cardoso (marlonhenrique6@gmail.com) and Prof. Octávio L. Franco (ocfranco@gmail.com).

ABSTRACT

Mastoparans are cationic peptides with multifunctional pharmacological properties. Mastoparans-R1 and R4 were computationally designed based on native mastoparan-L from wasps and have improved therapeutic potential for the control of bacterial infections. Here we evaluated whether these peptides maintain their activity against *Escherichia coli* strains under a range of salt concentrations. We found that mastoparans-R1 and R4 preserved their activity under the conditions tested, including having antibacterial activities at physiological salt concentrations. The overall structure of the peptides was investigated using circular dichroism spectroscopy in a range of solvents. No significant changes in secondary structure were observed (random coil in aqueous solutions and α-helix in hydrophobic and anionic environments). The three-dimensional structures of mastoparan-R1 and R4 were elucidated through nuclear magnetic resonance spectroscopy, revealing amphipathic α-helical segments for Leu3-Ile13 (mastoparan-R1) and Leu3-Ile14 (mastoparan-R4). Possible membrane-association mechanisms for mastoparan-R1 and R4 were investigated through surface plasmon resonance and leakage studies with synthetic POPC and POPC/POPG (4:1) lipid bilayers. Mastoparan-L had the highest affinity for both membrane systems, whereas the two analogs had weaker association, but improved selectivity for lysing anionic membranes. This finding was also supported by molecular dynamics simulations, in which mastoparan-R1 and R4 were found to have greater interactions with bacteria-like membranes compared to model mammalian membranes. Despite having a few differences in their functional and structural profiles, the mastoparan-R1 analog stood out with the highest activity, greater bacteriostatic potential, and selectivity for lysing anionic membranes. This study reinforces the potential of mastoparan-R1 as a drug candidate.

Keywords: mastoparan; antimicrobial peptide; structural biology.

INTRODUCTION

Diverse natural host defense peptides, including antimicrobial peptides (AMPs), are found in humans, animals, and plants, and most act against pathogens through interactions with their surfaces, including cell walls and plasma membranes [1, 2]. Naturally occurring AMPs have a broad range of sizes, stabilities, antibacterial potential, and toxicities towards mammalian cells [2]. Peptides, especially linear peptides, are generally highly flexible, allowing them to adapt to different environments and to interact with a wide range of molecular targets. For example, AMP secondary structures can change after membrane association [3]. They are considered promising candidates for neutralizing resistant pathogens because of their variety of mechanisms of action (*e.g.*, membrane-associated mechanisms or interaction with intracellular targets) [4-7]. Their ability to adapt to different environments (structural flexibility) can help AMPs to overcome the various defense mechanisms that microorganisms use to evade antimicrobial agents [5, 8]. Additionally, AMPs have a high degree of sequence variability and there are many different possible amino acid sequences with antimicrobial potential [2, 4, 9].

While the flexibility of AMPs is an important factor for their antimicrobial activity and explains their broad spectrum of action and ability to overcome microorganisms' defense mechanisms [3], it can also trigger undesired effects, including cytotoxicity, hemolysis, low bioavailability, proteolytic degradation, plasma instability, as well as their sensitivity to salt, since they interact electrostatically with microbial membranes [6]. Therefore, AMP design must consider other parameters apart from flexibility, including charge distribution, hydrophobic moment, and hydrophobicity [10].

Mastoparans are naturally occurring wasp peptides that have pharmaceutical potential due to their multifunctional properties [11, 12]. Two peptides derived from mastoparan-L,

named mastoparan-R1 and mastoparan-R4, were computer-designed in a previous study, with the aim of enhancing and extending antimicrobial activity, as well as reducing toxic effects on mammalian cells [13]. Mastoparan-R1 and R4 have antimicrobial activity against several strains, especially *Escherichia coli* (ATCC 25922, and BL21), and *Klebsiella pneumoniae* carbapenemase gene positive (KPC+). The peptides were evaluated for hemolytic potential against human erythrocytes, and at 100 μM mastoparan-L induced more than 45% of hemolysis, whereas R1 and R4 caused less than 10 % hemolysis [13]. With these results in mind, in the present study mastoparan-R1 and R4 were evaluated at physiological saline concentrations, seeking to understand how physicochemical properties and structures could affect their affinity for bacterial membranes and antibacterial activity.

RESULTS AND DISCUSSION

Peptide synthesis and target bacteria

Studies were conducted on synthetic samples of mastoparan-L, R1 and R4 with purity > 95 %. MALDI-ToF analyses confirmed ions with m/z of 1479.89 Da, 1636.14 Da and 1636.39 Da, corresponding to mastoparan-L, R1 and R4, respectively (Figure S1). Antimicrobial assays were conducted with two *E. coli* strains. Growth curves showed that the addition of sodium chloride (NaCl 150 mM) to the MHB growth medium did not interfere with the growth pattern of the *E. coli* ATCC 25922 and *E. coli* clinical isolate LACEN 9921447 strains (Figure S2). We obtained colony forming unit (CFU mL^{-1}) values from 5.5×10^{11} to 6.8×10^{11} CFU mL^{-1} in the presence and absence of salt, suggesting that the different ionic strengths did not significantly interfere with bacterial cell viability (Figure S2).

Antimicrobial kinetic activities for mastoparan-L, R1 and R4

The sensitivity of AMPs to salt is considered one of the major limitations in antimicrobial development as it is important to develop AMPs that maintain their antimicrobial activity at physiological salt concentration. In the present work, the minimal inhibitory concentration (MIC) values are expressed as a function of time (kinetics) in which the peptides can, or cannot, inhibit bacterial growth (bacteriostatic), thus preventing their proliferation and multiplication over the incubation time. Moreover, the bactericidal potential for each peptide was also evaluated as their ability to compromise the bacterial cell viability (minimal bactericidal concentration, MBC). For the susceptible *E. coli* ATCC 25922 strain we observed that mastoparan-L had MIC and MBC values of 16 µM in the absence of salt. By contrast, the activity of this peptide is abolished (up to 32 µM) in NaCl-supplemented medium, over 24 h of incubation. For mastoparan-R1 in the absence of salt, the lowest MIC value (2 µM) was recorded, whereas 4 µM was the necessary concentration to inhibit bacterial growth in salt conditions. Mastoparan-R4 showed bactericidal activity at 8 µM in the absence of salt but when evaluated in NaCl-supplemented medium, lost its inhibitory activity after 3 h, impairing its inhibitory and bactericidal potential (Figure 1.a-b). In summary, mastoparan-R1 showed the best performance in terms of MIC and MBC, both in the presence and the absence of 150 mM NaCl (Figure 1.a-d).

For the clinical isolate *E. coli* LACEN 9921447, mastoparan-L did not show bacteriostatic (MIC) or bactericidal (MBC) activity, even at the highest concentration tested (32 µM). However, mastoparan-R1 inhibited bacterial growth at 8 µM (MIC), and eradicated *E. coli* bacterial cells at 16 µM (MBC). For this same strain, but in the presence of salt, mastoparan-R1 showed improved antibacterial activity (MIC = 2 µM), thus supporting our data against *E. coli* ATCC, in which mastoparan-R1 showed the best performance under all conditions tested. For mastoparan-R4, similar behavior was observed at higher concentrations in the absence of

salt, with MIC and MBC values of 16 μM and 32 μM, respectively. With the addition of salt, the peptide showed improvement in the inhibitory and bactericidal activity (8 μM) (Figure 1.c-d). We conclude that mastoparan-R1 was the only peptide that preserved or improved its antibacterial activities against both *E. coli* strains in the absence and presence of 150 mM NaCl.

Characteristics such as helicity, hydrophobicity and hydrophobic moment can affect the salt-tolerance and antimicrobial activity of α-helical AMPs [14, 15]. Park and co-workers [14] tested different peptides with RLLR repeats, suggesting that structural instability may interfere with electrostatic interactions and, therefore, could be responsible for salt sensitivity in AMPs. A more recent study found that replacing lysine residues with other cationic residues could enhance antimicrobial activity under various salt concentrations, suggesting that the charge distribution along the peptide backbone may be relevant for salt sensitivity [16, 17].

In our previous study, we discussed whether lysine residues distributed along mastoparan sequences could boost their antimicrobial activity [13]. Interestingly, in the present study, mastoparan-R1 was the most potent and stable peptide in salt-supplemented medium (Figure 1). This may be explained by the positively charged amino acid residues distributed along this peptide structure, which follow the pattern K-2-KR-3-K-1-KK-2 (mastoparan-R1 full sequence: **K**IL**KR**LAA**K**I**KK**IL-NH_2), where the numbers indicate the spaces between the Lys and Arg residues. This pattern for mastoparan-R1 shows a wide distribution of positive charge throughout the peptide sequence (four sections of lysine and arginine residues). The same does not apply for mastoparan-L (3-K-6-KK-2 – two sections; mastoparan-L full sequence: INL**K**ALAALA**KK**IL-NH_2) and R4 (3-KK-3-R-1-KKK-1 – three sections; mastoparan-R4 full sequence: INL**KK**LAA**R**I**KKK**I-NH_2), which may explain the low performance of these two peptides compared to mastoparan-R1.

Apart from different ionic strengths, one of the major challenges in working with mastoparan-like peptides is their hemolytic and cytotoxic effects on mammalian cells. Thus, here the hemolytic activities were evaluated against mice erythrocytes at a maximum concentration of 128 μM. Mastoparan-L showed a higher hemolytic effect (21.6 %) than its analogs, which were not hemolytic at the same concentration (Figure S3). Associating these data with those previously published, we can infer that mastoparan-L consists of a non-specific cytolytic peptide, whereas mastoparan-R1 and mastoparan-R4 have better selectivity for microbial cells [13]. Some studies claim that peptides with greater hydrophobicity can cause lysis of neutral zwitterionic membranes, thus explaining more pronounced hemolytic effects [18, 19]. Previously, the physicochemical properties obtained through the HeliQuest server [20] showed the parent peptide mastoparan-L has a higher rate of hydrophobicity (57.6 %) and a lower hydrophobic moment (0.398) compared to its analogs mastoparan-R1 (36.9 % hydrophobicity; 0.775 hydrophobic moment) and R4 (20.4 % hydrophobicity; 0.472 hydrophobic moment). Characteristics such as high amphipathicity may favor the interaction of the peptide with cell membranes. Therefore, these characteristics are intrinsically involved in the cytolytic character of mastoparan-L [13, 21, 22].

Structural Analysis

CD spectroscopy was used to characterize the overall structure of the parental peptide, mastoparan-L, and its analogs in water, 10 mM KH_2PO_4 (pH 7.4) buffer, 50 % TFE and 75 - 100 mM SDS, at 25 °C. In general, the peptides had CD signatures characteristic of random coiled structures in water and buffer. Only mastoparan-L revealed a slight α-helix profile in 10 mM KH_2PO_4 (pH 7.4) In hydrophobic (50 % TFE) and anionic environments (75 and 100 mM SDS), all the peptides showed strong α-helical signatures (Figure 2), the helical contents in

SDS-containing solutions presented only slightly changes, ranging from 69 – 73 % for mastoparan-L, 36 – 45 % for mastoparan-R1, and 52 – 47 % for mastoparan-R4. (Table S2).

Helical structure and amphipathicity of AMPs influence their antimicrobial activity and contribute to a membrane-active mechanism [11, 14]. However, the importance of structural stability of α-helical AMPs still needs to be clarified. For instance, some studies report that the ability of a peptide to adopt a well-defined amphipathic α-helix could be strongly correlated with its antimicrobial activity [16, 23]. Bearing this in mind, further structural experiments (*e.g.*, nuclear magnetic resonance (NMR) and molecular dynamics (MD)) were carried out in the present work to examine this hypothesis.

The structures of mastoparan-R1 and R4 were elucidated through NMR spectroscopy in 75 mM SDS-d_{25}. ^{1}H resonance assignments were obtained by analysis of TOCSY and NOESY spectra, as reported by Wuthrich [24]. The structural statistics for low-energy structures are summarized in Table 1. The ^{1}H-^{1}H NOESY spectra revealed a total of 200 distance restraints for mastoparan-R1. The 200 (mastoparan-R1) or 166 (mastoparan-R4) distance restraints and 22 dihedral angles restraints predicted by the DANGLE algorithm in CcpNMR Analysis program were employed as data input in the ARIA protocol. We performed the structural calculation for 200 structures for each iteration, it0 until it8, starting with an extended structure until the MDSA protocol for energy minimization and to determine the secondary conformation of the peptide. The 10 lowest structures of the last iteration (it8) were refined in water, resulting in 10 structures used for the structure ensemble of mastoparan-R1 and R4.

Secondary structure was predicted by *phi* (ϕ) and *psi* (ψ) angles obtained using the DANGLE algorithm, by means of the experimental chemical shift of $^{1}H_{N}$, $^{1}H_{\alpha}$, $^{13}C_{\alpha}$ and $^{13}C_{\beta}$. Other relevant NMR data are summarised in Figure S4.a, including NOE connections. For mastoparan-R1, medium sequential NOE connectivities (Hα-HN and HN-HN) were observed

for almost the entire peptide sequence, except for H_{α}-HN *i, i*+1 for residues Ile2, Leu3, Ile13 and Leu14, and sequential HN-HN NOEs for residues Lys1, Ile10, Ile13 and Leu14. Sequential NOE connectivity (H_{β}-HN *i, i*+1) was observed only between residues Lys4H_{β}-Arg5H and Leu6H_{β}-Ala7H. Short distance (HN-HN *i, i*+2; H_{α}-HN *i, i*+3; and H_{α}-H_{β} *i, i*+3) and medium distance (H_{α}-HN *i, i*+4) NOEs characteristic of α-helix were observed for mastoparan-R1, as shown in Figure S4.a. Short distances (HN-HN *i, i*+2) were observed between residues Ala7H-Lys9H, Ala8H-Ile10H and Ile10H-12LysH_{α}. NOE connections (H_{α}-HN *i, i*+3) were observed among residues Lys4H_{α}-Ala7H, Ala7H_{α}-Ile10H, Ala8H_{α}-Lys11H, Ile10H_{α}-Ile13H and Lys11H_{α}-Leu14H. Similarly, (H_{α}-H_{β} *i, i*+3) connections were observed between residues Ile2H_{α}-Arg5H_{β}, Lys4H_{α}-Ala7H_{β}, Ile10H_{α}-Ile13H_{β} and Lys11H_{α}-Leu14H_{β}. Finally, medium distances (H_{α}-HN *i, i*+4) were observed for Ala6H_{α}-Ile10H and Ile10H_{α}-Leu14H.

Secondary chemical shifts (SCS) of the α and β carbons of mastoparan-R1showed positive and negative values, respectively (except for the α-carbon of Leu14, which showed a large negative value). The SCS values for α-hydrogens were negative. SCS values represent the difference in the chemical shift of $^{13}C_{\alpha}$, $^{13}C_{\beta}$ and $^{1}H_{\alpha}$ resonances relative to random coil values, and the positive values for the α-carbons and negative values for the β-carbons and α-hydrogens indicates an α-helical structure (Table S3). Structure prediction suggests an α-helix for mastoparan-R1 between Leu3 to Ile13, as can be observed in the secondary structure chart in Figure S4.a. The dihedral angles ϕ and ψ generated by Dangle in the CcpNmr analysis program were classified as good and consistent, since the values of dihedral angles for each residue were found in just one island of the Ramachandran plot, all in allowed regions, indicating excellent stereochemistry (Figure S4.a).

For mastoparan-R4, sequential NOE connectivity *i, i*+1 (H_{α}-HN and HN-HN) was observed for almost the entire peptide sequence, except for H_{α}-HN *i, i*+1 for residues Lys5 and

Ala8, and for sequential HN-HN for residues Ile1, Asn2, Leu6, Ile10 and Lys11. Sequential NOE connectivity (H_β-HN *i, i*+1) was observed between residues Leu3H_β-Lys4H, Lys4H_β-Lys5H, Lys5H_β-Leu6H, Leu6H_β-Ala7H, Ala7H_β-Ala8H, Arg9H_β-Ile10H, Lys12H_β-Lys13H and Lys13H_β-Ile14H. Short distance (HN-HN *i, i*+2; H_α-HN *i, i*+2 and H_α-HN *i, i*+3) and medium distance (H_α-HN *i, i*+4) NOEs characteristic of α-helix secondary structure were observed for mastoparan-R4 as shown in the chart NOE connectivity (Figure S4.b). Short distances (HN-HN *i, i*+2) were observed only for residues Lys5H-Ala7H and Ala7H-Arg9H. NOEs connections (H_α-HN *i, i*+2 and *i, i*+3) were observed among residues Ala8H_α-Ile10H, Ala7H_α-Ile10H, Ala8H_α-Lys11H and Ile10H_α-Lys13H. Finally, medium distances (H_α-HN *i, i*+4) were observed only for the connection Leu3H_α-Ala7H. Moreover, for mastoparan-R4, SCSs of all α and β carbons showed positive and negative values, respectively (except for α carbon of residues Asn2 and Ile10, which showed intense negative deviation). The SCSs of α-hydrogens show negative values, except for the α-hydrogen of Asn2, which has a positive value. These data indicate an α-helical structure (Table S4). Structure prediction suggested an α-helix for mastoparan-R4 between Leu3 to Lys13, as can be observed in the secondary structure chart (Figure S4.b).

As observed in Figure 3, the structural calculation shows that the peptides adopted an α-helical conformation between residues Leu3-Ile13 (mastoparan-R1) and Leu3-Ile14 (mastoparan-R4) for the lowest energy structure in 75 mM of SDS-d25 micelles. Figure 3 shows the superposition of the 10 lowest energy structures for mastoparan-L (PDB: 6DUL), previously determined by our group using a similar protocol (Figure 3.a), mastoparan-R1 (Figure 3.b) and mastoparan-R4 (Figure 3.c). The structural statistics are summarized in Table 1. Additional validations, including clash score, Ramachandran outliers and side-chain outliers, are available in the Protein Data Bank (PDB) under PDB IDs: 8EP5 and 8ERU for mastoparan-R1 and

mastoparan-R4, respectively. Previously, we reported that mastoparans-L, R1 and R4 have an environment-dependent structure, whereby in more hydrophobic conditions (30% TFE, 25 mM SDS, POPC and POPC/POPG) they adopt an α-helix secondary structure, while in an aqueous environment (water and 10 mM KH_2PO_4 buffer) mastoparan-R1 and R4 reduced their helix percentages in relation to the mastoparan-L analog [13]. Here we observed similar behavior, and through the NMR results we found that mastoparan-R1 and R4 adopt an α-helix structure; other studies have also reported that peptides of this class have a tendency for this environment-dependent structural organization [11, 12, 25, 26].

Factors such as sequence symmetry, residue distribution, flexibility and secondary structure may be beneficial to increase antimicrobial activity and decrease cytotoxicity, improve selectivity and stability [15, 23, 27, 28]. Mohanram et al.,[29] designed an AMP called RR12 with cationic and hydrophobic characteristics with 12 residues distributed in such a way as to obtain a well-defined polar and non-polar face, demonstrating a predominant amphipathic character and two parent peptides with specific modifications, namely the substitution of Arg5 by Trp5 and another which substitution of Trp5 by Ile7 [29]. With these modifications, they verified that the presence of the Arg5 residue on the cationic surface helix has the potential to confer salt resistance through the formation of multiple hydrogen bonds and/or ionic interactions with the outer and inner membranes of bacteria [29].

More recently, Wu and co-workers,[30] investigated how the structural properties of RR12 could interact with membranes and the structure attached to membrane mimetic micelles. RR12 demonstrated disordered folding for a well-defined α-helix structure when interacting with SDS micelles [30]. The structure orientation concentrated from residue Arg2 to Ile7 with the C-terminus more exposed to the solvent, and they stated that the helix segment could contribute to bactericidal activity [30]. Similarly, we observed that the short and medium

distance connections observed in mastoparan-R1 may allow a more relaxed folding of the structure in SDS when compared to mastoparan-R4, which, nevertheless also folds in α-helices, presents lower connectivity of the short-distance intra-residual.

AMP structures, including those of mastoparan peptides, may be influenced by factors such as specific residue position along the helix, amino acid composition, and physicochemical characteristics, which can affect their selectivity for microbial and mammalian cell membranes. This selectivity is crucial for developing AMPs as potential therapeutics [31]. Some AMPs, mainly those derived from animal toxins, may require modifications to improve their selectivity, while others possess optimal selectivity [32, 33]. Therefore, the structure of AMPs plays a key role in determining their mechanism of action and selectivity, making it an important consideration for new antimicrobial agents' development.

Insights about membrane-associated mechanisms of action

SPR was employed to evaluate peptide-lipid binding affinities for the parent peptide mastoparan-L and analogs R1 and R4 were evaluated for their binding to model phospholipid bilayers, including zwitterionic POPC (pure) which is included to represent the neutral outer surface of healthy mammalian cells, and anionic POPC/POPG (4:1), included to represent the negatively charged surface of bacterial membranes. (Figure 4.a-b). Mastoparan-L had the highest affinity for both POPC and POPC/POPG (4:1) bilayers, followed by mastoparan-R1 and R4. Each of the peptides showed higher affinity binding for the negatively charged POPC/POPG (4:1) bilayers compared to the neutral POPC bilayers, at a range of peptide concentrations (0 – 32 μM). Rapid association and dissociation rates were observed in all cases, but mastoparan-L was observed to remove lipids from the SPR L1 chip (commencing during association and shown in Figure 4.a for POPC/POPG (4:1)), suggesting detergent-like

properties at higher concentrations. This phenomenon has previously been observed for other hydrophobic membrane-disruptive peptides [34].

Membrane-disruptive properties were examined by measuring peptide-induced leakage of CF from LUVs, comprised of POPC or POPC/POPG (4:1). Dose-response curves (Figure 4.c) show that mastoparan-L lysed neutral and anionic vesicles at all concentrations tested (down to 0.01 μM), and like control membrane-disruptive peptide melittin, did not show any difference in the amount of peptide required to lyse 50 % of neutral compared to anionic vesicles (LC50). The LC50 values were at least ten-fold higher for mastoparan-R1 and R4 compared to parent mastoparan-L, which is consistent with the differences in lipid-binding affinities observed for analogues with SPR. Also, mastoparan-R1 lysed POPC/POPG (4:1) vesicles at ~3-fold lower concentration than POPC vesicles, which is consistent with the lower hemolytic potential observed for this peptide.

NMR studies revealed well-defined a-helical structures in the presence of 75 mM and the CD data show that these peptides have environment-dependent structures. When considering membrane systems, it is thus relevant to evaluate the structural arrangements of the peptides, aimed at better characterizing their mechanisms of action. We observed that mastoparan-R1 and R4 tend to organize themselves in a well-defined α-helix, with different flexibility levels depending on the environment in which they are inserted. Previously, Oshiro co-workers[13] reported the α-helix signatures of mastoparan-R1 and R4 in 30 % TFE-*d3* through two-dimensional NMR experiments, with α-helical segments from residues 4 to 13 and from residues 4 to 12 for mastoparan-R1 and R4, respectively. Mastoparan-L exhibited consistently higher intrapeptide hydrogen bonds than its analogs. Moreover, mastoparan-R1 had the lowest number of residues shielded from the solvent. These findings reinforce the hypothesis that mastoparan-R1 is the most structurally flexible peptide studied here, which is

supported by NMR temperature coefficient data [13]. The greater the amide proton shift with temperature, the lower the number of intrapeptide hydrogen bonds, thus influencing peptide flexibility. Overall, the flexibility patterns observed in our previous and current study reveal the ability of these peptides to change their conformation in response to external stimuli, which may include changes in pH, and ionic strength.

Chou and co-workers,[27] used variable physicochemical characteristics, sequence length, and composition that included the amino acids Gly, Lys, Leu, and Trp, along with modified residue distribution. They confirmed that the symmetrical and rational helical distribution of these parameters indicates a promising strategy for designing AMPs that are more selective and specific to pathogens [27]. Of the 12 generated peptides (F1-F12), F1 and F4 stood out with promising activities against gram-negative bacteria, low toxicity, low sensitivity to salt and tendency for helical formation in a mimetic membrane environment [27]. Moreover, the investigation of how AMPs interact with bacterial membranes and the associated antimicrobial performance can contribute to the design of new AMPs, minimizing toxicity to healthy mammalian cells and maximizing their actions against human pathogens [18]. Numerous studies have shown that changes in physicochemical properties, including increased hydrophobic moment and decreased overall hydrophobicity, may be responsible for cell selectivity [11, 35].

In addition to the SPR and leakage studies with model phospholipid bilayers, MD simulations over 1 μs were carried out to better understand at atomic level the structural preferences and interactions between mastoparan-R1 and R4 and pure POPC and POPC/POPG (4:1) bilayers. The simulations were carried out with the structures with the lowest free energy solution NMR structures for R1 and R4 in the presence of SDS micelles. In addition, the systems were programmed at 150 mM NaCl ionic strength similar to the antimicrobial assays,

as well as SPR and leakage experiments. In the simulations with POPC, we observed that the peptides tend to lose their initial α-helical structure, and that mastoparan-R1 had a greater variation in the RMSD compared to mastoparan-R4 (Figure S5.a-e). Moreover, the root mean square fluctuation (RMSF) analyses showed that mastoparan-R1 has a larger deviation at the terminal regions, N-terminal (1 – 3) and C-terminal (11 – 14), whereas mastoparan-R4 has a smaller fluctuation, except for the C-terminal region at position 12 (Figure S5.b-f). Moreover, mastoparan-R1 has a greater variation in its solvent accessible area (SASA) from 0.2 μs of the MD simulation, whereas mastoparan-R4 was more stable over 1 μs of MD simulations (Figure S5.c-g). Finally, mastoparan-R1 had a greater deviation from its center of mass, with radius of gyration values ranging from 0.8 to 1.4 nm, indicating that this peptide adopts a more extended structural profile compared to mastoparan-R4 (stable radius of gyration in both membrane constitutions) as shown in Figure S5.d-h. For the simulation in POPC/POPG (4:1) bilayers, mastoparan-R1 had a higher deviation in its trajectory than peptide R4, although the peptides presented similar residue fluctuations (mainly at the C-terminus), surface accessible solvent area and radius of gyration values (Figure S5.a-e).

In the partial density maps, we observed that N-terminal region of mastoparan-R1 attaches to the POPC bilayer at the at the end of the MD simulation (Figure 5.a), whereas mastoparan-R4 is completely detached from the membrane in the last 0.1 μs of the simulations (Figure 5.e). In both cases, the peptides had a higher number of hydrogen bonds with water molecules than with POPC phospholipids (Figure 5.b). By contrast, the partial density maps for mastoparan-R1 and R4 showed that these peptides fully penetrate the POPC/POPG (4:1) bilayer, with greater interactions in the last 0.1 μs of the simulations (Figure 5.c-d). Moreover, the number of hydrogen bonds for mastoparan-R1 and R4 were higher in contact with POPC and POPG phospholipids than for the POPC bilayer (Figure 5.a-b).

For mastoparan-R1 in POPC/POPG (4:1), at the end of 1 μs of MD simulations, we observed that most of the atomic interactions occur between Lys1, Leu3, Arg5, Lys9, 11 and 12 and the bilayer phospholipids (Table S6). For mastoparan-R4 in the same membrane constitution, the peptide adopted an α-helical structure in contact with the phospholipids. Moreover, the interactions involved residues Ile1, Asp2, Leu3, Arg9 and Lys12. More specifically, Ile1 established four interactions, including one hydrophobic interaction, whereas Arg9 was involved in six hydrogen bonds (Table S6). These data reveal the preference of both peptide analogs for POPC: POPG (4:1) membranes, demonstrating binding specificity.

Here, we observed that mastoparan-R1 and R4 have antibacterial properties, acting against susceptible and clinical isolates resistant. Mastoparan-R1 showed the best antibacterial performance in our biological assays (2 μM – 16 μM), including under physiological salt conditions. Antibacterial data associated with observations of electrostatic interaction with negatively charged membranes suggest that the analogues do not have membrane disruption as their main mechanism of action. The analogs are 10 times less disruptive than the parent, mastoparan-L, but their membrane interactions appear more selective for lysing anionic membranes. Mastoparan-R1 had a different functional and structural profile compared to the parent mastoparan-L, and demonstrated superior antimicrobial activity at lower concentrations, stronger bacteriostatic and bactericidal potential. Furthermore, mastoparan-R1 maintained its activity in the presence of 150 mM NaCl, had the most potent activity toward a clinical isolate of *E. coli* under these conditions, and importantly had a lower hemolytic potential. All these advantages may be explained by the more flexible α-helical structural scaffold observed for mastoparan-R1 compared to its parent peptide. Moreover, by comparing these structural features with the observed functional properties for this peptide, including potency, bacteriostatic and bactericidal effect, and selective binding and lysis of anionic membranes, it

is possible to identify structural and physicochemical determinants that contribute to the peptide's activity and mechanism of action. These findings highlight mastoparan-R1 as a promising candidate for antimicrobial therapy, which could be further used as a template molecule for further AMP optimization.

MATERIAL AND METHODS

Chemical synthesis of mastoparan-L, R1 and R4

Mastoparan-L, R1 and R4 were purchased from Peptide 2.0 Incorporated (USA), which synthesized the peptides through F-moc (9-fluorenylmethyloxycarbonyl) protected solid phase methodology and verified as > 95% pure.

Minimal inhibitory concentration kinetics assay

The MICs for mastoparan-L, R1 and R4 were evaluated against *E. coli* (ATCC 25922) and *E. coli* ((clinical isolate) LACEN 9921447) provided by LACEN - *Laboratório Central de Saúde Pública, Brasília – DF*, Brazil. The bacterial strains were plated on Mueller-Hinton agar plates (MHA) and incubated at 37 °C for approximately 18 h. Three colonies isolated from each bacterium were separately inoculated in 5 mL of Mueller-Hinton broth (MHB), under two salt conditions (0 mM NaCl and 150 mM NaCl) and incubated at 37 °C, overnight, at 200 rpm. Bacterial growth was measured in a spectrophotometer at 600 nm using 100 µL of each replicate. MIC assays were performed according to the protocol established by the Clinical & Laboratory Standards Institute (CLSI) using the 96-well microplate dilution method [36]. Three biological replicates were organized in the microplates at a bacterial concentration of 5×10^5 CFU mL^{-1}. The peptides were tested at concentrations ranging from 0.5 to 32 µM. The antibiotic meropenem was used as positive control at the peptide concentrations, and the bacterial

suspension (5×10^5 CFU mL^{-1}) in MHB supplemented or not with 150 mM NaCl was used as negative control. The microplates were incubated at 37 °C in kinectics cicles conditions (49 spot readings), for 24 h. The readings were recorded in a microplate reader at 600 nm, at 30 min intervals. To obtain the minimum bactericidal concentrations (MBC), 10 µL microdroplets were plated in MHA medium pipetted from the wells in which MICs were detected. After 24 h of incubation, the Petri dishes were evaluated for CFUs, and no bacterial growth was interpreted as bactericidal activity.

Hemolytic Assays

Hemolytic assays were evaluated against murine erythrocytes, in accordance with the Committee on Ethics in the Use of Animals (CEUA) of *Universidade Católica Dom Bosco* (UCDB - Brazil) (CEUA/UCDB number: 015/2018). Blood was collected by cardiac puncture from a healthy animal and transferred into tubes containing phosphate-buffered saline (PBS). Blood samples were centrifuged at 4,000 rpm for 1 min. The supernatant was discarded, and the blood cells were washed three times in 1 mL PBS. Solutions of 0.25 % erythrocytes were prepared in PBS. The stock of peptides was prepared from serial dilutions, where the initial concentration used was 100 µM (highest concentration per well in 96-well microplates). PBS was used as a negative control, and 1 % Triton X-100 (100 % lysis of erythrocytes) was used as positive control. Assays were performed on 96-well polypropylene plates at 37 °C for 1 h. After that, the plates were centrifuged at 1,000 rpm for 5 min and the supernatants (from 100 µM wells) transferred to 96-well flat-bottom plates. Absorbances were measured at 415 nm. Three independent experiments were performed.

Circular Dichroism Spectroscopy

The characterization of the overall structures of mastoparan-L, R1 and R4 was performed in ultrapure water, 10 mM KH_2PO_4 (pH 7.4), 50 % (v/v) 2,2,2-trifluoroethanol (TFE), and 75 - 100 mM dodecyl sodium sulfate (SDS), at 25 °C. CD measurements were carried out on a JASCO spectropolarimeter (J-1100) equipped with a Peltier temperature controller, using wavelengths from 185 to 260 nm and five scanning accumulations for each sample, using cuvettes of 0.5 mm path length at a scan speed of 50 nm min^{-1}. The resolution was 0.1 nm, with a 1 s response time and five scan accumulations for each sample. Measurements in solvents were conducted at a peptide concentration of 50 µM. All spectra were smoothed using the Jasco Fast Fourier algorithm and baseline corrected.

Nuclear Magnetic Resonance (NMR) Spectroscopy

Mastoparan-L (INLKALAALAKKIL-NH_2) was not studied by NMR as there are already two solution NMR structures deposited in the Protein Data Bank (PDB IDs: 1D7N and 7DUL). NMR spectroscopy for mastoparan-R1 (KILKRLAAKIKKIL-NH_2) was performed using 75 mM of deuterated SDS (SDS-d_{25}), pH 4.0, and the peptide stocks were prepared at 1.5 mM in 500 µL of H_2O/D_2O (90/10, v/v). NMR spectroscopy for mastoparan-R4 (INLKKLAARIKKKI-NH_2) was performed using 75 mM of deuterated SDS (SDS-d_{25}), pH 3.98, and the peptide stocks were prepared at 1.5 mM in 350 µL of H_2O/D_2O (90/10, v/v). All spectra were recorded at 298 K on a Bruker Avance III 500 spectrometer equipped with a 5 mm broadband inverse (BBI) probe head. ^1H-^1H TOCSY experiments were acquired using the *dipsi2gpph* [37, 38] pulse sequence with 56 transients of 4096 x 1024 points (F2, F1) and spinlock mixing time of 70 ms. The ^1H-^1H NOESY spectra were acquired using the *noesygpphw5* [39] pulse sequence with 48 transients of 4096 x 1024 points and mixing time of 200 ms. Water signal suppression was achieved by applying Watergate W5. ^1H-^{13}C HSQC

experiments were acquired using the *hsqcetedetgp* [40] pulse sequence with 88 transients of 4096 x 512 points and 1.5s relaxation delay (d1). All 2D NMR data were processed using Bruker TopsSpin 3.6.3 and analyzed using CcpNMR Analysis 2.5.2 [41, 42]. The Wuthrich method [24] was used for assignment of the spin systems of the ^{1}H resonances observed in TOCSY and NOESY spectra. DSS-d_6 3-(trimethylsilyl)-1-propanesulfonic acid-d6 sodium salt at 0.05 % was used as internal reference. ^{1}H-^{13}C HSQC heteronuclear spectra were used in assisting with the assignment of spin systems and confirmation for the assignment of chemical shifts.

Structure determination

Determination of the three-dimensional structures was done using ARIA [43-46] software version 2.3 with the compilation of the CNS program [47] and by molecular dynamics simulated annealing protocol (MDSA) [48]. Peak intensities/volumes, classified as strong, medium, and weak, obtained by NOE peak correlations from the NOESY spectra, were semi-quantitatively converted into distance restraints using 1.72, 3.2 and 8.0 Å as lower limit, reference distance and upper distance limit, respectively. Dihedral angle restraints were determined from the chemical shifts of ^{1}HN, ^{1}Hα, ^{13}Cα and ^{13}Cβ by using the DANGLE algorithm [49] from CcpNMR Analysis software [42]. Both distance and dihedral angle restraints were employed as data input from the CCPN [41] in the calculation in ARIA 2.3 software. Two-hundred structures were generated for each iteration in a protocol of 8 iterations and, for the last iteration, the refinement of structures was performed using the water refinement protocol [50, 51], resulting in 10 refined structures. Structures were visualized using the PyMOL [52] and MOLMOL program [53]. The 10 lowest energy conformations were selected to represent the structures' ensemble. The structural analysis was performed by packages

PROCHECK [54], WHAT IF [55] and MolProbity [56] integrated with ARIA software. The quality of the structures was analyzed based on the values of root mean square deviation (RMSD), stereochemical quality using PROCHECK, the Ramachandran diagram and ProSA (Protein Structure Analysis), which indicates the peptide's fold quality [57]. Furthermore, the minimum total energy was required by the structures in calculation. Electrostatic potential calculation was measured for the lowest energy three-dimensional structures resolved by NMR. Conversion of .pdb files into .pqr files was performed on the PDB2PQR server using the AMBER force field. Grid dimensions for calculating Adaptive Poisson−Boltzmann solver (APBS) were also determined by PDB2PQR [58]. Solvation potential energy was calculated in APBS [59]. Surface visualization was performed using the APBS plugin for PyMOL [52].

Preparation of small (SUV) unilamellar vesicles

Liposomes were prepared with the synthetic lipids 1-palmitoyl-2-oleoyl-sn-glycero-3-phosphocholine (POPC) (1:1) and POPC/1-palmitoyl-2-oleoylphosphatidylglycerol (POPG) (4:1) from Avanti Polar Lipids. Lipids were solubilized in chloroform and mixed in the quantities required to prepare the desired lipid mixtures and small unilamellar vesicles (SUVs; diameter of 50 nm) were prepared in a HEPES buffer (10 mM HEPES containing 150 mM NaCl, pH 7.4) by extrusion method, as previously described [60]. SUVs were used for SPR studies to facilitate bilayer deposition on the chip surface [60].

Surface Plasmon Resonance (SPR)

The binding affinities of the peptides for model membranes composed of pure POPC and POPC/POPG (4:1) were measured using SPR. Solutions were freshly prepared and filtered (0.22 μm pore size). L1 sensor chips with a BIAcore 3000 system (BIAcore, GE Healthcare)

were used for analysis. SUVs were prepared by freeze-thaw fracturing and sized by extrusion. Vesicle suspensions were deposited on an L1 chip over 40 min at a flow rate of 2 μL min^{-1} to allow the vesicles to bind, fuse and form a stable lipid bilayer. Loosely bound vesicles were removed with a short pulse of 10 mM sodium hydroxide (36 s at 50 μL min^{-1} flow rate). Running buffer was flowed over the lipid bilayer to ensure signal stabilization, before injection of peptide samples. The association of the peptide sample to the lipid bilayer was evaluated by injection for 180 s at flow rate of 5 μL min^{-1}, and the dissociation was followed for 600 s, at the same flow rate. The L1 chip was regenerated after each injection cycle, by an injection of 3-[(3-cholamidopropyl)dimethylammonio]-1-propanesulfonate (CHAPS) (5 μL min^{-1}, 60 s), followed by an injection of 10 mM sodium hydroxide in 20 % methanol (w/w) (50 μL min^{-1}, 60 s) and, to finish, an injection of 10 mM sodium hydroxide (50 μL min^{-1}, 36 s). All measurements were conducted at 25 °C. 10 mM HEPES pH 7.4, containing 150 mM NaCl was used as the running buffer and to prepare samples and lipid vesicles cited above. The peptide samples were prepared at seven different concentrations, starting from 32 to 0.5 μM following 2-fold dilution steps. Running buffer was included as the 0 μM sample. The lipid deposited onto the chip surface is dependent on the lipid mixture; therefore, the response units were converted into peptide to lipid ratio (mol/mol).

Vesicle leakage

Synthetic lipids POPC and POPC/POPG (4:1) were prepared in chloroform, and a lipid film was prepared by drying under nitrogen then in a vacuum desiccator for > 2 h. Lipid vesicles were prepared using repeated freeze/thaw cycles followed by extrusion of 1 mM lipid mixtures in 50 mM carboxyfluorescein (CF), 10 mM HEPES, 150 mM NaCl, pH 7.4. Large unilamellar vesicles (LUVs) were prepared by extrusion through membranes with 100 nm pores. CF-loaded

vesicles were purified using a 10 mL gel filtration column prepared from pre-swollen Sephadex G-50 beads in 10 mM HEPES, 150 mM NaCl, pH 7.4. The lipid concentration of the purified vesicles was determined against a standard curve prepared with Ferro thiocyanate Reagent (100 mM $FeCl_3 \times 6H_2O$, 400 mM NH_4SCN; Stewart assay). Serial dilutions of peptide were incubated with LUVs containing 5 µM lipid in black 96-well plates. The fluorescence intensity (FI; λex = 489 nm, λem = 515 nm) was measured using a Tecan fluorescence spectrometer plate-reader after a 20 min incubation. Triton X-100 (0.1 % v/v) was included to measure 100 % leakage, and 10 mM HEPES, 150 mM NaCl, pH 7.4 to measure 0 % leakage. The percentage of leakage induced by the peptides was calculated using the formula: (FI sample - FI buffer) / (FI TX-100 - FI buffer) x 100. Data were collected from a single experiment with three technical replicates.

Molecular dynamics in lipid bilayers

MD simulations were performed for the mastoparan-R1 and R4 peptides in various lipid bilayers, including zwitterionic POPC and anionic POPC: POPG (4:1), under similar conditions to the SPR studies. The CHARMM-GUI server [61] was used to place mastoparan-R1 and R4 at ~0.25 nm from the lipid bilayers. The simulations were programmed using the CHARMM36 force field. The simulations were performed at 150 mM NaCl ionic strength. The steepest descent algorithm (50,000 steps) was applied for energy minimization. The peptide/bilayer systems were subjected to six rounds (125,000 steps for the first three rounds each; 250,000 for the last three rounds each) of equilibration at 310 K and 1 bar, as described above. The systems with minimized energy and balanced temperature and pressure were submitted to MD simulations for 1 µs (1000 ns), using the leap-frog algorithm. The simulations were carried out using the GROMACS v.5.0.4 computational package [62]. MD simulations were analyzed

through root mean square deviation (RMSD), root mean square fluctuation (RMSF), solvent accessible area (SASA), radius of gyration (RG), partial density maps and number of hydrogen bonds.

AUTHOR CONTRIBUTIONS

K.G.N.O., M.H.C. and O.L.F. designed the research.

K.G.N.O. performed and analyzed the antimicrobial assays.

K.G.N.O performed and analyzed the hemolytic assays.

K.G.N.O., R.M.Q.O., M.H.C. performed and analyzed the CD experiments.

C.D.P.F., K.G.N.O. performed and analyzed the NMR experiments.

K.G.N.O., S.B.R., M.H.C. performed and analyzed the MD simulations.

L.Y.C., N.L. performed the leakage and SPR experiments.

K.G.N.O., M.H.C., O.L.F. wrote the paper with input from all authors.

L.M.L., M.L.R.M., D.J.C., M.H.C., O.L.F. supervised the research.

All authors reviewed and accepted the final manuscript version.

ACKNOWLEDGMENTS

This work was supported by grants from Coordenação de Aperfeiçoamento de Pessoal de Nível Superior (CAPES), Conselho Nacional de Desenvolvimento e Tecnológico (CNPq) and Fundação de Apoio ao Desenvolvimento do Ensino, Ciência e Tecnologia do Estado de Mato Grosso do Sul (FUNDECT), Brazil. M.L.R.M. and M.H.C. acknowledge the Universidade Federal de Mato Grosso do Sul (UFMS). D. J. C. is National Health and Medical Research Council (NHMRC) Leadership Fellow (GNT2009546) and his work on peptides is supported by the Australian Research Council Centre of Excellence for Innovations in Peptide and Protein

Science (CE200100012). L. Y. C. was supported by the Advance Queensland Women's Academic Fund (WAF-6884942288). N.L was supported by NHMRC grant 1183927.

CONFLICTS OF INTEREST

The authors declare no competing financial interests.

ABBREVIATIONS

AMP, antimicrobial peptide; APBS, Adaptive Poisson-Boltzmann Solver; CD, circular dichroism; CF, carboxyfluorescein; DSS, 4,4-Dimethyl-4-silapentane-1-sulfonic acid; LUV, large unilamellar vesicle; MALDI-TOF, matrix-assisted laser desorption/ionization - time of flight; MBC, minimal bactericidal concentration; MDSA, molecular dynamics simulated annealing protocol; MIC, minimal inhibitory concentration; NMR, nuclear magnetic resonance; PDB, protein data bank; POPC, 1-palmitoyl-2-oleoyl-sn-glycero-3-phosphocholine; POPG, 1-palmitoyl-2-oleoylphosphatidylglycerol; RG, Radius of gyration; RMSD, root mean square deviation; RMSF, root mean square fluctuation; SASA, solvent accessible area, SCS, Secondary chemical shifts; SUV, small unilamellar vesicle; TFE, 2,2,2-trifluoroethanol; UHPLC, ultra-high performance liquid chromatography.

REFERENCES

1. Hancock, R. E. (2001) Cationic peptides: effectors in innate immunity and novel antimicrobials. *Trends in Microbiol,* **1**, 156-164.

2. Kumar, P., Kizhakkedathu, J. N. & Straus, S. K. (2018) Antimicrobial peptides: diversity, mechanism of action and strategies to improve the activity and biocompatibility *in vivo.* *Biomolecules,* **8**, 4.

3. Benfield, A. H. & Henriques, S. T. (2020) Mode-of-action of antimicrobial peptides: membrane disruption vs. intracellular mechanisms. *Front Med Technol,* **2,** 610997.

4. Fjell, C. D., Hiss, J. A., Hancock, R. E. & Schneider, G. (2012) Designing antimicrobial peptides: form follows function. *Nat Rev Drug Discov*, **11**(1), 37-51.

5. Park, S.-C., Son, H., Kim, Y.-M., Lee, J.-K., Park, S., Lim, H. S., Lee, J. R. & Jang, M. (2022) Design of Antimicrobial Peptides with Cell-Selective Activity and Membrane-Acting Mechanism against Drug-Resistant Bacteria. *Antibiotics*, **11**(11), 1619.

6. Gan, B. H., Gaynord, J., Rowe, S. M., Deingruber, T. & Spring, D. R. (2021) The multifaceted nature of antimicrobial peptides: Current synthetic chemistry approaches and future directions. *Chem Soc Rev*, **50**(13), 7820-7880.

7. Torres, M. D., Sothiselvam, S., Lu, T. K. & de la Fuente-Nunez, C. (2019) Peptide design principles for antimicrobial applications. *J Mol Biol*, **431**(18), 3547-3567.

8. Koehbach, J. & Craik, D. J. (2019) The vast structural diversity of antimicrobial peptides. *Trends in Pharmacol Sci*, **40**(7), 517-528.

9. Zhang, C. & Yang, M. J. A. (2022) Antimicrobial peptides: From design to clinical application. *Antibiotics*, **11**(3), 349.

10. Cardoso, M. H., Orozco, R. Q., Rezende, S. B., Rodrigues, G., Oshiro, K. G., Cândido, E. S. & Franco, O. L. (2020) Computer-aided design of antimicrobial peptides: are we generating effective drug candidates? *Front in Microbiol*, **10**, 3097.

11. Rungsa, P., Peigneur, S., Jangpromma, N., Klaynongsruang, S., Tytgat, J. & Daduang, S. (2022) *In silico* and *in vitro* structure-activity relationship of mastoparan and its analogs. *Molecules*, **27**(2), 561.

12. Howl, J., Howl, L. & Jones, S. (2018) The cationic tetradecapeptide mastoparan as a privileged structure for drug discovery: Enhanced antimicrobial properties of mitoparan analogues modified at position-14, *Peptides.* **101**, 95-105.

13. Oshiro, K. G., Cândido, E. S., Chan, L. Y., Torres, M. D., Monges, B. E., Rodrigues, S. G., ... & Cardoso, M. H. (2019) Computer-aided design of mastoparan-like peptides enables the generation of nontoxic variants with extended antibacterial properties, *J Med Chem.* **62**, 8140-8151.

14. Park, I. Y., Cho, J. H., Kim, K. S., Kim, Y.-B., Kim, M. S. & Kim, S. C. (2004) Helix stability confers salt resistance upon helical antimicrobial peptides. *J Biol Chem.* **279**(14), 13896-13901.

15. Cardoso, M. H., Chan, L. Y., Cândido, E. S., Buccini, D. F., Rezende, S. B., Torres, M. D., Torres, M. D., ... & Franco, O. L. (2022) An N-capping asparagine–lysine–proline (NKP) motif contributes to a hybrid flexible/stable multifunctional peptide scaffold. *Chem Sci*, **13**(32), 9410-9424.

16. Takada, M., Ito, T., Kurashima, M., Matsunaga, N., Demizu, Y. & Misawa, T. (2023) Structure-activity relationship studies of substitutions of cationic amino acid residues on antimicrobial peptides. *Antibiotics*, **12**(1), 19.

17. Goto, C., Hirano, M., Hayashi, K., Kikuchi, Y., Hara-Kudo, Y., Misawa, T. & Demizu, Y. J. C. (2019) Development of amphipathic antimicrobial peptide foldamers based on Magainin 2 sequence. *Chem Med Chem*, **14**(22), 1911-1916.

18. Hollmann, A., Martínez, M., Noguera, M. E., Augusto, M. T., Disalvo, A., Santos, N. C., Semorile, L. & Maffía, P. C. (2016) Role of amphipathicity and hydrophobicity in the balance between hemolysis and peptide–membrane interactions of three related antimicrobial peptides. *Colloids Surf B: Biointerfaces.* **141**, 528-536.

19. Chen, Y., Guarnieri, M. T., Vasil, A. I., Vasil, M. L., Mant, C. T., Hodges, R. S. (2007) Role of peptide hydrophobicity in the mechanism of action of α-helical antimicrobial peptides. *Antimicrob Agents Chemother.* **51**(4), 1398-1406.

20. Gautier, R., Douguet, D., Antonny, B. & Drin, G. J. (2008) HELIQUEST: a web server to screen sequences with specific α-helical properties. *Bioinformatics*, **24**(18), 2101-2102.

21. Irazazabal, L. N., Porto, W. F., Ribeiro, S. M., Casale, S., Humblot, V., Ladram, A. & Franco, O. L. (2016) Selective amino acid substitution reduces cytotoxicity of the antimicrobial peptide mastoparan. *Biochim Biophys Acta Biomembr.* **1858**(11), 2699-2708.

22. dos Santos Cabrera, M. P., Rangel, M., Ruggiero Neto, J. & Konno, K. (2019) Chemical and biological characteristics of antimicrobial α-helical peptides found in solitary wasp venoms and their interactions with model membranes. *Toxins*, **11**(10), 559.

23. Souza, B. M. d., Cabrera, M. P. d. S., Gomes, P. C., Dias, N. B., Stabeli, R. G., Leite, N. B., Neto, J. R. & Palma, M. S. (2015) Structure–activity relationship of mastoparan analogs: Effects of the number and positioning of Lys residues on secondary structure, interaction with membrane-mimetic systems and biological activity, *Peptides.* **72,** 164-174.

24. Wüthrich, K. J. (1990) Protein structure determination in solution by NMR spectroscopy. *J Biol Chem*, **265**(36), 22059-22062.

25. Zhu, N., Zhong, C., Liu, T., Zhu, Y., Gou, S., Bao, H., & Ni, J. (2021) Newly designed antimicrobial peptides with potent bioactivity and enhanced cell selectivity prevent and reverse rifampin resistance in Gram-negative bacteria. *Eur J Pharm Sci*, **158**, 105665.

26. Whiles, J. A., Brasseur, R., Glover, K. J., Melacini, G., Komives, E. A. & Vold, R. R. (2001) Orientation and effects of mastoparan X on phospholipid bicelles. *Biophys J.* **80**, 280-293.

27. Chou, S., Wang, J., Shang, L., Akhtar, M. U., Wang, Z., Shi, B., Feng, X. & Shan, A. (2019) Short, symmetric-helical peptides have narrow-spectrum activity with low resistance potential and high selectivity. *Biomater Sci.* **7**(6), 2394-2409.

28. Dong, N., Zhu, X., Chou, S., Shan, A., Li, W. & Jiang, J. (2014) Antimicrobial potency and selectivity of simplified symmetric-end peptides. *Biomaterials*, **35**(27), 8028-8039

29. Mohanram, H. & Bhattacharjya, S. (2016) Salt-resistant short antimicrobial peptides. *Pept Sci*, **106**(3), 345-356.

30. Wu, P.-S., Lai, S.-J., Fung, K.-M. & Tseng, T. (2020) Characterization of the structure–function relationship of a novel salt-resistant antimicrobial peptide, RR12, *RSC Adv.* **10**, 23624-23631.

31. Henriksen, J. R., Etzerodt, T., Gjetting, T. & Andresen, T. L. (2014) Side Chain Hydrophobicity Modulates Therapeutic Activity and Membrane Selectivity of Antimicrobial Peptide Mastoparan-X, *Plos One*, **9**, e91007.

32. Yeung, A. T., Gellatly, S. L., Hancock, R. E. (2011) Multifunctional cationic host defence peptides and their clinical applications. *Cell Mol Life Sci*, **68,** 2161-2176.

33. Guido-Patiño, J. C. & Plisson, F. J. (2022) Profiling hymenopteran venom toxins: Protein families, structural landscape, biological activities, and pharmacological benefits. *Toxicon: X*, **14**, 100119.

34. Lawrence, N., Philippe, G. J. B., Harvey, P. J., Condon, N. D., Benfield, A. H., Cheneval, O., Craik, D. J. & Henriques, S. T. (2020) Cyclic peptide scaffold with ability to stabilize and deliver a helical cell-impermeable cargo across membranes of cultured cancer cells, *RSC Chem Biol.* **1**, 405-420.

35. Ko, S. J., Park, E., Asandei, A., Choi, J.-Y., Lee, S.-C., Seo, C. H., Luchian, T. & Park, Y. (2020) Bee venom-derived antimicrobial peptide melectin has broad-spectrum potency, cell selectivity, and salt-resistant properties, *Sci Rep.* **10**, 10145.

36. Clinical and Laboratory Standards Institute (CLSI). Performance standards for antimicrobial susceptibility testing, Twenty-Second Informational Supplement. CLSI Document M100-S22; Clinical and Laboratory Standards Institute: Wayne, PA, 2012.

37. Shaka, A., Lee, C. & Pines, A. J. J. o. M. R. (1988) Iterative schemes for bilinear operators; application to spin decoupling. *J Magn Reson*, **77**(2), 274-293.

38. Hwang, T.-L. & Shaka, A. J. J. o. M. R., Series A (1995) Water suppression that works. Excitation sculpting using arbitrary wave-forms and pulsed-field gradients. *J Magn Reson.* **112**(2), 275-279.

39. Liu, M., Mao, X.-a., Ye, C., Huang, H., Nicholson, J. K. & Lindon, J. C. (1998) Improved WATERGATE pulse sequences for solvent suppression in NMR spectroscopy. *J Magn Reson*, **132**(1), 125-129.

40. Willker, W., Leibfritz, D., Kerssebaum, R. & Bermel, W. J. (1993) Gradient selection in inverse heteronuclear correlation spectroscopy. *Magn Reson Chem.* **31**(3), 287-292.

41. Vranken, W. F., Boucher, W., Stevens, T. J., Fogh, R. H., Pajon, A., Llinas, M., Ulrich, E. L., Markley, J. L., Ionides, J., Laue, E. D. (2005) The CCPN data model for NMR spectroscopy: development of a software pipeline. *Proteins: Struct, Funct and Bioinform*, **59**(4), 687-696.

42. Skinner, S. P., Goult, B. T., Fogh, R. H., Boucher, W., Stevens, T. J., Laue, E. D. & Vuister, G. W. (2015) Structure calculation, refinement and validation using CcpNmr Analysis. *Acta Crystallog D Biol Crystallog*, **71**(1), 154-161.

43. Nilges, M. & O'Donoghue, S. I. (1998) Ambiguous NOEs and automated NOE assignment. *Prog Nucl Magn Reson Spectrosc*, **32**(2), 107-139.

44. Linge, J. P., O'Donoghue, S. I. & Nilges, M. (2001) Automated assignment of ambiguous nuclear overhauser effects with ARIA. *Meth Enzymol*, **339**, 71-90.

45. Linge, J. P., Habeck, M., Rieping, W. & Nilges, M. (2003) ARIA: automated NOE assignment and NMR structure calculation. *Bioinformatics*, **19**(2), 315-316.

46. Rieping, W., Habeck, M., Bardiaux, B., Bernard, A., Malliavin, T. E. & Nilges, M. (2007) ARIA2: automated NOE assignment and data integration in NMR structure calculation. *Bioinformatics*, **23**(3), 381-382.

47. Brünger, A. T., Adams, P. D., Clore, G. M., DeLano, W. L., Gros, P., Grosse-Kunstleve, R. W., Jiang, J.-S., Kuszewski, J., Nilges, M. & Pannu, N. S. (1998) Crystallography & NMR system: A new software suite for macromolecular structure determination. *Acta Crystallog D Biol Crystallog* **54**(5), 905-921.

48. Nilges, M., Bernard, A., Bardiaux, B., Malliavin, T., Habeck, M. & Rieping, W. (2008) Accurate NMR structures through minimization of an extended hybrid energy. *Structure*, **16**(9), 1305-1312.

49. Cheung, M.-S., Maguire, M. L., Stevens, T. J. & Broadhurst, R. W. (2010) DANGLE: A Bayesian inferential method for predicting protein backbone dihedral angles and secondary structure. *J Magn Reson*, **202**(2), 223-233.

50. Linge, J. P., Williams, M. A., Spronk, C. A., Bonvin, A. M., Nilges, M. (2003) Refinement of protein structures in explicit solvent. *Proteins: Struct, Funct and Bioinform*, **50**(3), 496-506.

51. Linge, J. & Nilges, M. J. (1999) Influence of non-bonded parameters on the quality of NMR structures: a new force field for NMR structure calculation. *J Biomol NMR*, **13**(1), 51.

52. DeLano, W. L. (2002) Pymol: An open-source molecular graphics tool. *CCP4 Newsl. Protein Crystallogr*, **40**(1), 82-92.

53. Koradi, R., Billeter, M. & Wüthrich, K. J. (1996) MOLMOL: a program for display and analysis of macromolecular structures. *J Mol Graph*, **14**(1), 51-55.

54. MacArthur, M. W., Laskowski, R. A. & Thornton, J. M. (1994) Knowledge-based validation of protein structure coordinates derived by X-ray crystallography and NMR spectroscopy. *Curr Opin Struct Biol*, **4**(5), 731-737.

55. Vriend, G. J. (1990) WHAT IF: a molecular modeling and drug design program. *J Mol Graph*, ***8***(1), 52-56.

56. Davis, I. W., Leaver-Fay, A., Chen, V. B., Block, J. N., Kapral, G. J., Wang, X., Murray, L. W., Arendall III, W. B., Snoeyink, J. & Richardson, J. (2007) MolProbity: all-atom contacts and structure validation for proteins and nucleic acids. *Nucleic Acids Res*, **35**, W375-W383.

57. Wiederstein, M. & Sippl, M. J. (2007) ProSA-web: interactive web service for the recognition of errors in three-dimensional structures of proteins. *Nucleic Acids Res*, **35**, W407-W410.

58. Dolinsky, T. J., Nielsen, J. E., McCammon, J. A. & Baker, N. A. (2004) PDB2PQR: an automated pipeline for the setup of Poisson–Boltzmann electrostatics calculations. *Nucleic Acids Res*, **32**, W665-W667.

59. Jurrus, E., Engel, D., Star, K., Monson, K., Brandi, J., Felberg, L. E., Brookes, D. H., Wilson, L., Chen, J. & Liles, K. J. (2018) Improvements to the APBS biomolecular solvation software suite. *Protein Sci*, **27**(1), 112-128.

60. Henriques, S. T., Pattenden, L. K., Aguilar, M.-I. & Castanho, M. A. (2008) PrP (106-126) does not interact with membranes under physiological conditions *Biophys J*, **95**(4), 1877-1889.

61. Jo, S., Kim, T., Iyer, V. G. & Im, W. (2008) CHARMM-GUI: a web-based graphical user interface for CHARMM, *J Comput Chem.* **29**, 1859-1865.

762 62. Abraham, M. J., Murtola, T., Schulz, R., Páll, S., Smith, J. C., Hess, B. & Lindahl, E.
763 (2015) GROMACS: High performance molecular simulations through multi-level parallelism
764 from laptops to supercomputers, *SoftwareX.* **1**, 19-25.

765

TABLES

Table 1. NMR and refinement statistics of mastoparan-R1 and mastoparan-R4 structures in 75 mM SDS-*d25* micelles.

	Peptides	
NMR distance and dihedral constraints		
Distance constraints	**mastoparan-R1**	**mastoparan-R4**
Total NOE	200	166
Intra-residue	94	71
Sequential ($\|i-j\|=1$)	23	23
Short-range ($2 \le \|i-j\| \le 3$)	16	6
Medium-range ($4 \le \|i-j\| \le 5$)	2	1
Long-range ($\|i-j\| > 5$)	0	0
Total unambiguous	135	101
Ambiguous	65	65
Total dihedral angle restraints		
ϕ + ψ	22	22
Structure statistics		
Violations (mean and s.d.)		
Distance constraints (Å)	0.0360 ± 0.0083	0.0228 ± 0.0045
Dihedral angle constraints (°)	0.0405 ± 0.0634	0.0295 ± 0.0505
Max. dihedral angle violation (°)	0	0
Max. distance constraint violation (Å)	0.7	0
Deviations from idealized geometry		
Bond lengths (Å)	0.0053 ± 0.0084 10^{-2}	0.0044 ± 0.0019 10^{-1}
Bond angles (°)	0.5527 ± 0.0083	0.5380 ± 0.0172
Impropers (°)	1.2330 ± 0.1695	0.9385 ± 0.1406
Average pairwise r.m.s. deviation (Å)**		
Backbone (2nd structure)[a]	0.0987 ± 0.0406	0.2486 ± 0.0818
Heavy atoms (2nd structure)[a]	0.9307 ± 0.1729	0.9247 ± 0.1729
Backbone (all residues)[b]	0.5531 ± 0.1639	0.6435 ± 0.2308

Heavy atoms (all residues)[b]	1.1646 ± 0.1897	1.1950 ± 0.2193
Ramachandran Plot (%)		
Most favored regions	95.0	94.5
Additional allowed regions	5.0	5.5
Generously allowed regions	0	0
Disallowed region	0	0
ProSA-web		
Z-score[c]	-2.09	-1.53
PROCHECK G-factors[d]	0.175	0.325

[a] Pairwise r.m.s deviation was calculated among 10 refined structures for residues in helical segment 3-13 to mastoparan-R1.

[b] Pairwise r.m.s deviation was calculated among 10 refined structures for residues 1-14 and more C-terminal amidation (NH_2).

[c] Z-score value within the expected for NMR structures deposited in the PDB with similar size and fold compared to mastoparan-R1 calculated structures.

[d] G-factors score for dihedral angles and covalent forces of the main chain within the expected range for a reliable structure (> -0.05).

**All r.m.s deviations were calculated by the CNS in refinement protocol.

FIGURES LEGENDS

Figure 1. Bacterial growth curves and minimum inhibitory concentration values for mastoparan-L, R1 and R4 from 32 to 0.5 µM, over 24 h, at 30 min intervals. (a) Mastoparan peptides against *E. coli* ATCC 25922 in MHB, and **(b)** against *E. coli* ATCC 25922 in 150 mM NaCl supplemented MHB. **(c)** Mastoparan peptides against *E. coli* (clinical isolate – LACEN 9921447) in MHB, and **(d)** against *E. coli* (clinical isolate – LACEN 9921447) in 150 mM NaCl supplemented MHB. The color legend denotes the concentrations (µM) and growth control (BAC) of the experiments.

Figure 2. Mastoparan-L, R1 and R4 circular dichroism analysis. CD spectra were recorded in ultrapure water, 10 mM potassium phosphate buffer (KH_2PO_4, 10 mM (pH 7.4)), 50 % TFE in water (v/v), 75 mM SDS, and 100 mM SDS. In **(a)** CD spectra for mastoparan-L, **(b)** mastoparan-R1 and **(c)** mastoparan-R4.

Figure 3. NMR structures of mastoparan-L, R1 and R4. The 3D structures of mastoparan-R1 and R4 were elucidated through NMR spectroscopy in 75 mM SDS-*d*25. The sequence of figures horizontally from left to right are: (i) Superposition of the 10 lowest energy structures of mastoparan-L (PDB: 6DUL) in orange **(a)**, R1 (PDB: 8EP5) in green **(b)**, and R4 (PDB: 8ERU) in blue **(c)** in the presence of 75 mM of SDS-d25 micelles. (ii) Lowest free energy model in Adaptive Poisson−Boltzmann solver (APBS) electrostatic potential of peptides with potential ranging from −5 kT/e (red) to +5 kT/e (blue) in 0° and 180° of rotation. (iii) Front view of the inside of the α-helix, showing the cationic face and the hydrophobic face and the cationic residues are in gray.

Figure 4. Peptide-lipid binding and membrane-lytic properties of mastoparan-L and analogs mastoparan-R1 and R4. The lipid-binding affinity of each peptide was determined for bilayers composed of POPC and POPC/POPG (PC/PG) (4:1). SPR sensorgrams were obtained for peptides injected over lipid bilayers deposited on an L1 chip for 180 s with dissociation monitored for 600 s. Response units (RU) at the end of the association phase were converted to peptide to lipid ratios (P/L mol/mol) by converting RU to moles of peptide and normalized to the amount of lipid deposited on the lipid surface (1 RU = 1 pg/mm^2 of peptide or lipid). **(a)** Representative sensorgrams for 32 μM peptide show peptide-lipid association (50 – 230 s) and dissociation (280 – 800 s). **(b)** peptide to lipid ratios (P/L, mol/mol) recorded at the end of the association phase (indicated by arrow) were used to plot dose response curves, by fitting [inhibitor] vs response in GraphPad Prism v9. **(c)** Peptide-induced membrane lysis was examined by measuring the leakage of CF, from LUVs. Leakage induced by Triton X-100 (100 %) and buffer (0 %) were used to calculate % leakage induced by the peptides. Dose-response curves were fitted with [inhibitor] vs response with variable slope in GraphPad Prism v9. Data represents three technical replicates.

Figure 5. MD analyses of peptide interaction with POPC and POPC/POPG (4:1) bilayers. Partial density profile obtained in the last 0.1 μs of MD simulations; hydrogen bonds over 1 μs of the analysis and the snapshot plotted at 1 μs of MD simulations. Interaction with POPC for mastoparan-R1 **(a)** and mastoparan-R4 **(b)** interaction with POPC/POPG (4:1) for mastoparan-R1 **(c)** and mastoparan-R4 **(d)**.

FIGURE 1

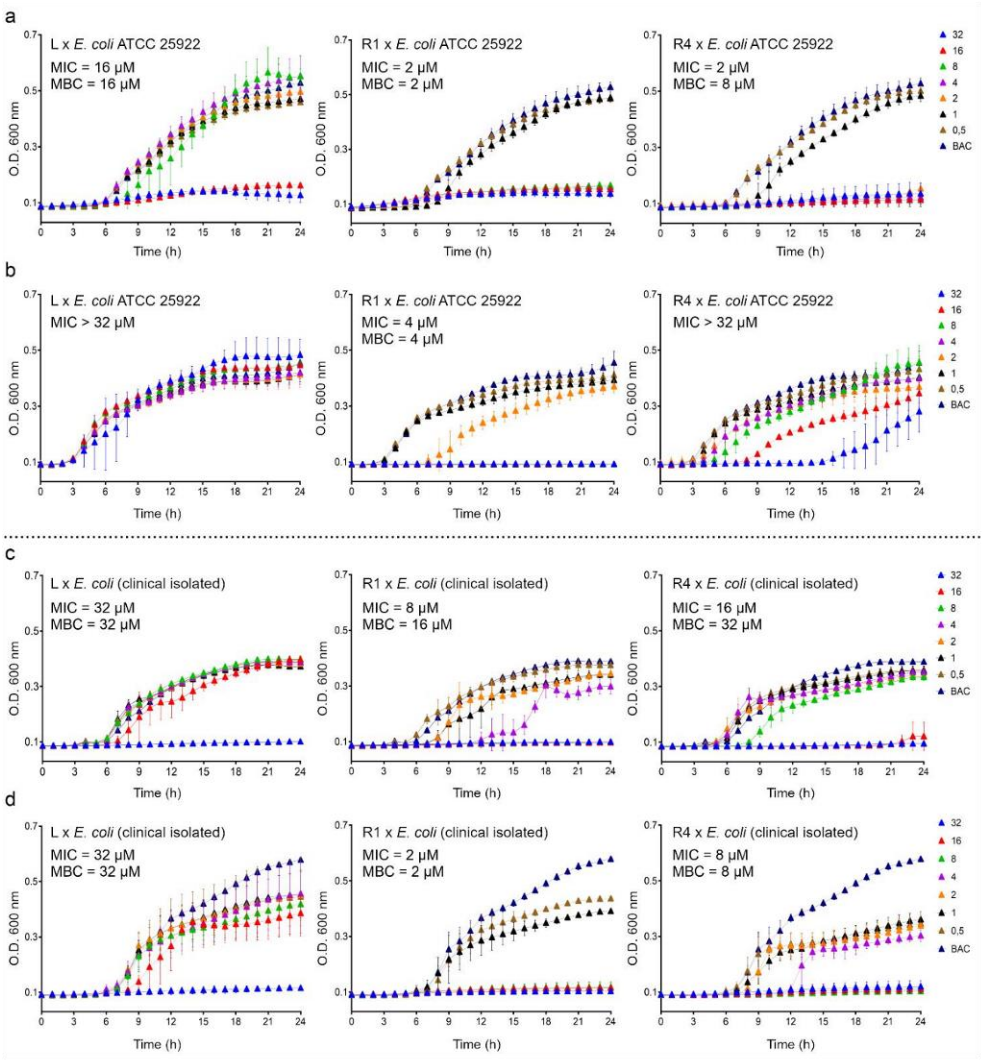
a
L x E. coli ATCC 25922
MIC = 16 µM
MBC = 16 µM
R1 x E. coli ATCC 25922
MIC = 2 µM
MBC = 2 µM
R4 x E. coli ATCC 25922
MIC = 2 µM
MBC = 8 µM
b
L x E. coli ATCC 25922
MIC > 32 µM
R1 x E. coli ATCC 25922
MIC = 4 µM
MBC = 4 µM
R4 x E. coli ATCC 25922
MIC > 32 µM
c
L x E. coli (clinical isolated)
MIC = 32 µM
MBC = 32 µM
R1 x E. coli (clinical isolated)
MIC = 8 µM
MBC = 16 µM
R4 x E. coli (clinical isolated)
MIC = 16 µM
MBC = 32 µM
d
L x E. coli (clinical isolated)
MIC = 32 µM
MBC = 32 µM
R1 x E. coli (clinical isolated)
MIC = 2 µM
MBC = 2 µM
R4 x E. coli (clinical isolated)
MIC = 8 µM
MBC = 8 µM
O.D. 600 nm
Time (h)
32
16
8
4
2
1
0,5
BAC

FIGURE 2

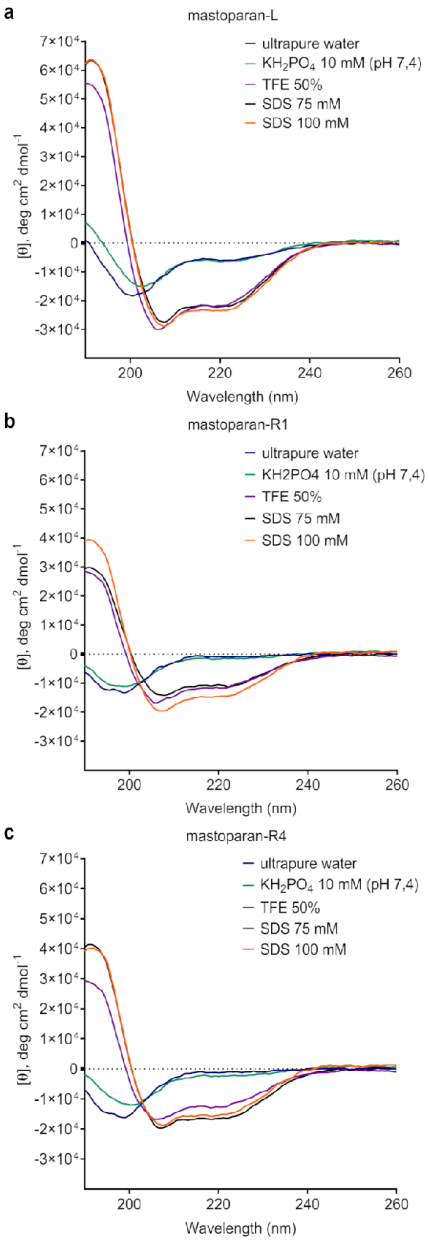

822 **FIGURE 3**

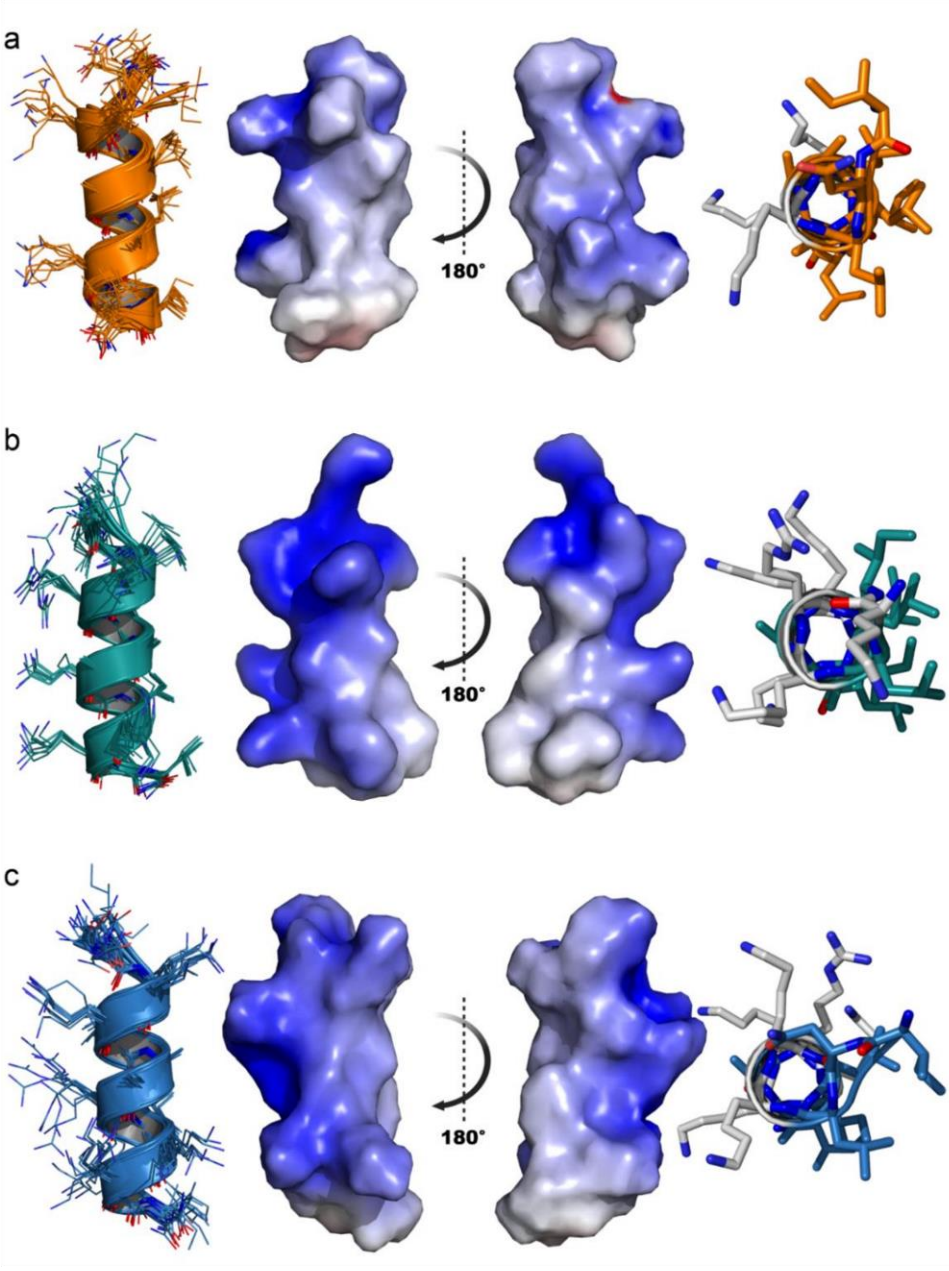

823

FIGURE 4

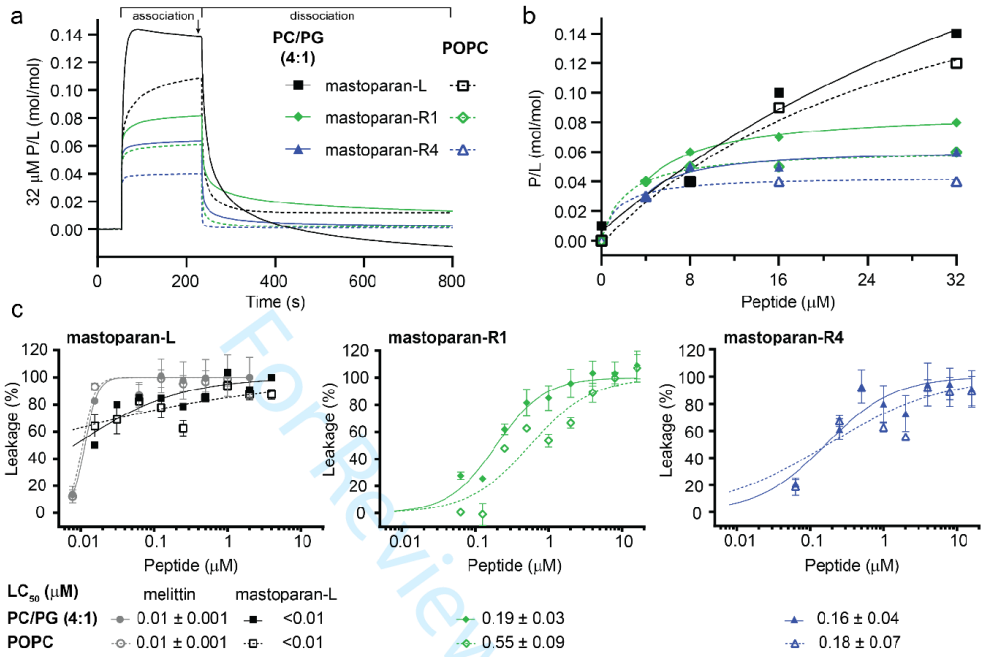

827 **FIGURE 5**

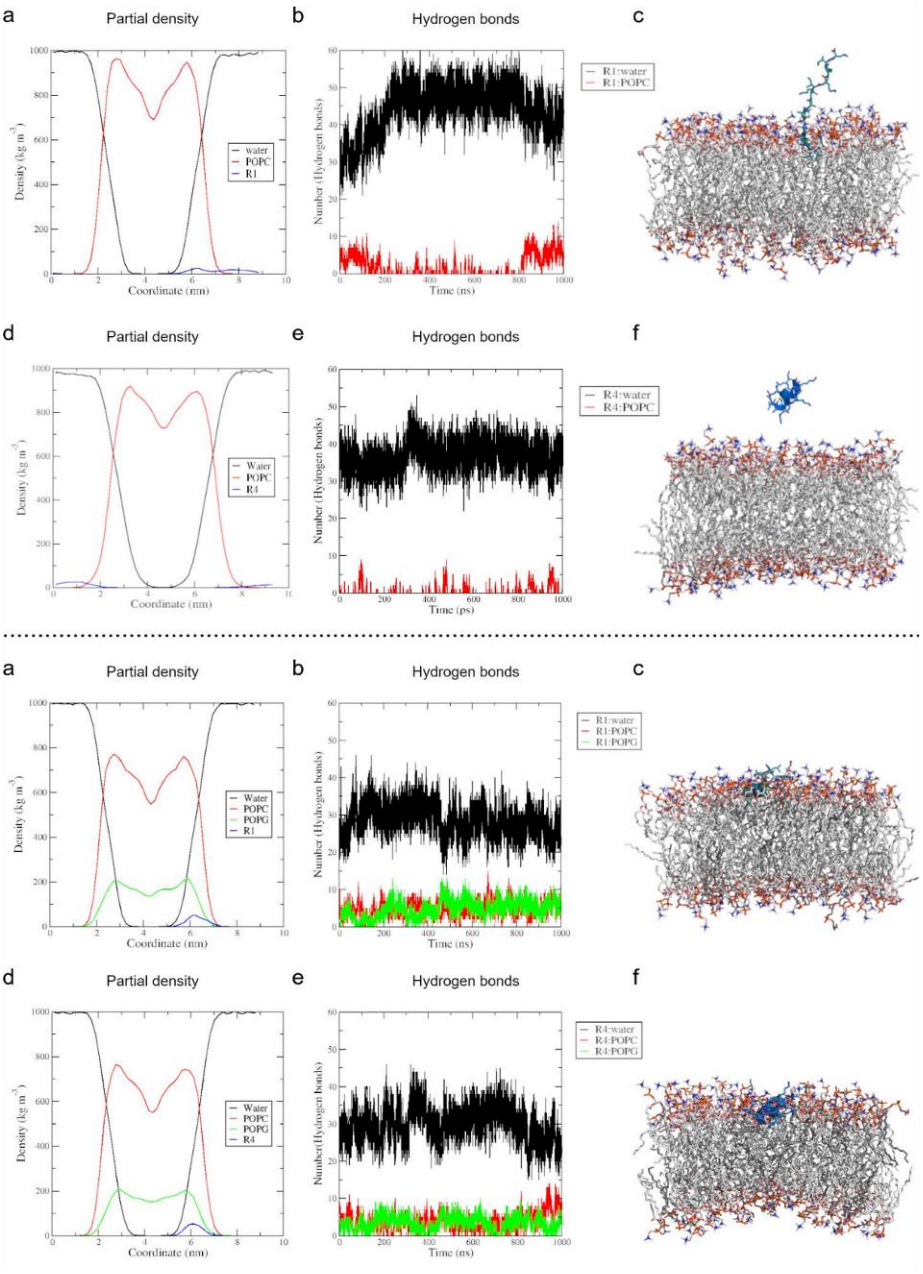

828

Supplementary information

Karen G. N. Oshiro[a,b,c], Carlos D. P. Freitas[d], Samilla B. Rezende[b,c], Raquel M. Q. Orozco[b,c], Lai Y. Chan[e], Nicole Lawrence[e], Luciano M. Lião[d], Maria L. R. Macedo[f], David J. Craik[e], Marlon H. Cardoso[a,b,c,f *] and Octávio L. Franco[a,b,c*]

[a] Programa de Pós-Graduação em Patologia Molecular, Faculdade de Medicina, Universidade de Brasília, Brasília/DF, 70910900, Brazil;

[b] S-inova Biotech, Programa de Pós-Graduação em Biotecnologia, Universidade Católica Dom Bosco, Campo Grande/MS, 79117900, Brazil;

[c] Centro de Análises Proteômicas e Bioquímicas, Pós-Graduação em Ciências Genômicas e Biotecnologia, Universidade Católica de Brasília, Brasília/DF, 70790160, Brazil;

[d] Laboratório de RMN, Instituto de Química, Universidade Federal de Goiás, Goiânia/GO, 74690-900, Brazil;

[e] Institute for Molecular Bioscience, Australian Research Council Centre of Excellence for Innovations in Peptide and Protein Science, The University of Queensland, Brisbane, QLD, 4072, Australia;

[f] Laboratório de Purificação de Proteínas e suas Funções Biológicas, Universidade Federal de Mato Grosso do Sul, Campo Grande/MS 79070-900, Brazil.

[*]**Corresponding authors:** Prof. Marlon H. Cardoso (marlonhenrique6@gmail.com) and Prof. Octávio L. Franco (ocfranco@gmail.com).

SUPPLEMENTARY TABLES

Table S1. Minimal inhibitory concentration (MIC) and minimal bactericidal concentration (MBC) of mastoparan-L, R1 and R4 from 32 to 0.5 µM, over 24 h. Mastoparan peptides against *E. coli* ATCC 25922 in MHB 0 mM NaCl, and MHB + 150 mM NaCl; and *E. coli* (clinical isolate – LACEN 9921447) in MHB 0 mM NaCl, and MHB + 150 mM NaCl.

Peptides (µM)		**mastoparan-L**		**mastoparan-R1**		**mastoparan-R4**	
***E. coli* strains**	**medium and salinity**	**MIC**	**MBC**	**MIC**	**MBC**	**MIC**	**MBC**
ATCC 25922	MHB 0 mM NaCl	16	16	2	2	2	8
	MHB 150 mM NaCl	>32		4	4	>32	
clinical isolate (9921447)	MHB 0 mM NaCl	32	32	8	16	16	32
	MHB 150 mM NaCl	32	32	2	2	8	8

Table S2. Helix content for mastoparan peptides were calculated from the mean residue ellipticity at 222 nm ($[\theta]_{222}$) according to the following equation: % helix = $100([\theta]_{222}/(-39{,}500(1-2.57/n)))$, where n is the total number of peptide bonds (Chen et al., 1974).

biomimetics conditions	mastoparan-L	mastoparan-R1	mastoparan-R4
	25 °C	**25 °C**	**25 °C**
ultrapure water	18	3	3
10 mM KH_2PO_4	20	5	7
50 % TFE	67	36	39
75 mM SDS	69	36	52
100 mM SDS	73	45	47

Table S3. Chemical shift of mastoparan-R1 in 75 mM SDS-d_{25}.

Residue	H	Hα	Hβ	Hγ	Hδ	Hε	Cα	Cβ	Cγ	Cδ	Cε
Lys1	NF	4.21	1.97, 2.32	1.61, 1.61	1.84,1.84	3.09, 3.09	56.12	32.41	24.77	28.80	42.03
Ile2	8.63	4.03	2.04	0.96, 1.30, 1.58	0.96	-	63.75	38.53	17.80, 28.58	13.87	-
Leu3	8.22	4.06	1.96,1.96	NF	0.87, 0.89	-	57.64	40.62	NF	23.17, 23.43	-
Lys4	7.56	3.98	1.88,1.88	1.46, 1.46	1.70, 1.70	3.00, 3.00	59.38	32.14	25.50	29.07	42.11
Arg5	7.73	4.10	1.97, 1.97	1.62, 1.62	3.19, 3.19	7.08	58.98	30.23	27.41	43.76	-
Leu6	8.20	4.05	1.70, 1.77	1.82	0.87, 0.91	-	58.41	41.90	26.94	24.43, 24.53	-
Ala7	8.49	3.89	1.51	-	-	-	55.54	18.28	-	-	-
Ala8	7.74	4.04	1.50	-	-	-	54.71	18.26	-	-	-
Lys9	7.55	4.14	2.07, 2.07	1.54, 1.54	NF	2.97, 2.97	58.18	32.25	24.73	NF	42.14
Ile10	8.12	3.69	1.95	0.90, 1.14, 1.14	0.80	-	64.41	37.54	17.77	13.03	-
Lys11	8.16	3.90	1.85, 1.93	1.44, 1.44	1.70, 1.70	2.95, 2.95	59.19	32.24	25.53	29.12	42.15
Lys12	7.33	4.14	1.99, 1.99	1.50, 1.63	1.71, 1.71	NF	58.02	32.47	24.82	29.11	NF
Ile13	7.60	4.20	2.02	0.96, 1.36, 1.36	0.87	-	62.09	39.06	17.80, 27.43	13.95	-
Leu14	7.58	4.36	1.63, 1.73	1.84	0.89, 0.98	-	53.87	42.00	26.80	25.44, 25.69	-
NF: not found											

Table S4. Chemical shift of mastoparan-R4 in 75 mM SDS-d_{25}.

Residue	H	Hα	Hβ	Hγ	Hδ	Hε	Cα	Cβ	Cγ	Cδ	Cε
Ile1	NF	3.95	NF	1.00, NF, NF	0.94	-	NF	NF	16.49	14.01	-
Asn2	8.57	5.01	2.78,3.05	-	6.92, 7.74	-	52.16	NF	-	-	-
Leu3	8.69	4.10	1.83,1.83	NF	0.90, 1.01	-	58.30	41.59	NF	23.57, 25.58	-
Lys4	8.15	3.95	1.93,1.93	1.42, 1.42	1.67, 1.67	3.04, 3.04	60.21	32.31	25.69	NF	42.12
Lys5	7.78	4.05	1.87, 1.94	1.50, 1.50	1.72, 1.72	3.01, 3.01	58.97	32.34	24.97	29.24	42.13
Leu6	7.87	4.14	1.83, 1.83	NF	0.93, 1.00	-	57.96	41.65	NF	23.99, 25.52	-
Ala7	8.53	3.93	1.53	-	-	-	55.38	18.24	-	-	-
Ala8	7.90	4.07	1.55	-	-	-	55.17	18.22	-	-	-
Arg9	7.87	4.08	2.10, 210	1.69, 1.69	3.19, 3.19	7.33	58.86	30.40	27.70	43.77	-
Ile10	8.12	3.62	2.00	0.92, 1.06, 1.06	0.85	-	59.60	39.12	17.80, 31.28	13.56	-
Lys11	8.52	3.87	1.87,1.99	1.47, 1.47	1.70, 1.70	NF	59.86	32.37	25.02	29.30	NF
Lys12	7.74	4.06	1.94,1.94	1.54, 1.54	1.73, 1.73	NF	58.81	32.45	25.16	29.40	NF
Lys13	7.66	4.25	2.02,2.02	1.51, 1.51	1.73, 1.73	3.00, 3.00	57.21	32.39	25.10	29.29	42.17
Ile14	7.89	4.05	1.97	0.98, NF, NF	0.86	-	62.42	38.70	17.69	13.58	-
NF: not found											

Table S5. Atomic interactions involving the POPC membrane with backbone atoms from the mastoparan-R1 (PDB: 8EP5) after 0.1 μs of MD simulations.

mastoparan-R1

Residues	Position	Atom Name	Distance (A)	Lipid	Atom Name	Interactions
Arg	5	O	3.3	POPC	N	HB
Arg	5	O	3.8	POPC	O14	HB
Arg	5	NH1	3.1	POPC	O12	HB
Arg	5	NH1	2.8	POPC	O11	HB
Arg	5	NH1	3.5	POPC	O21	HB
Arg	5	N	2.8	POPC	O13	HB
Lys	1	NZ	2.8	POPC	O13	HB
Lys	1	NZ	2.9	POPC	O14	HB
Lys	1	NZ	3.2	POPC	O13	HB

H: hydrophobic interaction; HB: hydrogen bonds.

Table S6. Atomic interactions involving the POPC:POPG (4:1) membrane with backbone atoms from the mastoparan-R1 (PDB: 8EP5) and mastoparan-R4 (PDB: 8ERU) after 0.1 μs of MD simulations.

mastoparan-R1						
Residues	**Position**	**Atom name**	**Distance (A)**	**Lipid**	**Atom name**	**Interactions**
Lys	1	NZ	3.0	POPG	O14	SB
Leu	3	N	3.8	POPG	O12	HB
Leu	3	N	2.7	POPG	O14	HB
Leu	3	CB	3.5	POPG	C1	H
Arg	5	NE	3.3	POPC	O13	HB
Arg	5	NH1	2.8	POPC	O13	HB
Arg	5	NH1	3.8	POPC	O22	HB
Arg	5	NH2	3.8	POPG	O13	SB
Lys	9	NZ	3.4	POPG	O13	SB
Lys	9	NZ	2.8	POPG	O13	SB
Lys	11	NZ	2.8	POPC	O22	HB
Lys	12	NZ	2.6	POPG	O13	SB
Lys	12	NZ	3.0	POPG	O14	SB
Lys	12	NZ	3.3	POPG	OC3	HB
mastoparan-R4						
Residues	**Position**	**Atom name**	**Distance (A)**	**Lipid**	**Atom name**	**Interactions**
Ile	1	N	3.2	POPC	O22	HB
Ile	1	O	3.6	POPC	O22	HB
Ile	1	O	3.8	POPC	O21	HB
Ile	1	CD	3.8	POPC	C32	H
Asn	2	ND2	2.8	POPC	O13	HB
Asn	2	ND2	3.3	POPC	O14	HB
Leu	3	CD2	3.8	POPG	O32	HB
Arg	9	NH2	2.7	POPC	O14	HB
Arg	9	NH2	3.7	POPC	O21	HB

Arg	9	NH2	2.9	POPC	O11	HB
Arg	9	NH2	3.6	POPC	O13	HB
Arg	9	NH1	2.7	POPC	O13	HB
Arg	9	NH1	2.9	POPG	O32	HB
Lys	12	CG	3.4	POPG	OC3	HB

H: hydrophobic interaction; HB: hydrogen bonds; SB: saline bonds.

SUPPLEMENTARY FIGURES

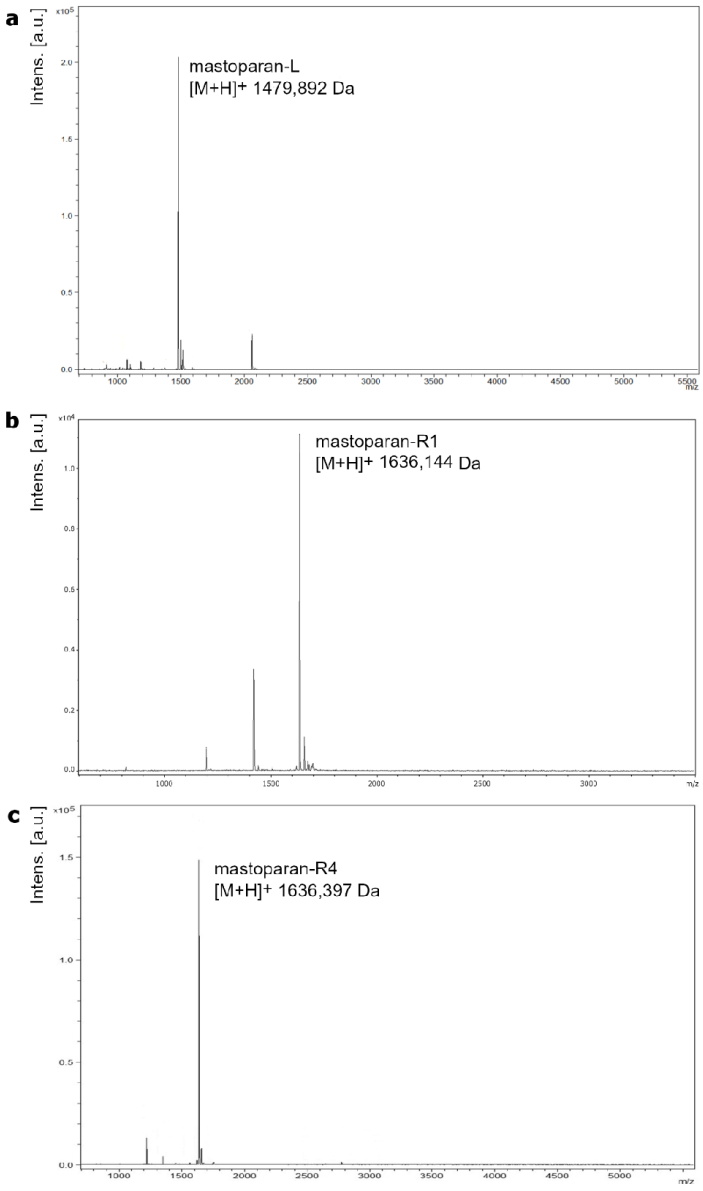

Figure S1. MALDI-ToF analyzes for mastoparan-L, R1 and R4. The molecular mass of mastoparan-L was confirmed by MALDI-ToF, revealing a monoisotopic mass of 1479.84 Da **(a)**; mastoparan-R1 1636.14 Da **(b)**; and mastoparan-R4 1636.39 Da **(c)**.

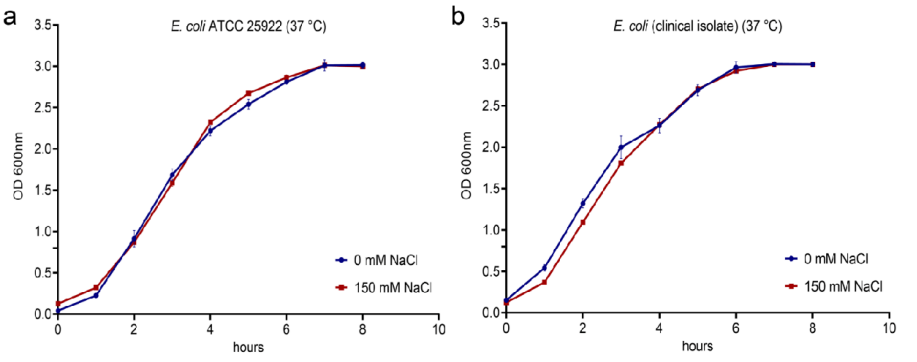

Strain	MHB	CFU
E. coli ATCC 25922	0 mM NaCl	6.8 x 10^{11} CFU mL^{-1}
E. coli ATCC 25922	150 mM NaCl	5.6 x 10^{11} CFU mL^{-1}

Strain	MHB	CFU
E. coli LACEN 9921447	0 mM NaCl	5.5 x 10^{11} CFU mL^{-1}
E. coli LACEN 9921447	150 mM NaCl	6.5 x 10^{11} CFU mL^{-1}

Figure S2. Growth curves for *E. coli* strains at different salt concentrations. **(a)** Growth curve of *E. coli* ATCC 25922 grown in MHB 0 mM NaCl (blue line) and MHB 150 mM NaCl (red line); **(b)** Growth curve of *E. coli* ((clinical isolate) LACEN 9921447) grown in MHB 0 mM NaCl (blue line) and MHB 150 mM NaCl (red line). The points represent the mean density of the reading of three independent replicates. The error bars represent the standard deviation of the mean. The tables inform the CFUs obtained for each strain under different conditions.

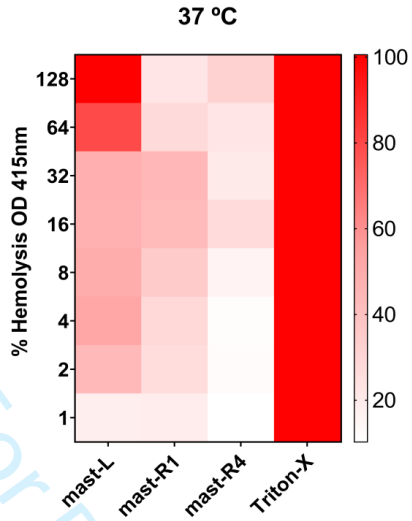

Figure S3. Hemolytic assay. The hemolytic activity of mastoparan-L, mastoparan-R1 and mastoparan-R4 was evaluated using murine erythrocytes. Triton-X 1% was used as positive controls.

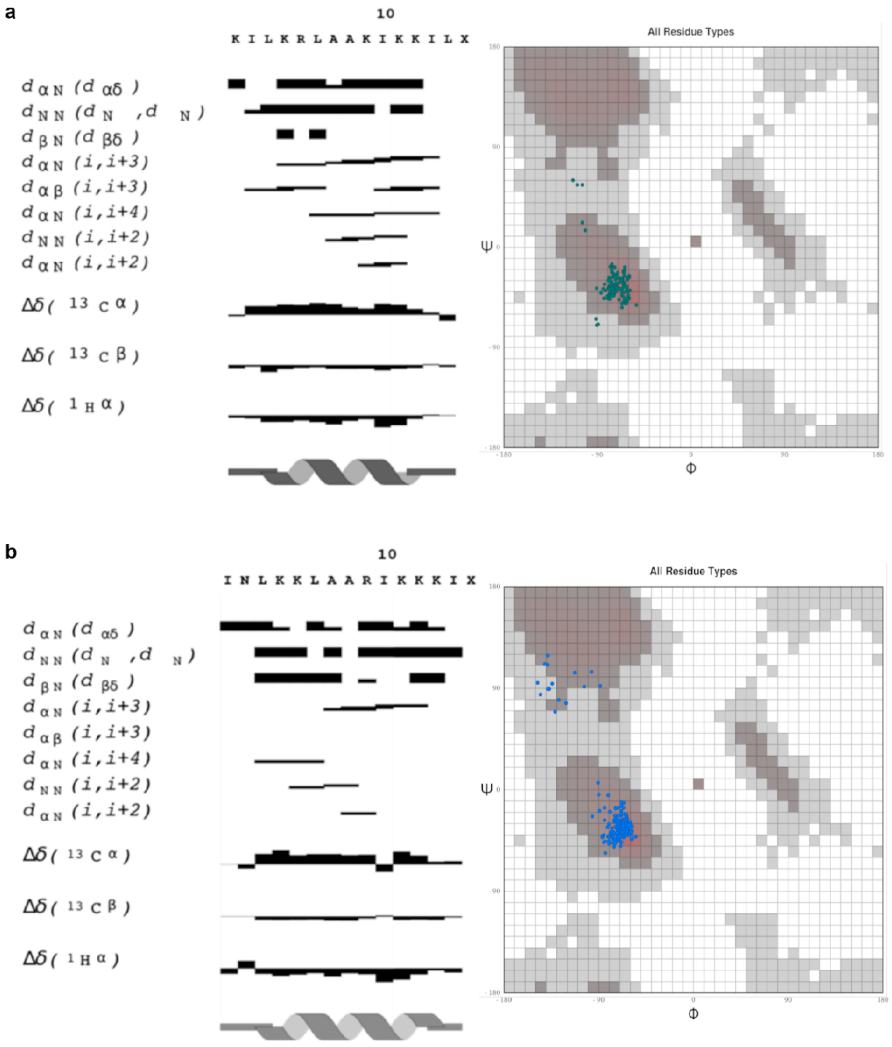

Figure S4. Sequential, short, and medium range NOE connectivity for mastoparan-R1 **(a)** and mastoparan-R4 **(b)** in 75 mM SDS-*d25* micelles. The peptide sequence is described at the top with the one-letter code ("X" is used to represent the C-terminal amidation). The chart presents the NOE connectivity, the variation of secondary chemical shift assigned for the resonances $^{13}C\alpha$, $^{13}C\beta$ and $^{1}H\alpha$ (difference to random coil value) and the predicted secondary structure. Ramachandran plot of the 10 lowest-energy solution NMR structures of mastoparan-R1 and mastoparan-R4.

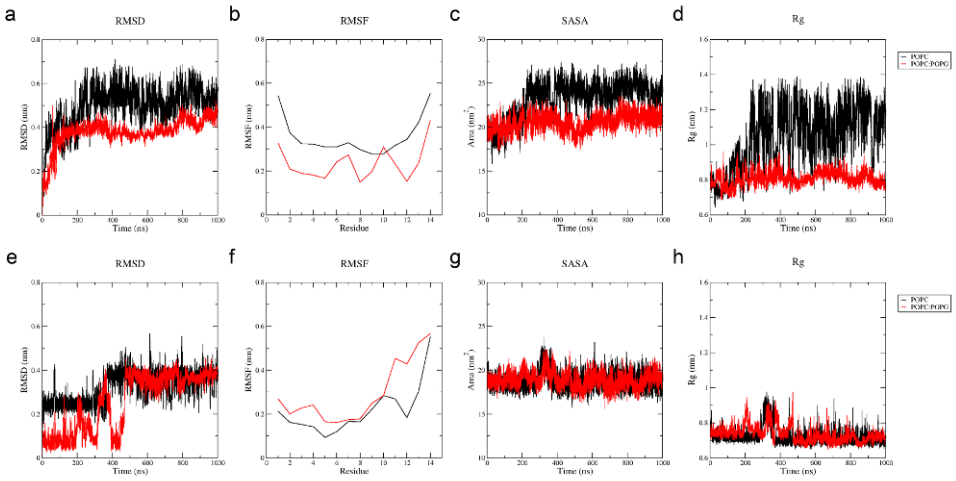

Figure S5. MD simulation analyses for mastoparan-R1 and R4 were carried out in contact with POPC and POPC:POPG (4:1) bilayers with 150 mM NaCl. Analysis for mastoparan-R1 included **(a)** root mean square deviation (RMSD), **(b)** root mean square fluctuation (RMSF), **(c)** solvent accessible area (SASA), **(d)** radius of gyration (Rg); Analysis for mastoparan-R4 included **(e)** RMSD **(f)** RMSF **(g)** SASA **(h)** Rg.

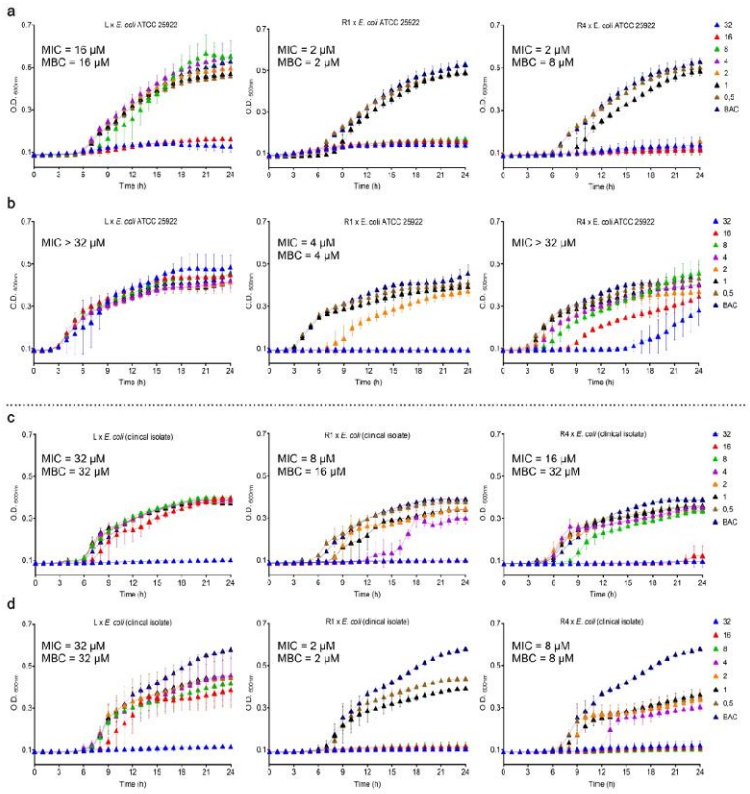

Figure 1. Bacterial growth curves and minimum inhibitory concentration values for mastoparan-L, R1 and R4 from 32 to 0.5 µM, over 24 h, at 30 min intervals. (a) Mastoparan peptides against *E. coli* ATCC 25922 in MHB, and (b) against *E. coli* ATCC 25922 in 150 mM NaCl supplemented MHB. (c) Mastoparan peptides against *E. coli* (clinical isolate – LACEN 9921447) in MHB, and (d) against *E. coli* (clinical isolate – LACEN 9921447) in 150 mM NaCl supplemented MHB. The color legend denotes the concentrations (µM) and growth control (BAC) of the experiments.

284x307mm (300 x 300 DPI)

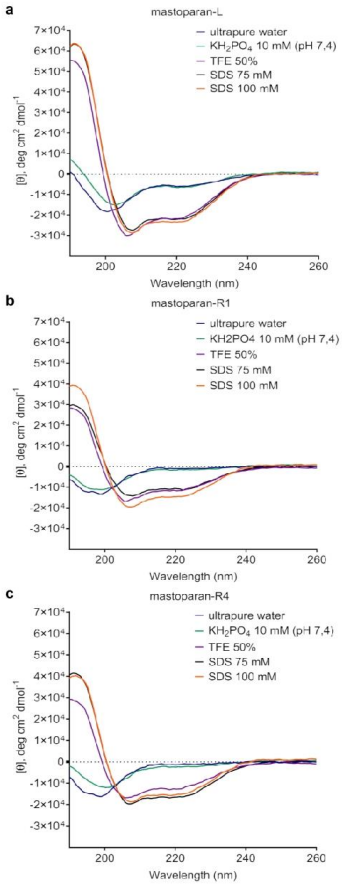

Figure 2. Mastoparan-L, R1 and R4 circular dichroism analysis. CD spectra were recorded in ultrapure water, 10 mM potassium phosphate buffer (KH2PO4, 10 mM (pH 7.4)), 50 % TFE in water (v/v), 75 mM SDS, and 100 mM SDS. In (a) CD spectra for mastoparan-L, (b) mastoparan-R1 and (c) mastoparan-R4.

325x755mm (118 x 118 DPI)

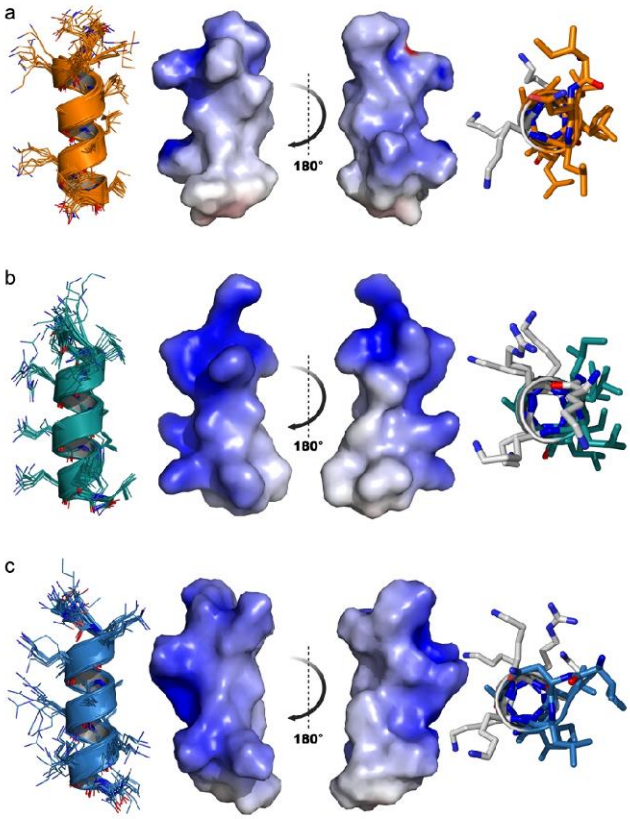

Figure 3. NMR structures of mastoparan-L, R1 and R4. The 3D structures of mastoparan-R1 and R4 were elucidated through NMR spectroscopy in 75 mM SDS-d25. The sequence of figures horizontally from left to right are: (i) Superposition of the 10 lowest energy structures of mastoparan-L (PDB: 6DUL) in orange (a), R1 (PDB: 8EP5) in green (b), and R4 (PDB: 8ERU) in blue (c) in the presence of 75 mM of SDS-d25 micelles. (ii) Lowest free energy model in Adaptive Poisson−Boltzmann solver (APBS) electrostatic potential of peptides with potential ranging from −5 kT/e (red) to +5 kT/e (blue) in 0° and 180° of rotation. (iii) Front view of the inside of the α-helix, showing the cationic face and the hydrophobic face and the cationic residues are in gray.

209x297mm (300 x 300 DPI)

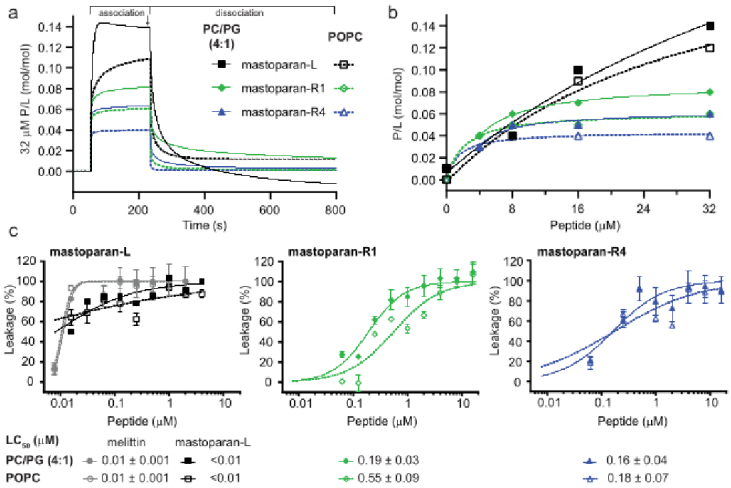

Figure 4. Peptide-lipid binding and membrane-lytic properties of mastoparan-L and analogs mastoparan-R1 and R4. The lipid-binding affinity of each peptide was determined for bilayers composed of POPC and POPC/POPG (PC/PG) (4:1). SPR sensorgrams were obtained for peptides injected over lipid bilayers deposited on an L1 chip for 180 s with dissociation monitored for 600 s. Response units (RU) at the end of the association phase were converted to peptide to lipid ratios (P/L mol/mol) by converting RU to moles of peptide and normalized to the amount of lipid deposited on the lipid surface (1 RU = 1 pg/mm2 of peptide or lipid). (a) Representative sensorgrams for 32 µM peptide show peptide-lipid association (50 – 230 s) and dissociation (280 – 800 s). (b) peptide to lipid ratios (P/L, mol/mol) recorded at the end of the association phase (indicated by arrow) were used to plot dose response curves, by fitting [inhibitor] vs response in GraphPad Prism v9. (c) Peptide-induced membrane lysis was examined by measuring the leakage of CF, from LUVs. Leakage induced by Triton X-100 (100 %) and buffer (0 %) were used to calculate % leakage induced by the peptides. Dose-response curves were fitted with [inhibitor] vs response with variable slope in GraphPad Prism v9. Data represents three technical replicates.

435x288mm (39 x 39 DPI)

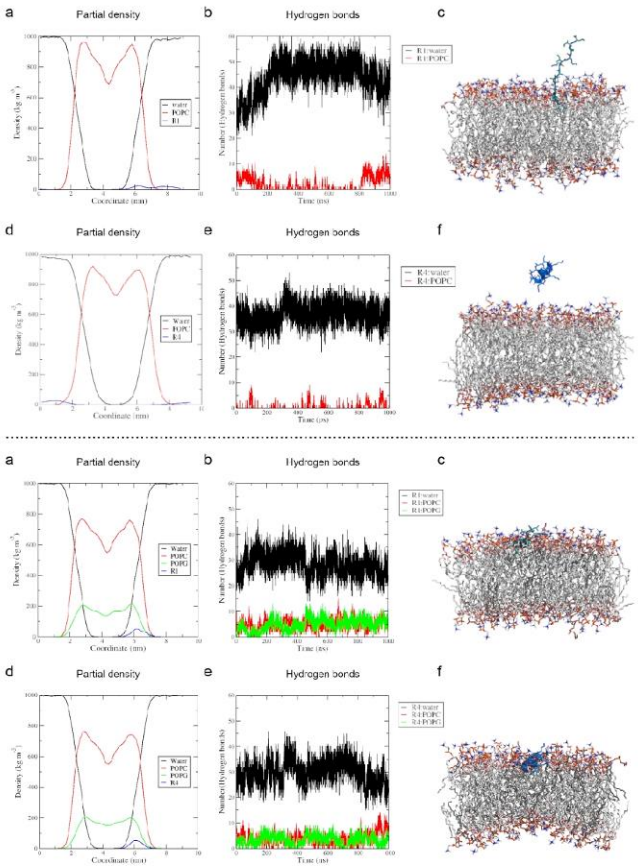

Figure 5. MD analyses of peptide interaction with POPC and POPC/POPG (4:1) bilayers. Partial density profile obtained in the last 0.1 μs of MD simulations; hydrogen bonds over 1 μs of the analysis and the snapshot plotted at 1 μs of MD simulations. Interaction with POPC for mastoparan-R1 (a) and mastoparan-R4 (b) interaction with POPC/POPG (4:1) for mastoparan-R1 (c) and mastoparan-R4 (d).

533x755mm (118 x 118 DPI)

5. ARTIGO DE REVISÃO

Artigo 2 publicado na revista *Frontiers in Microbiology*

(DOI:10.3389/fmicb.2019.02169).

Peptídeos bioativos contra biofilmes fúngicos

Resumo: Infecções causadas por biofilmes fúngicos invasivos têm sido amplamente associadas a altas taxas de morbidade e mortalidade, principalmente devido ao advento da resistência a antibióticos. Além disso, os biofilmes fúngicos impõem um desafio adicional, levando à resistência a múltiplas drogas. Este fato, juntamente com a contaminação de dispositivos médicos e o número limitado de agentes antifúngicos eficazes disponíveis no mercado, demonstra a importância de encontrar novos candidatos a medicamentos direcionados a células fúngicas e biofilmes patogênicos. Nesse contexto, uma estratégia alternativa é o uso de peptídeos antifúngicos (AFPs) contra biofilmes fúngicos. Os AFPs são considerados um grupo de moléculas bioativas com atividades de amplo espectro e múltiplos mecanismos de ação que têm sido amplamente utilizados como moléculas modelo para estratégias de design de medicamentos visando maior especificidade e eficácia biológica. Dentre as classes de AFP mais estudadas no contexto de biofilmes fúngicos, têm sido descritas defensinas, catelicidinas e histatinas. Os AFPs também podem atuar prevenindo a formação de biofilmes fúngicos e erradicando biofilmes pré-formados por meio de mecanismos associados à perturbação da parede celular, inibição da adesão de células fúngicas planctônicas em superfícies, regulação de genes e geração de espécies reativas de oxigênio (ROS). Assim, considerando o cenário crítico imposto por biofilmes fúngicos e infecções associadas e a aplicação de AFPs como um possível tratamento, esta revisão se concentrará nos peptídeos antifúngicos mais eficazes descritos até o momento, com foco central nos peptídeos antibiofilmes, bem como em sua eficácia *in vivo*, aplicação em superfícies e mecanismos de ação propostos.

frontiers in Microbiology

REVIEW
published: 04 October 2019
doi: 10.3389/fmicb.2019.02169

Bioactive Peptides Against Fungal Biofilms

*Karen G. N. Oshiro[1,2], Gisele Rodrigues[3], Bruna Estéfani D. Monges[2], Marlon Henrique Cardoso[2,3] and Octávio Luiz Franco[1,2,3]**

[1] *Programa de Pós-Graduação em Patologia Molecular, Faculdade de Medicina, Universidade de Brasília, Brasília, Brazil,* [2] *S-Inova Biotech, Programa de Pós-Graduação em Biotecnologia, Universidade Católica Dom Bosco, Campo Grande, Brazil,* [3] *Centro de Análises Proteômicas e Bioquímicas, Programa de Pós-Graduação em Ciências Genômicas e Biotecnologia, Universidade Católica de Brasília, Brasília, Brazil*

Infections caused by invasive fungal biofilms have been widely associated with high morbidity and mortality rates, mainly due to the advent of antibiotic resistance. Moreover, fungal biofilms impose an additional challenge, leading to multidrug resistance. This fact, along with the contamination of medical devices and the limited number of effective antifungal agents available on the market, demonstrates the importance of finding novel drug candidates targeting pathogenic fungal cells and biofilms. In this context, an alternative strategy is the use of antifungal peptides (AFPs) against fungal biofilms. AFPs are considered a group of bioactive molecules with broad-spectrum activities and multiple mechanisms of action that have been widely used as template molecules for drug design strategies aiming at greater specificity and biological efficacy. Among the AFP classes most studied in the context of fungal biofilms, defensins, cathelicidins and histatins have been described. AFPs can also act by preventing the formation of fungal biofilms and eradicating preformed biofilms through mechanisms associated with cell wall perturbation, inhibition of planktonic fungal cells' adhesion onto surfaces, gene regulation and generation of reactive oxygen species (ROS). Thus, considering the critical scenario imposed by fungal biofilms and associated infections and the application of AFPs as a possible treatment, this review will focus on the most effective AFPs described to date, with a core focus on antibiofilm peptides, as well as their efficacy *in vivo*, application on surfaces and proposed mechanisms of action.

Keywords: antifungal peptides, fungal infections, fungal biofilms, antimicrobial peptides, mechanisms of action

OPEN ACCESS

Edited by:
Jose F. Marcos, Instituto de Agroquímica y Tecnología de Alimentos (IATA), Spain

Reviewed by:
Anand K. Ramasubramanian, San Jose State University, United States
Dilip Shah, Donald Danforth Plant Science Center, United States

****Correspondence:***
Octávio Luiz Franco
ocfranco@gmail.com

Specialty section:
This article was submitted to Fungi and Their Interactions, a section of the journal Frontiers in Microbiology

Received: *26 March 2019*
Accepted: *04 September 2019*
Published: *04 October 2019*

Citation:
Oshiro KGN, Rodrigues G, Monges BED, Cardoso MH and Franco OL (2019) Bioactive Peptides Against Fungal Biofilms. Front. Microbiol. 10:2169. doi: 10.3389/fmicb.2019.02169

INTRODUCTION

Fungal infections are recurrent in the clinical environment and, annually, affect ~25% of the general population worldwide, causing high morbidity and mortality rates (Brown et al., 2012; Gamaletsou et al., 2018). The indiscriminate use of broad-spectrum antibiotics, along with parenteral nutrition, permanent catheters, chemotherapy and radiotherapy, as well as immunosuppression in patients, are the most important predisposing factors for invasive fungal

Abbreviations: AFM, atomic force microscopy; AFPs, antifungal peptides; AMPs, antimicrobial peptides; BIC, biofilm inhibition concentration; BIC50, concentration required to reduce biofilm formation by 50%; Csf, caspofungin; GlcCer, glucosylceramide; Mcf, micafungin; MFC, minimal fungicidal concentration; MIC, minimal inhibitory concentration; PI, phosphatidylinositol.

infections (Lionakis and Levitz, 2018). Fungi are classified according to their morphologies, including yeasts (*Cryptococcus* spp.), fungi with branched hyphae (*Aspergillus* spp./*Rhizopus* spp.), as well as fungi with both morphologies (yeasts and pseudohyphas, as for *Candida* spp.), which have all been associated with fungal infections in humans (Brown et al., 2012; Lionakis and Levitz, 2018). In addition, fungal pathogens can also organize multicellular consortia, known as biofilms, which establish resistant communities on a variety of biotic and abiotic surfaces (Nett and Andes, 2015). Fungal adhesion to biotic and abiotic surfaces represents an initial stage by which fungi establish biofilms. Consequently, this cellular mechanism has been investigated as a potential target for antibiofilm therapies (Nett and Andes, 2015).

Fungal Biofilms

Apart from their planktonic development, microorganisms can also establish biofilms in nature, and these biofilms allow microbial cells to survive in the host environment and be dispersed to colonize new niches (Hall-Stoodley et al., 2004). Fungal biofilms are composed of adherent cells covered by an extracellular matrix. First, free-floating cells adhere to a substrate followed by the secretion of an extracellular matrix, which confers additional mechanical protection on the fungal colonies. The release of biofilm cells is a regulated process by which organisms can spread throughout the host and establish new sites of infection (Nett et al., 2010; Uppuluri et al., 2010).

Studies have shown that biofilm-constituting cells usually present a different phenotype from that presented by planktonic cells. Among these differences, the elaborate architecture of biofilms has been highlighted as an additional challenge in the treatment of patients with systemic infections, mainly due to fungi's increased resistance to conventional antibiotics and lower performance of the host immune system (Gulati and Nobile, 2016). Medical devices, including catheters and artificial heart valves, are in constant contact with body fluids, facilitating glycoprotein substrate deposition and favoring fungal cell adhesion, followed by their colonization and biofilm formation (Giles et al., 2018). Biofilm formation has been well described in *Candida albicans*, the most common fungal pathogen in the hospital setting (Douglas, 2002). *C. albicans* biofilms are composed of yeast and hyphalic cells, both of which are necessary for biofilm formation on biotic and abiotic surfaces (Dongari-Bagtzoglou et al., 2009; Harriott et al., 2010). Moreover, *Aspergillosis* and *Cryptococcus neoformans* biofilms are among the major causes of nosocomial infections caused by fungi (Ajesh and Sreejith, 2012; Kaur and Singh, 2013).

Overview on Antifungal Peptides (AFPs)

Currently, antifungal therapies are scarce and include only four chemical classes of antifungal agents, namely polyenes, triazoles, echinocandins and flucytosine (Chowdhary et al., 2017). Moreover, the misuse of antifungal agents over the last two decades has contributed to antifungal resistance development (Perlin et al., 2017). Fungal resistance emergence has important clinical implications, as it limits the already small arsenal of antifungal agents, raising the idea of a "post-antifungal" era (Chowdhary et al., 2017). Therefore, an alternative is the use of AFPs against fungal infections and biofilms (Matejuk et al., 2010). AFPs have been tested as promising therapeutic agents for biofilm-related infections (Di Luca et al., 2014). In this context, AFPs have been considered a bioactive molecule group with broad-spectrum activities and multiple mechanisms of action. The search for AFPs capable of acting on fungal biofilms with lower toxic effects on mammalian cells either alone or in combination with conventional antibiotics has been the subject of diverse studies (Fjell et al., 2012). Although biofilm-active AFPs have not been achieved in clinical and commercial use, the development, design and optimization of such molecules remain as an alternative treatment (Duncan and O'Neil, 2013).

Antifungal peptides are structurally diverse. Moreover, AFPs comprise amphipathic molecules capable of interacting with biological membranes (De Lucca and Walsh, 1999; Faruck et al., 2016; Rautenbach et al., 2016). In the past decade, an increasing number of works have reported AFPs capable of either inhibiting fungal biofilm formation or eradicating preformed biofilms, as well as some AFPs with both inhibitory and eradication properties (Matejuk et al., 2010; Delattin et al., 2017). Most AFPs display their biological activities through membrane-associated mechanisms of action. When compared to other eukaryotic cells (e.g., mammalian cells), fungal membranes present few differences, including sphingolipid composition, PI content and the presence of ergosterol as the main sterol (Rautenbach et al., 2016). These differences, along with specific targets in the fungal pathogen, including fungal proteins, mannosyldiinositol phosphorylceramide and GlcCer, provide useful information for the generation of selective AFPs, avoiding toxicity toward human cells (Rautenbach et al., 2016). In this context, this review will focus on the therapeutic potential of AFPs, highlighting the most effective AFPs described to date, with a core focus on antibiofilm properties. Finally, we will explore the application of AFPs and their proposed antibiofilm mechanisms of action.

PEPTIDES WITH DELETERIOUS ACTIVITY TOWARD FUNGAL BIOFILMS

Defensin-Like Peptides

Defensins comprise AFPs isolated from various organisms, including plants and mammals (Cools et al., 2017a). Structurally, defensins are organized in an αβ motif, generally with an α-helix and a triple-stranded antiparallel β-sheet, which is stabilized by disulfide bonds that ensure high stability, thus retaining their functions under extreme conditions by avoiding/decreasing degradation (Shafee et al., 2016). Many defensins share the CSαβ motif, including plants, fungi and invertebrates. Therefore, the following subsections will address the structural characteristics, activity and mechanism of action of plant defensins, α-defensins and β-defensins on fungal biofilms.

Plant Defensins

Plant defensins are cationic and have 45–54 amino acids in length. These peptides have typically been isolated from seeds, but can also be found in other plant tissues including leaves,

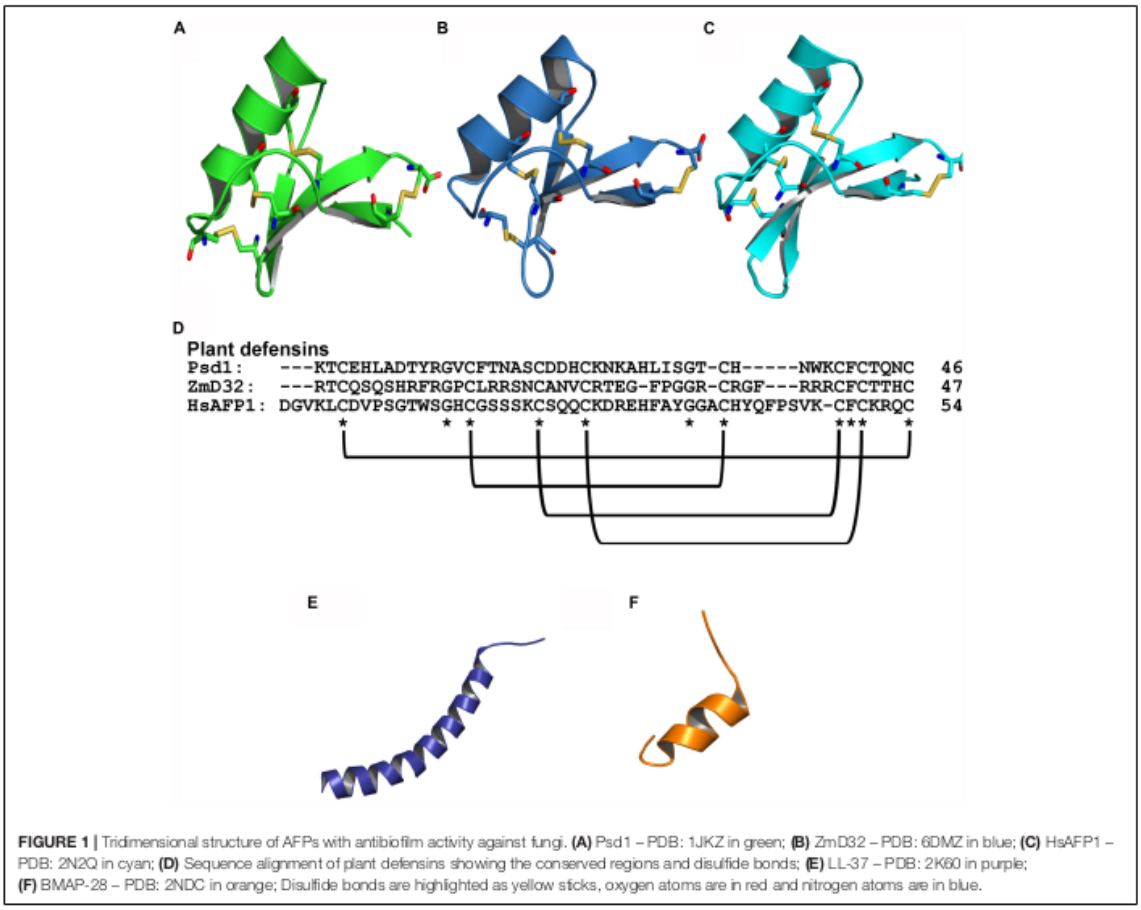

FIGURE 1 | Tridimensional structure of AFPs with antibiofilm activity against fungi. **(A)** Psd1 – PDB: 1JKZ in green; **(B)** ZmD32 – PDB: 6DMZ in blue; **(C)** HsAFP1 – PDB: 2N2Q in cyan; **(D)** Sequence alignment of plant defensins showing the conserved regions and disulfide bonds; **(E)** LL-37 – PDB: 2K60 in purple; **(F)** BMAP-28 – PDB: 2NDC in orange; Disulfide bonds are highlighted as yellow sticks, oxygen atoms are in red and nitrogen atoms are in blue.

flowers, roots and stems (Lay and Anderson, 2005). Most of the plant defensins identified so far have eight cysteine residues that favor structural stability by the formation of four disulfide bonds. In addition, structural studies have shown that plant defensins comprise a triple β-sheet with a parallel helix (Thomma et al., 2002) (**Figure 1**). Regarding their biological properties, plant defensins have shown activity against bacteria (Sathoff and Samac, 2019) and fungi, both in their planktonic and biofilm modes of growth (Vriens et al., 2016; Gonçalves et al., 2017).

Psd1, for instance, is a plant defensin first isolated from *Pisum sativum seeds*, which has shown promising effects on *C. albicans* planktonic cells and biofilm (Gonçalves et al., 2017). Confocal microscopy and AFM analyses revealed that Psd1, at 20 μM, eradicates *C. albicans* planktonic cells; however, total inhibition or partial eradication of biofilms were observed at a concentration 10 x greater than the inhibitory value (approximately 200 μM) (Gonçalves et al., 2017). One of the main differences between mammalian and fungal cells is the presence of a cell wall in the latter. Thus, to access the fungal membrane, AFPs have first to interact with cell wall and plasma membrane components, which include sphingolipids, chitin, β-glucans and mannoproteins. The glycosphingolipid GlcCer, for instance, has been reported as a crucial plasma membrane component for anticandidal activity (planktonic cells and biofilms) of plant defensins (Aerts et al., 2008; Gonçalves et al., 2017). Psd1 acts on *C. albicans* biofilms by disaggregating the polysaccharide matrix of the cell wall (increasing cell roughness and decreasing its rigidity), followed by membrane permeabilization via interaction with GlcCer (Gonçalves et al., 2017). Once inside the fungal cells, Psd1 accumulation triggers an intracellular mechanism of action by interrupting the cell cycle, leading to apoptosis (Gonçalves et al., 2017). These mechanisms allowed Psd1 to decrease *C. albicans* planktonic cells' adhesion, leading to the inhibition of biofilm formation, along with the eradication of preformed biofilms (**Figures 2A,C**).

In addition to Psd1, other plant defensins from *Heuchera sanguinea* coral bell seeds, named HsAFP1 and HsAFP2, have displayed deleterious antifungal activities against pathogenic fungi (Osborn et al., 1995; Aerts et al., 2011). Interestingly, HsAFP1 has been produced by heterologous expression using the yeast *Pichia pastoris*, and further denominated rHsAFP1 (r - recombinant). rHsAFP1 has shown inhibitory activity against

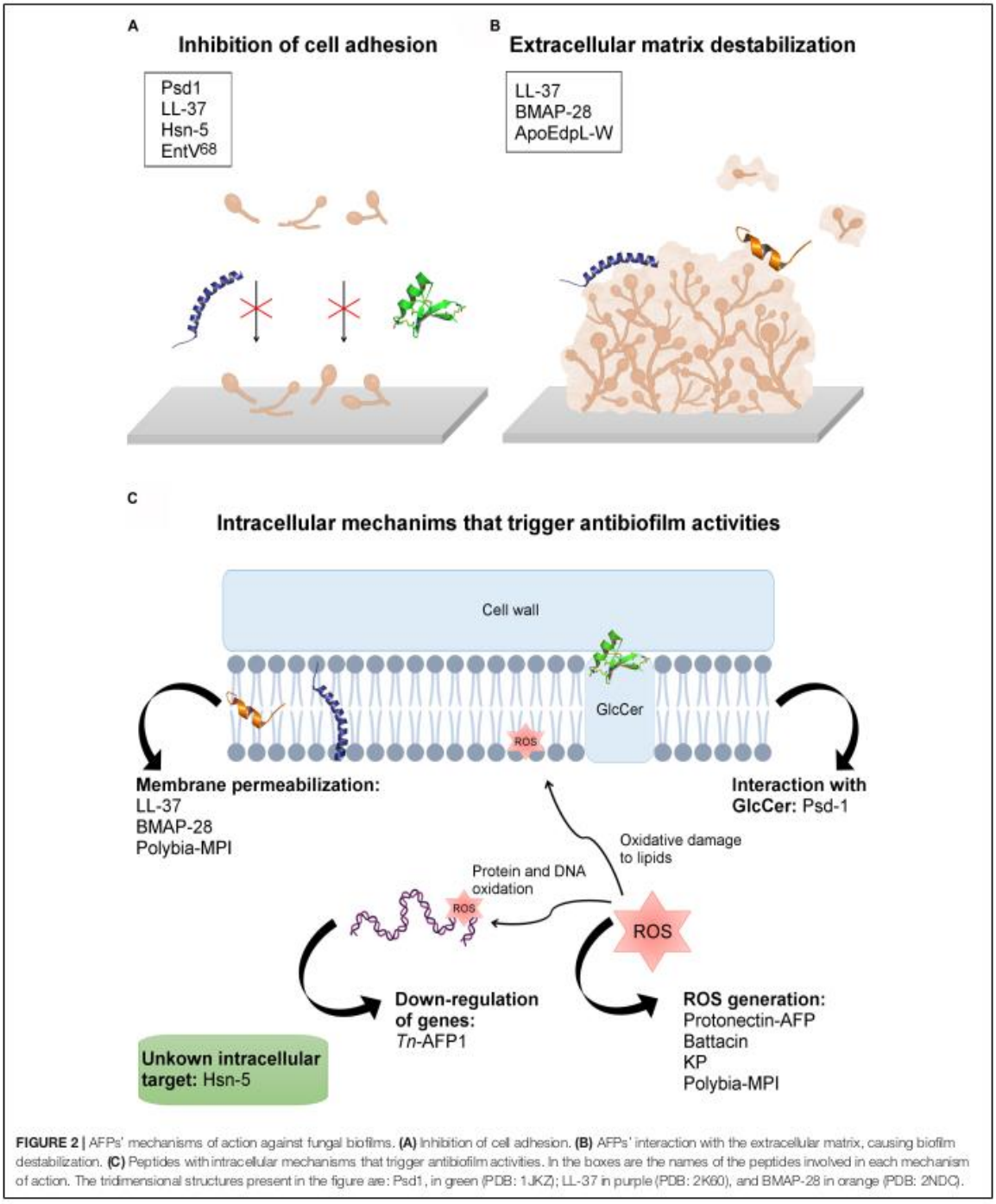

FIGURE 2 | AFPs' mechanisms of action against fungal biofilms. **(A)** Inhibition of cell adhesion. **(B)** AFPs' interaction with the extracellular matrix, causing biofilm destabilization. **(C)** Peptides with intracellular mechanisms that trigger antibiofilm activities. In the boxes are the names of the peptides involved in each mechanism of action. The tridimensional structures present in the figure are: Psd1, in green (PDB: 1JKZ); LL-37 in purple (PDB: 2K60), and BMAP-28 in orange (PDB: 2NDC).

planktonic *C. albicans* with a value for its MIC 50 (half maximal inhibitory concentration – 50%) of 18 μM. In addition, the minimal BIC50 was 11 μM (Vriens et al., 2015). In another study, 44 linear peptides derived from HsAFP1 were identified, among which the peptide HsLin06_18 showed antifungal activity (Cools et al., 2017b). This peptide (HsLin06_18) was evaluated against biofilms of *C. albicans*, obtaining a BIC value >2 μM. Interestingly, however, when in synergism with Csf this value

(BIC) is reduced to 0.5 μM. In another study, a plant defensin isolated from *Raphanus sativus* antifungal protein 2 (RsAFP2) has also been expressed in *P. pastoris*. The recombinant peptide, rRsAFP2, has been proved to prevent *C. albicans* biofilm formation 330 μM (BIC). In contrary, rRsAFP2 is not capable of eradicating *C. albicans* biofilm (Vriens et al., 2016).

Plant defensins represent a large class of AFPs that exhibit remarkable stability at extreme pH and elevated temperature, as well as resistance to protease digestion (Kerenga et al., 2019). Kerenga et al. (2019) carried out a screening for plant defensin sequences in a database with more than 1,200 plant defensins, and identified a *Zea mays* defensin, named ZmD32, with the highest charge (+10) at pH 7. In this context, the objective of the work was to evaluate whether ZmD32 with an increased positive charge would retain the activity of the parent peptide at higher salt concentrations. It was observed that ZmD32 retained activity against a variety of fungal species in media containing high salt concentrations. In addition, ZmD32 has been shown to be multifunctional, as this peptide acted on fungi and on Gram-negative and Gram-positive bacteria. Moreover, the most prominent activity was observed against *C. albicans* biofilms, as ZmD32 eliminated biofilm viable cells from 20 to 40 μM at a physiological sodium concentration (132.1 mM). These findings demonstrate the potential of ZmD32 as a candidate for antifungal therapies (Kerenga et al., 2019).

α-Defensin

Defensins from vertebrate animals are cationic and amphipathic peptides containing 18–45 amino acid residues. These defensins have been divided into two subfamilies named α and β-defensins (Parisi et al., 2019). Human peptides have been isolated from neutrophils, playing important roles in processes related to host defense (Szyk et al., 2006; Jarczak et al., 2013). These peptides are cationic (arginine rich), with 3–5 kDa molecular masses, and they are stabilized by disulfide bonds (generally three) (Szyk et al., 2006). Human α-defensins have tertiary structure, and these defensins have a short helix structure and β-sheet stabilized by three disulfide bonds (Szyk et al., 2006).

An example of an α-defensin studied for its antifungal actions was human α-defensin 6 (HD6). This peptide demonstrated a blocking action of *C. albicans* adhesion in human intestinal epithelial cells, and treatment with HD6 at concentrations of 10 or 20 μM resulted in the prevention of biofilm formation (Chairatana et al., 2017). Some HBDs (e.g., HBD 2, 3, and 4) present antimicrobial properties and, in some cases (Krishnakumari et al., 2009) antifungal activities have been reported (Dhople et al., 2006; Krishnakumari et al., 2009). For instance, the α-defensin 6 (HD6) has demonstrated the potential to block *C. albicans* cells' adhesion on human intestinal epithelial cells. Moreover, the treatment with HD6, at 10 or 20 μM, resulted in the prevention of biofilm formation (Chairatana et al., 2017).

β-Defensin

β-defensins comprise a large family of AMPs distributed in plants, mammals and insects. These cysteine-rich peptides are cationic and present approximately 45 amino acid residues (Taylor et al., 2008). The tertiary structures of β-defensins resemble α-defensin, the difference being in the position of the disulfide bonds responsible for stabilizing the β-sheet (Szyk et al., 2006; Shafee et al., 2016). Moreover, β-defensins have been reported for their multifunctional properties, including antifungal and antifungal biofilm activities (Taylor et al., 2008).

β-defensins comprise the majority of human defensins described with fungal antibiofilm activity. β-Human defensins (HBDs) are cationic peptides expressed in inflamed dental pulp (Paris et al., 2009). Similarly, different synthetic defensin-like peptides, including α-defensin-3, β-defensin-1, β-defensin-3 and PG-1, have demonstrated potent antifungal activity against *C. neoformans* biofilms. These peptides were effective against planktonic cells and mature biofilms, whereas PG-1, at 8 μM, reduced the survival percentage of cryptococcal biofilms by approximately 50%. β-defensin-1, at the same concentration, reduced biofilm survival by 60%, whereas α-defensin-3 and β-defensin-3 reduced biofilm survival by approximately 30% (Martinez and Casadevall, 2006). Interestingly, a 15-amino acid residue peptide derived from the C-terminus region of the human defensin 3 (HBD3-C15) has also revealed antifungal activity in a dose-dependent manner (28.3 – 169.8 μM) against *C. albicans* biofilm when evaluated on dentin disks (Lim et al., 2016).

The AFPs here cited are mainly active against *C. albicans* and *C. neoformans*. Plant defensins are stable AFPs with antifungal action and are capable of inhibiting biofilm formation, as well as eradicating preformed biofilms. In addition, these AFPs have also been proved to act in synergism with conventional antifungal agents, including HsLin06_18 peptide in combination with Csf, which acts on *C. albicans* biofilm formation (Vriens et al., 2016). Although these defensins have been proved to prevent fungal cell adhesion and, consequently, biofilm formation, more detailed studies regarding their antifungal biofilm activities are still scarce (van der Weerden et al., 2010). Therefore, further investigations with α-defensins are needed to demonstrate the real potential and mechanisms of action for this class of AFP. The same could be expected for β-defensins, which are active against fungal planktonic cells and biofilms, although the mechanisms by which they operate on different cellular organizations have not been yet elucidated. Thus, the findings here summarized, especially for plant defensins, represent an attractive field for further structure-function studies, aiming at correlating some of the already available tridimensional structures with AFPs' mechanisms of action and, finally, identifying determinants for the generation of optimized AFPs that specifically target fungal biofilms. The AFPs described in the Defensin-like peptides section, their respective antibiofilm activities, and their proposed mechanisms of action are summarized in **Table 1**.

Cathelicidins

Peptides from the cathelicidin family have been isolated from different species of mammals and exhibit broad-spectrum activities against fungi (Zanetti, 2004). Cathelicidins are characterized as cationic peptides, consisting of 12–80 amino acids that adopt an α-helix or β-sheet as secondary structures, most of which have 23–37 amino acid residues distributed in amphipathic helices, including LL-37 and BMAP-28 (**Figure 1**) (Zanetti et al., 1995; Gennaro and Zanetti, 2000).

TABLE 1 | Defensin-like peptides against pathogenic fungi and biofilms and their proposed mechanisms of action.

Peptide	Source	Activity	Concentration (μM)	Pathogen	Mechanism of actions	References
Psd1	*P. sativum* seeds	Biofilm inhibition	~ 200	*C. albicans*	Cell cycle interruption, leading to apoptosis	Gonçalves et al., 2017
rHsAFP1	*H. sanguinea* coral bell seeds (r - recombinant)	Biofilm inhibition	BIC50* 11	*C. albicans*	Not determined	Vriens et al., 2015
rRsAFP2	*H. sanguinea* coral bell seeds (r - recombinant)	Biofilm inhibition	BIC* 330	*C. albicans*	Not determined	Vriens et al., 2016
HsLin06_18	Derived from rHsAFP1	Biofilm inhibition	BIC* > 2; and 0.5 synergism with Csf	*C. albicans*	Not determined	Cools et al., 2017b
ZmD32	*Z. mays*	Biofilm inhibition	20 – 40	*C. albicans*	Not determined	Kerenga et al., 2019
HD6	Human defensin	Biofilm inhibition	10 – 20	*C. albicans*	Not determined	Chairatana et al., 2017
β-defensin 1, β-defensin 3, PG-1	Human defensins	Biofilm inhibition	8	*C. neoformans*	Not determined	Martinez and Casadevall, 2006
HBD3-C15	Human defensin	Biofilm inhibition	Dose-dependent (28,3 – 169,8)	*C. albicans*	Not determined	Lim et al., 2016

*References values for each experiment, which can be: BIC, biofilm inhibition concentration; BIC50, concentration required to reduce biofilm formation by 50%.

The activities of LL-37 and BMAP-28 have been investigated against *Candida* spp. strains (clinical isolates of vaginal infections) in terms of planktonic cells' growth inhibition and interference in fungal cell adhesion on polystyrene and silicone surfaces (biofilm formation) (Scarsini et al., 2015). LL-37, at 64 μM, was capable of inhibiting *C. albicans* cell adhesion on the tested surfaces (Scarsini et al., 2015). In that same work, BMAP-28, at 16 μM, was capable of inhibiting 70–90% of *C. albicans* and *Candida krusei* mature biofilms. BMAP-28 also reduced the number of *C. albicans* adherent cells on silicone surfaces, indicating its usage as an antifungal agent in coaching strategies (medical devices) (Scarsini et al., 2015). In addition to LL-37 and BMAP-18, a peptide derived from a cathelicidin-related AMP (CRAMP), named AS10, inhibited *C. albicans* biofilm formation at 0.22 μM (De Brucker et al., 2014). Furthermore, in synergism with Csf or amphotericin B, AS10 also acted on *C. albicans* mature biofilms (De Brucker et al., 2014). In that same work, another peptide, named P318, demonstrated even higher antifungal activity (0.15 μM) against *C. albicans* biofilms, without affecting planktonic cells' survival (De Brucker et al., 2014).

The human cathelicidin LL-37 inhibits *C. albicans* adhesion and aggregation (2.2 and 4.5 μM) on biotic and abiotic surfaces by interacting with chitin, glucan and, especially, mannan present in the cell wall of this pathogen (**Figure 2C**) (Tsai et al., 2011). This ability has also been emphasized as a crucial mechanism by which LL-37 inhibits *C. albicans* biofilm formation on both medical devices and biological tissues in the course of *C. albicans* infections (Tsai et al., 2011). Moreover, to evaluate whether LL-37 interaction with mannan is selective for *C. albicans* or not, this AFP was also tested regarding its ability to interact with *Saccharomyces cerevisiae* mannan. As a result, LL-37 was not recovered by mannan from *S. cerevisiae* and, therefore, this AFP had no influence on cell aggregation and cell adhesion in this fungal strain (**Figure 2A**) (Tsai et al., 2011). It is known that the main difference between *C. albicans* and *S. cerevisiae* mannan is the presence of β-1,2 linkages in the first one (Shibata et al., 1985). This exclusive feature in *C. albicans* mannan was also proposed in that work (Tsai et al., 2011) as an important factor for LL-37 cell adhesion inhibitory potential, highlighting the application of this AFP in antibiofilm strategies.

Cathelicidins are peptides that are well described in the literature for their broad-spectrum activities and relatively stable structures. Cathelecidins have potential for the development of drugs that could be used on medical devices to combat fungal biofilms. Furthermore, the studies cited here demonstrate that this class can act synergistically with the conventional antifungal agents, rendering these peptides a promising starting point for future combinatorial therapies. The AFPs described in this section, their respective antibiofilm activities, and their proposed mechanisms of action are summarized in **Table 2**.

Histatins

Human salivary histatins are a group of small histidine-rich proteins constituted from 7 to 38 amino acids first isolated from human parotid saliva (Oppenheim et al., 1988). In general, histatins are a multifunctional group of proteins with antimicrobial properties that vary from broad-spectrum to moderate activities (Troxler et al., 1990). Moreover, histatins have been reported for their effective antifungal activity (Troxler et al., 1990; Tsai and Bobek, 1998). Histatins are divided into three major peptides, named histatin-1, histantin-3 and histatin-5, varying from 24 to 38 amino acid residues in length. They are polar and hydrophilic peptides presenting an α-helical structural conformation in organic solutions (Oppenheim et al., 1988). Therefore, histatin peptides have promising antifungal activities and their membrane affinity has been studied in the context of fungal infections (Brewer et al., 1998).

It is known that diverse pathogenic fungi can form biofilms on polymer surfaces, oral prostheses and medical devices. In that

context, the activity of the Hst-5 peptide has been evaluated against *C. albicans* biofilms (CAI-4), demonstrating that this peptide, at 50 μM, inhibited biofilm formation on acrylic dentures *in vitro* (Pusateri et al., 2009). In another study, the potential of Hsn-5 was evaluated against planktonic cells and biofilms of *C. albicans* and *C. glabrata* growth on poly (methyl methacrylate) disks, simulating oral prostheses (Konopka et al., 2010). Hsn-5 was capable of inhibiting planktonic *C. albicans* strains with MICs ranging from 2.6 to 4.8 μM. In contrast, planktonic *C. glabrata* cells were insensitive to Hsn-5. Moreover, this peptide also caused a reduction in the biofilm metabolic activity (RMA) with concentrations ranging from 1.7 to 6.9 μM and from 31.2 and 62.5 μM against *C. albicans* and *C. glabrata* biofilms, respectively (Konopka et al., 2010).

Diverse studies have been carried out over recent decades aiming to understand the mechanism of histatin fungicidal activity. According to the literature, Hsn-5 acts by a multistep mechanism. First, the peptide is internalized by endocytosis, followed by its binding to the cell wall and further translocation across the membrane to act on intracellular targets (**Figure 2C**) (Sun et al., 2008). Hsn-5 can enter *C. albicans* by means of an energy-dependent or -independent mechanism (Moffa et al., 2015). Although we do not have complete evidence on the mechanisms of action of Hsn-5, studies have shown that the same peptide often has different mechanisms against planktonic cells and biofilms (Sun et al., 2008).

Some authors report that histidine-rich peptides, including the histatins cited in this section, are highly selective antifungals and have little toxicity toward mammalian cells. According to data here summarized, histatins demonstrate promising antifungal activities, making these AFPs potential candidates for biofilm treatment, especially oral fungal infections. However, although they have elucidated mechanisms of action against planktonic cells, histatin studies still lack deeper information on fungal antibiofilm properties and mechanisms of action, making this class a potential subject for further studies aimed at combating fungal biofilms, determining their tridimensional structures, as well as unraveling their mechanisms of action. The AFPs described in this section, their respective antibiofilm activities, and their proposed mechanisms of action are summarized in **Table 3**.

Miscellaneous AFPs That Act on Fungal Biofilms

In addition to the above-mentioned classes of AFPs with antibiofilm potential, studies have also described additional AFPs from different sources that target fungal cell adhesion, thus inhibiting biofilm formation, as well as preformed biofilms. Ergosterol is the main sterol that constitutes fungal membranes. Moreover, studies have shown that the overexpression of genes involved in the biosynthesis of ergosterol (e.g., *ERG11*, *ERG16* and *ERG25*) may be crucial for *Candida* species biofilm formation (Garcia-Sanchez et al., 2004). For instance, the peptide *Tn*-AFP1, which is derived from *Trapa natans*, demonstrated antifungal potential by inhibiting planktonic cells of *C. tropicalis* at 26 μM. Moreover, it has been reported that *Tn*-AFP1 is capable of inhibiting fungal biofilm formation in a dose-dependent manner, as well as eradicating preformed biofilms (Mandal et al., 2011). In addition, when evaluating the levels of expression of two

TABLE 2 | Cathelicidin peptides against pathogenic fungi and biofilms and their proposed mechanisms of action.

Peptide	Source	Activity	Concentration (μM)	Pathogen	Mechanism of actions	References
LL-37	Human cathelicidin	Inhibited cell adhesion	64	*C. krusei* *C. albicans*	Membrane permeabilization	Scarsini et al., 2015
BMAP-28	Bovine cathelicidin	Biofilm inhibition - Biofilm eradication	16	*C. albicans*, *C. glabrata*, *C. krusei*	Membrane permeabilization	Scarsini et al., 2015
AS10 P318c	Derived from BMAP-18	Biofilm inhibition	0.22 0.15	*C. albicans*	Not determined	De Brucker et al., 2014
LL-37	Human cathelicidin	Biofilm inhibition	2.2 and 4.5	*C. albicans*	Adhesion and aggregation inhibition on biotic and abiotic surfaces	Tsai et al., 2011

TABLE 3 | Histatin peptides against pathogenic fungi and biofilms and their proposed mechanisms of action.

Peptide	Source	Activity	Concentration (μM)	Pathogen	Mechanism of actions	References
Hst-5	Human salivary histatins	Biofilm inhibiton	50	*C. albicans*	Not determined	Pusateri et al., 2009
Hsn-5	Human salivary histatins	Biofilm inhibiton	1.7 – 6.9 4.8 31.2 – 62.5	*C. albicans* *C. glabrata*	Peptide is internalized by endocytosis, then it binds to the cell wall and translocates into the cell to act on intracellular targets	Sun et al., 2008; Konopka et al., 2010

genes related to biofilm formation, including *ERG11* (ergosterol biosynthesis) and *MDR1* (ATP-binding cassettes pump) it was observed that planktonic cells treated with *Tn*-AFP1 presented the down-regulation of these genes and, therefore, could not establish biofilms (**Figure 2C**) (Mandal et al., 2011). Moreover, this AFP also induced morphological cell changes, along with fungicidal effects on biofilm-constituting cells.

In addition, a decapeptide isolated from *Arabidopsis thaliana*, called OSIP108, was evaluated regarding its antifungal and antibiofilm properties on *C. albicans* (De Coninck et al., 2013). As a result, the authors observed that OSIP108, from 2 to >200 μM, did not display antifungal activity against *C. albicans* planktonic cells, whereas OSIP108, from 6.25 to 100 μM, reduced *C. albicans* biofilm formation when administrated during the cell adhesion stage. These findings indicate that, despite using the same AFP, its antifungal and antibiofilm modes of action are most likely to be independent, as AFPs that are promising against planktonic cells may present ineffective antibiofilm properties and vice versa.

As described above, human-derived peptides have also been pinpointed as promising antifungal agents. A tryptophan-rich peptide derived from the human ApoE apolipoprotein (ApoEdpL-W), for instance, has shown antifungal activity against pathogenic yeasts of the *Candida* species, except for *C. glabrata* (Rossignol et al., 2011). ApoEdpL-W was active against planktonic cells and biofilms at early stages, but less active against mature biofilms (10 to 80 μM). In addition, ApoEdpL-W partially prevented biofilm formation on medical devices (Rossignol et al., 2011). Fungal cells in biofilms are embedded in an extracellular matrix composed of exopolymeric compounds, including β-1,3 glucan. Taking that into account, Rodrigues et al. (2018) evaluated the susceptibility of *C. glabrata* biofilms to echinocandins (cyclic lipo-hexapeptides), including Csf and micafugin (Mcf), also shedding some light on how these two AFPs interfere in β-1,3 glucan concentration in the matrix of *C. glabrata* biofilms. The authors observed that *C. glabrata* preformed biofilms treated with Csf and Mcf presented adjustments in the matrix composition due to a decrease in β-1,3 glucan concentration (Rodrigues et al., 2018). These findings were further correlated with the antibiofilm potential of these two AFPs, partially elucidating their antibiofilm mechanism (Rodrigues et al., 2018). A similar hypothesis has also been proposed for the higher antibiofilm activity of the tryptophan-rich AFP, ApoEdpL-W, against early-stage *C. albicans* biofilms when compared to mature biofilms (Rossignol et al., 2011). This finding can be partially explained by the affinity of ApoEdpL-W for extracellular matrix β-glucans in mature biofilms (e.g., β-1,3 glucan), which is known to trap antifungal agents and, consequently, confer biofilm tolerance (**Figure 2B**) (Rossignol et al., 2011).

Insect peptides are also known for their broad-spectrum of biological activities. Polybia-MPI, for instance, was originally isolated from the venom of the social wasp *Polybia paulista* and presented potent antibacterial activity (Souza et al., 2005). To better understand peptide biological potential, Polybia-MPI was evaluated for its inhibitory, fungicidal and antibiofilm activities against *Candida* spp. (Wang et al., 2014). Polybia-MPI revealed MIC and MFC values of 16 and 32 μM against *C. albicans*, respectively, whereas *C. glabrata* was inhibited (MIC) and killed (MFC) by Polybia-MPI at 8 and 32 μM, respectively. In addition, Polybia-MPI inhibited *C. glabrata* biofilm formation on polystyrene surface from 2 × MIC to 8 × MIC, resulting in a drastic decrease of biofilm biomass (Wang et al., 2014).

Another example of an AFP isolated from wasp toxin is the protonectin peptide, which was originally isolated from *Agelaia pallipes pallipes* (Mendes et al., 2004). Protonectin has been evaluated against *C. glabrata*, *C. albicans*, *C. parapsilosis*, *C. tropicalis* and *C. krusei*, revealing MICs from 8 to 128 μM. Protonectin was also found to disrupt fungal membrane integrity and induce the production of cellular reactive oxygen species (ROS), inhibiting the formation of *C. glabrata* biofilms (Wang et al., 2015). Wang et al. (2015), for instance, observed that a protonectin AFP, derived from the venom of a social wasp, has potent antifungal and fungicidal activities. Moreover, this AFP not only inhibited biofilm formation, but also killed adherent biofilm cells. All these activities were further correlated with membrane-associated mechanisms, along with the generation of ROS (**Figure 2C**) (Wang et al., 2015). In fungi, ROS are generated as metabolic products from an endogenous or exogenous source and include hydrogen peroxide and hydroxyl radicals, which act as signaling molecules for gene regulation (Scandalios, 2002; Cho and Lee, 2011). Inside fungal cells, ROS generation is balanced by the production of antioxidants. However, when this balance is compromised (for instance, by the presence of AFPs) ROS accumulation may lead to oxidative damage to lipids, proteins and DNA, resulting in cell death (Scandalios, 2002; Cho and Lee, 2011). In antifungal therapies focusing on AFPs, antifungal properties toward fungal biofilms have been reported and, in some cases, associated with ROS generation. Similar findings were reported for linear battacin peptides against *C. albicans* mature biofilms (**Figure 2C**) (De Zoysa et al., 2018).

Peptides derived from insect venom have also been submitted to sequence optimization strategies aiming at improved antifungal properties. Lasioglossin-III (LL-III) and halitin (HAL-2), for instance, represent two peptides derived from bee venom (Čeřovský et al., 2009) that were used as template molecules for the generation of synthetic analogs, named LL-III/43 and peptide VIII, respectively. These analogs were evaluated for their antifungal and antibiofilm activities against *Candida* spp. The lowest MIC (0.8 μM) value was observed for LL-III/43 against *C. tropicalis*. Moreover, both analogs inhibited *Candida* spp. biofilm formation, with concentrations ranging from 0.9 to 58.6 μM. Biofilm eradication for almost all *Candida* species tested ranged from 12.8 to 200 μM (Kočendová et al., 2019).

Bacteriocins are examples of peptides produced by various bacterial species with antifungal action (Sang and Blecha, 2008). EntV is a bacteriocin encoded by the entV locus (ef1097) from *Enterococcus faecalis* (Graham et al., 2017), originally studied for its antibacterial activity against Gram-positive strains (Swe et al., 2007). Graham et al. (2017) have reported a synthetic bacteriocin version, named $EntV^{68}$, which is constituted of 68 amino acid residues with one disulfide bond involved in structure cyclization. $EntV^{68}$ has been shown to be effective for reducing virulence of *C. albicans* strains and biofilm formation by inhibiting hyphae formation (BIC50 = 0.0003 μM) (**Figure 2A**). Furthermore, this

peptide potentially blocks biofilm development in solid substrates under multi-media conditions and has been proved to disturb preformed biofilms that are resistant to current antifungal agents (Graham et al., 2017). In addition, that work also evaluates whether $EntV^{68}$ protected phagocytes from *C. albicans*-induced damage or not (Graham et al., 2017). The murine RAW 264.7 macrophages were incubated with *C. albicans* cells in the presence and absence of $EntV^{68}$, at 100 nM (0.0001 μM). Under the peptide presence, the authors observed a decrease in the release of lactate dehydrogenase (LDH), an enzyme present in the macrophage membrane. Moreover, the analysis showed fewer surviving fungal cells, indicating that $EntV^{68}$ reduces fungus-induced cytotoxicity and may potentiate macrophage antifungal activity (Graham et al., 2017). Therefore, $EntV^{68}$ has clear pharmacological potential, as this peptide is capable of inhibiting biofilm formation and also disturbing preformed biofilms, without causing cytotoxicity in macrophages. In addition, two *in vivo* experiments were performed, which will be described later in the section "AFPs used to counter fungal infections in animal models."

In addition to insects, other arthropods and also bacteria can be a rich source of bioactive peptide screening. Lichosin-1, which is derived from *Lycosa singoriensi* spider venom (Tan et al., 2018), showed antifungal activity against clinical isolates of fluconazole-resistant *C. albicans*, with MIC values from 0.31 and 0.67 μM. When this peptide was evaluated against *C. albicans* biofilm, it was capable of inhibiting biofilm formation from 2.75 to 70.73 μM. However, higher concentrations ranging from 136.25 to 694.47 μM were required for antibiofilm activities against mature biofilms (Tan et al., 2018). In addition, Lycosin-1 acts against *C. tropicalis* through several types of morphological damage, leading to decreased biofilm filamentation, along with an increased number of gaps between cell clusters within the biofilms (Tan et al., 2018).

Another study evaluated optimized synthetic peptides called kaxins, capable of inhibiting fluconazole-susceptible and –resistant *C. albicans*, *C. tropicalis* and *C. glabrata* strains (128 to 512 μM) (Burrows et al., 2006). In that work, it was observed that a kaxin peptide, named dF21-10K, completely eradicated *C. albicans* and *C. tropicalis* preformed biofilms in a concentration 10-fold higher than the MIC against these strains (61.5 to 246.1 μM) (Burrows et al., 2006).

Also in the field of synthetic peptides, a decapeptide known as killer peptide (KP) was described (Paulone et al., 2017). This peptide was tested against fluconazole-resistant and -susceptible *C. albicans* biofilms at different development stages (cell adhesion, development of hyphae and extracellular matrix production). KP exerted fungicidal activity against all planktonic strains investigated, with MFC from 0.31 to 0.67 μM. The inhibitory effects of KP in *C. albicans* biofilm's early stages showed that 124.2 μM, KP impaired the biofilms, reducing the total biomass by more than 45% in four strains. Furthermore, the inhibitory effects of KP on mature (2-day old) biofilms of *C. albicans* showed that, at 124.2 μM, KP significantly impaired the total biomass of mature biofilms. In addition, KP administration led to an increased oxidative stress response in *C. albicans*, showing that this peptide has inhibitory effects on *C. albicans* biofilm regardless of whether this pathogen is resistant or susceptible to fluconazole (Paulone et al., 2017). AFPs can present multiple mechanisms against fungal biofilms depending on their stage, including early and mature biofilms. Recently, it was reported that a synthetic killer decapeptide (KP) was capable of inhibiting fluconazole-susceptible and -resistant *C. albicans* biofilm formation, also significantly affecting the viability of preformed biofilms (Paulone et al., 2017). In that work, KP induced ROS production in mature biofilms and also decreased the viability of biofilm-constituting fungal cells through membrane permeabilization (Paulone et al., 2017). Moreover, the transcriptional profile of *C. albicans* biofilms in early and mature stages treated with KP indicates that this AFP reduced the expression of biofilm-associated genes, including matrix-related genes and hyphal-specific genes (**Figure 2C**) (Rodrigues et al., 2018).

Battacin, a cyclic lipopeptide isolated from *Paenibacillus tianmuensis*, has shown promising antibacterial activities (Qian et al., 2012). De Zoysa et al. (2015) developed 16 battacin linear analogs, observing an improvement in their activity against bacterial biofilms. Based on that, these analogs were also submitted to fungal antibiofilm assays. As a result, the authors identified the three most effective analogs (3, 12, and 13), which were capable of inhibiting planktonic cells of *C. albicans* at 50, 12.5, and 6.25 μM, respectively. Since the lowest inhibitory concentration was observed for analog 13, it was evaluated against *C. albicans* biofilms. Analog 13 showed BIC50 values of 6.25 μM and was able to eradicate pre-formed biofilms 62.5 μM (10 times its MIC) (De Zoysa et al., 2018). The AFPs described in this section, their respective antibiofilm activities, and their proposed mechanisms of action are summarized in **Table 4**.

AFPs USED TO COUNTER FUNGAL INFECTIONS IN ANIMAL MODELS

In general, antifungal and antibiofilm peptides are tested in murine models, although different models have been developed in primates, rabbits, guinea pigs, birds, and canines (Hohl, 2014; Dijck et al., 2018). Animal models are an effective method by which to evaluate the progression of fungal pathogenesis and host immune responses and to investigate the antifungal properties of drug candidates (Capilla et al., 2007; Hohl, 2014; Dijck et al., 2018). These models allow the control of different biological variables, mimicking human diseases and monitoring disease progress (Capilla et al., 2007; Dijck et al., 2018). Recently, studies have used non-vertebrate models to optimize the screening of candidate drugs and evaluate fungal virulence. Non-vertebrate and other animal models are described in **Table 5**. According to Segal and Frenkel (2018), animal models are classified based on methods of therapeutic evaluation, including superficial (skin, nails), mucosal (oral, vaginal), gastrointestinal and lung or systemic infections (intravenous, intraperitoneal)

TABLE 4 | Unusual AFP classes of peptides against pathogenic fungi and biofilms and their proposed mechanisms of action.

Peptide	Source	Activity	Concentration (μM)	Pathogen	Mechanism of actions	References
Tn-AFP1	*T. natans*	Antifungal- Biofilm inhibition - Biofilm eradication	26 (inhibition) 52 (eradication)	*C. tropicalis*	Down-regulation of genes (*ERG11* and *MD1R*) and, therefore, cannot establish biofilms	Mandal et al., 2011
dF21-10K	Synthetic peptide	Biofilm eradication	61.5 – 246.1	*C. albicans* *C. tropicalis*	Not determined	Burrows et al., 2006
OSIP108	*A. thaliana*	Biofilm inhibition	6.25 – 100	*C. albicans*	Not determined	Delattin et al., 2014
ApoEdpl-W	Human ApoE apolipoprotein	Biofilm inhibition	10 – 80	*Candida* spp., except for *C. glabrata*	Affinity for extracellular matrix β-glucans in mature biofilms, conferring biofilm tolerance	Rossignol et al., 2011
Polybia-MPI	*P. paulista*	Biofilm inhibition	16 – 32 8 – 32	*C. albicans*, *C. glabrata*	Generation of ROS	Wang et al., 2014
LL-III/43 Peptide VIII	Bee venom	Biofilm inhibition - Biofilm eradication	0.9 – 58.6 (inhibition) 12.8 – 200 (eradication)	*C. tropicalis Candida* spp.	Not determined	Kočendová et al., 2019
KP	Synthetic peptide	Biofilm inhibition Biofilm eradication	0.31 – 0.67 124.2	*C. albicans*	ROS generation in mature biofilms and membrane permeabilization	Paulone et al., 2017
Protonectin AFP	*A pallipes pallipes*	Biofilm inhibition - Biofilm eradication	–	*C. albicans*	ROS generation	Wang et al., 2015
Battacin	*P. tianmuensis*	Biofilm inhibition - Biofilm eradication	BIC50* 6.25 (inhibition) 62.5 (eradication)	*C. albicans*	ROS generation	De Zoysa et al., 2018
Lichosin-1	*L. singoriensi*	Biofilm inhibition - Biofilm eradication	2.75 – 70.73	*C. albicans*	Not determined	Tan et al., 2018
$EntV^{68}$	bacteriocin of *E. faecalis*	Biofilm inhibition - blocking biofilm development	BIC50* 0.0003 0.0001	*C. albicans* (virulence and biofilm development) *C. albicans*, *C. tropicalis*, *C. parapsilosis C. glabrata* (inhibition of formed biofilms)	Reduces virulence of *C. albicans* strains and biofilm formation by inhibiting hyphae formation blocking biofilm development in solid substrates under multi-media conditions	Graham et al., 2017

**Reference values for each experiment, which can be: BIC50, concentration required to reduce biofilm formation by 50%.*

(Capilla et al., 2007; Hohl, 2014; Dijck et al., 2018). In addition, antifungal drugs have limited efficiency against invasive fungal infections, directly impacting increasing mortality rates (Hohl, 2014).

In this context, studies with animal models demonstrate a reliable strategy for evaluating the effectiveness of AFPs on biofilm-associated fungal infections, thus helping researchers to elucidate the therapeutic application of these antifungal agents in the clinic. Therefore, here we described different AFPs with activity against fungal biofilm in distinct animal models. Cools et al. (2017b) tested HsLin06_18 (derived from the plant defensin HsAFP1) in association with Csf. This combination was tested in immunosuppressed female Sprague–Dawley rats. *C. albicans* biofilms were formed inside catheters (5×10^4 cells. mL^{-1}), which were further implanted into the back area of the rats. The antibiofilm treatment aiming to inhibit biofilm formation was initiated immediately after the implant. The combination Csf + HsLin06_18 and the control group were administered intravenously or subcutaneously once daily for 7 days. It was demonstrated that the combination Csf + HsLin06_18 reduced *C. albicans* biofilm formation *in vivo* compared to the untreated control, besides not presenting cytotoxicity in healthy cells. Similar effects have been observed for an insect defensin, named drosomycin, against *Botrytis cinerea* strain B05-10 and *Colletotrichum gloeosporioides*. Drosomycin inhibited the growth of both fungi at 1.5 and 15 μM, respectively (Cohen et al., 2009). Another group demonstrated the efficiency of AFPs to combat planktonic fungi and biofilm formation. In a study using OSIP108, a *Caenorhabditis elegans in vivo* model was used to test synergic effects using different combinations of OSIP108 with Csf. The worms were infected with *C. albicans* and subsequently treated with 100 μM OSIP108, 0.095 μM Csf, and 100 μM OSIP108 + 0.095 μM Csf, and 0.6% DMSO (negative control) after 3, 5, and 7 days. The

TABLE 5 | | Overview of different animal models for screening for antifungal drugs.

Animal models	*Candida* sp.	*Aspergillus* sp.	*Cryotococcus* sp.
Galleria mellonella (greater wax moth)	Rowan et al., 2009; Lopez-Moya et al., 2015; Souza et al., 2015; Aneja et al., 2016; Ames et al., 2017; Gu et al., 2018; Lu et al., 2018	Alcazar-Fuoli et al., 2015; Forastiero et al., 2015; Maurer et al., 2015; Ben Yaakov et al., 2016; Ben Yaakov et al., 2017	Sangalli-Leite et al., 2016; Palanco et al., 2017; de Sá et al., 2018
Bombyx mori (silkworm)	Uchida et al., 2016	Nakamura et al., 2017	Ishii et al., 2016; Matsumoto et al., 2017
Caenorhabditis elegans	Delattin et al., 2013; Muhammed et al., 2016; Graham et al., 2017; Mohammad et al., 2018; Subramenium et al., 2018; Sun et al., 2018		de Aguiar Cordeiro et al., 2016; Thangamani et al., 2017
Drosophila melanogaster	Glittenberg et al., 2011; Zanette and Kontoyiannis, 2013	Lionakis and Kontoyiannis, 2012	
Danio rerio Zebrafish larvae			Palanco et al., 2017
Mice	López-García et al., 2005; Graham et al., 2017; Li et al., 2017; Peters et al., 2017; Wu et al., 2017; Dostert et al., 2018; Singulani et al., 2017; Lepak et al., 2018; Ci et al., 2018	Ben-Ami et al., 2010; Kai et al., 2013; Paulussen et al., 2015	Rathore et al., 2017; Nixon et al., 2018
Rats	Bink et al., 2012; Kucharíková et al., 2013; De Cremer et al., 2014; Kucharíková et al., 2014; Li et al., 2014; Cools et al., 2017b; Holtappels et al., 2018		
Guinea pigs	Maiolo et al., 2016	Wiederhold et al., 2015; Zhao et al., 2015	Kirkpatrick et al., 2007
Rabbit		Walsh et al., 1995; Petraitiene et al., 2002	

authors reported that OSIP108 alone did not present activity in *C. albicans* infected worms. However, the combination 100 μM OSIP108 + 0.095 μM Csf improved worms' survival. In accordance with these results, OSIP108 can be used for coating strategies in some medical devices, assisting in the fight against biofilm formation. The studies described above show that AFPs derived from plants are very efficient in inhibiting or controlling fungal biofilms tested in different *in vivo* models, demonstrating their therapeutic potential (Thevissen et al., 2007; Delattin et al., 2014).

Different groups of peptides have been tested by Yu et al. (2016). These authors have demonstrated the potential of four cathelicidins (cathelicidin-BF, Pc-CATH1, Cc-CATH2, Cc-CATH3) in combating *C. albicans* biofilm formation (Yu et al., 2016). The cathelicidins were tested in a murine oral candidiasis model using LL-37 and amphotericin B as control. Mice were infected by intramuscular injection and then infected by topical inoculation with *C. albicans* dilutions (0.1 mL) on the oral mucosa surface. The cathelicidin-BF inhibited *C. albicans* biofilm formation, demonstrating better results compared to other peptides. Similar results were also described by De Brucker et al. (2014) in *in vitro* tests using AS10 to inhibit fungal biofilm formation. As a result, AS10 was capable of inhibiting biofilm formation at 0.22 μM, and acted synergistically with amphotericin B and Csf against mature biofilms. In addition, this peptide did not exert a cytotoxic effect on mammalian cells.

Furthermore, synthetic peptides (β-peptides) have shown promising antifungal and antibiofilm properties against *C. albicans*. These AFPs act by reducing fungal metabolic activities and preventing or compromising biofilm formation (Delattin et al., 2014; Raman et al., 2014). The great activity of synthetic β-sheet peptides was also demonstrated by Wu et al. (2015). These authors tested the peptides $(IKIK)_2$-NH_2 and $(IRIK)_2$-NH_2 *in vivo* against fungal keratitis in comparison with the commercially available amphotericin B (Wu et al., 2015). They used contact lenses containing a layer of *C. albicans* biofilm, subsequently transferred onto the de-epithelia cornea surface of mice. The inoculum was maintained for 18 h, and eye ulcers developed with a leathery, tough, raised surface. Treatment was performed with peptide 1 (3000 $mg.L^{-1}$), peptide 2 (3000 $mg.L^{-1}$), amphotericin B (1000 $mg.L^{-1}$) and water (control), and further applied topically as eye drops (20 mL) on the corneal surface. After treatment, the authors observed a significant decrease in keratitis infection, suggesting that synthetic β-sheet peptides are effective in removing keratitis-related fungal biofilms from mouse eyes.

Additionally to the previously mentioned *in vitro* experiments, the potential of $EntV^{68}$ was evaluated in two fungal infection models in which this peptide showed to be protective during *C. albicans* infection via inhibition of hyphal morphogenesis at low concentrations. The nematode infection model used *C. elegans* to evaluate *C. albicans* filamentation by microscopy. Thus, it was observed that, in the presence of $EntV^{68}$ at subnanomolar concentrations (100 nM = 0.0001 μM), the virulence of *C. albicans* in the nematodes was nullified. Furthermore, the authors suggest that $EntV^{68}$ is effective

in protecting *C. elegans* during *C. albicans* infection via inhibition of *C. albicans* hyphal morphogenesis (Graham et al., 2017). In murines (immunosuppressed Balb-C mice), the evaluated model was oropharyngeal candidiasis (OPC). The results obtained showed that, based on a treatment with 100 nM (0.0001 μM) of EntV^{68}, mice had a significant reduction in fungal cell invasion, showing once again the ability of this peptide to inhibit morphological differentiation (Graham et al., 2017). Other peptides tested in animal models against fungal strains and biofilms are summarized in **Table 6**.

BIOTECHNOLOGICAL POTENTIAL

In recent years, fungal infections have become a worldwide health problem (Brown et al., 2012; Gamaletsou et al., 2018). Fungal biofilm formation is nowadays increasingly reported in systemic, superficial and mucosal fungal infections (Duncan and O'Neil, 2013; Nett and Andes, 2015). In addition to that, therapeutic strategies are still scarce and show limited effectiveness (Chowdhary et al., 2017; Santos et al., 2017). Moreover, one of the ways to correlate the challenges of working with AFPs is by looking at the failures of working with AMPs. In both cases, one of the obstacles in developing such molecules as pharmaceuticals is the substantial activity loss under physiological saline concentrations (Kerenga et al., 2019). Some authors have reported additional disadvantages, including systemic and local toxicity, susceptibility to proteolysis, sensitization and allergy after repeated application, and high costs in discovering, screening and manufacturing these peptides (Koczulla and Bals, 2003; Gordon et al., 2005). However, there are promising advantages as well, including AFPs' broad-spectrum action (antibacterial, antifungal, antiviral), rapid action upon contact with the pathogen, potentially low levels of induced resistance, as well as anti-inflammatory and immunomodulatory activity (Koczulla and Bals, 2003; Gordon et al., 2005). After years without any innovation in chemical antifungal agents, the AFPs initiated a new prospect for fungal treatment (Duncan and O'Neil, 2013; Santos et al., 2017). The study of AFPs is an emerging field, and recent works have focused on new strategies to improve their stability, safety, and efficacy (Kerenga et al., 2019). Moreover, an increasing number of studies have shown the advantages of combination therapies and drug delivery systems for AFPs' efficacy (Mahlapuu et al., 2016; Koo et al., 2017; Gomes et al., 2018; Revie et al., 2018).

According to the Food and Drug Administration (FDA), the number of approved bioactive peptides is growing. This rise is associated with the understanding of biofilm microenvironments, allowing the development of multi-targeted therapeutic approaches to prevent biofilm formation and combat preformed biofilms, enhancing drug efficacy (Koo et al., 2017; Lee et al., 2019). Some AFPs have been proved to act synergically with conventional antifungals, improving the success of antifungal therapies (Cohen et al., 2009; De Brucker et al., 2014). Thus, AFPs have shown great efficiency against fungal biofilms, along with the lack of side effects that are recurrent in conventional antifungal treatments. Moreover, some AMPs are undergoing pre-clinical and clinical trials, including the treatment of infections related to contaminated catheters, topical formulations for acne, treatment of peritoneal infections caused by bacteria (e.g., pneumonia), as well as treatment of gingivitis and oral biofilms (Guaní-Guerra et al., 2010). However, to date, AFPs with fungal antibiofilm activity have not yet reached the market.

Therefore, in this review we described different applications for AFPs, with a core focus on antibiofilm properties toward fungi. This includes the use of AFPs as topical agents for the treatment of superficial vulvovaginal candidiasis (Kovács et al., 2018). Another application is against fungal keratitis, in which AFPs can be used as eye drops (Wu et al., 2015), as well as for oral administration (Yu et al., 2016). Furthermore, AFPs can be immobilized on medical devices (e.g., catheter, prosthesis and implants) to prevent fungal biofilm formation (De Brucker et al., 2014; Gonçalves et al., 2017). Besides that, nanoformulation strategies may allow the maintenance of AFPs stability and activity, thus improving the treatment's effectiveness by creating drug delivery systems (Batoni et al., 2011; Kovalainen et al., 2015; Mahlapuu et al., 2016; Cavalheiro and Teixeira, 2018; Dostert et al., 2018). Apart from their strong performance in the therapeutic area, AFPs can also be used in cosmetics (Bedoux et al., 2014; Rahnamaeian and Vilcinskas, 2015; Carvalho et al., 2016), diagnostics (Ribeiro et al., 2016; Young-Speirs et al., 2018), functional food and nutraceuticals (Gianfranceschi et al., 2018), vaccines (Nami et al., 2019), and in agriculture for pest control (Subbanna et al., 2019).

When combined with their activity against fungal biofilms, heat stability, pH, degradation and proteolysis, we can provide a solid basis for the development of AFPs as antimicrobial therapeutic agents for clinical use. Their multifunctionality with respect to antifungal and antibacterial properties is particularly stimulating, as there is potential utility against polymicrobial infections. Taken together, all the findings highlighted in this review suggest the promising application of AFPs as new biomolecules in pre-clinical and clinical trials, reinforcing a

TABLE 6 | Overview of antifungal peptides tested *in vivo* against free-floating fungi and biofilms.

Peptides	AFP classes	References
hBD1hDB3, Psd1, HsAFP1, RsAFP2, NFAP2,	Defensins	Martinez and Casadevall, 2006; Pusateri et al., 2009; Delattin et al., 2014; Gonçalves et al., 2017; Menzel et al., 2017; Kovács et al., 2018
LL-37, P318, AS10	Cathelicidins	Benincasa et al., 2006; De Brucker et al., 2014; Yu et al., 2016; Niemirowicz et al., 2017; Sun et al., 2018
Histatin-5, $Hst5_{4-15}Spd$	Histatins	Sung et al., 2008; Tati et al., 2014
Tn-AFP, OSIPI08, EntV^{68}	Unusual AFPs	Gonçalves et al., 2017; Kovács et al., 2018
β-peptides, mPE	Synthetic β-sheet	Raman et al., 2014; Wu et al., 2015

growing movement in which bioactive peptides may assume a lead role in modern medicine and pharmaceutics.

AUTHOR CONTRIBUTIONS

KO, GR, BM, and MC wrote the manuscript. KO and MC idealized and organized the figures. MC and OF corrected the manuscript. OF supervised and managed all authors.

FUNDING

This work was supported by grants from the Fundação de Apoio à Pesquisa do Distrito Federal (FAPDF), Coordenação de Aperfeiçoamento de Pessoal de Nível Superior (CAPES), Conselho Nacional de Desenvolvimento e Tecnológico (CNPq), and Fundação de Apoio ao Desenvolvimento do Ensino, Ciência e Tecnologia do Estado de Mato Grosso do Sul (FUNDECT), Brazil.

REFERENCES

Aerts, A. M., Bammens, L., Govaert, G., Carmona-Gutierrez, D., Madeo, F., Cammue, B., et al. (2011). The antifungal plant defensin HsAFP1 from *Heuchera sanguinea* induces apoptosis in *Candida albicans*. *Front. Microbiol.* 2:47. doi: 10.3389/fmicb.2011.00047

Aerts, A. M., François, I. E. J. A., Cammue, B. P. A., and Thevissen, K. (2008). The mode of antifungal action of plant, insect and human defensins. *Cell. Mol. Life Sci.* 65, 2069–2079. doi: 10.1007/s00018-008-8035-0

Ajesh, K., and Sreejith, K. (2012). *Cryptococcus laurentii* biofilms: structure, development and antifungal drug resistance. *Mycopathologia* 174, 5–6. doi: 10.1007/s11046-012-9575-2

Alcazar-Fuoli, L., Buitrago, M., Gomez-Lopez, A., and Mellado, E. (2015). An alternative host model of a mixed fungal infection by azole susceptible and resistant *Aspergillus* spp. strains. *Virulence* 6, 376–384. doi: 10.1080/21505594.2015.1025192

Ames, L., Duxbury, S., Pawlowska, B., Ho, H. L., Haynes, K., and Bates, S. (2017). *Galleria mellonella* as a host model to study *Candida glabrata* virulence and antifungal efficacy. *Virulence* 8, 1909–1917. doi: 10.1080/21505594.2017.1347744

Aneja, B., Irfan, M., Kapil, C., Jairajpuri, M. A., Maguire, R., Kavanagh, K., et al. (2016). Effect of novel triazole–amino acid hybrids on growth and virulence of *Candida species*: *in vitro* and *in vivo* studies. *Org. Biomol. Chem.* 14, 10599–10619. doi: 10.1039/c6ob01718e

Batoni, G., Maisetta, G., Lisa Brancatisano, F., Esin, S., and Campa, M. (2011). Use of antimicrobial peptides against microbial biofilms: advantages and limits. *Curr. Med. Chem.* 18, 256–279. doi: 10.2174/092986711794088399

Bedoux, G., Hardouin, K., Burlot, A. S., and Bourgougnon, N. (2014). Bioactive components from seaweeds: cosmetic applications and future development. *Adv. Bot. Res.* 71, 345–378. doi: 10.1016/B978-0-12-408062-1.00012-3

Ben Yaakov, D., Rivkin, A., Mircus, G., Albert, N., Dietl, A. M., Kovalerchick, D., et al. (2016). Identification and characterization of haemofungin, a novel antifungal compound that inhibits the final step of haem biosynthesis. *J. Antimicrob. Chemoter.* 71, 946–952. doi: 10.1093/jac/dkv446

Ben Yaakov, D., Shadkchan, Y., Albert, N., Kontoyiannis, D. P., and Osherov, N. (2017). The quinoline bromoquinol exhibits broad-spectrum antifungal activity and induces oxidative stress and apoptosis in *Aspergillus fumigatus*. *J. Antimicrob. Chemother.* 72, 2263–2272. doi: 10.1093/jac/dkx117

Ben-Ami, R., Lewis, R. E., Leventakos, K., Latgé, J. P., and Kontoyiannis, D. P. (2010). Cutaneous model of invasive aspergillosis. *Antimicrob. Agents Chemother.* 54, 1848–1854. doi: 10.1128/AAC.01504-09

Benincasa, M., Scocchi, M., Pacor, S., Tossi, A., Nobili, D., Basaglia, G., et al. (2006). Fungicidal activity of five cathelicidin peptides against clinically isolated yeasts. *J. Antimicrob. Chemother.* 58, 950–959. doi: 10.1093/jac/dkl382

Bink, A., Kucharíková, S., Neirinck, B., Vleugels, J., Van Dijck, P., Cammue, B. P., et al. (2012). The nonsteroidal antiinflammatory drug diclofenac potentiates the *in vivo* activity of caspofungin against *Candida albicans* biofilms. *J. Infect. Dis.* 206, 1790–1797. doi: 10.1093/infdis/jis594

Brewer, D., Hunter, H., and Lajoie, G. (1998). NMR studies of the antimicrobial salivary peptides histatin 3 and histatin 5 in aqueous and nonaqueous solutions. *Biochem. Cell Biol.* 76, 247–256. doi: 10.1139/o98-066

Brown, G. D., Denning, D. W., Gow, N. A., Levitz, S. M., Netea, M. G., and White, T. C. (2012). Hidden killers: human fungal infections. *Sci. Transl. Med.* 4:165rv13. doi: 10.1126/scitranslmed.3004404

Burrows, L. L., Stark, M., Chan, C., Glukhov, E., Sinnadurai, S., and Deber, C. M. (2006). Activity of novel non-amphipathic cationic antimicrobial peptides against *Candida* species. *J. Antimicrob. Chemother.* 57, 899–907. doi: 10.1093/jac/dkl056

Capilla, J., Clemons, K. V., and Stevens, D. A. (2007). Animal models: an important tool in mycology. *Med. Mycol.* 45, 657–684. doi: 10.1080/13693780701644140

Carvalho, I. T., Estevinho, B. N., and Santos, L. (2016). Application of microencapsulated essential oils in cosmetic and personal healthcare products–a review. *Inter. J. Cosm. Sci.* 38, 109–119. doi: 10.1111/ics.12232

Cavalheiro, M., and Teixeira, M. C. (2018). Candida biofilms: threats, challenges, and promising strategies. *Front. Med.* 5:28. doi: 10.3389/fmed.2018.00028

Čeřovský, V., Budějínský, M., Hovorka, O., Cvačka, J., Voburka, Z., Slaninová, J., et al. (2009). Lasioglossins: three novel antimicrobial peptides from the venom of the eusocial bee *Lasioglossum laticeps* (Hymenoptera: Halictidae). *ChemBioChem* 10, 2089–2099. doi: 10.1002/cbic.200900133

Chairatana, P., Chiang, I. L., and Nolan, E. M. (2017). Human α-defensin 6 self-assembly prevents adhesion and suppresses virulence traits of *Candida albicans*. *Biochemistry* 56, 1033–1041. doi: 10.1021/acs.biochem.6b01111

Cho, J., and Lee, D. G. (2011). Oxidative stress by antimicrobial peptide pleurocidin triggers apoptosis in *Candida albicans*. *Biochimie* 93, 1873–1879. doi: 10.1016/j.biochi.2011.07.011

Chowdhary, A., Sharma, C., and Meis, J. F. (2017). Azole-resistant aspergillosis: epidemiology, molecular mechanisms, and treatment. *J. Infec. Dis.* 216(Suppl._3), S436–S444. doi: 10.1093/infdis/jix210

Ci, T., Yuan, L., Bao, X., Hou, Y., Wu, H., Sun, H., et al. (2018). Development and anti-*Candida* evaluation of the vaginal delivery system of amphotericin B nanosuspension-loaded thermogel. *J. Drug Target* 26, 829–839. doi: 10.1080/1061186X.2018.1434660

Cohen, L., Moran, Y., Sharon, A., Segal, D., Gordon, D., and Gurevitz, M. (2009). Drosomycin, an innate immunity peptide of *Drosophila melanogaster*, interacts with the fly voltage-gated sodium channel. *J. Biol. Chem.* 284, 23558–23563. doi: 10.1074/jbc.M109.023358

Cools, T. L., Struyfs, C., Cammue, B. P., and Thevissen, K. (2017a). Antifungal plant defensins: increased insight in their mode of action as a basis for their use to combat fungal infections. *Future Microbiol.* 12, 441–454. doi: 10.2217/fmb-2016-0181

Cools, T. L., Struyfs, C., Drijfhout, J. W., Kucharíková, S., Lobo Romero, C., Van Dijck, P., et al. (2017b). A linear 19-mer plant defensin-derived peptide acts synergistically with caspofungin against *Candida albicans* biofilms. *Front. Microbiol.* 8:2051. doi: 10.3389/fmicb.2017.02051

de Aguiar Cordeiro, R., de Jesus Evangelista, A. J., Serpa, R., de Farias Marques, F. J., de Melo, C. V. S., de Oliveira, J. S., et al. (2016). Inhibition of heat-shock protein 90 enhances the susceptibility to antifungals and reduces the virulence of *Cryptococcus neoformans*/*Cryptococcus gattii* species complex. *Microbiology* 162, 309–317. doi: 10.1099/mic.0.000222

De Brucker, K., Delattin, N., Robijns, S., Steenackers, H., Verstraeten, N., Landuyt, B., et al. (2014). Derivatives of the mouse cathelicidin-related antimicrobial peptide (CRAMP) inhibit fungal and bacterial biofilm formation. *Antimicrob. Agents Chemother.* 58, 5395–5404. doi: 10.1128/aac.03045-14

De Coninck, B., Carron, D., Tavormina, P., Willem, L., Craik, D. J., Vos, C., et al. (2013). Mining the genome of *Arabidopsis thaliana* as a basis for the identification of novel bioactive peptides involved in oxidative stress tolerance. *J. Exp. Bot.* 64, 5297–5307. doi: 10.1093/jxb/ert295

De Cremer, K., Delattin, N., De Brucker, K., Peeters, A., Kucharíková, S., Gerits, E., et al. (2014). Oral administration of the broad-spectrum antibiofilm

compound toremifene inhibits *Candida albicans* and *Staphylococcus aureus* biofilm formation *in vivo*. *Antimicrob. Agents Chemother.* 58, 7606–7610. doi: 10.1128/AAC.03869-14

De Lucca, A. J., and Walsh, T. J. (1999). Antifungal peptides: novel therapeutic compounds against emerging pathogens. *Antimicrob. Agents Chemother.* 43, 1–11. doi: 10.1128/AAC.03869-1

de Sá, N. P., de Barros, P. P., Junqueira, J. C., Vaz, J. A., de Oliveira, R. B., Rosa, C. A., et al. (2018). Thiazole derivatives act on virulence factors of *Cryptococcus* spp. *Med. Mycol.* 1, 84–91. doi: 10.1093/mmy/myx158

De Zoysa, G. H., Cameron, A. J., Hegde, V. V., Raghothama, S., and Sarojini, V. (2015). Antimicrobial peptides with potential for biofilm eradication: synthesis and structure activity relationship studies of battacin peptides. *J. Med. Chem.* 58, 625–639. doi: 10.1021/jm501084q

De Zoysa, G. H., Glossop, H. D., and Sarojini, V. (2018). Unexplored antifungal activity of linear battacin lipopeptides against planktonic and mature biofilms of *C. albicans*. *Eur. J. Med. Chem.* 146, 344–353. doi: 10.1016/j.ejmech.2018.01.023

Delattin, N., De Brucker, K., Craik, D. J., Cheneval, O., Fröhlich, M., Veber, M., et al. (2014). The plant-derived decapeptide OSIP108 interferes with *Candida albicans* biofilm formation without affecting cell viability. *Antimicrob. Agents Chemother.* 58, 2647–2656. doi: 10.1128/AAC.01274-13

Delattin, N., De Brucker, K., De Cremer, K., Pa Cammue, B., and Thevissen, K. (2017). Antimicrobial peptides as a strategy to combat fungal biofilms. *Curr. Top. Med. Chem.* 17, 604–612. doi: 10.2174/1568026616666160713142228

Delattin, N., De Brucker, K., Vandamme, K., Meert, E., Marchand, A., Chaltin, P., et al. (2013). Repurposing as a means to increase the activity of amphotericin B and caspofungin against *Candida albicans* biofilms. *J. Antimicrob. Chemoter.* 69, 1035–1044. doi: 10.1093/jac/dkt449

Dhople, V., Krukemeyer, A., and Ramamoorthy, A. (2006). The human beta-defensin-3, an antibacterial peptide with multiple biological functions. *Biochim. Biophys. Acta Biomembr.* 1758, 1499–1512. doi: 10.1016/j.bbamem.2006.07.007

Di Luca, M., Maccari, G., and Nifosì, R. (2014). Treatment of microbial biofilms in the post-antibiotic era: prophylactic and therapeutic use of antimicrobial peptides and their design by bioinformatics tools. *Pathog. Dis.* 70, 257–270. doi: 10.1111/2049-632x.12151

Dijck, P. V., Sjollema, J., Cammue, B. P., Lagrou, K., Berman, J., d'Enfert, C., et al. (2018). Methodologies for *in vitro* and *in vivo* evaluation of efficacy of antifungal and antibiofilm agents and surface coatings against fungal biofilms. *Microb. Cell.* 5, 300–326. doi: 10.15698/mic2018.07.638

Dongari-Bagtzoglou, A., Kashleva, H., Dwivedi, P., Diaz, P., and Vasilakos, J. (2009). Characterization of mucosal *Candida albicans* biofilms. *PLoS One* 4:e7967. doi: 10.1371/journal.pone.0007967

Dostert, M., Belanger, C. R., and Hancock, R. E. W. (2018). Design and assessment of anti-biofilm peptides: steps toward clinical application. *J. Innate Immun.* 11, 193–204. doi: 10.1159/000491497

Douglas, L. J. (2002). Medical importance of biofilms in *Candida* infections. *Rev. Iberoam. Micol.* 19, 139–143.

Duncan, V. M., and O'Neil, D. A. (2013). Commercialization of antifungal peptides. *Fungal Biol. Rev.* 26, 156–165. doi: 10.1016/j.fbr.2012.11.001

Faruck, M. O., Yusof, F., and Chowdhury, S. (2016). An overview of antifungal peptides derived from insect. *Peptides* 80, 80–88. doi: 10.1016/j.peptides.2015.06.001

Fjell, C. D., Hiss, J. A., Hancock, R. E., and Schneider, G. (2012). Designing antimicrobial peptides: form follows function. *Nat. Rev. Drug Discov.* 11, 37–51. doi: 10.1038/nrd3591

Forastiero, A., Bernal-Martínez, L., Mellado, E., Cendejas, E., and Gomez-Lopez, A. (2015). *In vivo* efficacy of voriconazole and posaconazole therapy in a novel invertebrate model of *Aspergillus fumigatus* infection. *Int. J. Antimicrob. Agents* 46, 511–517. doi: 10.1016/j.ijantimicag.2015.07.007

Gamaletsou, M. N., Walsh, T. J., and Sipsas, N. V. (2018). Invasive fungal infections in patients with hematological malignancies: emergence of resistant pathogens and new antifungal therapies. *Turk. J. Haematol.* 35, 1–11. doi: 10.4274/tjh.2018.0007

Garcia-Sanchez, S. S., Aubert, S., Iraqui, I., Janbon, G., Ghigo, J. M., and d'Enfert, C. (2004). *Candida albicans* biofilms: a developmental state associated with specific and stable gene expression patterns. *Eukaryot. Cell* 3, 536–545. doi: 10.1128/EC.3.2.536-545.2004

Gennaro, R., and Zanetti, M. (2000). Structural features and biological activities of the cathelicidin-derived antimicrobial peptides. *Biopolymers* 55, 31–49.

Gianfranceschi, G. L., Gianfranceschi, G., Quassinti, L., and Bramucci, M. (2018). Biochemical requirements of bioactive peptides for nutraceutical efficacy. *J. Funct. Foods* 47, 252–263. doi: 10.1016/j.jff.2018.05.034

Giles, C., Lamont-Friedrich, S. J., Michl, T. D., Griesser, H. J., and Coad, B. R. (2018). The importance of fungal pathogens and antifungal coatings in medical device infections. *Biotechnol. Adv.* 36, 264–280. doi: 10.1016/j.biotechadv.2017.11.010

Glittenberg, M. T., Silas, S., MacCallum, D. M., Gow, N. A., and Ligoxygakis, P. (2011). Wild-type *Drosophila melanogaster* as an alternative model system for investigating the pathogenicity of *Candida albicans*. *Dis. Models Mech.* 4, 504–514. doi: 10.1242/dmm.006619

Gomes, B., Augusto, M. T., Felício, M. R., Hollmann, A., Franco, O. L., Gonçalves, S., et al. (2018). Designing improved active peptides for therapeutic approaches against infectious diseases. *Biotech. Adv.* 36, 415–429. doi: 10.1016/j.biotechadv.2018.01.004

Gonçalves, S., Silva, P. M., Felício, M. R., de Medeiros, L. N., Kurtenbach, E., and Santos, N. C. (2017). Psd1 effects on *Candida albicans* planktonic cells and biofilms. *Front. Cell. Infect. Microbiol.* 7:249. doi: 10.3389/fcimb.2017.00249

Gordon, Y. J., Romanowski, E. G., and McDermott, A. M. (2005). A review of antimicrobial peptides and their therapeutic potential as anti-infective drugs. *Curr. Eye Res.* 30, 505–515. doi: 10.1080/02713680590968637

Graham, C. E., Cruz, M. R., Garsin, D. A., and Lorenz, M. C. (2017). Enterococcus faecalis bacteriocin EntV inhibits hyphal morphogenesis, biofilm formation, and virulence of *Candida albicans*. *Proc. Natl. Acad. Sci. U.S.A.* 114, 4507–4512. doi: 10.1073/pnas.1620432114

Gu, W., Yu, Q., Yu, C., and Sun, S. (2018). *In vivo* activity of fluconazole/tetracycline combinations in *Galleria mellonella* with resistant *Candida albicans* infection. *J. Glob. Antimicrob. Resist.* 13, 74–80. doi: 10.1016/j.jgar.2017.11.011

Guaní-Guerra, E., Santos-Mendoza, T., Lugo-Reyes, S. O., and Terán, L. M. (2010). Antimicrobial peptides: general overview and clinical implications in human health and disease. *J. Clin. Immunol.* 135, 1–11. doi: 10.1016/j.clim.2009.12.004

Gulati, M., and Nobile, C. J. (2016). *Candida albicans* biofilms: development, regulation, and molecular mechanisms. *Microb. Infect.* 18, 310–321. doi: 10.1016/j.micinf.2016.01.002

Hall-Stoodley, L., Costerton, J. W., and Stoodley, P. (2004). Bacterial biofilms: from the natural environment to infectious diseases. *Nat. Rev. Microbiol.* 2, 95–108. doi: 10.1038/nrmicro821

Harriott, M., Lilly, E. A., Rodriguez, T. E., Fidel, P. L. Jr., and Noverr, M. C. (2010). *Candida albicans* forms biofilms on the vaginal mucosa. *Microbiology* 156, 3635–3644. doi: 10.1099/mic.0.039354-0

Hohl, T. M. (2014). Overview of vertebrate animal models of fungal infection. *J. Immunol. Methods* 410, 100–112. doi: 10.1016/j.jim.2014.03.022

Holtappels, M., Swinnen, E., De Groef, L., Wuyts, J., Moons, L., Lagrou, K., et al. (2018). Antifungal activity of oleylphosphocholine on *in vitro* and *in vivo Candida albicans* biofilms. *Antimicrob. Agents Chemother.* 62:e01767-17. doi: 10.1128/AAC.01767-17

Ishii, M., Matsumoto, Y., and Sekimizu, K. (2016). Usefulness of silkworm as a host animal for understanding pathogenicity of *Cryptococcus neoformans*. *Drug Discov. Ther.* 10, 9–13. doi: 10.5582/ddt.2016.01015

Jarczak, J., Kościuczuk, E. M., Lisowski, P., Strzałkowska, N., Jóźwik, A., Horbańczuk, J., et al. (2013). Defensins: natural component of human innate immunity. *Hum. Immunol.* 74, 1069–1079. doi: 10.1016/j.humimm.2013.05.008

Kai, H., Yamashita, M., Nakamura, I., Yoshikawa, K., Nitta, K., Watanabe, M., et al. (2013). Synergistic antifungal activity of KB425796-C in combination with micafungin against *Aspergillus fumigatus* and its efficacy in murine infection models. *J. Antibiot.* 66, 479–484. doi: 10.1038/ja.2013.57

Kaur, S., and Singh, S. (2013). Biofilm formation by *Aspergillus fumigatus*. *Med. Mycol.* 52, 2–9. doi: 10.3109/13693786.2013.819592

Kerenga, B. K., McKenna, J. A., Harvey, P. J., Quimbar, P., Garcia, D., Lay, F. T., et al. (2019). Salt-tolerant antifungal and antibacterial activities of the corn defensin ZmD32. *Front. Microbiol.* 10:795. doi: 10.3389/fmicb.2019.00795

Kirkpatrick, W. R., Najvar, L. K., Bocanegra, R., Patterson, T. F., and Graybill, J. R. (2007). New guinea pig model of *Cryptococcal meningitis*. *Antimicrob. Agent Chemother.* 51, 3011–3013. doi: 10.1128/AAC.00085-07

Kočendová, J., Vaňková, E., Volejníková, A., Nešuta, O., Buděšínský, M., Socha, O., et al. (2019). Antifungal activity of analogues of antimicrobial peptides isolated

from bee venoms against vulvovaginal *Candida* spp. *FEMS Yeast Res.* 19:foz013. doi: 10.1093/femsyr/foz013

Koczulla, A. R., and Bals, R. (2003). Antimicrobial peptides. *Drugs* 63, 389–406. doi: 10.2165/00003495-200363040-00005

Konopka, K., Dorocka-Bobkowska, B., Gebremedhin, S., and Düzgüneş, N. (2010). Susceptibility of *Candida* biofilms to histatin 5 and fluconazole. *Antonie van Leeuwenhoek* 97, 413–417. doi: 10.1007/s10482-010-9417-5

Koo, H., Allan, R. N., Howlin, R. P., Stoodley, P., and Hall-Stoodley, L. J. N. R. M. (2017). Targeting microbial biofilms: current and prospective therapeutic strategies. *Nat. Rev. Microbiol.* 5, 740–755. doi: 10.1038/nrmicro.2017.99

Kovács, R., Holzknecht, J., Hargitai, Z., Papp, C., Farkas, A., Borics, A., et al. (2018). *In vivo* applicability of *Neosartorya fischeri* antifungal protein 2 (NFAP2) in treatment of vulvovaginal candidiasis. *Antimicrob. Agents Chemother.* 63:e01777-18. doi: 10.1128/AAC.01777-18

Kovalainen, M., Mönkäre, J., Riikonen, J., Pesonen, U., Vlasova, M., Salonen, J., et al. (2015). Novel delivery systems for improving the clinical use of peptides. *Pharmacol. Rev.* 67, 541–561. doi: 10.1124/pr.113.008367

Krishnakumari, V., Rangaraj, N., and Nagaraj, R. (2009). Antifungal activities of human beta-defensins HBD-1 to HBD-3 and their C-terminal analogs Phd1 to Phd3. *Antimicrob. Agents Chemother.* 53, 256–260. doi: 10.1128/AAC.00470-08

Kucharíková, S., Neirinck, B., Sharma, N., Vleugels, J., Lagrou, K., and Van Dijck, P. (2014). *In vivo Candida glabrata* biofilm development on foreign bodies in a rat subcutaneous model. *J. Antimicrob. Chemother.* 70, 846–856. doi: 10.1093/jac/dku447

Kucharíková, S., Sharma, N., Spriet, I., Maertens, J., Van Dijck, P., and Lagrou, K. (2013). Activity of systemically administered echinocandins against *in vivo* mature *Candida albicans* biofilms developed in a rat subcutaneous model. *Antimicrob. Agents Chemother.* 57, 2365–2368. doi: 10.1128/AAC.02288-12

Lay, F., and Anderson, M. (2005). Defensins-components of the innate immune system in plants. *Curr. Protein Pept. Sci.* 6, 85–101. doi: 10.2174/1389203053027575

Lee, M. R., Raman, N., Ortiz-Bermudez, P., Lynn, D. M., and Palecek, S. P. (2019). 14-Helical beta-peptides elicit toxicity against *C. albicans* by forming pores in the cell membrane and subsequently disrupting intracellular organelles. *Cell Chem. Biol.* 26, 289–299. doi: 10.1016/j.chembiol.2018.11.002

Lepak, A. J., Zhao, M., VanScoy, B., Ambrose, P. G., and Andes, D. R. (2018). Pharmacodynamics of a long-acting echinocandin, CD101, in a neutropenic invasive-candidiasis murine model using an extended-interval dosing design. *Antimicrob. Agents Chemother.* 62:e02154-17. doi: 10.1128/AAC.02154-17

Li, D.-D., Zhao, L. X., Mylonakis, E., Hu, G. H., Zou, Y., Huang, T. K., et al. (2014). *In vitro* and *in vivo* activity of pterostilbene against *Candida albicans* biofilms. *Antimicrob. Agents Chemother.* 58, 2344–2355. doi: 10.1128/AAC.01583-13

Li, R., Zhang, L., Zhang, H., Yi, Y., Wang, L., Chen, L., et al. (2017). Protective effect of a novel antifungal peptide derived from human chromogranin a on the immunity of mice infected with *Candida krusei*. *Exp. Ther. Med.* 13, 2429–2434. doi: 10.3892/etm.2017.4290

Lim, S.-M., Ahn, K. B., Kim, C., Kum, J. W., Perinpanayagam, H., Gu, Y., et al. (2016). Antifungal effects of synthetic human β-defensin 3-C15 peptide. *Restor. Dent. Endod.* 43, 1857–1861. doi: 10.5395/rde.2016.41.2.91

Lionakis, M. S., and Kontoyiannis, D. P. (2012). Drosophila melanogaster as a model organism for invasive aspergillosis. In host-fungus interactions. *Methods Mol. Biol.* 845, 455–468. doi: 10.1007/978-1-61779-539-8_32

Lionakis, M. S., and Levitz, S. M. (2018). Host control of fungal infections: lessons from basic studies and human cohorts. *Ann. Rev. Immunol.* 36, 157–191. doi: 10.1146/annurev-immunol-042617-053318

López-García, B., Lee, P. H., Yamasaki, K., and Gallo, R. L. (2005). Anti-fungal activity of cathelicidins and their potential role in *Candida albicans* skin infection. *J. Invest. Dermatol.* 125, 108–115. doi: 10.1111/j.0022-202X.2005.23713.x

Lopez-Moya, F., Colom-Valiente, M. F., Martinez-Peinado, P., Martinez-Lopez, J. E., Puelles, E., Sempere-Ortells, J. M., et al. (2015). Carbon and nitrogen limitation increase chitosan antifungal activity in *Neurospora crassa* and fungal human pathogens. *Fungal Biol.* 119, 154–169. doi: 10.1016/j.funbio.2014.12.003

Lu, M., Yu, C., Cui, X., Shi, J., Yuan, L., and Sun, S. (2018). Gentamicin synergises with azoles against drug-resistant *Candida albicans*. *Int. J. Antimicrob. Agents* 51, 107–114. doi: 10.1016/j.ijantimicag.2017.09.012

Mahlapuu, M., Håkansson, J., Ringstad, L., and Björn, C. (2016). Antimicrobial peptides: an emerging category of therapeutic agents. *Front. Cell. Infect. Microbiol.* 6:194. doi: 10.3389/fcimb.2016.00194

Maiolo, E. M., Oliva, A., Tafin, U. F., Perrotet, N., Borens, O., and Trampuz, A. (2016). Antifungal activity against planktonic and biofilm *Candida albicans* in an experimental model of foreign-body infection. *J. Infect.* 72, 386–392. doi: 10.1016/j.jinf.2015.12.008

Mandal, S. M., Migliolo, L., Franco, O. L., and Ghosh, A. K. (2011). Identification of an antifungal peptide from *Trapa natans* fruits with inhibitory effects on *Candida tropicalis* biofilm formation. *Peptides* 32, 1741–1747. doi: 10.1016/j.peptides.2011.06.020

Martinez, L. R., and Casadevall, A. (2006). *Cryptococcus neoformans* cells in biofilms are less susceptible than planktonic cells to antimicrobial molecules produced by the innate immune system. *Infect. Immun.* 74, 6118–6123. doi: 10.1128/IAI.00995-06

Matejuk, A., Leng, Q., Begum, M. D., Woodle, M. C., Scaria, P., Chou, S. T., et al. (2010). Peptide-based antifungal therapies against emerging infections. *Drugs Future* 35:197. doi: 10.1358/dof.2010.035.03.1452077

Matsumoto, Y., Ishii, M., Shimizu, K., Kawamoto, S., and Sekimizu, K. (2017). A silkworm infection model to evaluate antifungal drugs for cryptococcosis. *Med. Mycol. J.* 112, 138–146. doi: 10.1111/j.1365-2672.2011.05186.x

Maurer, E., Browne, N., Surlis, C., Jukic, E., Moser, P., Kavanagh, K., et al. (2015). *Galleria mellonella* as a host model to study *Aspergillus terreus* virulence and amphotericin B resistance. *Virulence* 6, 591–598. doi: 10.1080/21505594.2015.1045183

Mendes, M. A., de Souza, B. M., Marques, M. R., and Palma, M. S. (2004). Structural and biological characterization of two novel peptides from the venom of the neotropical social wasp *Agelaia pallipes pallipes*. *Toxicon* 44, 67–74. doi: 10.1016/j.toxicon.2004.04.009

Menzel, L. P., Chowdhury, H. M., Masso-Silva, J. A., Ruddick, W., Falkovsky, K., Vorona, R., et al. (2017). Potent *in vitro* and *in vivo* antifungal activity of a small molecule host defense peptide mimic through a membrane-active mechanism. *Sci. Rep.* 7, 1–10. doi: 10.1038/s41598-017-04462-6

Moffa, E. B., Mussi, M., Xiao, Y., Garrido, S. S., Machado, M. A., Giampaolo, E. T., et al. (2015). Histatin 5 inhibits adhesion of *C. albicans* to reconstructed human oral epithelium. *Front. Microbiol.* 6:885. doi: 10.3389/fmicb.2015.00885

Mohammad, H., Elghazawy, N. H., Eldesouky, H. E., Hegazy, Y. A., Younis, W., Avrimova, L., et al. (2018). Discovery of a novel dibromoquinoline compound exhibiting potent antifungal and antivirulence activity that targets metal ion homeostasis. *ACS Infect. Dis.* 4, 403–414. doi: 10.1021/acsinfecdis.7b00215

Muhammed, M., Arvanitis, M., and Mylonakis, E. (2016). Whole animal HTS of small molecules for antifungal compounds. *Expert. Opin. Drugs Discov.* 11, 177–184. doi: 10.1517/17460441.2016.1122591

Nakamura, I., Kanasaki, R., Yoshikawa, K., Furukawa, S., Fujie, A., Hamamoto, H., et al. (2017). Discovery of a new antifungal agent ASP2397 using a silkworm model of *Aspergillus fumigatus* infection. *J. Antibiot.* 70, 41–44. doi: 10.1038/ja.2016.106

Nami, S., Aghebati-Maleki, A., Morovati, H., and Aghebati-Maleki, L. (2019). Current antifungal drugs and immunotherapeutic approaches as promising strategies to treatment of fungal diseases. *Biomed. Pharmacother.* 110, 857–868. doi: 10.1016/j.biopha.2018.12.009

Nett, J. E., and Andes, D. (2015). Fungal biofilms: *in vivo* models for discovery of anti-biofilm drugs. *Microbiol. Spectr.* 3, 1–25. doi: 10.1128/microbiolspec.MB-0008-2014

Nett, J. E., Marchillo, K., Spiegel, C. A., and Andes, D. R. (2010). Development and validation of an *in vivo Candida albicans* biofilm denture model. *Infect. Immun.* 78, 3650–3659. doi: 10.1128/IAI.00480-10

Niemirowicz, K., Durnaś, B., Tokajuk, G., Piktel, E., Michalak, G., Gu, X., et al. (2017). Formulation and candidacidal activity of magnetic nanoparticles coated with cathelicidin LL-37 and ceragenin CSA-13. *Sci. Rep.* 7, 1–12. doi: 10.1038/s41598-017-04653-1

Nixon, G. L., McEntee, L., Johnson, A., Farrington, N., Whalley, S., Livermore, J., et al. (2018). Pharmacodynamics of flubendazole for cryptococcal meningoencephalitis: repurposing and reformulation of an anti-parasitic agent for a neglected fungal disease. *Antimicrob. Agents Chemother.* 62:e01909-17. doi: 10.1128/AAC.01909-17

Oppenheim, F., Xu, T., McMillian, F. M., Levitz, S. M., Diamond, R. D., Offner, G. D., et al. (1988). Histatins, a novel family of histidine-rich proteins in human parotid secretion. Isolation, characterization, primary structure, and fungistatic effects on *Candida albicans*. *J. Biol. Chem.* 263, 7472–7477.

Osborn, R. W., De Samblanx, G. W., Thevissen, K., Goderis, I., Torrekens, S., Van Leuven, F., et al. (1995). Isolation and characterisation of plant defensins from seeds of Asteraceae, Fabaceae, Hippocastanaceae and Saxifragaceae. *FEBS Lett.* 368, 257–262. doi: 10.1016/0014-5793(95)00666-W

Palanco, A. C., Lacorte Singulani, J. D., Costa-Orlandi, C. B., Gullo, F. P., Strohmayer Lourencetti, N. M., Gomes, P. C., et al. (2017). Activity of 3′-hydroxychalcone against *Cryptococcus gattii* and toxicity, and efficacy in alternative animal models. *Future Microbiol.* 12, 1123–1134. doi: 10.2217/fmb-2017-0062

Paris, S., Wolgin, M., Kielbassa, A. M., Pries, A., and Zakrzewicz, A. (2009). Gene expression of human beta-defensins in healthy and inflamed human dental pulps. *J. Endodon.* 35, 520–523. doi: 10.1016/j.joen.2008.12.015

Parisi, K., Shafee, T. M. A., Quimbar, P., van der Weerden, N. L., Bleackley, M. R., and Anderson, M. A. (2019). The evolution, function and mechanisms of action for plant defensins. *Semin. Cell Dev. Biol.* 88, 107–118. doi: 10.1016/j.semcdb.2018.02.004

Paulone, S., Ardizzoni, A., Tavanti, A., Piccinelli, S., Rizzato, C., Lupetti, A., et al. (2017). The synthetic killer peptide KP impairs *Candida albicans* biofilm *in vitro*. *PLoS One* 12:e0181278. doi: 10.1371/journal.pone.0181278

Paulussen, C., Boulet, G., Bosschaerts, T., Cos, P., Fortin, A., and Maes, L. (2015). Efficacy of oleylphosphocholine (Ol PC) *in vitro* and in a mouse model of invasive aspergillosis. *Mycoses* 58, 127–132. doi: 10.1111/myc.12286

Perlin, D. S., Rautemaa-Richardson, R., and Alastruey-Izquierdo, A. (2017). The global problem of antifungal resistance: prevalence, mechanisms, and management. *Lancet Infect. Dis.* 17, e383–e392. doi: 10.1016/S1473-3099(17)30316-X

Peters, B. M., Luna-Tapia, A., Tournu, H., Rybak, J. M., Rogers, P. D., and Palmer, G. E. (2017). An azole-tolerant endosomal trafficking mutant of *Candida albicans* is susceptible to azole treatment in a mouse model of vaginal candidiasis. *Antimicrob. Agents Chemother.* 61:e00084-17. doi: 10.1128/AAC.00084-17

Petraitiene, R., Petraitis, V., Groll, A. H., Sein, T., Schaufele, R. L., Francesconi, A., et al. (2002). Antifungal efficacy of caspofungin (MK-0991) in experimental pulmonary aspergillosis in persistently neutropenic rabbits: pharmacokinetics, drug disposition, and relationship to galactomannan antigenemia. *Antimicrob. Agents Chemother.* 46, 12–23. doi: 10.1128/AAC.46.1.12-23.2002

Pusateri, C. R., Monaco, E. A., and Edgerton, M. (2009). Sensitivity of *Candida albicans* biofilm cells grown on denture acrylic to antifungal proteins and chlorhexidine. *Arch. Oral Biol.* 54, 588–594. doi: 10.1016/j.archoralbio.2009.01.016

Qian, C.-D., Wu, X. C., Teng, Y., Zhao, W. P., Li, O., Fang, S. G., et al. (2012). Battacin (Octapeptin B5), a new cyclic lipopeptide antibiotic from *Paenibacillus tianmuensis* active against multidrug-resistant Gram-negative bacteria. *Antimicrob. Agents Chemother.* 56, 1458–1465. doi: 10.1128/AAC.05580-11

Rahnamaeian, M., and Vilcinskas, A. (2015). Short antimicrobial peptides as cosmetic ingredients to deter dermatological pathogens. *Appl. Microbiol. Biotechnol.* 99, 8847–8855. doi: 10.1007/s00253-015-6926-1

Raman, N., Lee, M. R., Palecek, S. P., and Lynn, D. M. (2014). Polymer multilayers loaded with antifungal β-peptides kill planktonic *Candida albicans* and reduce formation of fungal biofilms on the surfaces of flexible catheter tubes. *J. Control. Release* 191, 54–62. doi: 10.1016/j.jconrel.2014.05.026

Rathore, S. S., Isravel, M., Vellaisamy, S., Chellappan, D. R., Cheepurupalli, L., Raman, T., et al. (2017). Exploration of antifungal and immunomodulatory potentials of a furanone derivative to rescue disseminated cryptococosis in mice. *Sci. Rep.* 7, 1–14. doi: 10.1038/s41598-017-15500-8

Rautenbach, M., Troskie, A. M., and Vosloo, J. A. (2016). Antifungal peptides: to be or not to be membrane active. *Biochimie* 130, 132–145. doi: 10.1016/j.biochi.2016.05.013

Revie, N. M., Iyer, K. R., Robbins, N., and Cowen, L. E. (2018). Antifungal drug resistance: evolution, mechanisms and impact. *Curr. Opin. Microbiol.* 45, 70–76. doi: 10.1016/j.mib.2018.02.005

Ribeiro, S. M., Felicio, M. R., Boas, E. V., Goncalves, S., Costa, F. F., Samy, R. P., et al. (2016). New frontiers for anti-biofilm drug development. *Pharmacol. Therap.* 160, 133–144. doi: 10.1016/j.pharmthera.2016.02.006

Rodrigues, C. F., Rodrigues, M. E., and Henriques, M. (2018). Susceptibility of *Candida glabrata* biofilms to echinocandins: alterations in the matrix composition. *Biofouling* 34, 569–578. doi: 10.1080/08927014.2018.1472244

Rossignol, T., Kelly, B., Dobson, C., and d'Enfert, C. (2011). Endocytosis-mediated vacuolar accumulation of the human ApoE apolipoprotein-derived ApoEdpL-W antimicrobial peptide contributes to its antifungal activity in *Candida albicans*. *Antimicrob. Agents Chemother.* 55, 4670–4681. doi: 10.1128/AAC.00319-11

Rowan, R., Moran, C., McCann, M., and Kavanagh, K. J. B. (2009). Use of *Galleria mellonella* larvae to evaluate the *in vivo* anti-fungal activity of [Ag2(mal)(phen)3]. *Biometals* 22, 461–467. doi: 10.1007/s10534-008-9182-3

Sang, Y., and Blecha, F. (2008). Antimicrobial peptides and bacteriocins: alternatives to traditional antibiotics. *Anim. Health Res. Rev.* 9, 227–235. doi: 10.1017/S1466252308001497

Sangalli-Leite, F., Scorzoni, L., da Silva, J. D. F., de Oliveira, H. C., de Lacorte Singulani, J., Gullo, F. P., et al. (2016). Synergistic effect of pedalitin and amphotericin B against *Cryptococcus neoformans* by *in vitro* and *in vivo* evaluation. *Int. J. Antimicrob. Agents* 48, 504–511. doi: 10.1016/j.ijantimicag.2016.07.025

Santos, J. R. A., Ribeiro, N. Q., Bastos, R. W., Holanda, R. A., Silva, L. C., Queiroz, E. R., et al. (2017). High-dose fluconazole in combination with amphotericin B is more efficient than monotherapy in murine model of cryptococcosis. *Sci. Rep.* 7:4661. doi: 10.1038/s41598-017-04588-7

Sathoff, A. E., and Samac, D. A. (2019). Antibacterial activity of plant defensins. *Mol. Plant Microbe Interact.* 32, 507–514. doi: 10.1094/mpmi-08-18-0229-cr

Scandalios, J. G. (2002). The rise of ROS. *Trends Biochem. Sci.* 27, 483–486. doi: 10.1016/S0968-0004(02)02170-9

Scarsini, M., Tomasinsig, L., Arzese, A., D'Este, F., Oro, D., and Skerlavaj, B. (2015). Antifungal activity of cathelicidin peptides against planktonic and biofilm cultures of *Candida* species isolated from vaginal infections. *Peptides* 71, 211–221. doi: 10.1016/j.peptides.2015.07.023

Segal, E., and Frenkel, M. J. (2018). Experimental *in vivo* models of candidiasis. *J. Fungi* 21:E21. doi: 10.3390/jof4010021

Shafee, T. M., Lay, F. T., Hulett, M. D., and Anderson, M. A. (2016). The defensins consist of two independent, convergent protein superfamilies. *Mol. Biol. Evol.* 33, 2345–2356. doi: 10.1093/molbev/msw106

Shibata, N., Ichikawa, T., Tojo, M., Takahashi, M., Ito, N., Okubo, Y., et al. (1985). Immunochemical study on the mannans of *Candida albicans* NIH A-207, NIH B-792, and J-1012 strains prepared by fractional precipitation with cetyltrimethylammonium bromide. *Arch. Biochem. Biophys.* 243, 338–348. doi: 10.1016/0003-9861(85)90511-9

Singulani, J. L., Scorzoni, L., Gomes, P. C., Nazaré, A. C., Polaquini, C. R., Regasini, L. O., et al. (2017). Activity of gallic acid and its ester derivatives in *Caenorhabditis elegans* and zebrafish (*Danio rerio*) models. *Future Med. Chem.* 9, 1863–1872. doi: 10.4155/fmc-2017-0096

Souza, A. C. R., Fuchs, B. B., Pinhati, H. M., Siqueira, R. A., Hagen, F., Meis, J. F., et al. (2015). *Candida parapsilosis* resistance to fluconazole: molecular mechanisms and *in vivo* impact in infected *Galleria mellonella* larvae. *Antimicrob. Agents Chemoter.* 59, 6581–6587. doi: 10.1128/AAC.01177-15

Souza, B. M., Mendes, M. A., Santos, L. D., Marques, M. R., César, L. M., Almeida, R. N., et al. (2005). Structural and functional characterization of two novel peptide toxins isolated from the venom of the social wasp *Polybia paulista*. *Peptides* 26, 2157–2164. doi: 10.1016/j.peptides.2005.04.026

Subbanna, A. R. N. S., Chandrashekara, C., Stanley, J., Mishra, K. K., Mishra, P. K., and Pattanayak, A. (2019). Bio-efficacy of chitinolytic *Bacillus thuringiensis* isolates native to northwestern Indian Himalayas and their synergistic toxicity with selected insecticides. *Pest. Biochem. Physiol.* 158, 166–174. doi: 10.1016/j.pestbp.2019.05.005

Subramenium, G. A., Swetha, T. K., Iyer, P. M., Balamurugan, K., and Pandian, S. K. (2018). 5-hydroxymethyl-2-furaldehyde from marine bacterium *Bacillus subtilis* inhibits biofilm and virulence of *Candida albicans*. *Am. J. Microbiol. Res.* 207, 19–32. doi: 10.1016/j.micres.2017.11.002

Sun, J. N., Li, W., Jang, W. S., Nayyar, N., Sutton, M. D., and Edgerton, M. (2008). Uptake of the antifungal cationic peptide Histatin 5 by *Candida albicans* Ssa2p

requires binding to non-conventional sites within the ATPase domain. *Mol. Microbiol.* 70, 1246–1260. doi: 10.1111/j.1365-2958.2008.06480.x

Sun, L., Liao, K., and Hang, C. J. P. (2018). Caffeic acid phenethyl ester synergistically enhances the antifungal activity of fluconazole against resistant *Candida albicans*. *Phytomedicine* 40, 55–58. doi: 10.1016/j.phymed.2017.12.033

Sung, W. S., Lee, J., and Lee, D. G. (2008). Fungicidal effect and the mode of action of piscidin 2 derived from hybrid striped bass. *Biochem. Biophys. Res. Commun.* 371, 551–555. doi: 10.1016/j.bbrc.2008.04.107

Swe, P. M., Heng, N. C., Ting, Y.-T., Baird, H. J., Carne, A., Tauch, A., et al. (2007). ef1097 and ypkK encode enterococcin V583 and corynicin JK, members of a new family of antimicrobial proteins (bacteriocins) with modular structure from Gram-positive bacteria. *Microbiology* 153, 3218–3227. doi: 10.1099/mic.0.2007/010777-0

Szyk, A., Wu, Z., Tucker, K., Yang, D., Lu, W., and Lubkowski, J. (2006). Crystal structures of human α-defensins HNP4, HD5, and HD6. *Protein Sci.* 15, 2749–2760. doi: 10.1110/ps.062336606

Tan, L., Bai, L., Wang, L., He, L., Li, G., Du, W., et al. (2018). Antifungal activity of spider venom-derived peptide lycosin-I against *Candida tropicalis*. *Microbiol. Res.* 216, 120–128. doi: 10.1016/j.micres.2018.08.012

Tati, S., Li, R., Puri, S., Kumar, R., Davidow, P., and Edgerton, M. (2014). Histatin 5-spermidine conjugates have enhanced fungicidal activity and efficacy as a topical therapeutic for oral candidiasis. *Antimicrob. Agents Chemother.* 58, 756–766. doi: 10.1128/AAC.01851-13

Taylor, K., Barran, P. E., and Dorin, J. R. (2008). Structure–activity relationships in β-defensin peptides. *J. Pept. Sci.* 90, 1–7. doi: 10.1002/bip.20900

Thangamani, S., Eldesouky, H. E., Mohammad, H., Pascuzzi, P. E., Avramova, L., Hazbun, T. R., et al. (2017). Ebselen exerts antifungal activity by regulating glutathione (GSH) and reactive oxygen species (ROS) production in fungal cells. *Biochim. Biophys. Acta Gen. Subj.* 1861, 3002–3010. doi: 10.1016/j.bbagen.2016.09.029

Thevissen, K., Kristensen, H. H., Thomma, B. P., Cammue, B. P., and Francois, I. E. (2007). Therapeutic potential of antifungal plant and insect defensins. *Drug Discov. Today* 12, 966–971. doi: 10.1016/j.drudis.2007.07.016

Thomma, B. P., Cammue, B. P., and Thevissen, K. (2002). Plant defensins. *Planta* 216, 193–202. doi: 10.1007/s00425-002-0902-6

Troxler, R. F., Offner, G. D., Xu, T., Vanderspek, J. C., and Oppenheim, F. G. (1990). Structural relationship between human salivary histatins. *J. Dent. Res.* 69, 2–6. doi: 10.1177/00220345900690010101

Tsai, H., and Bobek, L. A. (1998). Human salivary histatins: promising anti-fungal therapeutic agents. *Crit. Rev. Oral Biol. Med.* 9, 480–497.

Tsai, P. W., Yang, C. Y., Chang, H. T., and Lan, C. Y. (2011). Human antimicrobial peptide LL-37 inhibits adhesion of *Candida albicans* by interacting with yeast cell-wall carbohydrates. *PLoS One* 6:e17755. doi: 10.1371/journal.pone.0017755

Uchida, R., Namiguchi, S., Ishijima, H., and Tomoda, H. (2016). Therapeutic effects of three trichothecenes in the silkworm infection assay with *Candida albicans*. *Drug Discov. Ther.* 10, 44–48. doi: 10.5582/ddt.2016.01013

Uppuluri, P., Chaturvedi, A. K., Srinivasan, A., Banerjee, M., Ramasubramaniam, A. K., Köhler, J. R., et al. (2010). Dispersion as an important step in the *Candida albicans* biofilm developmental cycle. *PLoS Pathog.* 6:e1000828. doi: 10.1371/journal.ppat.1000828

van der Weerden, N. L., Hancock, R. E., and Anderson, M. A. (2010). Permeabilization of fungal hyphae by the plant defensin NaD1 occurs through a cell wall-dependent process. *J. Biol. Chem.* 285, 37513–37520. doi: 10.1074/jbc.M110.134882

Vriens, K., Cools, T. L., Harvey, P. J., Craik, D. J., Braem, A., Vleugels, J., et al. (2016). The radish defensins RsAFP1 and RsAFP2 act synergistically with caspofungin against *Candida albicans* biofilms. *Peptides* 75, 71–79. doi: 10.1016/j.peptides.2015.11.001

Vriens, K., Cools, T. L., Harvey, P. J., Craik, D. J., Spincemaille, P., Cassiman, D., et al. (2015). Synergistic activity of the plant defensin HsAFP1 and caspofungin against *Candida albicans* biofilms and planktonic cultures. *PLoS One* 10:e0132701. doi: 10.1371/journal.pone.0132701

Walsh, T. J., Garrett, K., Feurerstein, E., Girton, M., Allende, M., Bacher, J., et al. (1995). Therapeutic monitoring of experimental invasive pulmonary aspergillosis by ultrafast computerized tomography, a novel, noninvasive method for measuring responses to antifungal therapy. *Antimicrob. Agents Chemother.* 39, 1065–1069. doi: 10.1128/AAC.39.5.1065

Wang, K., Dang, W., Xie, J., Zhu, R., Sun, M., Jia, F., et al. (2015). Antimicrobial peptide protonectin disturbs the membrane integrity and induces ROS production in yeast cells. *Biochim. Biophys. Acta Biomembr.* 1848, 2365–2373. doi: 10.1016/j.bbamem.2015.07.008

Wang, K., Yan, J., Dang, W., Xie, J., Yan, B., Yan, W., et al. (2014). Dual antifungal properties of cationic antimicrobial peptides polybia-MPI: membrane integrity disruption and inhibition of biofilm formation. *Peptides* 56, 22–29. doi: 10.1016/j.peptides.2014.03.005

Wiederhold, N. P., Najvar, L. K., Matsumoto, S., Bocanegra, R. A., Herrera, M. L., Wickes, B. L., et al. (2015). Efficacy of the investigational echinocandin ASP9726 in a guinea pig model of invasive pulmonary aspergillosis. *Antimicrob. Agents Chemother.* 59, 2875–2881. doi: 10.1128/AAC.04857-14

Wu, H., Liu, S., Wiradharma, N., Ong, Z. Y., Li, Y., Yang, Y. Y., et al. (2017). Short synthetic α-helical-forming peptide amphiphiles for fungal keratitis treatment *in vivo*. *Adv. Healthc. Mater.* 6, 1–7. doi: 10.1002/adhm.201600777

Wu, H., Ong, Z. Y., Liu, S., Li, Y., Wiradharma, N., Yang, Y. Y., et al. (2015). Synthetic β-sheet forming peptide amphiphiles for treatment of fungal keratitis. *Biomaterials* 43, 44–49. doi: 10.1016/j.biomaterials.2014.11.052

Young-Speirs, M., Drouin, D., Cavalcante, P. A., Barkema, H. W., and Cobo, E. R. (2018). Host defense cathelicidins in cattle: types, production, bioactive functions and potential therapeutic and diagnostic applications. *Int. J. Antimicrob. Agents* 51, 813–821. doi: 10.1016/j.ijantimicag.2018.02.006

Yu, H., Liu, X., Wang, C., Qiao, X., Wu, S., Wang, H., et al. (2016). Assessing the potential of four cathelicidins for the management of mouse candidiasis and *Candida albicans* biofilms. *Biochimie* 121, 268–277. doi: 10.1016/j.biochi.2015.11.028

Zanette, R. A., and Kontoyiannis, D. P. (2013). Paradoxical effect to caspofungin in *Candida* species does not confer survival advantage in a *Drosophila* model of candidiasis. *J. Virulence* 4, 497–498. doi: 10.1016/j.biochi.2015.11.028

Zanetti, M. (2004). Cathelicidins, multifunctional peptides of the innate immunity. *J. Leukoc. Biol.* 75, 39–48. doi: 10.1189/jlb.0403147

Zanetti, M., Gennaro, R., and Romeo, D. (1995). Cathelicidins: a novel protein family with a common proregion and a variable C-terminal antimicrobial domain. *FEBS Lett.* 374, 1–5. doi: 10.1016/0014-5793(95)01050-O

Zhao, J., Cheng, Y., Song, X., Wang, C., Su, G., and Liu, Z. (2015). A comparative treatment study of intravitreal voriconazole and liposomal amphotericin B in an *Aspergillus fumigatus* endophthalmitis model. *Invest. Ophthalmol. Vis. Sci.* 56, 7369–7376. doi: 10.1167/iovs.15-17266

Conflict of Interest: The authors declare that the research was conducted in the absence of any commercial or financial relationships that could be construed as a potential conflict of interest.

6. DISCUSSÃO

O acesso facilitado ao uso de antibióticos convencionais pode resultar em recorrências de resistência antimicrobiana e, consequentemente, em danos à saúde pública (Fuentes et al., 2018; Carratalá et al., 2020). Diante da resistência emergente aos antibióticos e a falta de novos e eficazes agentes antibacterianos, uma nova direção para o desenvolvimento de novos antimicrobianos torna-se cada vez mais urgente (Durand et al., 2019). Nesse contexto, esforços têm sido feitos pela comunidade científica para desenvolver alternativas viáveis para conter infecções causadas por esses patógenos. Frente a essa problemática, PAMs têm aparecido como candidatos promissores, representando uma classe de moléculas multifuncionais (Gan et al., 2021).

O desenvolvimento de peptídeos como agentes terapêuticos ainda enfrenta desafios diante da compreensão limitada sobre seus mecanismos de ação. Apesar de extensas pesquisas, o mecanismo preciso pelo qual os PAMs erradicam patógenos não parece ser totalmente compreendido, dificultando a otimização e desenho dessas moléculas (Benfield and Henriques, 2020). No entanto, a otimização dessas moléculas requer consideração de vários parâmetros, e embora existam diversos métodos para geração de novos candidatos a PAMs, muitos deles se baseiam em tecnologias computacionais (Kliger, 2010; Magana et al., 2020). A otimização dessas sequências pode envolver a modificação de sua sequência de aminoácidos por meio de técnicas como substituição, deleção ou adição de aminoácidos para aumentar sua atividade e estabilidade. Isso pode ser feito por meio de métodos empíricos, como triagem de alto rendimento ou abordagens mais direcionadas, como mutagênese direcionada ao local (Porto et al., 2018b). Consequentemente, novas sequências de peptídeos podem ser geradas sem o uso de informações de função de estrutura, mas com uma combinação de padrões de aminoácidos. Dentro deste conceito, Porto e colaboradores (2018a), desenvolveram um algoritmo baseado em métodos linguísticos para projetar sequências peptídicas otimizadas, chamado *Joker*, por meio da inserção de padrões antimicrobianos em sequências peptídicas (PAMs ou não) em uma janela deslizante.

Recentemente descrevemos o desenho auxiliado por computador de novos peptídeos mastoparanos por meio do algoritmo *Joker* (Oshiro et al., 2019). Para isso, utilizamos a sequência do peptídeo citolítico mastoparano-L como entrada para o algoritmo *Joker* com o objetivo de otimizar as atividades antimicrobianas das variantes projetadas e reduzir seus efeitos tóxicos nas células de mamíferos quando comparadas ao peptídeo parental. Peptídeos mastoparanos consistem em peptídeos catiônicos, geralmente contendo resíduos hidrofóbicos,

incluindo leucina, isoleucina, valina, lisina, bem como um C-terminal amidado (Nakajima et al., 1986; Higashijima et al., 1988). O peptídeo mastoparano-L foi isolado inicialmente do veneno de *Vespula lewissii* possuindo atividades citolítica, além de promover a degranulação de mastócitos (Hirai et al., 1979). Além disso, foram descritos diversos peptídeos baseados nessa sequência como potenciais antimicrobianos. Dessa forma, essa classe de peptídeos é considerada promissora para estudos visando maior seletividade celular (Souza et al., 2015; Howl et al., 2018; de Santana et al., 2022).

Como observado a partir de sua sequência primária (INLKALAALAKKIL-NH_2) (Hirai et al., 1979; Hori et al., 2001), mastoparano-L possui carga líquida igual a +3, 57,6% de hidrofobicidade e um momento hidrofóbico de 0,398 <μH>. As variantes geradas com base nessa sequência foram optimizados em relação a suas características físico-químicas, assim, os resíduos de leucina (L), isoleucina (I) e lisina (K) foram mantidos nas sequências primárias dos análogos R1 e R4, bem como C-terminal amidado (-NH_2). Contudo, ao contrário da sequência do parental, mastoparano-L (PDB 1D7N), os análogos R1 e R4 avaliados apresentam argininas (R), bem como um aumento nos números de lisina ou arginina onde o arranjo dos resíduos ao longo da hélice pode levar ao aumento de interações eletrostáticas peptídeos-membranas aniônicas (Chen et al., 2005).

A triagem inicial para atividades antibacterianas contra *P. aeruginosa* mostrou que R1 e R4 tiveram a maior eficácia (Oshiro et al., 2019). Os resíduos Ile1, Asn2, Ala5, Leu9 e Ala10 no mastoparano-L foram substituídos por Lys1, Ile2, Arg5, Lys9 e Ile10 em R1, enquanto os resíduos Ala5, Leu9, Ala10, Ile13 e Leu14 no mastoparan-L foram substituídos por Lys5, Arg9, Ile10, Lys13 e Ile14, em R4. Essas modificações resultaram em aumento da carga líquida positiva (+6) e momento hidrofóbico, bem como redução da hidrofobicidade em R1 e R4. Além disso, observamos que a modificação tanto em R1 quanto em R4 interferiu na reorganização das faces hidrofílica e hidrofóbica nessas duas variantes. Lopez Cascales et al. (2018) relataram que a carga líquida positiva dos peptídeos, bem como sua anfipaticidade, pode ser um aspecto crucial na ação e seletividade antimicrobiana. Nesse contexto, observamos que as modificações físico-químicas nas variantes R1 e R4 podem estar diretamente relacionadas à perda das atividades hemolítica e citotóxica quando comparadas ao seu peptídeo parental. Achados semelhantes também foram relatados por Irazazabal e colaboradores (Irazazabal et al., 2016), a qual aplicou técnicas de desenho racional para modificar a sequência do mastoparano-L, gerando uma variante denominada [I^5R^8] (INLKILARLAKKIL-NH_2). Substituições pontuais nas posições 5 e 8, onde os resíduos de

alanina no mastoparano-L foram substituídos por resíduos de isoleucina e arginina em [I^5R^8], respectivamente, resultaram no aumento da carga líquida positiva de +3 para +4 no [I^5R^8] em relação a seu parental, mastoparano-L, o que foi descrito pelos autores como a causa de sua maior atividade antimicrobiana e menor toxicidade contra células de mamíferos.

Diversos peptídeos semelhantes ao mastoparanos têm sido relatados como tendo atividade antimicrobiana, principalmente agindo contra bactérias (Silva et al., 2017; Howl et al., 2018; de Santana et al., 2022). Em nosso estudo prévio, foram relatados os potenciais antimicrobianos dos peptídeos mastoparano-L, R1 e R4, verificando que as variantes R1 e R4 inibem o crescimento de *E. coli* suscetível e resistente a 4 μM e 8 μM, respectivamente, enquanto o peptídeo mastoparano-L inibe as mesmas cepas a 32 μM, já os peptídeos R1 e R4 inibem *E. coli* (BL21) a 2 μM (Oshiro et al., 2019). O estudo também avaliou a atividade desses peptídeos contra bactérias Gram-positivas, constatando que mastoparano-L e R1 não foram ativos contra *S. aureus* (ATCC 25923). Por outro lado, todos os peptídeos foram ativos contra *S. aureus* (ATCC 12600). Curiosamente, apenas a variante R4 inibiu o crescimento de MRSA a 8 μM, que é um valor de atividade maior do que outros peptídeos mastoparanos descritos na literatura, incluindo o mastoparano-1 (Memariani et al., 2018). De forma geral, o estudo sugere que os peptídeos mastoparanos têm propriedades antimicrobianas promissoras, particularmente R1 e R4 apresentam atividade contra cepas específicas (Oshiro et al., 2019).

Como desafios, podemos citar a toxicidade em células de mamíferos, falta de especificidade, produção das moléculas e entrega nos sítios de ação, e instabilidade correlacionada a atividade bactericida comprometida em soluções salinas fisiológicas (Chen et al., 2007; Kumar et al., 2018; Benfield and Henriques, 2020). Geralmente, PAMs interagem eletrostaticamente com a membrana microbiana de maneira sensível ao sal. Assim, uma vez que o fluido corporal humano possui alta concentração de sal, isso poderia interferir em sua atividade antimicrobiana (Park et al., 2004; Mohanram and Bhattacharjya, 2016). Além disso, alguns autores relatam que a presença do sal no meio de crescimento pode alterar o metabolismo das bactérias (Li et al., 2021). Ainda assim, no presente estudo a adição de sal no meio de crescimento não alterou seu padrão de crescimento, sugerindo que as diferentes forças iônicas não interferiram na viabilidade celular bacteriana.

Características como helicidade, hidrofobicidade e momento hidrofóbico podem afetar a tolerância ao sal e a atividade antimicrobiana dos PAMs α-helicoidais (Park et al., 2004; Cardoso et al., 2022). Park e colaboradores (2004) testaram diferentes peptídeos com repetições RLLR, sugerindo que a instabilidade estrutural pode interferir nas interações

eletrostáticas e, portanto, poderia ser responsável pela sensibilidade ao sal em PAMs. Um estudo mais recente descobriu que a substituição de resíduos de lisina por outros resíduos catiônicos podem aumentar a atividade antimicrobiana sob várias concentrações de sal, sugerindo que a distribuição de carga ao longo da sequência do peptídeo pode ser relevante para a sensibilidade ao sal (Goto et al., 2019; Takada et al., 2023).

A sensibilidade ao sal também é um fator importante a ser considerado, uma vez que a presença de altas concentrações de íons salinos pode interferir nas interações eletrostáticas entre as PAMs e as membranas microbianas, reduzindo sua atividade antimicrobiana (Benfield and Henriques, 2020). Em nosso estudo anterior, discutimos se resíduos de lisina distribuídos ao longo das sequências de mastoparanos poderiam aumentar sua atividade antimicrobiana (Oshiro et al., 2019). Curiosamente, no presente estudo, mastoparano-R1 foi o peptídeo mais potente e estável em meio suplementado com sal. Isso pode ser explicado pelos resíduos de aminoácidos carregados positivamente distribuídos ao longo dessa estrutura peptídica, que seguem o padrão K-2-KR-3-K-1-KK-2 (sequência completa do mastoparano-R1: KILKRLAAKIKKIL-NH_2), onde o os números indicam os espaços entre os resíduos Lys e Arg. Este padrão para mastoparano-R1 mostra uma ampla distribuição de carga positiva ao longo da sequência peptídica (quatro seções de resíduos de lisina e arginina). O mesmo padrão não se aplica ao mastoparano-L (3-K-6-KK-2 – duas seções; sequência completa do mastoparano-L: INLKALAALAKKIL-NH_2) e mastoparano-R4 (3-KK-3-R-1-KKK-1 – três seções; sequência completa do mastoparano-R4: INLKKLAARIKKKI-NH_2), o que pode explicar o baixo desempenho desses dois peptídeos em comparação com o mastoparano-R1.

Além das diferentes forças iônicas, um dos maiores desafios no trabalho com peptídeos mastoparanos são seus efeitos hemolíticos e citotóxicos em células de mamíferos (Hollmann et al., 2016). Alguns estudos afirmam que peptídeos com maior hidrofobicidade podem causar lise de membranas zwiteriônicas neutras explicando, assim, efeitos hemolíticos mais pronunciados (Chen et al., 2007; Hollmann et al., 2016). Anteriormente, as propriedades físico-químicas obtidas através do servidor *HeliQuest* (Gautier et al., 2008) mostraram que o peptídeo original mastoparano-L tem uma taxa mais alta de hidrofobicidade (57,6 %) e um momento hidrofóbico mais baixo (0,398 <μH>) em comparação com seus análogos mastoparano-R1 (36,9 % de hidrofobicidade; 0,775 <μH> momento hidrofóbico) e R4 (20,4 % de hidrofobicidade; 0,472 momento hidrofóbico). Características como alta anfipaticidade podem favorecer a interação do peptídeo com as membranas celulares. Portanto, essas

características estão intrinsecamente envolvidas no caráter citolítico do mastoparano-L (Irazazabal et al., 2016; dos Santos Cabrera et al., 2019; Oshiro et al., 2019).

A estrutura helicoidal e a anfipaticidade dos PAMs influenciam na sua atividade antimicrobiana e contribuem para seu mecanismo de ação em membranas (Park et al., 2004; Rungsa et al., 2022). No entanto, a importância da estabilidade estrutural dos PAMs α-helicoidais ainda precisa ser esclarecida. Por exemplo, alguns estudos relatam que a capacidade de um peptídeo de adotar uma α-hélice anfipática bem definida pode estar fortemente correlacionada com sua atividade antimicrobiana (Souza et al., 2015; Takada et al., 2023). A espectroscopia de dicroísmo circular (DC) foi usada para caracterizar a estrutura geral do peptídeo parental, mastoparano-L, e seus análogos R1 e R4 em água, tampão KH_2PO_4 (pH 7,4) 10 mM, TFE 50% e SDS 75 - 100 mM, a 25 °C. Em geral, os peptídeos tinham assinaturas de CD características de estruturas estendidas aleatórias *(random coil*) em água e tampão. Apenas o mastoparano-L revelou um leve perfil de α-hélice em 10 mM KH_2PO_4 (pH 7,4). De forma geral, os peptídeos mastoparanos apresentam estruturas helicoidais dependentes do ambiente. Em um trabalho semelhante, Lin e colaboradores (2011) caracterizaram a estrutura secundária de seis mastoparanos em diferentes ambientes, observando que apenas uma variante apresentou conteúdo helicoidal em sistema aquoso; enquanto os outros cinco mastoparanos mostraram arranjo em *random coil* (Lin et al., 2011).

Anteriormente, relatamos que os peptídeos mastoparano-L, R1 e R4 possuem estrutura ambiente dependente, em ambiente aquoso (água e tampão KH_2PO_4 10 mM) R1 e R4 reduziram suas porcentagens de hélice quando comparados ao parental mastoparano-L, enquanto em ambientes mais hidrofóbicos, como por exemplo, TFE 30%, SDS 25 mM e POPC/POPG, mostraram assinaturas características de α-hélice (Oshiro et al., 2019). No presente trabalho o conteúdo helicoidal em soluções contendo SDS apresentou apenas pequenas alterações respectivas a concentração de SDS (75 – 100 mM), variando o conteúdo de hélice em 222 nm em 69 – 73% para mastoparano-L, 36 – 45% para mastoparano-R1 e 52 – 47% para mastoparano-R4. Tendo isso em mente, outros experimentos estruturais complementares de ressonância magnética nuclear (RMN) e dinâmica molecular (DM) foram realizados no presente trabalho para examinar a hipótese de que a flexibilidade desses peptídeos pode interferir em sua afinidade de ligação com membranas.

A RMN pode ser considerada uma técnica capaz de capturar diferentes conformações e estados conformacionais de moléculas. Dessa forma, torna-se especialmente relevante para estudos com moléculas flexíveis ou que sofrem mudanças conformacionais de acordo com o

ambiente de estudo (Wüthrich, 1990). Diversas abordagens complementares a técnica de RMN foram utilizadas para estudar a interação de peptídeos mastoparanos com membranas lipídicas. A primeira estrutura de mastoparano resolvida por RMN, por exemplo, o foi mastoparano-x (PDB 1A13), considerado um bom peptídeo modelo por seu baixo peso molecular acoplado a proteínas reguladoras de ligação a proteínas G (Kusunoki et al., 1998). O modelo parental usado utilizado desde a projeção do peptídeo, mastoparano-L (PDB 1D7N) também teve sua estrutura resolvida por RMN, sendo resolvida em micela de SDS-*d25* (Hori et al., 2001). Os resultados estruturais observados nos trabalhos com R1 e R4 em 30% TFE-*d3* mostraram que os peptídeos possuíam assinaturas de hélice dos resíduos 4 – 13 e 4 – 12, respectivamente, associados a isso, os dados de coeficiente de temperatura sugeriram diferentes níveis de estabilidade/flexibilidade estrutural (Oshiro et al., 2019). No presente trabalho, em SDS-*d25* observamos comportamento semelhante, e através dos resultados de RMN descobrimos que mastoparano-R1 e R4 adotam uma estrutura α-hélice; outros estudos também relataram que os peptídeos dessa classe têm uma tendência para essa organização estrutural dependente do ambiente (Whiles et al., 2001; Howl et al., 2018; Rungsa et al., 2022). Dessa forma, o presente trabalho apresentou as estruturas dos peptídeos mastoparano-R1 e R4 seguindo a mesma técnica do parental (mastoparano-L). Os dados completos e de validações estão disponíveis no banco de dados de proteínas (PDB) sob IDs PDB: 8EP5 e 8ERU para mastoparano-R1 e mastoparano-R4, respectivamente.

Fatores como simetria de sequência, distribuição de resíduos, flexibilidade e estrutura secundária podem ser benéficos para aumentar a atividade antimicrobiana e diminuir a citotoxicidade, melhorar a seletividade e a estabilidade em PAMs (Dong et al., 2014; Souza et al., 2015; Chou et al., 2019; Cardoso et al., 2022). Mohanram e colaboradores (Mohanram and Bhattacharjya, 2016) projetaram um PAM denominado RR12 com características catiônicas e hidrofóbicas contendo 12 resíduos distribuídos de forma a obter uma face polar e apolar bem definida. Dessa forma, o peptídeo redesenhado demonstraria um caráter anfipático predominante e os dois peptídeos progenitores tiveram modificações específicas, com substituições pontuais de Arg5 por Trp5 e outro cuja substituição foi Trp5 por Ile7 (Mohanram and Bhattacharjya, 2016). Com essas modificações, eles verificaram que a presença do resíduo Arg5 na hélice de superfície catiônica tem o potencial de conferir resistência ao sal por meio da formação de múltiplas ligações de hidrogênio e/ou interações iônicas com as membranas externa e interna das bactérias (Mohanram and Bhattacharjya, 2016).

Mais recentemente, Wu e colaboradores (Wu et al., 2020), investigaram como as propriedades estruturais do RR12 poderiam interagir com as membranas e a estrutura ligada às micelas miméticas da membrana. RR12 demonstrou dobramento desordenado para uma estrutura α-hélice bem definida ao interagir com micelas SDS (Wu et al., 2020). A orientação da estrutura concentrou-se do resíduo Arg2 para Ile7 com o C-terminal mais exposto ao solvente, e eles afirmaram que o segmento da hélice poderia contribuir para atividade bactericida (Wu et al., 2020). Mastoparano-L exibiu ligações de hidrogênio intrapeptídicas consistentemente mais altas do que seus análogos. Além disso, o mastoparano-R1 apresentou o menor número de resíduos protegidos do solvente. Esses achados reforçam a hipótese de que o mastoparano-R1 é o peptídeo estruturalmente mais flexível estudado aqui, o que é suportado pelos dados do coeficiente de temperatura de RMN (Oshiro et al., 2019). Quanto maior o deslocamento do próton amídico com a temperatura, menor o número de ligações de hidrogênio intrapeptídeo, influenciando assim a flexibilidade do peptídeo. No geral, os padrões de flexibilidade observados em nosso estudo anterior e atual revelam a capacidade desses peptídeos de alterar sua conformação em resposta a estímulos externos, que podem incluir alterações no pH e na força iônica.

As estruturas do PAMs, incluindo as dos peptídeos do mastoparano, podem ser influenciadas por fatores como posição específica do resíduo ao longo da hélice, composição de aminoácidos e características físico-químicas, que podem afetar sua seletividade para membranas celulares microbianas e de mamíferos. Essa seletividade é crucial para o desenvolvimento de PAMs como potencial terapêutico (Henriksen et al., 2014). Alguns PAMs, principalmente aqueles derivados de toxinas animais, podem exigir modificações para melhorar sua seletividade, enquanto outros possuem seletividade ideal (Yeung et al., 2011; Guido-Patiño and Plisson, 2022). Portanto, a estrutura dos PAMs desempenha um papel fundamental na determinando seu mecanismo de ação e seletividade, tornando-se uma consideração importante para o desenvolvimento de novos agentes antimicrobianos.

Ao considerar sistemas de membranas, torna-se relevante avaliar os arranjos estruturais dos peptídeos, visando melhor caracterizar seus mecanismos de ação. Observamos que os mastoparano-R1 e R4 tendem a se organizar em uma α-hélice bem definida, com diferentes níveis de flexibilidade dependendo do ambiente em que estão inseridos. Chou e colaboradores (2019) usaram características físico-químicas variáveis, comprimento de sequência e composição que incluíam os aminoácidos Gly, Lys, Leu e Trp, juntamente com distribuição de resíduos modificados. Os autores confirmaram que a distribuição helicoidal

simétrica e racional desses parâmetros indica uma estratégia promissora para projetar PAMs mais seletivos e específicos para patógenos (Chou et al., 2019). Dos 12 peptídeos gerados (F1-F12), F1 e F4 se destacaram com atividades promissoras contra bactérias Gram-negativas, baixa toxicidade, baixa sensibilidade ao sal e tendência para formação helicoidal em um ambiente de membrana mimético (Chou et al., 2019). Além disso, a investigação de como os PAMs interagem com as membranas bacterianas e o desempenho antimicrobiano associado podem contribuir para o design de novos peptídeos, minimizando a toxicidade à células de mamíferos saudáveis e maximizando suas ações contra patógenos humanos (Hollmann et al., 2016). Numerosos estudos mostraram que alterações nas propriedades físico-químicas, incluindo aumento do momento hidrofóbico e diminuição da hidrofobicidade geral, podem ser responsáveis pela seletividade celular (Ko et al., 2020; Rungsa et al., 2022).

A afinidade de ligação à membrana de peptídeos pode ser determinada através da metodologia de ressonância plasmônica de superfície (RPS) utilizando membranas modelo depositadas em um chip biossensor (Cooper et al., 2000). Para mimetizar a superfície neutra das membranas celulares de mamíferos podem ser usadas bicamadas compostas de POPC, e para mimetizar a superfície aniônica das membranas celulares bacterianas podem ser utilizadas bicamadas compostas com fosfolipídios carregados negativamente, como por exemplo, POPG, POPS, entre outros (Li et al., 2015). Para investigar o efeito da proporção de lipídios carregados negativamente, podem ser utilizados modelos de membranas com adaptações de razão molar de acordo com o objetivo (Epand and Epand, 2011). O presente trabalho avaliou as afinidades de ligação peptídeo-lipídio quanto à sua ligação a modelos de bicamadas fosfolipídicas, incluindo POPC zwitteriônico (puro) e POPC/POPG (4:1) aniônico, o parental mastoparano-L apresentou a maior afinidade pelas bicamadas POPC e POPC/POPG (4:1), seguido pelo mastoparano-R1 e R4. Cada um dos peptídeos mostrou maior afinidade de ligação para as bicamadas POPC/POPG (4:1) carregadas negativamente em comparação com as bicamadas neutras de POPC. Taxas rápidas de associação e dissociação foram observadas em todos os casos, mas observou-se que o mastoparano-L removeu lipídios do chip SPR. Este fenômeno foi observado anteriormente para outros peptídeos destrutivos de membrana hidrofóbicos (Lawrence et al., 2020).

A permeabilização de membranas se apresenta como um mecanismo crucial empregado pelos PAMs para prevenir o desenvolvimento de resistência em patógenos. Um estudo, utilizando as mesmas constituições de bicamadas avaliando o peptídeo arenicina AA139 demonstrou que mudanças simples de aminoácidos podem levar a variações sutis na

interação do peptídeo com membranas e, alterar sua seletividade e toxicidade (Edwards et al., 2022). Dessa forma, Edwards e colaboradores (2022) mostraram que ambos os peptídeos (aericina AA139 e parental arenicina-3) se ligam a diferentes composições de vesículas lipídicas, porém apresentam preferência (cerca de 2 a 3 vezes maior) por membranas modelo carregadas negativamente (POPC/POPG), em comparação com membranas zwitteriônicas, mostrando que propriedades de ligação e inserção mais específicas podem tornar peptídeos mais seletivos. Além disso, arenicin-3 e AA139 não induziram agregação de vesículas compostas apenas por POPC, no entanto induziram agregação substancial de vesículas carregadas negativamente, reforçando novamente a hipótese que esses peptídeos também apresentam maior seletividade para se ligar e permeabilizar vesículas com carga mais negativa (Edwards et al., 2022).

As propriedades de ruptura de membrana foram examinadas medindo o extravazamento induzido por peptídeo de CF de LUVs, composto de POPC ou POPC/POPG (4:1). Em nosso trabalho, os valores de LC50 foram pelo menos dez vezes maiores para mastoparano-R1 e R4 em comparação com o mastoparano-L, o que é consistente com as diferenças nas afinidades de ligação lipídica observadas para análogos com SPR. Além disso, mastoparano-R1 lisa vesículas de POPC/POPG (4:1) em concentração ~3 vezes menor do que vesículas POPC, o que é consistente com o menor potencial hemolítico observado para este peptídeo. Reafirmando que a indução de vazamento parcial pode ser explicada pela atração eletrostática dos peptídeos catiônicos para uma bicamada lipídica carregada negativamente e, portanto, sugerindo que a permeabilização da membrana pode não ser o único mecanismo de ação que causa ação antibacteriana.

Outro trabalho utilizando o mesmo algoritmo computacional caracterizou o PAM PaDBS1R6 como potencial candidato para o tratamento de infecções causadas por bactérias Gram-negativas (Fensterseifer et al., 2019). Semelhante a nosso presente trabalho, o peptídeo PaDBS1R6 adotou uma estrutura de espiral aleatória em meio aquoso confirmou a tendência de adotar uma conformação α-helicoidal em meio altamente hidrofóbico. Com outros estudos complementares, os autores observaram um aumento da agregação/maior partição do peptídeo para bactérias Gram-negativas como vesículas, além disso, o peptídeo apresentou desestabilização da membrana interna, levando à ruptura da membrana e à morte celular (Fensterseifer et al., 2019). Dessa forma, podemos observar que para avaliar o mecanismo de ação em bactérias também seriam necessários mais estudos envolvendo diferentes

constituições de membranas, bem como avaliações de mecanismos internos de ação antibacteriana (Benfield and Henriques, 2020).

Além dos estudos de RPS e de extravasamento com bicamadas fosfolipídicas, simulações de MD em 1 μs foram realizadas para entender melhor em nível atômico as preferências estruturais e interações entre mastoparano-R1 e R4 em POPC puro e bicamadas POPC/POPG (4:1). As simulações foram realizadas com as estruturas com menor energia livre para R1 e R4 na presença de micelas SDS. A flexibilidade pode ser considerada uma característica chave dos PAMs que contribui para sua atividade antimicrobiana. Ela permite que esses peptídeos se adaptem e interajam com uma ampla variedade de microrganismos, superando suas defesas e causando danos à membrana celular (Cardoso et al., 2022). No entanto, essa flexibilidade também pode levar a efeitos indesejados, como citotoxicidade e hemólise, o que limita sua aplicação clínica. Além disso, PAMs podem sofrer degradação proteolítica e instabilidade plasmática, o que reduz sua eficácia terapêutica. Uma abordagem balanceada e integrada considerando todos esses fatores pode levar ao desenvolvimento de PAMs mais eficazes e com menor toxicidade, melhorando sua aplicabilidade como agentes antimicrobianos (Cardoso et al., 2020; Gan et al., 2021).

7. CONCLUSÕES

No presente trabalho observamos que os peptídeos R1 e R4 possuem propriedades antibacterianas, atuando contra cepas bacterianas suscetíveis e resistentes. O peptídeo R1 apresentou o melhor desempenho antibacteriano em nossos ensaios biológicos (2 μM – 16 μM), inclusive sob condições salinas fisiológicas. A partir dos resultados, observamos que por meio de sua interação eletrostática com membranas carregadas negativamente, esse peptídeo pode exercer seu mecanismo de ação com maior seletividade. Portanto, apesar de apresentar algumas diferenças em seus perfis funcional e estrutural, o análogo R1 se destacou por demonstrar atividade superior em concentrações mais baixas, maior potencial bacteriostático e seletividade para membranas aniônicas. Todas essas vantagens podem ser explicadas pela conformação estrutural α-helicoidal mais flexível observado para o peptídeo R1 em comparação com seu peptídeo parental.

Além disso, comparando essas características estruturais com as propriedades funcionais observadas para esse peptídeo (R1), incluindo potência, efeito bacteriostático e afinidade seletiva por membranas aniônicas, é possível identificar determinantes estruturais e físico-químicos que contribuem para a atividade do peptídeo e mecanismo de ação. Essas

descobertas destacam o peptídeo R1 como um candidato promissor para a terapia antimicrobiana, que pode ser usado posteriormente como uma molécula modelo para otimização adicional de peptídeos com maior seletividade.

8. PERSPECTIVAS

Considerando o cenário acerca das infecções bacterianas, torna-se interessante o desenvolvimento de novos compostos eficazes contra cepas resistentes. Como apresentado e discutido ao longo deste trabalho, dois mastoparanos redesenhados computacionalmente foram caracterizados como moléculas modelo e de interesse farmacológico. Contudo, algumas perguntas ainda precisam ser respondidas em relação a esses candidatos a fármaco.

Mastoparano-R1 e R4 possuem promissor potencial antibacteriano e afinidade com membrana Gram-negativa, o que lhes garantem maior especificidade, ainda assim, mais experimentos tornam-se necessários para a confirmação do seu potencial terapêutico, incluindo definição de seus mecanismos de ação em membranas, ensaios de estabilidade, bem como a utilização desses peptídeos no tratamento de infecções bacterianas em modelos animais. O presente trabalho sugere que R1 e R4 possuem uma flexibilidade estrutural que podem interferir na sua capacidade de atravessar membranas biológicas para exercer sua atividade antibacteriana. Entretanto, também seria interessante comprovar possíveis alvos intracelulares, encorajando maiores estudos neste sentido.

Mais estudos seriam necessários visando a elucidação dos mecanismos de ação dos peptídeos. Nesse âmbito, as metodologias aplicadas poderiam incluir microscopia de força atômica, permeabilização e rompimento de vesículas miméticas em outras constituições fosfolipídicas e acoplamento/dinâmica molecular com membranas modelo, poderiam ser estendidas a adição de mais peptídeos no sistema. Por meio dessas e outras diversas abordagens é esperado que os mastoparanos apresentados neste trabalho, assim como toda a caracterização atrelada a eles, encoraje seu uso como moléculas modelo para o desenvolvimento guiado de PAMs cada vez mais seletivos, efetivos e seguros que possam, futuramente, ser submetidos a testes pré-clínicos.

9. ANEXOS

Artigo 1

DOI: 10.1016/bs.apcsb.2018.01.008

CHAPTER TEN

The Structure/Function Relationship in Antimicrobial Peptides: What Can we Obtain From Structural Data?

Marlon H. Cardoso[*,†,‡,2], Karen G.N. Oshiro[‡,2], Samilla B. Rezende[‡], Elizabete S. Cândido[†,‡], Octávio L. Franco[*,†,‡,1]

[*]Programa de Pós-Graduação em Patologia Molecular, Faculdade de Medicina, Universidade de Brasília, Brasília, Brazil
[†]Centro de Análises Proteômicas e Bioquímicas, Programa de Pós-Graduação em Ciências Genômicas e Biotecnologia, Universidade Católica de Brasília, Brasília, Brazil
[‡]S-inova Biotech, Programa de Pós-Graduação em Biotecnologia, Universidade Católica Dom Bosco, Campo Grande, Brazil
[1]Corresponding author: e-mail address: ocfranco@gmail.com

Contents

Abstract

Antimicrobial peptides (AMPs) have been widely isolated from most organisms in nature. This class of antimicrobials may undergo changes in their sequence for improved physicochemical properties, including charge, hydrophobicity, and hydrophobic moment. It is known that such properties may be directly associated with AMPs' structural arrangements and, consequently, could interfere in their modes of action against microorganisms. In this scenario, biophysical methodologies, such as nuclear magnetic resonance spectroscopy, X-ray crystallography, and cryo-electron

[2] These authors contributed equally.

Advances in Protein Chemistry and Structural Biology, Volume 112
ISSN 1876-1623
https://doi.org/10.1016/bs.apcsb.2018.01.008

Artigo 2

DOI: 10.1016/bs.apcsb.2018.01.008

NJC

PAPER

Check for updates

Cite this: *New J. Chem.*, 2018, 42, 13948

Synthesis and cytotoxic characteristics displayed by a series of Ag(I)-, Au(I)- and Au(III)-complexes supported by a common N-heterocyclic carbene†

Lalmohan Jhulki,[a] Parul Dutta,[b] Manas Kumar Santra,[b] Marlon H. Cardoso,[cde] Karen G. N. Oshiro,[ce] Octávio L. Franco,[cde] Valerio Bertolasi,[f] Anvarhusein A. Isab,[g] Christopher W. Bielawski[hi] and Joydev Dinda[*j]

Received 25th April 2018,
Accepted 13th July 2018

DOI: 10.1039/c8nj02008f

rsc.li/njc

The synthesis, structures and anticancer studies of a series of precious metal complexes supported by 1-methyl-2-(phenyl)imidazo[1,5-*a*]pyridine-2-ylidene (**1**) have been highlighted. The Ag(I) (**2**), Au(I) (**3**) and Au(III) (**4**) complexes were prepared using standard methods and characterized by a range of techniques, including NMR spectroscopy, X-ray crystallography and elemental analyses. The *in vitro* cytotoxicity activities displayed by **2–4** were explored against human colon adenocarcinoma (HCT116), lung cancer (A549) and breast cancer (MCF7) cell lines. A series of assays showed that all of the complexes exhibited significant growth inhibition in the aforementioned cell lines. Inspection of the data collected revealed that the Au(I) and Ag(I) complexes were more potent than their Au(III) congener, a trend that was found to be consistent with molecular docking studies that utilized BCL-2 as a model as this protein regulates cell death through apoptosis.

Introduction

The N-heterocyclic carbenes (NHCs) have emerged as an important class of ancillary ligands for a broad range of transition metals.[1] When compared to their phosphine analogues, metal complexes supported by NHCs often exhibit increased stabilities toward elevated temperatures, oxygen, and water, which frequently facilitates practicality.[2] Silver(I) complexes bearing NHCs, in particular, have attracted significant attention for their chemical,[3] structural[4] and photophysical properties.[5] More recently, the biological applications[6] displayed by Ag(I) and Au(I)–NHC complexes have steadily gained interest for their potential as new classes of metal-based drugs,[7] especially for the treatment of cancer and drug-resistant pathogens.[8,9] Although several reviews describe the utilities of Ag(I)–NHC complexes against various cancer lines, analogous Au(I) complexes may hold greater potential.[10] Gold has a long history of use as a medicine in ancient China and numerous gold-based drugs are being investigated for their activities against various ailments (*e.g.*, auranofin as an anti-rheumatic agent), including cancer.[11] Unfortunately, many of these complexes are readily metabolized *in vivo* by thiols,[12] which significantly reduces their activities. To overcome this limitation, gold-complexes bearing stabilizing NHCs have been explored as alternatives, often with good results.[13] For example, Panda and Ghosh reported[14] that Au(I)–NHC complex, [1-benzyl-3-*t*butylimidazol-2-ylidene]AuCl, exhibited excellent efficiency against the proliferation of HeLa cells (1.7% proliferation at $[Au]_0$ = 10 μM). Ott and co-workers discovered[15] that Au(I)–NHC-based thiotetrazolates are effective thioredoxin reductase inhibitors and antiproliferative agents against breast and colon carcinoma cells. Likewise, Berners-Price and Filipovska described[16] a new approach to based antitumor agents, where selective mitochondria targeting and thioredoxin by Picquet and Casini as anticancer agents against human

[a] *School of Applied Science, Haldia Institute of Technology, Haldia 721657, West Bengal, India*
[b] *National Centre for Cell Science, Pune 411007, Maharastra, India*
[c] *Programa de Pós-Graduação em Patologia Molecular, Faculdade de Medicina, Universidade de Brasília, Brasília-DF, Brazil*
[d] *Centro de Análises Proteômicas e Bioquímicas, Programa de Pós-Graduação em Ciências Genômicas e Biotecnologia, Universidade Católica de Brasília, Brasília-DF, Brazil*
[e] *Biotecnologia, Universidade Católica de Brasília, Brasília-DF, Brazil*
[f] *Dipartimento di Scienze Chimiche e Farmaceutiche, Centro di Strutturistica Diffrattometrica, Universita' di Ferrara, Via L. Borsari, 46, Italy*
[g] *Department of Chemistry, King Fahd University of Petroleum and Minerals, Dhahran 31261, Saudi Arabia*
[h] *Center for Multidimensional Carbon Materials (CMCM), Institute for Basic Science (IBS), Ulsan 44919, Republic of Korea*
[i] *Department of Chemistry and Department of Energy Engineering, Ulsan National Institute of Science and Technology (UNIST), Ulsan 44919, Republic of Korea*
[j] *Department of Chemistry, Utkal University, Vani Bihar, Bhubaneswar 751004, Odisha, India. E-mail: joydevdinda@gmail.com, dindajoy@yahoo.com*

† Electronic supplementary information (ESI) available: Crystallographic data for the complexes **2**, **3** and **4** in CIF format. CCDC 1562513–1562515. For ESI and crystallographic data in CIF or other electronic format see DOI: 10.1039/c8nj02008f

Artigo 3

DOI: 10.1021/acsinfecdis.8b00219

ACS Infectious Diseases

Article

Cite This: ACS Infect. Dis. XXXX, XXX, XXX−XXX

pubs.acs.org/journal/aidcbc

A Computationally Designed Peptide Derived from *Escherichia coli* as a Potential Drug Template for Antibacterial and Antibiofilm Therapies

Marlon H. Cardoso,[†,‡,§,∥] Elizabete S. Cândido,[‡,§] Lai Y. Chan,[∥] Marcelo Der Torossian Torres,[⊥,#,▽] Karen G. N. Oshiro,[†,§] Samilla B. Rezende,[§] William F. Porto,[‡,§,⊗] Timothy K. Lu,[⊥,#] Cesar de la Fuente-Nunez,[⊥,#] David J. Craik,[∥] and Octávio L. Franco*[,†,‡,§]

[†]Programa de Pós-Graduação em Patologia Molecular, Faculdade de Medicina, Universidade de Brasília, Campus Darcy Ribeiro, Asa Norte, Brasília, DF 70910900, Brazil

[‡]Centro de Análises Proteômicas e Bioquímicas, Pós-Graduação em Ciências Genômicas e Biotecnologia, Universidade Católica de Brasília, SGAN 916 Módulo B, Asa Norte, Brasília, DF 70790160, Brazil

[§]S-inova Biotech, Programa de Pós-Graduação em Biotecnologia, Universidade Católica Dom Bosco Avenida Tamandaré 6000, Campo Grande, MS 79117900, Brazil

[∥]Institute for Molecular Bioscience, The University of Queensland, 306 Carmody Road, Brisbane, QLD 4072, Australia

[⊥]Synthetic Biology Group, MIT Synthetic Biology Center; The Center for Microbiome Informatics and Therapeutics; Research Laboratory of Electronics, Department of Biological Engineering, and Department of Electrical Engineering and Computer Science, Massachusetts Institute of Technology, Cambridge, Massachusetts 02139, United States

[#]Broad Institute of MIT and Harvard, Cambridge, Massachusetts 02139, United States

[▽]Centro de Ciências Naturais e Humanas, Universidade Federal do ABC, Santo André, SP 09210170, Brazil

[⊗]Porto Reports, Brasília, DF 70790160, Brazil

Supporting Information

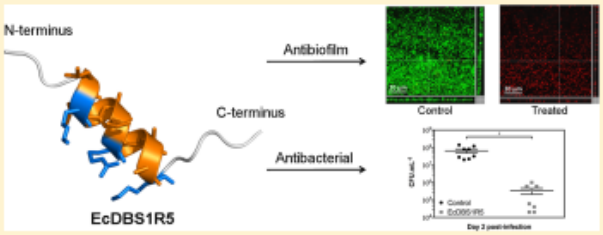

ABSTRACT: Computer-aided screening of antimicrobial peptides (AMPs) is a promising approach for discovering novel therapies against multidrug-resistant bacterial infections. Here, we functionally and structurally characterized an *Escherichia coli*-derived AMP (EcDBS1R5) previously designed through pattern identification [α-helical set (KK[ILV]$_{(3)}$[AILV])], followed by sequence optimization. EcDBS1R5 inhibited the growth of Gram-negative and Gram-positive, susceptible and resistant bacterial strains at low doses (2−32 μM), with no cytotoxicity observed against non-cancerous and cancerous cell lines in the concentration range analyzed (<100 μM). Furthermore, EcDBS1R5 (16 μM) acted on *Pseudomonas aeruginosa* pre-formed biofilms by compromising the viability of biofilm-constituting cells. The *in vivo* antibacterial potential of EcDBS1R5 was confirmed as the peptide reduced bacterial counts by two-logs 2 days post-infection using a skin scarification mouse model. Structurally, circular dichroism analysis revealed that EcDBS1R5 is unstructured in hydrophilic environments, but has strong helicity in 2,2,2-trifluoroethanol (TFE)/water mixtures (v/v) and sodium dodecyl sulfate (SDS) micelles. The TFE-induced nuclear magnetic resonance structure of EcDBS1R5 was determined and showed an amphipathic helical segment with flexible termini. Moreover, we observed that the amide protons for residues Met2-Ala8, Arg10, Ala13-Ala16, and Trp19 in EcDBS1R5 are protected from the solvent, as their temperature coefficients values are more positive than −4.6 ppb-K^{-1}. In summary, this study reports a novel dual-antibacterial/antibiofilm α-helical peptide with therapeutic potential *in vitro* and *in vivo* against clinically relevant bacterial strains.

KEYWORDS: *antimicrobial peptides, bacterial resistance, bacterial biofilm, skin infection, biophysics*

Multidrug bacterial resistance is among the most significant health threats of the 21st century.[1] Approximately 15 million deaths were associated with bacterial infections in 2010, and

Received: August 24, 2018
Published: October 22, 2018

DOI: 10.1021/acsinfecdis.8b00219
ACS Infect. Dis. XXXX, XXX, XXX−XXX

Artigo 4

DOI: 10.1038/s42003-018-0224-2

COMMUNICATIONS BIOLOGY

ARTICLE

DOI: 10.1038/s42003-018-0224-2 OPEN

Structure-function-guided exploration of the antimicrobial peptide polybia-CP identifies activity determinants and generates synthetic therapeutic candidates

Marcelo D.T. Torres[1,2,3], Cibele N. Pedron[3], Yasutomi Higashikuni et al.[#]

Antimicrobial peptides (AMPs) constitute promising alternatives to classical antibiotics for the treatment of drug-resistant infections, which are a rapidly emerging global health challenge. However, our understanding of the structure-function relationships of AMPs is limited, and we are just beginning to rationally engineer peptides in order to develop them as therapeutics. Here, we leverage a physicochemical-guided peptide design strategy to identify specific functional hotspots in the wasp-derived AMP polybia-CP and turn this toxic peptide into a viable antimicrobial. Helical fraction, hydrophobicity, and hydrophobic moment are identified as key structural and physicochemical determinants of antimicrobial activity, utilized in combination with rational engineering to generate synthetic AMPs with therapeutic activity in a mouse model. We demonstrate that, by tuning these physicochemical parameters, it is possible to design nontoxic synthetic peptides with enhanced sub-micromolar antimicrobial potency in vitro and anti-infective activity in vivo. We present a physicochemical-guided rational design strategy to generate peptide antibiotics.

Marcelo D.T. Torres[1,2,3], Cibele N. Pedron[3], Yasutomi Higashikuni[1,2], Robin M. Kramer[4], Marlon H. Cardoso[5,6,7], Karen G.N. Oshiro[7], Octávio L. Franco[5,6,7], Pedro I. Silva Junior[8], Fernanda D. Silva[3], Vani X. Oliveira Junior[3], Timothy K. Lu[1,2] & Cesar de la Fuente-Nunez[1,2]

[1]Synthetic Biology Group, MIT Synthetic Biology Center; The Center for Microbiome Informatics and Therapeutics; Research Laboratory of Electronics, Department of Biological Engineering, and Department of Electrical Engineering and Computer Science, Massachusetts Institute of Technology, Cambridge, MA 02139, USA. [2]Broad Institute of MIT and Harvard, Cambridge, MA 02142, USA. [3]Centro de Ciências Naturais e Humanas, Universidade Federal do ABC, Santo André, SP 09210580, Brazil. [4]Division of Comparative Medicine, Massachusetts Institute of Technology, Cambridge, MA 02139, USA. [5]Programa de Pós-Graduação em Patologia Molecular, Faculdade de Medicina, Universidade de Brasília, Brasília, DF 70297400, Brazil. [6]Centro de Análises Proteômicas e Bioquímicas, Universidade Católica de Brasília, Brasília, DF 71966700, Brazil. [7]S-inova Biotech, Programa de Pós-Graduação em Biotecnologia, Universidade Católica Dom Bosco, Campo Grande, MS 79117010, Brazil. [8]Laboratório Especial de Toxinologia Aplicada, Instituto Butantan, São Paulo, SP 05503900, Brazil

. Correspondence and requests for materials should be addressed to V.X.O.J. (email: vani.junior@ufabc.edu.br) or to T.K.L. (email: timlu@mit.edu) or to C.d.l.F.-N. (email: cfuente@mit.edu). [#]A full list of authors and their affiliations appears at the end of the paper.

Artigo 5

DOI: 10.1021/acsinfecdis.9b00073

ACS Infectious Diseases

Letter

Cite This: ACS Infect. Dis. XXXX, XXX, XXX−XXX

pubs.acs.org/journal/aidcbc

Short Cationic Peptide Derived from Archaea with Dual Antibacterial Properties and Anti-Infective Potential

Elizabete S. Cândido,[†,‡,#] Marlon H. Cardoso,[†,‡,§,∥,#] Lai Y. Chan,[∥] Marcelo D. T. Torres,[⊥,¶,▽,α,β] Karen G. N. Oshiro,[‡,§] William F. Porto,[‡,○] Suzana M. Ribeiro,[‡] Evan F. Haney,[◆] Robert E. W. Hancock,[◆] Timothy K. Lu,[⊥,¶] Cesar de la Fuente-Nunez,[⊥,¶,α,β] David J. Craik,[∥] and Octávio L. Franco[*,†,‡,§]

[†]Centro de Análises Proteômicas e Bioquímicas, Pós-Graduação em Ciências Genômicas e Biotecnologia, Universidade Católica de Brasília, SGAN 916 Módulo B, Asa Norte, Brasília, Distrito Federal 70790160, Brazil

[‡]S-Inova Biotech, Programa de Pós-Graduação em Biotecnologia, Universidade Católica Dom Bosco, Avenida Tamandaré 6000, Campo Grande, Mato Grosso do Sul 79117900, Brazil

[§]Programa de Pós-Graduação em Patologia Molecular, Faculdade de Medicina, Universidade de Brasília, Campus Darcy Ribeiro, Asa Norte, Brasília, Distrito Federal 70910900, Brazil

[∥]Institute for Molecular Bioscience, The University of Queensland, 306 Carmody Road, Brisbane, Queensland 4072, Australia

[⊥]Synthetic Biology Group, MIT Synthetic Biology Center; The Center for Microbiome Informatics and Therapeutics; Research Laboratory of Electronics, Department of Biological Engineering, and Department of Electrical Engineering and Computer Science, Massachusetts Institute of Technology, Cambridge, Massachusetts 02139, United States of America

[¶]Broad Institute of MIT and Harvard, Cambridge, Massachusetts 02139, United States of America

[▽]Centro de Ciências Naturais e Humanas, Universidade Federal do ABC, Santo André, São Paulo 09210170, Brazil

[○]Porto Reports, Brasília, Distrito Federal 70790160, Brazil

[◆]Centre for Microbial Diseases and Immunity Research, University of British Columbia, Vancouver, British Columbia V6T 1Z4, Canada

ABSTRACT: Bacterial biofilms and associated infections represent one of the biggest challenges in the clinic, and as an alternative to counter bacterial infections, antimicrobial peptides have attracted great attention in the past decade. Here, ten short cationic antimicrobial peptides were generated through a sliding-window strategy on the basis of the 19-amino acid residue peptide, derived from a *Pyrobaculum aerophilum* ribosomal protein. PaDBS1R6F10 exhibited anti-infective potential as it decreased the bacterial burden in murine *Pseudomonas aeruginosa* cutaneous infections by more than 1000-fold. Adverse cytotoxic and hemolytic effects were not detected against mammalian cells. The peptide demonstrated structural plasticity in terms of its secondary structure in the different environments tested. PaDBS1R6F10 represents a promising antimicrobial agent against bacteria infections, without harming human cells.

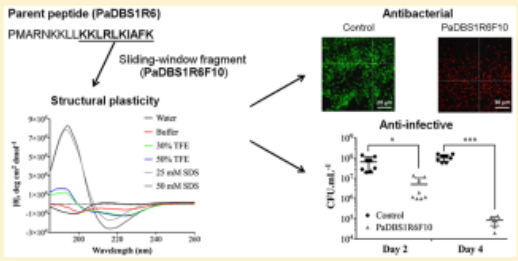

KEYWORDS: *antimicrobial peptide, biofilm, cutaneous infection, CD spectroscopy*

The high incidence of drug-resistant bacterial and biofilm-related infections currently represents a global health concern, demanding an urgent search for new antimicrobial strategies.[1] Interestingly, despite recent efforts aimed at eradicating biofilm-related infections, only a few new antimicrobial drugs are specially aimed at biofilms.[2] Moreover, the resistance associated with bacterial biofilms imposes numerous challenges for the use of conventional antimicrobials to treat these infections.

Natural antimicrobial peptides (AMPs) represent a promising alternative therapy for the treatment of drug-resistant infections. These molecules present high structural diversity and broad-spectrum antimicrobial activity.[3] Natural AMPs have been explored with the aim of making a new generation of synthetic bioinspired molecules, which are a promising option for the engineering of more active and multifunctional drugs.[4] The use of rational design approaches has enabled the generation of improved AMP synthetic analogues, reducing the limitations and increasing the advantages of these natural molecules.[5] In particular, short AMPs represent attractive

Received: February 20, 2019
Published: April 24, 2019

DOI: 10.1021/acsinfecdis.9b00073
ACS Infect. Dis. XXXX, XXX, XXX−XXX

Artigo 6

DOI: 10.1021/acs.jmedchem.9b00915

Journal of Medicinal Chemistry

Article

pubs.acs.org/jmc

Computer-Aided Design of Mastoparan-like Peptides Enables the Generation of Nontoxic Variants with Extended Antibacterial Properties

Karen G. N. Oshiro,[†,‡] Elizabete S. Cândido,[‡,§] Lai Y. Chan,[∥] Marcelo D. T. Torres,[⊥,#,∇,○,◆] Bruna E. D. Monges,[‡] Silvia G. Rodrigues,[‡] William F. Porto,[‡,¶] Suzana M. Ribeiro,[⋈] Sónia T. Henriques,[⋈] Timothy K. Lu,[⊥,#] Cesar de la Fuente-Nunez,[⊥,#,○,◆] David J. Craik,[∥] Octávio L. Franco,[*,†,‡,§] and Marlon H. Cardoso[*,†,‡,§,∥]

[†]Programa de Pós-Graduação em Patologia Molecular, Faculdade de Medicina, Universidade de Brasília, Brasília 70910900, Brazil

[‡]S-Inova Biotech, Programa de Pós-Graduação em Biotecnologia, Universidade Católica Dom Bosco, Campo Grande 79117900, Brazil

[§]Centro de Análises Proteômicas e Bioquímicas, Pós-Graduação em Ciências Genômicas e Biotecnologia, Universidade Católica de Brasília, Brasília 70790160, Brazil

[∥]Institute for Molecular Bioscience, The University of Queensland, Brisbane, QLD 4072, Australia

[⊥]Synthetic Biology Group, MIT Synthetic Biology Center; The Center for Microbiome Informatics and Therapeutics; Research Laboratory of Electronics, Department of Biological Engineering, and Department of Electrical Engineering and Computer Science, Massachusetts Institute of Technology, Cambridge, Massachusetts 02139, United States

[#]Broad Institute of MIT and Harvard, Cambridge, Massachusetts 02139, United States

[∇]Centro de Ciências Naturais e Humanas, Universidade Federal do ABC, Santo André, SP, 09210170, Brazil

[○]Department of Psychiatry and Department of Microbiology, Perelman School of Medicine and [◆]Department of Bioengineering, University of Pennsylvania, Philadelphia, Pennsylvania, 19104, United States

[¶]Porto Reports, Brasília, DF 70790160, Brazil

[⋈]Programa de Pós-Graduação em Ciências da Saúde, Universidade Federal da Grande Dourados, Dourados, MS 79825070, Brazil

[⋈]Faculty of Health, School of Biomedical Sciences, Institute of Health & Biomedical Innovation, Queensland University of Technology, Translational Research Institute, Brisbane, QLD 4102, Australia

Supporting Information

ABSTRACT: Diverse peptides have been evaluated for their activity against pathogenic microorganisms. Here, five mastoparan variants were designed based on mastoparan-L, among which two (R1 and R4) were selected for in-depth analysis. Mastoparan-L (parent/control), R1, and R4 inhibited susceptible/resistant bacteria at concentrations ranging from 2 to 32 μM, whereas only R1 and R4 eradicated *Pseudomonas aeruginosa* biofilms at 16 μM. Moreover, the toxic effects of mastoparan-L toward mammalian cells were drastically reduced in both variants. In skin infections, R1 at 64 μM was the most effective variant, reducing *P. aeruginosa* bacterial counts 1000 times on day 4 post-infection. Structurally, all of the peptides showed varying levels of helicity and structural stability in aqueous and membrane-like conditions, which may affect the different bioactivities observed here. By computationally modifying the physicochemical properties of R1 and R4, we reduced the cytotoxicity and optimized the therapeutic potential of these mastoparan-like peptides both in vitro and in vivo.

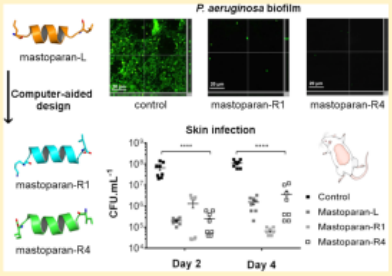

INTRODUCTION

Persistent bacterial infections are among the greatest threats to human health and are directly responsible for high levels of morbidity and mortality.[1] Bacteria from the *Enterococcus faecium*, *Staphylococcus aureus*, *Klebsiella pneumoniae*, *Acinetobacter baumannii*, *Pseudomonas aeruginosa*, and *Enterobacter* spp. group[2,3] are often associated with resistance events and hospital infections.[2] Moreover, in the case of constant exposure to antimicrobial agents, nutrient limitation, or temperature

Received: June 7, 2019
Published: August 14, 2019

DOI: 10.1021/acs.jmedchem.9b00915
J. Med. Chem. XXXX, XXX, XXX−XXX

Artigo 7

DOI: 10.3389/fmicb.2019.02169

frontiers in Microbiology

REVIEW
published: 04 October 2019
doi: 10.3389/fmicb.2019.02169

Bioactive Peptides Against Fungal Biofilms

*Karen G. N. Oshiro[1,2], Gisele Rodrigues[3], Bruna Estéfani D. Monges[2], Marlon Henrique Cardoso[2,3] and Octávio Luiz Franco[1,2,3]**

[1] *Programa de Pós-Graduação em Patologia Molecular, Faculdade de Medicina, Universidade de Brasília, Brasília, Brazil,* [2] *S-Inova Biotech, Programa de Pós-Graduação em Biotecnologia, Universidade Católica Dom Bosco, Campo Grande, Brazil,* [3] *Centro de Análises Proteômicas e Bioquímicas, Programa de Pós-Graduação em Ciências Genômicas e Biotecnologia, Universidade Católica de Brasília, Brasília, Brazil*

Infections caused by invasive fungal biofilms have been widely associated with high morbidity and mortality rates, mainly due to the advent of antibiotic resistance. Moreover, fungal biofilms impose an additional challenge, leading to multidrug resistance. This fact, along with the contamination of medical devices and the limited number of effective antifungal agents available on the market, demonstrates the importance of finding novel drug candidates targeting pathogenic fungal cells and biofilms. In this context, an alternative strategy is the use of antifungal peptides (AFPs) against fungal biofilms. AFPs are considered a group of bioactive molecules with broad-spectrum activities and multiple mechanisms of action that have been widely used as template molecules for drug design strategies aiming at greater specificity and biological efficacy. Among the AFP classes most studied in the context of fungal biofilms, defensins, cathelicidins and histatins have been described. AFPs can also act by preventing the formation of fungal biofilms and eradicating preformed biofilms through mechanisms associated with cell wall perturbation, inhibition of planktonic fungal cells' adhesion onto surfaces, gene regulation and generation of reactive oxygen species (ROS). Thus, considering the critical scenario imposed by fungal biofilms and associated infections and the application of AFPs as a possible treatment, this review will focus on the most effective AFPs described to date, with a core focus on antibiofilm peptides, as well as their efficacy *in vivo*, application on surfaces and proposed mechanisms of action.

Keywords: antifungal peptides, fungal infections, fungal biofilms, antimicrobial peptides, mechanisms of action

OPEN ACCESS

Edited by:
Jose F. Marcos,
Instituto de Agroquímica y Tecnología de Alimentos (IATA), Spain

Reviewed by:
Anand K. Ramasubramanian,
San Jose State University, United States
Dilip Shah,
Donald Danforth Plant Science Center, United States

****Correspondence:***
Octávio Luiz Franco
ocfranco@gmail.com

Specialty section:
This article was submitted to Fungi and Their Interactions, a section of the journal Frontiers in Microbiology

Received: *26 March 2019*
Accepted: *04 September 2019*
Published: *04 October 2019*

Citation:
Oshiro KGN, Rodrigues G, Monges BED, Cardoso MH and Franco OL (2019) Bioactive Peptides Against Fungal Biofilms. Front. Microbiol. 10:2169. doi: 10.3389/fmicb.2019.02169

INTRODUCTION

Fungal infections are recurrent in the clinical environment and, annually, affect ~25% of the general population worldwide, causing high morbidity and mortality rates (Brown et al., 2012; Gamaletsou et al., 2018). The indiscriminate use of broad-spectrum antibiotics, along with parenteral nutrition, permanent catheters, chemotherapy and radiotherapy, as well as immunosuppression in patients, are the most important predisposing factors for invasive fungal

Abbreviations: AFM, atomic force microscopy; AFPs, antifungal peptides; AMPs, antimicrobial peptides; BIC, biofilm inhibition concentration; BIC50, concentration required to reduce biofilm formation by 50%; Csf, caspofungin; GlcCer, glucosylceramide; Mcf, micafungin; MFC, minimal fungicidal concentration; MIC, minimal inhibitory concentration; PI, phosphatidylinositol.

Artigo 8

DOI: 10.3390/ijms20194877

International Journal of *Molecular Sciences*

MDPI

Review

Non-Lytic Antibacterial Peptides That Translocate Through Bacterial Membranes to Act on Intracellular Targets

Marlon H. Cardoso [1,2], Beatriz T. Meneguetti [1], Bruna O. Costa [1], Danieli F. Buccini [1], Karen G. N. Oshiro [1,3], Sergio L. E. Preza [1], Cristiano M. E. Carvalho [1], Ludovico Migliolo [1,4] and Octávio L. Franco [1,2,3,*]

1 S-inova Biotech, Programa de Pós-Graduação em Biotecnologia, Universidade Católica Dom Bosco, Campo Grande 79117-900, Brazil; marlonhenrique6@gmail.com (M.H.C.); biatmeneguetti@gmail.com (B.T.M.); ocostab@gmail.com (B.O.C.); dfbuccini@gmail.com (D.F.B.); oshiro.kgn@gmail.com (K.G.N.O.); dyrosha@gmail.com (S.L.E.P.); rf7085@ucdb.br (C.M.E.C.); ludovico.migliolo@gmail.com (L.M.)

2 Centro de Análises Proteômicas e Bioquímicas, Pós-Graduação em Ciências Genômicas e Biotecnologia, Universidade Católica de Brasília, Brasília 70790-160, Brazil

3 Programa de Pós-Graduação em Patologia Molecular, Faculdade de Medicina, Universidade de Brasília, Brasília 70910-900, Brazil

4 Programa de Pós-Graduação em Bioquímica, Universidade Federal do Rio Grande do Norte, Natal 59078-900, Brazil

* Correspondence: ocfranco@gmail.com; Tel.: +55-61-34487167 or +55-61-34487220

Received: 30 July 2019; Accepted: 14 September 2019; Published: 1 October 2019

Abstract: The advent of multidrug resistance among pathogenic bacteria has attracted great attention worldwide. As a response to this growing challenge, diverse studies have focused on the development of novel anti-infective therapies, including antimicrobial peptides (AMPs). The biological properties of this class of antimicrobials have been thoroughly investigated, and membranolytic activities are the most reported mechanisms by which AMPs kill bacteria. Nevertheless, an increasing number of works have pointed to a different direction, in which AMPs are seen to be capable of displaying non-lytic modes of action by internalizing bacterial cells. In this context, this review focused on the description of the in vitro and in vivo antibacterial and antibiofilm activities of non-lytic AMPs, including indolicidin, buforin II PR-39, bactenecins, apidaecin, and drosocin, also shedding light on how AMPs interact with and further translocate through bacterial membranes to act on intracellular targets, including DNA, RNA, cell wall and protein synthesis.

Keywords: antimicrobial peptides; non-lytic peptides; bacterial membranes

1. Introduction

The World Health Organization (WHO) has identified antimicrobial resistance as one of the three major threats to human health [1]. Bacteria can be efficient in the synthesis and sharing of genes involved in the development of antibiotic resistance mechanisms, leading to negative outcomes in the clinic [2]. This inefficiency may be related to the intrinsic resistance of a bacterium to a specific antibiotic, which can be explained by its ability to resist the action of this drug as a result of inherent structural or functional characteristics [3]. Therefore, the dissemination of antibiotic resistance factors, along with the misuse of these drugs, has made drug design a broad field of research [4]. In this scenario, the antimicrobial peptides (AMPs) have been considered as an alternative to conventional antibacterial treatments [5].

Artigo 9

DOI: 10.3390/molecules24234344

molecules

MDPI

Article

Dual Insecticidal Effects of *Adenanthera pavonina* Kunitz-Type Inhibitor on *Plodia interpunctella* is Mediated by Digestive Enzymes Inhibition and Chitin-Binding Properties

Caio Fernando Ramalho de Oliveira [1], Taylla Michelle de Oliveira Flores [2,3], Marlon Henrique Cardoso [2,4], Karen Garcia Nogueira Oshiro [2,5], Raphael Russi [6], Anderson Felipe Jácome de França [6], Elizeu Antunes dos Santos [6], Octávio Luiz Franco [2,4,5], Adeliana Silva de Oliveira [6] and Ludovico Migliolo [2,3,6,*]

1 Universidade Federal de Grande Dourados, Dourados, Mato Grosso do Sul, MS, 79825-070, Brazil; oliveiracfr@gmail.com
2 S-Inova Biotech, Programa de Pós-Graduação em Biotecnologia, Universidade Católica Dom Bosco, Campo Grande, MS, 79117-900, Brazil; taylla.flores@outlook.com (T.M.d.O.F.); marlonhenrique6@gmail.com (M.H.C.); oshiro.kgn@gmail.com (K.G.N.O.); ocfranco@gmail.com (O.L.F.)
3 Programa de Pós-Graduação em Biologia Celular e Molecular, Universidade Federal da Paraíba, João Pessoa, PB, 58059-900, Brazil
4 Centro de Análises Bioquímica e Proteômicas, Programa de Pós Graduação em Ciências Genômicas e Biotecnologia, Universidade Católica de Brasília, Brasília, DF, 70790-160, Brazil
5 Programa de Pós-Graduação em Patologia Molecular, Faculdade de Medicina, Universidade de Brasília, Brasília, DF, 70910-900, Brazil
6 Programa de Pós-Graduação em Bioquímica, Universidade Federal do Rio Grande do Norte, Natal, RN, 59078-900, Brazil; raphaelrussi@gmail.com (R.R.); andersonfjf@gmail.com (A.F.J.d.F.); elizeu.ufrn@gmail.com (E.A.d.S.); cisteana@yahoo.com.br (A.S.d.O.)
* Correspondence: ludovico@ucdb.br

Academic Editor: Massimiliano Fenice
Received: 19 September 2019; Accepted: 14 October 2019; Published: 28 November 2019

check for updates

Abstract: The Indianmeal moth, *Plodia interpunctella*, is one of the most damaging pests of stored products. We investigated the insecticidal properties of ApKTI, a Kunitz trypsin inhibitor from *Adenanthera pavonina* seeds, against *P. interpunctella* larvae through bioassays with artificial diet. ApKTI-fed larvae showed reduction of up to 88% on larval weight and 75% in survival. Trypsin enzymes extracted from *P. interpunctella* larvae were inhibited by ApKTI, which also demonstrated capacity to bind to chitin. Kinetic studies revealed a non-competitive inhibition mechanism of ApKTI for trypsin, which were further corroborated by molecular docking studies. Furthermore, we have demonstrated that ApKTI exhibits a hydrophobic pocket near the reactive site loop probably involved in chitin interactions. Taken together, these data suggested that the insecticidal activity of ApKTI for *P. interpunctella* larvae involves a dual and promiscuous mechanisms biding to two completely different targets. Both processes might impair the *P. interpunctella* larval digestive process, leading to larvae death before reaching the pupal stage. Further studies are encouraged using ApKTI as a biotechnological tool to control insect pests in field conditions.

Keywords: non-competitive inhibitor; trypsin inhibitor; peritrophic membrane

Highlights

- ApKTI increases mortality of *P. interpunctella* larvae.

Artigo 10

DOI: 10.3389/fmicb.2019.03097

frontiers in Microbiology

REVIEW
published: 22 January 2020
doi: 10.3389/fmicb.2019.03097

Computer-Aided Design of Antimicrobial Peptides: Are We Generating Effective Drug Candidates?

*Marlon H. Cardoso[1,2], Raquel Q. Orozco[1,3], Samilla B. Rezende[1], Gisele Rodrigues[2], Karen G. N. Oshiro[1,4], Elizabete S. Cândido[1,2] and Octávio L. Franco[1,2,3,4]**

[1] *S-Inova Biotech, Programa de Pós-Graduação em Biotecnologia, Universidade Católica Dom Bosco, Campo Grande, Brazil,* [2] *Centro de Análises Proteômicas e Bioquímicas, Pós-Graduação em Ciências Genômicas e Biotecnologia, Universidade Católica de Brasília, Brasília, Brazil,* [3] *Instituto de Ciências Biológicas, Departamento de Biologia, Programa de Pós-Graduação em Ciências Biológicas (Imunologia/Genética e Biotecnologia), Universidade Federal de Juiz de Fora, Juiz de Fora, Brazil,* [4] *Programa de Pós-Graduação em Patologia Molecular, Faculdade de Medicina, Universidade de Brasília, Brasília, Brazil*

OPEN ACCESS

Edited by:
Kai Hilpert,
St George's, University of London, United Kingdom

Reviewed by:
Ralf Mikut,
Karlsruhe Institute of Technology, Germany
Steven W. Polyak,
University of South Australia, Australia
Monique L. Van Hoek,
George Mason University, United States

****Correspondence:***
Octávio L. Franco
ocfranco@gmail.com

Specialty section:
This article was submitted to Antimicrobials, Resistance and Chemotherapy, a section of the journal Frontiers in Microbiology

Received: *28 September 2019*
Accepted: *20 December 2019*
Published: *22 January 2020*

Citation:
Cardoso MH, Orozco RQ, Rezende SB, Rodrigues G, Oshiro KGN, Cândido ES and Franco OL (2020) Computer-Aided Design of Antimicrobial Peptides: Are We Generating Effective Drug Candidates? Front. Microbiol. 10:3097. doi: 10.3389/fmicb.2019.03097

Antimicrobial peptides (AMPs), especially antibacterial peptides, have been widely investigated as potential alternatives to antibiotic-based therapies. Indeed, naturally occurring and synthetic AMPs have shown promising results against a series of clinically relevant bacteria. Even so, this class of antimicrobials has continuously failed clinical trials at some point, highlighting the importance of AMP optimization. In this context, the computer-aided design of AMPs has put together crucial information on chemical parameters and bioactivities in AMP sequences, thus providing modes of prediction to evaluate the antibacterial potential of a candidate sequence before synthesis. Quantitative structure-activity relationship (QSAR) computational models, for instance, have greatly contributed to AMP sequence optimization aimed at improved biological activities. In addition to machine-learning methods, the *de novo* design, linguistic model, pattern insertion methods, and genetic algorithms, have shown the potential to boost the automated design of AMPs. However, how successful have these approaches been in generating effective antibacterial drug candidates? Bearing this in mind, this review will focus on the main computational strategies that have generated AMPs with promising activities against pathogenic bacteria, as well as anti-infective potential in different animal models, including sepsis and cutaneous infections. Moreover, we will point out recent studies on the computer-aided design of antibiofilm peptides. As expected from automated design strategies, diverse candidate sequences with different structural arrangements have been generated and deposited in databases. We will, therefore, also discuss the structural diversity that has been engendered.

Keywords: computer-aided design, bacteria, biofilms, antimicrobial peptides, drug design

Artigo 11

DOI: 10.1093/jac/dkaa560

J Antimicrob Chemother
doi:10.1093/jac/dkaa560

Journal of Antimicrobial Chemotherapy

Polyalanine peptide variations may have different mechanisms of action against multidrug-resistant bacterial pathogens

Mário R. Felício[1], Gislaine G. O. S. Silveira[2], Karen G. N. Oshiro[2,3], Beatriz T. Meneguetti[2], Octávio L. Franco[2,3,4], Nuno C. Santos[1]† and Sónia Gonçalves[1]*†

[1]Instituto de Medicina Molecular, Faculdade de Medicina, Universidade de Lisboa, Avenida Professor Egas Moniz, 1649-028 Lisboa, Portugal; [2]S-Inova Biotech, Pós-graduação em Biotecnologia, Universidade Católica Dom Bosco, Campo Grande, MS, Brazil; [3]Programa de Pós-Graduação em Patologia Molecular, Universidade de Brasília, Brasília, DF, Brazil; [4]Centro de Análises Proteômicas e Bioquímicas, Pós-graduação em Ciências Genômicas e Biotecnologia, Universidade Católica de Brasília, Brasília, DF, Brazil

*Corresponding author. E-mail: sabreu@fm.ul.pt
†These two authors contributed equally to this article.

Received 10 July 2020; accepted 15 December 2020

Objectives: The number of bacterial pathogens resistant to the currently available antibiotics has dramatically increased, with antimicrobial peptides (AMPs) being among the most promising potential new drugs. In this study, the applicability and mechanisms of action of *Pa*-MAP 2 and *Pa*-MAP 1.9, two AMPs synthetically designed based on a natural AMP template, were evaluated.

Methods: *Pa*-MAP 2 and *Pa*-MAP 1.9 were tested against a clinically isolated multidrug-resistant (MDR) *Escherichia coli* strain. Biophysical approaches were used to evaluate the preference of both peptides for specific lipid membranes, and bacterial surface changes imaged by atomic force microscopy (AFM). The efficacy of both peptides was assessed both *in vitro* and *in vivo*.

Results: Experimental results showed that both peptides have antimicrobial activity against the *E. coli* MDR strain. Zeta potential and surface plasmon resonance assays showed that they interact extensively with negatively charged membranes, changing from a random coil structure, when free in solution, to an α-helical structure after membrane interaction. The antibacterial efficacy was evaluated *in vitro*, by several techniques, and *in vivo*, using a wound infection model, showing a concentration-dependent antibacterial effect. Different membrane properties were evaluated to understand the mechanism underlying peptide action, showing that both promote destabilization of the bacterial surface, as imaged by AFM, and change properties such as membrane surface and dipole potential.

Conclusions: Despite their similarity, data indicate that the mechanisms of action of the peptides are different, with *Pa*-MAP 1.9 being more effective than *Pa*-MAP 2. These results highlight their potential use as antimicrobial agents against MDR bacteria.

Introduction

Increased bacterial resistance to conventional antibiotics poses a serious health problem that needs to be overcome.[1–3] The indiscriminate use of conventional antibiotics has contributed to an increase in resistance to these therapeutic agents in different bacteria, such as *Escherichia coli*, *Klebsiella pneumoniae* and *Pseudomonas aeruginosa*.[4] Alternative therapeutics are urgently required, with the lack of development of new antibiotic molecules contributing to the emergence of this problem. Due to this, antimicrobial peptides (AMPs) have been gaining attention as future alternatives in microbial treatment.[5,6]

AMPs are small cationic and amphipathic peptides that are part of the innate immune system, acting against a wide range of microorganisms, including bacteria, viruses and fungi.[7,8] They have the advantage of being less prone to promoting bacterial resistance than conventional antibiotics, due to the more difficult development of resistance against AMP mechanisms of action at the membrane level.[9,10] Nevertheless, it has been shown that cells may still become resistant to these molecules.[11] AMP properties determine their selective interaction with the pathogen membrane, such as their positive net charge, promoting electrostatic attraction between the peptide and the bacterial membranes, which contain high numbers of negatively charged lipids, such as

Artigo 12

DOI: 10.1039/d1cc03793e

ChemComm

ROYAL SOCIETY OF CHEMISTRY

HIGHLIGHT

View Article Online
View Journal

Cite this: DOI: 10.1039/d1cc03793e

Advances on chemically modified antimicrobial peptides for generating peptide antibiotics

Samilla B. Rezende,[a] Karen G. N. Oshiro,[ab] Nelson G. O. Júnior,[c] Octávio L. Franco[abc] and Marlon H. Cardoso[*abc]

Antimicrobial peptides (AMPs) are pinpointed as promising molecules against antibiotic-resistant bacterial infections. Nevertheless, there is a discrepancy between the AMP sequences generated and the tangible outcomes in clinical trials. AMPs' limitations include enzymatic degradation, chemical/physical instability and toxicity toward healthy human cells. These factors compromise AMPs' bioavailability, resulting in limited therapeutic potential. To overcome such obstacles, peptidomimetic approaches, including glycosylation, PEGylation, lipidation, cyclization, grafting, D-amino acid insertion, stapling and dendrimers are promising strategies to fine-tune AMPs. Here we focused on chemical modifications applied for AMP optimization and how they have helped these peptide-based antibiotic candidates' design and translational potential.

Received 14th July 2021,
Accepted 5th October 2021

DOI: 10.1039/d1cc03793e

rsc.li/chemcomm

Nosocomial infections caused by antibiotic-resistant bacterial strains represent a severe threat to humanity. According to the World Health Organization (WHO), alarming levels of antimicrobial resistance have been reported in countries of all income levels. This resistance to second and third-line antibiotics is projected to increase 70% by 2030. Therefore, innovative antimicrobial molecules are urgently needed.[1]

Antimicrobial peptides (AMPs) represent an alternative treatment against multi-drug-resistant (MDR) bacterial infections. AMPs are found in all kinds of life, representing inherent defense mechanisms against microbial pathogens.[2] The properties of multifunctional AMPs are intrinsically related to their

[a] S-Inova Biotech, Universidade Católica Dom Bosco (UCDB), Campo Grande, MS, Brazil
[b] Programa de Pós-Graduação em Patologia Molecular, Universidade de Brasília (UnB), Brasília, DF, Brazil
[c] Centro de Análises Proteômicas e Bioquímicas Programa de Pós-Graduação em Ciências Genômicas e Biotecnologia, Universidade Católica de Brasília (UCB), Brasília, DF, Brazil. E-mail: marlonhenrique6@gmail.com

Octávio L. Franco

Dr Octávio L. Franco is a Head Professor at Universidade Católica Dom Bosco and Universidade Católica de Brasília. He graduated in Biological Sciences from Universidade Federal do Ceará and obtained his PhD from Universidade de Brasília. Prof. Franco is the Principal Investigator of two laboratories, including the Centro de Análises Proteômicas e Bioquímicas and S-inova Biotech. His contributions are documented in >300 career publication in international journals, mainly in the fields of peptide science, medicinal chemistry and biochemistry.

Marlon H. Cardoso

Dr Marlon H. Cardoso is an Assistant Professor at the Post-Graduation Program in Biotechnology (Universidade Católica Dom Bosco – UCDB). Prof. Cardoso obtained his bachelor's degree in Biological Sciences (Habilitation: Biotechnology) from Universidade Católica de Brasília. He obtained his PhD in Molecular Pathology from the Faculty of Medicine of the Universidade de Brasília. Prof. Cardoso was also a Visiting PhD student at the Institute for Molecular Bioscience, The University of Queensland, Australia. He has accumulated over 50 career publications as a young scientist, with a core focus on AMP design, functional/structural characterization of peptide-based drug candidates and peptidomimetics.

Artigo 13

DOI: 10.1039/d1sc06998e

Chemical Science

ROYAL SOCIETY OF CHEMISTRY

EDGE ARTICLE

View Article Online
View Journal

Check for updates

Cite this: DOI: 10.1039/d1sc06998e

All publication charges for this article have been paid for by the Royal Society of Chemistry

An N-capping asparagine–lysine–proline (NKP) motif contributes to a hybrid flexible/stable multifunctional peptide scaffold†

Marlon H. Cardoso, *abcd Lai Y. Chan, e Elizabete S. Cândido,ab Danieli F. Buccini,a Samilla B. Rezende, a Marcelo D. T. Torres, f Karen G. N. Oshiro, ac Ítala C. Silva, g Sónia Gonçalves,g Timothy K. Lu,h Nuno C. Santos, g Cesar de la Fuente-Nunez, f David J. Craik *e and Octávio L. Franco *abc

Structural diversity drives multiple biological activities and mechanisms of action in linear peptides. Here we describe an unusual N-capping asparagine-lysine-proline (NKP) motif that confers a hybrid multifunctional scaffold to a computationally designed peptide (PaDBS1R7). PaDBS1R7 has a shorter α-helix segment than other computationally designed peptides of similar sequence but with key residue substitutions. Although this motif acts as an α-helix breaker in PaDBS1R7, the Asn5 presents exclusive N-capping effects, forming a belt to establish hydrogen bonds for an amphipathic α-helix stabilization. The combination of these different structural profiles was described as a coil/N-cap/α-helix scaffold, which was also observed in diverse computational peptide mutants. Biological studies revealed that all peptides displayed antibacterial activities. However, only PaDBS1R7 displayed anticancer properties, eradicated *Pseudomonas aeruginosa* biofilms, decreased bacterial counts by 100–1000-fold *in vivo*, reduced lipopolysaccharide-induced macrophages stress, and stimulated fibroblast migration for wound healing. This study extends our understanding of an N-capping NKP motif to engineering hybrid multifunctional peptide drug candidates with potent anti-infective and immunomodulatory properties.

Received 16th December 2021
Accepted 10th July 2022

DOI: 10.1039/d1sc06998e

rsc.li/chemical-science

Introduction

Short bioactive peptides have dynamic structures that include diverse conformational states such as random coils, α-helices, β-turns and β-sheets.[1,2] The structures of peptides can be manipulated based on many parameters, ranging from amino acid composition to the biological environments into which they are inserted. For example, branched and bulky amino acids favor rigidity, whereas smaller amino acids elicit flexibility.[3] Moreover, depending on the net charge, hydrophobicity, fluidity, salt concentration and pH of its environment, a single peptide may adopt different structural profiles to achieve the lowest free-energy state for a specific molecular complex (*e.g.*, peptide-membrane, peptide–peptide or peptide–protein interactions).[4]

Much effort has been devoted to designing peptide-based drugs having constrained scaffolds and well-defined secondary structures.[5] Antimicrobial peptides (AMPs), for instance, are typically designed with the aim of having a well-defined α-helix conformation when in contact with a target microorganism to trigger membrane-associated mechanisms of

[a]S-Inova Biotech, Programa de Pós-Graduação em Biotecnologia, Universidade Católica Dom Bosco Avenida Tamandaré 6000, Campo Grande – MS, 79117900, Brazil. E-mail: marlonhenrique6@gmail.com; d.craik@imb.uq.edu.au; ocfranco@gmail.com

[b]Centro de Análises Proteômicas e Bioquímicas, Programa de Pós-Graduação em Ciências Genômicas e Biotecnologia, Universidade Católica de Brasília, SGAN 916 Módulo B, Asa Norte, Brasília – DF, 70790160, Brazil

[c]Programa de Pós-Graduação em Patologia Molecular, Faculdade de Medicina, Universidade de Brasília, Campus Darcy Ribeiro, Asa Norte, Brasília – DF, 70910900, Brazil

[d]Instituto de Biociências (INBIO), Universidade Federal de Mato Grosso do Sul, Cidade Universitária, 79070900, Campo Grande, Mato Grosso do Sul, Brazil

[e]Institute for Molecular Bioscience, Australian Research Council Centre of Excellence for Innovations in Peptide and Protein Science, The University of Queensland, Brisbane, QLD, 4072, Australia

[f]Machine Biology Group, Departments of Psychiatry and Microbiology, Institute for Biomedical Informatics, Institute for Translational Medicine and Therapeutics, Perelman School of Medicine, Departments of Bioengineering and Chemical and Biomolecular Engineering, School of Engineering and Applied Science, Penn Institute for Computational Science, University of Pennsylvania, Philadelphia, Pennsylvania, USA

[g]Instituto de Medicina Molecular, Faculdade de Medicina, Universidade de Lisboa, Lisbon, Portugal

[h]Synthetic Biology Group, MIT Synthetic Biology Center, The Center for Microbiome Informatics and Therapeutics, Research Laboratory of Electronics, Department of Biological Engineering, Department of Electrical Engineering and Computer Science, Massachusetts Institute of Technology, Cambridge – MA, 02139, USA

† Electronic supplementary information (ESI) available: Tables S1–S12, Fig. S1–S17,† and supplementary references. See https://doi.org/10.1039/d1sc06998e

10. REFERÊNCIA BIBLIOGRÁFICAS

Akram, F., Imtiaz, M., and Haq, I.u. (2023). Emergent crisis of antibiotic resistance: A silent pandemic threat to 21st century. *Microbial Pathogenesis,* 174**,** 105923.

Alanis, A.J. (2005). Resistance to antibiotics: are we in the post-antibiotic era? *Archives of medical research,* 36(6)**,** 697-705.

Alvares, D.S., Wilke, N., and Neto, J.R. (2018). Effect of N-terminal acetylation on lytic activity and lipid-packing perturbation induced in model membranes by a mastoparan-like peptide. *Biochimica et Biophysica Acta (BBA)-Biomembranes,* 1860(3)**,** 737-748.

Argiolas, A., and Pisano, J.J. (1984). Isolation and characterization of two new peptides, mastoparan C and crabrolin, from the venom of the European hornet, *Vespa crabro*. *Journal of Biological Chemistry,* 259(16)**,** 10106-10111.

Benfield, A.H., and Henriques, S.T. (2020). Mode-of-action of antimicrobial peptides: membrane disruption vs. intracellular mechanisms. *Frontiers in Medical Technology,* 2**,** 610997.

Blair, J.M.A., Webber, M.A., Baylay, A.J., Ogbolu, D.O., and Piddock, L.J.V. (2015). Molecular mechanisms of antibiotic resistance. *Nature reviews microbiology, 13*(1), 42-51.

Blanco, F.J., Rivas, G., and Serrano, L. (1994). A short linear peptide that folds into a native stable β-hairpin in aqueous solution. *Nature Structural & Molecular Biology* 1(9)**,** 584-590.

Blondelle, S., and Lohner, K. (2010). Optimization and high-throughput screening of antimicrobial peptides. *Current pharmaceutical design* 16(28)**,** 3204-3211.

Bradshaw, J.P. (2003). Cationic antimicrobial peptides. *BioDrugs,* 17(4)**,** 233-240.

Braff, M., and Gallo, R. (2006). "Antimicrobial peptides: an essential component of the skin defensive barrier," in *Antimicrobial Peptides and Human Disease*, 91-110.

Broekaert, W.F., Cammue, B.P., De Bolle, M.F., Thevissen, K., De Samblanx, G.W., Osborn, R.W., et al. (1997). Antimicrobial peptides from plants. *Critical reviews in plant sciences* 16(3)**,** 297-323.

Brogden, K.A. (2005). Antimicrobial peptides: pore formers or metabolic inhibitors in bacteria? *Nature Reviews Microbiology* 3(3)**,** 238-250.

Cardoso, M.H., Cândido, E.S., Oshiro, K.G., Rezende, S.B., and Franco, O.L. (2018). "Peptides containing D-amino acids and retro-inverso peptides: general applications and special focus on antimicrobial peptides," in *Peptide Applications in Biomedicine, Biotechnology and Bioengineering*, 131-155.

Cardoso, M.H., Chan, L.Y., Cândido, E.S., Buccini, D.F., Rezende, S.B., Torres, M.D., et al. (2022). An N-capping asparagine–lysine–proline (NKP) motif contributes to a hybrid flexible/stable multifunctional peptide scaffold. *Chemical Science*, 13(32)**,** 9410-9424.

Cardoso, M.H., Meneguetti, B.T., Costa, B.O., Buccini, D.F., Oshiro, K.G., Preza, S.L., et al. (2019). Non-lytic antibacterial peptides that translocate through bacterial membranes to act on intracellular targets. *International Journal of Molecular Sciences*, 20(19)**,** 4877.

Cardoso, M.H., Orozco, R.Q., Rezende, S.B., Rodrigues, G., Oshiro, K.G., Cândido, E.S., et al. (2020). Computer-aided design of antimicrobial peptides: are we generating effective drug candidates?. *Frontiers in microbiology*, 10**,** 3097.

Cardoso, M.H., Ribeiro, S.M., Nolasco, D.O., de La Fuente-Núñez, C., Felício, M.R., Gonçalves, S., et al. (2016). A polyalanine peptide derived from polar fish with anti-infectious activities. *Scientific reports*, 6.

Carratalá, J.V., Serna, N., Villaverde, A., Vázquez, E., and Ferrer-Miralles, N. (2020). Nanostructured antimicrobial peptides: The last push towards clinics. *Biotechnology advances*, 44**,** 107603.

Chen, Y., Guarnieri, M.T., Vasil, A.I., Vasil, M.L., Mant, C.T., Hodges, R.S.J.A.a., et al. (2007). Role of peptide hydrophobicity in the mechanism of action of α-helical antimicrobial peptides. *Antimicrobial agents and chemotherapy*, 51(4)**,** 1398-1406.

Chen, Y., Mant, C.T., Farmer, S.W., Hancock, R.E., Vasil, M.L., and Hodges, R.S. (2005). Rational design of α-helical antimicrobial peptides with enhanced activities and specificity/therapeutic index. *Journal of Biological Chemistry*, 280(13)**,** 12316-12329.

Chiang, L.H., Kotanchek, M.E., and Kordon, A.K. (2004). Fault diagnosis based on Fisher discriminant analysis and support vector machines. *Computers & chemical engineering*, 28(8)**,** 1389-1401.

Chou, S., Wang, J., Shang, L., Akhtar, M.U., Wang, Z., Shi, B., et al. (2019). Short, symmetric-helical peptides have narrow-spectrum activity with low resistance potential and high selectivity. *Biomaterials science*, 7(6)**,** 2394-2409.

Cooper, M.A., Hansson, A., Löfås, S., and Williams, D.H. (2000). A vesicle capture sensor chip for kinetic analysis of interactions with membrane-bound receptors. *Analytical biochemistry*, 277(2)**,** 196-205.

Costerton, J.W., Stewart, P.S., and Greenberg, E.P. (1999). Bacterial biofilms: a common cause of persistent infections. *Science*, 284(5418)**,** 1318-1322.

das Neves, R.C., Mortari, M.R., Schwartz, E.F., Kipnis, A., and Junqueira-Kipnis, A. (2019). Antimicrobial and antibiofilm effects of peptides from venom of social Wasp and scorpion on multidrug-resistant *Acinetobacter baumannii*. *Toxins*, 11(4)**,** 216.

Davies, A., and Shamu, C. (2014). An introduction to high content screening: imaging technology, assay development, and data analysis in biology and drug discovery. *John Wiley & Sons.*

de Azevedo, R.A., Figueiredo, C.R., Ferreira, A.K., Matsuo, A.L., Massaoka, M.H., Girola, N., et al. (2015). Mastoparan induces apoptosis in B16F10-Nex2 melanoma cells via the intrinsic mitochondrial pathway and displays antitumor activity in vivo. *Peptides*, 68**,** 113-119.

de la Fuente-Núñez, C., Reffuveille, F., Fernández, L., and Hancock, R.E. (2013). Bacterial biofilm development as a multicellular adaptation: antibiotic resistance and new therapeutic strategies. *Current opinion in microbiology*, 16(5)**,** 580-589.

de Lacorte Singulani, J., Galeane, M.C., Ramos, M.D., Gomes, P.C., dos Santos, C.T., de Souza, B.M., et al. (2019). Antifungal activity, toxicity, and membranolytic action of a mastoparan analog peptide. *Frontiers in cellular and infection microbiology*, 9, 419.

de Santana, C.J.C., Pires Júnior, O.R., Fontes, W., Palma, M.S., and Castro, M.S. (2022). Mastoparans: A Group of Multifunctional α-Helical Peptides With Promising Therapeutic Properties. *Frontiers in Molecular Biosciences,* 9, 824989.

de Souza, B.M., dos Santos Cabrera, M.P., Neto, J.R., and Palma, M.S. (2011). Investigating the effect of different positioning of lysine residues along the peptide chain of mastoparans for their secondary structures and biological activities. *Amino acids,* 40(1)**,** 77-90.

Dennison, S.R., Wallace, J., Harris, F., and Phoenix, D.A. (2005). Amphiphilic α-helical antimicrobial peptides and their structure/function relationships. *Protein and peptide letters* 12(1)**,** 31-39.

Dong, N., Zhu, X., Chou, S., Shan, A., Li, W., and Jiang, J. (2014). Antimicrobial potency and selectivity of simplified symmetric-end peptides. *Biomaterials,* 35(27)**,** 8028-8039.

Dongol, T., Dhananjaya, B., Shrestha, R.K., Aryal, G. (2014). Pharmacological and immunological properties of wasp venom. *Pharmacology and Therapeutics,* 47-81.

dos Santos Cabrera, M.P., Rangel, M., Ruggiero Neto, J., and Konno, K.J.T. (2019). Chemical and biological characteristics of antimicrobial α-helical peptides found in solitary wasp venoms and their interactions with model membranes. *Toxins,* 11(10)**,** 559.

Durand, G.A., Raoult, D., and Dubourg, G. (2019). Antibiotic discovery: history, methods and perspectives. *International journal of antimicrobial agents,* 53(4)**,** 371-382.

Eddy, S.R. (1998). Profile hidden Markov models. *Bioinformatics (Oxford, England),* 14(9)**,** 755-763.

Edwards, I.A., Henriques, S.T., Blaskovich, M.A.T., Elliott, A.G., and Cooper, M.A. (2022). Investigations into the membrane activity of arenicin antimicrobial peptide AA139. *Biochimica et Biophysica Acta (BBA) - General Subjects,* 1866(8)**,** 130156.

Epand, R.M., and Epand, R.F. (2011). Bacterial membrane lipids in the action of antimicrobial agents. *Journal of Peptide Science,* 17(5)**,** 298-305.

Epand, R.M., and Vogel, H.J. (1999). Diversity of antimicrobial peptides and their mechanisms of action. *Biochimica et Biophysica Acta (BBA)-Biomembranes,* 1462(1)**,** 11-28.

Fensterseifer, I.C.M., Felício, M.R., Alves, E.S.F., Cardoso, M.H., Torres, M.D.T., Matos, C.O., et al. (2019). Selective antibacterial activity of the cationic peptide PaDBS1R6 against Gram-negative bacteria. *Biochimica et Biophysica Acta (BBA) – Biomembranes,* 1861(7)**,** 1375-1387.

Fernández, L., and Hancock, R.E. (2012). Adaptive and mutational resistance: role of porins and efflux pumps in drug resistance. *Clinical microbiology reviews,* 25(4)**,** 661-681.

Fisher, R.A., Gollan, B., and Helaine, S. (2017). Persistent bacterial infections and persister cells. *Nature Reviews Microbiology*, *15*(8), 453-464.

Floss, H.G., and Yu, T.-W. (2005). Rifamycin mode of action, resistance, and biosynthesis. *Chemical reviews,* 105(2)**,** 621-632.

Founou, R.C., Founou, L.L., and Essack, S.Y. (2017). Clinical and economic impact of antibiotic resistance in developing countries: A systematic review and meta-analysis. *PloS one,* 12(12)**,** e0189621.

Franco, O.L. (2011). Peptide promiscuity: an evolutionary concept for plant defense. *FEBS letters* 585(7)**,** 995-1000.

Fuentes, A.V., Pineda, M.D., and Venkata, K.C.N. (2018). Comprehension of top 200 prescribed drugs in the US as a resource for pharmacy teaching, training and practice. *Pharmacy,* 6(2)**,** 43.

Gallo, R.L., Murakami, M., Ohtake, T., and Zaiou, M. (2002). Biology and clinical relevance of naturally occurring antimicrobial peptides. *Journal of Allergy and Clinical Immunology,* 110(6)**,** 823-831.

Gan, B.H., Gaynord, J., Rowe, S.M., Deingruber, T., and Spring, D.R. (2021). The multifaceted nature of antimicrobial peptides: Current synthetic chemistry approaches and future directions. *Chemical Society Reviews,* 50(13)**,** 7820-7880.

Gautier, R., Douguet, D., Antonny, B., and Drin, G.J.B. (2008). HELIQUEST: a web server to screen sequences with specific α-helical properties. *Bioinformatics,* 24(18)**,** 2101-2102.

Giuliani, A., Pirri, G., and Nicoletto, S. (2007). Antimicrobial peptides: an overview of a promising class of therapeutics. *Open Life Sciences,* 2(1)**,** 1-33.

Goto, C., Hirano, M., Hayashi, K., Kikuchi, Y., Hara-Kudo, Y., Misawa, T., et al. (2019). Development of amphipathic antimicrobial peptide foldamers based on Magainin 2 sequence. *ChemMedChem,* 14(22)**,** 1911-1916.

Guido-Patiño, J.C., and Plisson, F.J.T.X. (2022). Profiling hymenopteran venom toxins: Protein families, structural landscape, biological activities, and pharmacological benefits. *Toxicon,* 14**,** 100119.

Hale, J.D., and Hancock, R.E.W. (2007). Alternative mechanisms of action of cationic antimicrobial peptides on bacteria. *Expert review of anti-infective therapy,* 5(6)**,** 951-959.

Hall, C.W., and Mah, T.-F.M. (2017). Molecular mechanisms of biofilm-based antibiotic resistance and tolerance in pathogenic bacteria. *FEMS microbiology reviews,* 41(3)**,** 276-301.

Hancock, R., and Patrzykat, A. (2002). Clinical development of cationic antimicrobial peptides: from natural to novel antibiotics. *Current drug targets-Infectious disorders,* 2(1)**,** 79-83.

Hancock, R.E., and Diamond, G. (2000). The role of cationic antimicrobial peptides in innate host defences. *Trends in microbiology,* 8(9)**,** 402-410.

Hancock, R.E., and Lehrer, R. (1998). Cationic peptides: a new source of antibiotics. *Trends in biotechnology,* 16(2)**,** 82-88.

Hancock, R.E., and Rozek, A. (2002). Role of membranes in the activities of antimicrobial cationic peptides. *FEMS microbiology letters,* 206(2)**,** 143-149.

Hancock, R.E., and Sahl, H.-G. (2006). Antimicrobial and host-defense peptides as new anti-infective therapeutic strategies. *Nature biotechnology,* 24(12)**,** 1551-1557.

Hancock, R.E., and Scott, M.G. (2000). The role of antimicrobial peptides in animal defenses. *Proceedings of the national Academy of Sciences* 97(16)**,** 8856-8861.

Haney, E.F., Straus, S.K., and Hancock, R.E.J.F.i.c. (2019). Reassessing the host defense peptide landscape. *Frontiers in chemistry,* 43.

Henriksen, J.R., Etzerodt, T., Gjetting, T., and Andresen, T.L. (2014). Side Chain Hydrophobicity Modulates Therapeutic Activity and Membrane Selectivity of Antimicrobial Peptide Mastoparan-X. *Plos one,* 9(3)**,** e91007.

Higashijima, T., Uzu, S., Nakajima, T., and Ross, E.M. (1988). Mastoparan, a peptide toxin from wasp venom, mimics receptors by activating GTP-binding regulatory proteins (G proteins). *Journal of Biological Chemistry,* 263(14)**,** 6491-6494.

Hirai, Y., Yasuhara, T., Yoshida, H., Nakajima, T., Fujino, M., and Kitada, C. (1979). A new mast cell degranulating peptide "mastoparan" in the venom of *Vespula lewisii*. *Chem Pharm Bull (Tokyo),* 27(8)**,** 1942-1944.

Hiss, J., Hartenfeller, M., and Schneider, G. (2010). Concepts and applications of “natural computing” techniques in de novo drug and peptide design. *Current pharmaceutical design,* 16(15)**,** 1656-1665.

Ho, C.-L., Shih, Y.-P., Wang, K.-T., and Yu, H.-M. (2001). Enhancing the hypotensive effect and diminishing the cytolytic activity of hornet mastoparan B by D-amino acid substitution. *Toxicon,* 39(10)**,** 1561-1566.

Holland, J., and Goldberg, D. (1989). Genetic Algorithms in Search, Optimization and Machine Learning. *ed: Addison-Wesley, Reading, MA.*

Hollenbeck, B.L., and Rice, L.B. (2012). Intrinsic and acquired resistance mechanisms in enterococcus. *Virulence,* 3(5)**,** 421-569.

Hollmann, A., Martínez, M., Noguera, M.E., Augusto, M.T., Disalvo, A., Santos, N.C., et al. (2016). Role of amphipathicity and hydrophobicity in the balance between hemolysis and peptide–membrane interactions of three related antimicrobial peptides. *Colloids and Surfaces B: Biointerfaces,* 141**,** 528-536.

Hooper, D.C. (2002). Fluoroquinolone resistance among Gram-positive cocci. *The Lancet infectious diseases,* 2(9)**,** 530-538.

Hori, Y., Demura, M., Iwadate, M., Ulrich, A.S., Niidome, T., Aoyagi, H., et al. (2001). Interaction of mastoparan with membranes studied by 1H-NMR spectroscopy in detergent micelles and by solid-state 2H-NMR and 15N-NMR spectroscopy in oriented lipid bilayers. *European Journal of Biochemistry,* 268(2)**,** 302-309.

Howl, J., Howl, L., and Jones, S. (2018). The cationic tetradecapeptide mastoparan as a privileged structure for drug discovery: Enhanced antimicrobial properties of mitoparan analogues modified at position-14. *Peptides,* 101**,** 95-105.

Huang, D.B., Mohanty, A., DuPont, H.L., Okhuysen, P.C., and Chiang, T. (2006). A review of an emerging enteric pathogen: enteroaggregative *Escherichia coli*. *Journal of medical microbiology,* 55(10)**,** 1303-1311.

Irazazabal, L.N., Porto, W.F., Ribeiro, S.M., Casale, S., Humblot, V., Ladram, A., et al. (2016). Selective amino acid substitution reduces cytotoxicity of the antimicrobial peptide mastoparan. *Biochimica et Biophysica Acta (BBA)-Biomembranes,* 1858(11)**,** 2699-2708.

Izadpanah, A., and Gallo, R.L. (2005). Antimicrobial peptides. *Journal of the American Academy of Dermatology,* 52(3)**,** 381-390.

Jenssen, H., Hamill, P., and Hancock, R.E. (2006). Peptide antimicrobial agents. *Clinical microbiology reviews,* 19(3)**,** 491-511.

Jones, S., and Howl, J. (2006). Biological applications of the receptor mimetic peptide mastoparan. *Current Protein and Peptide Science,* 7(6)**,** 501-508.

Joo, S.H. (2012). Cyclic peptides as therapeutic agents and biochemical tools. *Biomol Ther (Seoul),* 20(1)**,** 19-26.

Kaper, J.B., Nataro, J.P., and Mobley, H.L. (2004). Pathogenic escherichia coli. *Nature reviews microbiology,* 2(2)**,** 123-140.

Karmali, M.A. (2018). Factors in the emergence of serious human infections associated with highly pathogenic strains of shiga toxin-producing Escherichia coli. *International Journal of Medical Microbiology,* 308(8)**,** 1067-1072.

Kliger, Y. (2010). Computational approaches to therapeutic peptide discovery. *Peptide Science,* 94(6)**,** 701-710.

Ko, S.J., Park, E., Asandei, A., Choi, J.-Y., Lee, S.-C., Seo, C.H., et al. (2020). Bee venom-derived antimicrobial peptide melectin has broad-spectrum potency, cell selectivity, and salt-resistant properties. *Scientific Reports,* 10(1)**,** 10145.

Koehbach, J., and Craik, D.J. (2019). The vast structural diversity of antimicrobial peptides. *Trends in pharmacological sciences,* 40(7)**,** 517-528.

Konno, K., Hisada, M., Fontana, R., Lorenzi, C.C., Naoki, H., Itagaki, Y., et al. (2001). Anoplin, a novel antimicrobial peptide from the venom of the solitary wasp *Anoplius samariensis*. *Biochimica et Biophysica Acta (BBA)-Protein Structure and Molecular Enzymology,* 1550(1)**,** 70-80.

Konno, K., Hisada, M., Naoki, H., Itagaki, Y., Fontana, R., Rangel, M., et al. (2006). Eumenitin, a novel antimicrobial peptide from the venom of the solitary eumenine wasp Eumenes rubronotatus. *Peptides,* 27(11)**,** 2624-2631.

Konno, K., Hisada, M., Naoki, H., Itagaki, Y., Kawai, N., Miwa, A., et al. (2000). Structure and biological activities of eumenine mastoparan-AF (EMP-AF), a new mast cell degranulating peptide in the venom of the solitary wasp (Anterhynchium flavomarginatum micado). *Toxicon,* 38(11)**,** 1505-1515.

Kostakioti, M., Hadjifrangiskou, M., and Hultgren, S.J. (2013). Bacterial biofilms: development, dispersal, and therapeutic strategies in the dawn of the postantibiotic era. *Cold Spring Harbor perspectives in medicine,* 3(4)**,** a010306.

Kotsiantis, S.B., Zaharakis, I., and Pintelas, P. (2007). Supervised machine learning: A review of classification techniques. *Emerging artificial intelligence applications in computer engineering, 160*(1), 3-24.

Kumar, P., Kizhakkedathu, J.N., and Straus, S.K.J.B. (2018). Antimicrobial peptides: diversity, mechanism of action and strategies to improve the activity and biocompatibility *in vivo*. *Biomolecules,* 8(1)**,** 4.

Kusunoki, H., Wakamatsu, K., Sato, K., Miyazawa, T., and Kohno, T. (1998). G protein-bound conformation of mastoparan-x: heteronuclear multidimensional transferred nuclear overhauser effect analysis of peptide uniformly enriched with 13C and 15N. *Biochemistry,* 37(14)**,** 4782-4790.

Lai, Y., and Gallo, R.L. (2009). AMPed up immunity: how antimicrobial peptides have multiple roles in immune defense. *Trends in immunology,* 30(3)**,** 131-141.

Lawrence, N., Philippe, G.J.B., Harvey, P.J., Condon, N.D., Benfield, A.H., Cheneval, O., et al. (2020). Cyclic peptide scaffold with ability to stabilize and deliver a helical cell-impermeable cargo across membranes of cultured cancer cells. *RSC Chemical Biology,* 1(5)**,** 405-420.

Lee, J., and Lee, D.G. (2015). Antimicrobial peptides (AMPs) with dual mechanisms: membrane disruption and apoptosis. *Journal of Microbiology and Biotechnology,* 25(6)**,** 759-764.

Li, F., Xiong, X.-S., Yang, Y.-Y., Wang, J.-J., Wang, M.-M., Tang, J.-W., et al. (2021). Effects of NaCl concentrations on growth patterns, phenotypes associated with virulence, and energy metabolism in *Escherichia coli* BW25113. *Frontiers in microbiology*, *12*, 705326.

Li, J., Wang, X., Zhang, T., Wang, C., Huang, Z., Luo, X., et al. (2015). A review on phospholipids and their main applications in drug delivery systems. *Asian Journal of Pharmaceutical Sciences,* 10(2)**,** 81-98.

Lin, C.-H., Tzen, J.T., Shyu, C.-L., Yang, M.J., and Tu, W.-C. (2011). Structural and biological characterization of mastoparans in the venom of *Vespa species* in Taiwan. *Peptides,* 32(10)**,** 2027-2036.

Llarrull, L.I., Testero, S.A., Fisher, J.F., and Mobashery, S. (2010). The future of the β-lactams. *Current opinion in microbiology,* 13(5)**,** 551-557.

Lopez Cascales, J.J., Zenak, S., García de La Torre, J., Lezama, O.G., Garro, A., and Enriz, R.D. (2018). Small cationic peptides: influence of charge on their antimicrobial activity. *ACS omega,* 3(5)**,** 5390-5398.

Lorin, C., Saidi, H., Belaid, A., Zairi, A., Baleux, F., Hocini, H., et al. (2005). The antimicrobial peptide dermaseptin S4 inhibits HIV-1 infectivity *in vitro*. *Virology,* 334(2)**,** 264-275.

Magana, M., Pushpanathan, M., Santos, A.L., Leanse, L., Fernandez, M., Ioannidis, A., et al. (2020). The value of antimicrobial peptides in the age of resistance. *The Lancet Infectious Diseases,* 20(9)**,** e216-e230.

Marr, A.K., Gooderham, W.J., and Hancock, R.E. (2006). Antibacterial peptides for therapeutic use: obstacles and realistic outlook. *Current opinion in pharmacology,* 6(5)**,** 468-472.

Martínez, J.L., and Baquero, F. (2002). Interactions among strategies associated with bacterial infection: pathogenicity, epidemicity, and antibiotic resistance. *Clinical microbiology reviews,* 15(4)**,** 647-679.

Mayor, S., and Pagano, R.E. (2007). Pathways of clathrin-independent endocytosis. *Nature reviews Molecular cell biology,* 8(8)**,** 603-612.

Memariani, H., Memariani, M., and Pourmand, M.R. (2018). Venom-derived peptide Mastoparan-1 eradicates planktonic and biofilm-embedded methicillin-resistant *Staphylococcus aureus* isolates. *Microbial Pathogenesis,*119**,** 72-80.

Miller, M.B., and Bassler, B.L. (2001). Quorum sensing in bacteria. *Annual Reviews in Microbiology,* 55(1)**,** 165-199.

Mitchell, J.B. (2014). Machine learning methods in chemoinformatics. *Wiley Interdisciplinary Reviews: Computational Molecular Science,* 4(5)**,** 468-481.

Mohanram, H., and Bhattacharjya, S. (2016). Salt-resistant short antimicrobial peptides. *Peptide Science,* 106(3)**,** 345-356.

Monte, A.A., Vasiliou, V., and Heard, K.J. (2012). Omics screening for pharmaceutical efficacy and safety in clinical practice. *Journal of pharmacogenomics & pharmacoproteomics*.

Monteiro, M.C., Romão, P.R., and Soares, A.M. (2009). Pharmacological perspectives of wasp venom. *Protein and peptide letters,* 16(8)**,** 944-952.

Moreno, M., and Giralt, E. (2015). Three valuable peptides from bee and wasp venoms for therapeutic and biotechnological use: melittin, apamin and mastoparan. *Toxins* 7(4)**,** 1126-1150.

Morens, D.M., Folkers, G.K., and Fauci, A.S. (2004). The challenge of emerging and re-emerging infectious diseases. *Nature,* 430(6996)**,** 242-249.

Morgenstern, B., Prohaska, S.J., Pöhler, D., and Stadler, P.F. (2006). Multiple sequence alignment with user-defined anchor points. *Algorithms for Molecular Biology* 1(1)**,** 6.

Munita, J.M., and Arias, C.A. (2016). Mechanisms of Antibiotic Resistance. *Microbiology spectrum.* 4(2).

Nakajima, T., Uzu, S., Wakamatsu, K., Saito, K., Miyazawa, T., Yasuhara, T., et al. (1986). Amphiphilic peptides in wasp venom. *Biopolymers,* 25 Suppl**,** S115-121.

Nataro, J.P., and Kaper, J.B. (1998). Diarrheagenic *Escherichia coli*. *Clinical microbiology reviews,* 11(1)**,** 142-201.

Neves, B.J., Braga, R.C., Melo-Filho, C.C., Moreira-Filho, J.T., Muratov, E.N., and Andrade, C.H. (2018). QSAR-based virtual screening: advances and applications in drug discovery. *Frontiers in pharmacology, 9,* 1275.

Nguyen, L.T., Haney, E.F., and Vogel, H.J. (2011). The expanding scope of antimicrobial peptide structures and their modes of action. *Trends in Biotechnology,* 29(9)**,** 464-472.

Nikaido, H. (2009). Multidrug resistance in bacteria. *Annual review of biochemistry,* 78**,** 119-146.

O'Toole, G., Kaplan, H.B., and Kolter, R. (2000). Biofilm formation as microbial development. *Annual Reviews in Microbiology,* 54(1)**,** 49-79.

Okeke, I.N., and Nataro, J.P. (2001). Enteroaggregative escherichia coli. *The Lancet infectious diseases,* 1(5)**,** 304-313.

Oliveira, D.M.P.D., Forde, B.M., Kidd, T.J., Harris, P.N.A., Schembri, M.A., Beatson, S.A., et al. (2020). Antimicrobial Resistance in ESKAPE Pathogens. *Clinical microbiology reviews,* 33(3)**,** e00181-00119.

Osborn, A.M., and Böltner, D. (2002). When phage, plasmids, and transposons collide: genomic islands, and conjugative-and mobilizable-transposons as a mosaic continuum. *Plasmid* 48(3)**,** 202-212.

Oshiro, K.G., Cândido, E.S., Chan, L.Y., Torres, M.D., Monges, B.E., Rodrigues, S.G., et al. (2019). Computer-Aided design of mastoparan-like peptides enables the generation of nontoxic variants with extended antibacterial properties. *Journal of medicinal chemistry,* 62(17)**,** 8140-8151.

Papo, N., and Shai, Y. (2003). Can we predict biological activity of antimicrobial peptides from their interactions with model phospholipid membranes?. *Peptides,* 24(11)**,** 1693-1703.

Park, I.Y., Cho, J.H., Kim, K.S., Kim, Y.-B., Kim, M.S., and Kim, S.C. (2004). Helix stability confers salt resistance upon helical antimicrobial peptides. *Journal of Biological Chemistry,* 279(14)**,** 13896-13901.

Park, S.-C., Son, H., Kim, Y.-M., Lee, J.-K., Park, S., Lim, H.S., et al. (2022). Design of antimicrobial peptides with cell-selective activity and membrane-acting mechanism against drug-resistant bacteria. *Antibiotics,* 11(11)**,** 1619.

Peleg, A.Y., and Hooper, D.C. (2010). Hospital-acquired infections due to gram-negative bacteria. *New England Journal of Medicine,* 362(19)**,** 1804-1813.

Pelegrini, P.B., del Sarto, R.P., Silva, O.N., Franco, O.L., and Grossi-de-Sa, M.F. (2011). Antibacterial peptides from plants: what they are and how they probably work. *Biochemistry Research International.*

Petsko, G.A. (1992). On the other hand. *Science,* 256(5062)**,** 1403-1404.

Porto, W.F., Fensterseifer, I.C., Ribeiro, S.M., and Franco, O.L. (2018a). Joker: An algorithm to insert patterns into sequences for designing antimicrobial peptides antimicrobial peptides. *Biochimica et Biophysica Acta (BBA)-General Subjects*, 1862(9), 2043-2052.

Porto, W.F., Irazazabal, L., Alves, E.S.F., Ribeiro, S.M., Matos, C.O., Pires, Á.S., et al. (2018b). *In silico* optimization of a guava antimicrobial peptide enables combinatorial exploration for peptide design. *Nature Communications,* 9(1)**,** 1490.

Porto, W.F., Silva, O.N., and Franco, O.L. (2012). "Prediction and rational design of antimicrobial peptides," in *Protein Structure*. InTech).

Powers, J.-P.S., and Hancock, R.E. (2003). The relationship between peptide structure and antibacterial activity. *Peptides,* 24(11)**,** 1681-1691.

Reddy, K., Yedery, R., and Aranha, C. (2004). Antimicrobial peptides: premises and promises. *International journal of antimicrobial agents*, 24(6)**,** 536-547.

Römling, U., and Balsalobre, C. (2012). Biofilm infections, their resilience to therapy and innovative treatment strategies. *Journal of internal medicine*, 272(6)**,** 541-561.

Rungsa, P., Peigneur, S., Jangpromma, N., Klaynongsruang, S., Tytgat, J., and Daduang, S. (2022). *In silico* and *in vitro* structure and activity relationship of mastoparan and its analogs. *Molecules*, 27(2)**,** 561.

Schneider, G., and Wrede, P. (1998). Artificial neural networks for computer-based molecular design. *Progress in biophysics and molecular biology*, 70(3)**,** 175-222.

Scornet, E., Biau, G., and Vert, J.-P. (2015). Consistency of random forests. *The Annals of Statistics*, 43(4)**,** 1716-1741.

Scott, M.G., Yan, H., and Hancock, R.E. (1999). Biological properties of structurally related α-helical cationic antimicrobial peptides. *Infection and immunity*, 67(4)**,** 2005-2009.

Shai, Y. (2002). Mode of action of membrane active antimicrobial peptides. *Peptide Science*, 66(4)**,** 236-248.

Silva, J.C., Neto, L.M., Neves, R.C., Gonçalves, J.C., Trentini, M.M., Mucury-Filho, R., et al. (2017). Evaluation of the antimicrobial activity of the mastoparan Polybia-MPII isolated from venom of the social wasp *Pseudopolybia vespiceps testacea* (Vespidae, Hymenoptera). *International Journal of Antimicrobial Agents*, 49(2)**,** 167-175.

Souza, B.M.d., Cabrera, M.P.d.S., Gomes, P.C., Dias, N.B., Stabeli, R.G., Leite, N.B., et al. (2015). Structure–activity relationship of mastoparan analogs: Effects of the number and positioning of Lys residues on secondary structure, interaction with membrane-mimetic systems and biological activity. *Peptides*, 72**,** 164-174.

Takada, M., Ito, T., Kurashima, M., Matsunaga, N., Demizu, Y., and Misawa, T. (2023). Structure and activity relationship studies of substitutions of cationic amino acid residues on antimicrobial peptides. *Antibiotics*, 12(1).

Teng, P., Shao, H., Huang, B., Xie, J., Cui, S., Wang, K., et al. (2023). Small molecular mimetics of antimicrobial peptides as a promising therapy to combat bacterial resistance. *Journal of Medicinal Chemistry*. 66(4), 2211-2234.

Torres, M.D., Sothiselvam, S., Lu, T.K., and de la Fuente-Nunez, C.J. (2019). Peptide design principles for antimicrobial applications. *Journal of molecular biology,* 431(18)**,** 3547-3567.

Tosteson, M., Holmes, S., Razin, M., and Tosteson, D. (1985). Melittin lysis of red cells. *The Journal of membrane biology,* 87(1)**,** 35-44.

Vila-Farres, X., Garcia de la Maria, C., López-Rojas, R., Pachón, J., Giralt, E., and Vila, J. (2012). *In vitro* activity of several antimicrobial peptides against colistin-susceptible and colistin-resistant Acinetobacter baumannii. *Clinical Microbiology and Infection,* 18(4)**,** 383-387.

Waghu, F.H., Barai, R.S., Gurung, P., and Idicula-Thomas, S. (2015). CAMPR3: a database on sequences, structures and signatures of antimicrobial peptides. *Nucleic acids research***,** gkv1051.

Wang, G., Li, X., and Wang, Z. (2008). APD2: the updated antimicrobial peptide database and its application in peptide design. *Nucleic acids research,* 37(suppl_1)**,** D933-D937.

Weiss, R.A., and McMichael, A.J. (2004). Social and environmental risk factors in the emergence of infectious diseases. *Nature medicine*, *10*(Suppl 12), S70-S76.

Wellington, E.M., Boxall, A.B., Cross, P., Feil, E.J., Gaze, W.H., Hawkey, P.M., et al. (2013). The role of the natural environment in the emergence of antibiotic resistance in Gram-negative bacteria. *The Lancet infectious diseases,* 13(2)**,** 155-165.

Whiles, J.A., Brasseur, R., Glover, K.J., Melacini, G., Komives, E.A., and Vold, R.R. (2001). Orientation and effects of mastoparan x on phospholipid bicelles. *Biophysical Journal,* 80(1)**,** 280-293.

WHO (2001). World Health Organization. *Global strategy for containment of antimicrobial resistance.* (No. WHO/CDS/CSR/DRS/2001.2).

WHO (2017). World Health Organization. *Prioritization of pathogens to guide discovery, research, and development of new antibiotics for drug-resistant bacterial infections, including tuberculosis* (No. WHO/EMP/IAU/2017.12).

Wright, G.D. (2011). Molecular mechanisms of antibiotic resistance. *Chemical communications,* 47(14)**,** 4055-4061.

Wu, P.-S., Lai, S.-J., Fung, K.-M., and Tseng, T.-S. (2020). Characterization of the structure–function relationship of a novel salt-resistant antimicrobial peptide, RR12. *RSC Advances,* 10(40)**,** 23624-23631.

Wüthrich, K.J.J.o.B.C. (1990). Protein structure determination in solution by NMR spectroscopy. *Journal of Biological Chemistry*, *265*(36), 22059-22062.

Yang, L., Harroun, T.A., Weiss, T.M., Ding, L., and Huang, H.W. (2001). Barrel-stave model or toroidal model? A case study on melittin pores. *Biophysical journal* 81(3)**,** 1475-1485.

Yeung, A.T., Gellatly, S.L., Hancock, R.E. (2011). Multifunctional cationic host defence peptides and their clinical applications. *Cellular and Molecular Life Sciences*, *68,* 2161-2176.

Zasloff, M., Martin, B., and Chen, H.-C. (1988). Antimicrobial activity of synthetic magainin peptides and several analogues. *Proceedings of the National Academy of Sciences,* 85(3)**,** 910-913.

Zhu, S., Li, W., O'Brien-Simpson, N., Separovic, F., and Sani, M.-A.J.A.A. (2021). C-terminus amidation influences biological activity and membrane interaction of maculatin 1.1. *Amino Acids,* 53(5)**,** 769-777.